Elche, 2015

Identification and characterisation of Whirlin as a novel modulator of TRPV1

Maria Grazia Ciardo

Doctoral Thesis

DIRECTORS:
Antonio Ferrer Montiel
Rosa Planells Cases

Instituto de Biología Molecular y Celular
Universidad Miguel Hernández

UNIVERSITAS
Miguel
Hernández

Dr. Antonio Ferrer Montiel, Catedrático y Director del Instituto de Biología Molecular y Celular de la Universidad Miguel Hernández de Elche.

DA SU CONFORMIDAD a la lectura de tesis doctoral titulada: “Identification and characterisation of Whirlin as a novel modulator of TRPV1”, presentada por Dña. Maria Grazia Ciardo.

Elche, Noviembre 2015

Fdo: Dr. Antonio Ferrer Montiel
Catedrático Universidad Miguel Hernández

UNIVERSITAS
Miguel
Hernández

Dr. Antonio Ferrer Montiel, Catedrático de la Universidad Miguel Hernández de Elche, y **Dra. Rosa Planells Cases**, Investigadora del Centro Max Delbrück para Medicina Molecular de Berlín,

CERTIFICAN que el trabajo de investigación que lleva por título "Identification and characterisation of Whirlin as a novel modulator of TRPV1", presentado por Dña. Maria Grazia Ciardo para optar al grado de Doctor, ha sido realizado bajo su dirección en el Instituto de Biología Molecular y Celular de la Universidad Miguel Hernández de Elche. Considerando que la presente tesis se halla concluida, **AUTORIZAN** su presentación para que pueda ser juzgada por el tribunal correspondiente.

Y para que así conste a los efectos oportunos, se expide el presente escrito.

Elche, Noviembre 2015

Fdo: Dr. Antonio Ferrer Montiel
Catedrático Universidad Miguel Hernández

Fdo: Dra. Rosa Planells Cases

UNIVERSITAS
Miguel
Hernández

El presente trabajo ha sido realizado en el Instituto de Biología Molecular y Celular (IBMC), de la Universidad Miguel Hernández de Elche.

Este trabajo se ha desarrollado gracias a la financiación procedente del Ministerio de Economía y competitividad y de la Generalitat Valenciana.

UNIVERSITAS
Miguel
Hernández

La ciencia siempre
vale la pena
porque sus descubrimientos,
tarde o temprano,
siempre se aplican.
Severo Ochoa

UNIVERSITAS
Miguel
Hernández

INDEX OF CONTENT

UNIVERSITAS
Miguel
Hernández

UNIVERSITAS
Miguel
Hernández

INDEX OF ABBREVIATIONS

AC	Adenyl Cyclase
AKAP	A-kinase Anchoring Protein
AMPA	α-Amino-3-hydroxyl-5-Methyl-4-isoxazole Propionic Acid
ANO1	Anoctamin 1
ARD	Ankyrin Repeat Domain
ASIC	Acid-Sensing Ion Channel
ATP	Adenosine 5'-Triphosphate
AUC	Area Under Curve
BCA	Bicinchoninic Acid
BK	Bradykinin
BSA	Bovine Serum Albumin
CaCC	Ca2+-activated Cl– Channels
CaM	Calmodulin
CaMKII	Ca2+/Calmodulin-dependent protein Kinase II
cAMP	cyclic Adenosine Monophosphate
CASK	Calmodulin-dependent Serine Kinase
CFA	Complete Freund's adjuvant
CGRP	Calcitonin-Gene Related Peptide
CIP98	CASK-Interacting Protein 98
CNS	Central Nervous System
cryo-EM	cryo-Electron Microscopy
DAG	1,2-Diacylglycerol
DAPI	4',6-Diamidino-2-Phenylindole
dlg	disc large
DMEM	Dulbecco's Modified Eagle's Medium
DRG	Dorsal Root Ganglia
DsRED	Discosoma sp. Red fluorescent protein
E	Epoxomicin
EDTA	Ethylenediaminetetraacetic acid
EGTA	Ethylene glycol tetraacetic acid
Epac	Exchange protein directly activated by cAMP
ePKC	eye specific PKC
EPSC	Excitatory Postsynaptic Currents
ER	Endoplasmic Reticulum
ERAD	ER-Associated Degradation
FBS	Fetal Bovine Serum
Fluo-4-AM	Fluo-4-Acetoxymethyl ester

GABA	γ-aminobutyric acid
GABARAP	GABA A Receptor Associated Protein
GDNF	Glial-Derived Neurotrophic Factor
GFP	Green Fluorescent Protein
GPCR	G-Protein-Coupled Receptor
Gs	Stimulatory G protein
GST	Glutathione S-Transferase
HB	Homogenisation Buffer
HEK293	Human embryonic kidney 293
HEPES	4-(2-Hydroxyethyl)-1-Piperazineethanesulfonic acid
His6	Hexahistidine
HIV-1	Human Immunodeficiency Virus-type 1
HRP	Horseradish Peroxidase
IASP	Isolectin B4
IB4	Insulin-like Growth Factor 1
IGF-1	Inner Hair Cells
IHC	International Association for the Study of Pain
INAD	Inactivation No Afterpotential D
IP3	Inositol 1,4,5-triphosphate
IPTG	Isopropyl β-D-1-Thiogalactopyranoside
Kvβ2	Voltage-gated K+ channel accessory subunit beta 2
L	Leupeptin
LB	Luria Broth
MAGUK	Membrane-Associated Guanylate Kinase
MAPK	Mitogen-Activated Protein Kinase
MES	2-(N-Morpholino)-Ethanesulfonic acid
MYCBP2	Myc-Binding Protein-2
MβCD	Methyl-β-cyclodextrin
NADA	N-arachidonoyl Dopamine
NGF	Nerve Growth Factor
NMDA	N-methyl-D-aspartate
NO	Nitric Oxide
NT	Non-transfected cells
NTC	Non-Template Control
o/n	overnight
OHC	Outer Hair Cells
P/S	Penicillin-Streptomycin Solution
PBM	PDZ-Binding Motif
PBS	Phosphate Buffered Saline
PDZ	Postsynaptic density protein 95, Disc large, ZO-1

PFA	Paraformaldehyde
PGE2	Prostaglandin E2
PGI2	Prostacyclin
PI3K	Phosphatidylinositol 3-Kinase
PI4K	Phosphatidylinositol 4-Kinase
PIP2	Phosphatidylinositol 4,5-bisphosphate
PKA	cAMP-dependent Protein Kinase A
PKC	Protein Kinase C
PLA2	Phospholipases A2
PLC	Phospholipase C
PMSF	Phenylmethylsulfonylfluoride
PP2B	Ca2+/Calmodulin dependent Ser/Thr phosphatase 2B
PSD95	Postsynaptic Density Protein 95
PTD	Protein Transduction Domain
qPCR	quantitative Polymerase Chain Reaction
RIPA	Radioimmunoprecipitation Assay
RT	Room Temperature
RT-PCR	Reverse Transcriptase PCR
RTX	Resiniferatoxin
SANS	Scaffolding protein containing Ankyrin repeats and SAM domain
sc-siRNA	scramble siRNA
SDS	Sodium Dodecyl Sulfate
SDS-PAGE	SDS Polyacrylamide Gel Electrophoresis
siRNA	small interfering RNA
SNARE	Soluble N-ethylmaleimide-sensitive factor Attachment Protein Receptor
SP	Substance P
TBS-T	Tris-buffered saline-Tween-20
TCA	Trichloroacetic Acid
TEMED	Tetramethylethylenediamine
TG	Trigeminal Ganglion
TrkA	Tyrosine Kinase Receptor A
TRP	Transient Receptor Potential
TRPV1	Transient Receptor Potential Vanilloid 1
Ub	Ubiquitin
UPS	Ubiquitin-Proteasome System
VLGR1b	Very large G-protein-coupled receptor-1
Y2H	Yeast two-Hybrid screening
YFP	Yellow Fluorescent Protein

UNIVERSITAS
Miguel
Hernández

SUMMARY

UNIVERSITAS
Miguel
Hernández

SUMMARY

TRPV1 receptor is a molecular transducer for both chemical and physical stimuli in high-threshold afferent neurons (or nociceptors), where it is abundantly expressed and plays an essential role in pain physiopathology. TRPV1 is known to interact with different proteins which modulate receptor activity and/or trafficking to the membrane. The formation of these multiproteic complexes, called signalplexes or transducisomes, can alter the activity and/or activation thresholds of TRPV1 receptor and it is crucial for the regulation of channel function. For this reason, the identification of new components of these signalling complexes would allow a more complete understanding of TRPV1 physiopathology, knowledge essential for the development of new pharmacological treatments.

In this context, the present study describes the interaction between TRPV1 and Whirlin, a cytosolic protein with PDZ domains previously identified through a yeast two hybrid assay by using the N-terminus of TRPV1 as bait. Specifically, the heterologous expression of Whirlin increases TRPV1 protein levels and promotes the clustering of the receptor to the plasma membrane. Whirlin downregulation through specific silencing RNA results in the concomitant degradation of TRPV1 receptor, which can be prevented by proteasome inhibition. Furthermore, the degradation kinetics of TRPV1 upon arresting protein translation mirrored that of Whirlin in cells co-expressing both proteins, suggesting a parallel degradation mechanism. Finally, Whirlin coexpression attenuated TRPV1 internalisation upon prolonged exposure to the agonist capsaicin.

Together, these findings indicate that the assembly of both proteins in a same complex stabilises TRPV1 expression and localisation in the plasma membrane, suggesting that the pharmacological perturbation of this macromolecular complex may represent a novel therapeutic strategy for pain management.

UNIVERSITAS
Miguel
Hernández

RESUMEN

El receptor TRPV1 es un transductor de estímulos químicos y físicos en las neuronas aferentes de alto umbral o nociceptores donde se expresa de forma abundante, y juega un papel esencial en la fisiopatología del dolor. Numerosas evidencias demuestran que el receptor TRPV1 interacciona activamente con diversas proteínas celulares que modulan su actividad y/o su tráfico hacia la membrana plasmática. La formación de estos complejos multiproteicos, llamados también signalosomas o transducisomas, puede alterar la actividad del receptor TRPV1 y/o su umbral de activación y juega por lo tanto un papel crucial en la regulación de su función. Por esta razón la identificación de nuevos componentes de estos complejos de señalización nos permitiría alcanzar un mejor conocimiento de la fisiopatología del receptor TRPV1, que se podría trasladar al desarrollo de nuevos tratamientos farmacológicos.

A este propósito, el presente trabajo describe la interacción del receptor TRPV1 con una proteína citosólica con dominios PDZ, conocida como Whirlin, inicialmente identificada mediante la técnica de doble híbrido en levaduras utilizando como cebo el dominio citosólico N-terminal de TRPV1. La coexpresión heterologa de Whirlin resulta en un aumento de la expresión del receptor TRPV1 y promueve la agrupación de receptores en la membrana plasmática. Por otro lado, el silenciamiento genético de Whirlin mediante ARN de interferencia resulta en la concomitante degradación del receptor TRPV1, que puede ser bloqueada por el tratamiento con un inhibidor del proteasoma. La degradación del receptor TRPV1, tras la inhibición de la síntesis proteica, sigue la misma cinética de degradación que Whirlin. Finalmente, la coexpresión de Whirlin reduce la internalización de TRPV1 inducida por la exposición prolongada al agonista del receptor, la capsaicina.

En conjunto, estos resultados indican que el ensamblaje de ambas proteínas en un mismo complejo proteico estabiliza la expresión del receptor TRPV1 y su localización en la membrana plasmática, lo que conlleva a pensar que la perturbación farmacológica de dicho complejo macromolecular podría representar una interesante estrategia terapéutica para el tratamiento del dolor.

UNIVERSITAS
Miguel
Hernández

INTRODUCTION

UNIVERSITAS
Miguel
Hernández

PAIN

A definition

The struggle against pain dates back to the birth of humanity. The etymological origin of the word can be found in the ancient Greek *poiné* that, as its Latin equivalent *poena*, means "penalty", according to the traditional idea of pain as an external force, something generated outside the body as a test of faith or a kind of punishment from God/s. It was essentially during the scientific Renaissance in Europe when pain started to be better understood and considered more as a physical sensation than a mystical experience. In his *Treatise of Man* (1664) René Descartes described pain as a disturbance within the body "machine" that passed through nerves to the brain. This work preceded the development of the 19th century specificity theory which considered pain as "a specific sensation with its own sensory apparatus independent of touch and other senses". Since then many other works have explored the concept of pain and many attempts have been made in the last centuries to describe mechanisms underlying pain perception. In 1979 the International Association for the Study of Pain (IASP) introduced the currently most widely used definition of pain as "an unpleasant sensory and emotional experience associated with actual or potential tissue damage, or described in terms of tissue damage, or both", emphasising that pain is a complex experience that involves multiple dimensions (Merskey *et al.* 1979).

Epidemiology

Due to its high prevalence and serious consequences, pain is one of the primary reasons for patients to visit their doctor. Actually, recent studies have estimated that globally between 10 and 25% of adults suffer from pain (Goldberg and McGee 2011). When not effectively treated, it has a detrimental effect on all aspects of life, from social relationships to productivity at work, at every age and for every type and source of pain itself. In addition to the physical and emotional impact on patients, also the financial cost it brings to society is tremendous, currently estimated at more than € 200 billion per year in Europe and $ 150 billion per year in the USA (Tracey and Bushnell 2009). All this aspects and factors explain how important is to establish an effective analgesic therapy and relieve pain in order to improve patients' quality of life and reduce its global impact on society (van *et al.* 2013).

Over the last several years, discovery and description of pathophysiological mechanisms of pain have helped the development of more effective pain management strategies and of new drugs with lower side effects, although in many cases pain still remains underrecognised and undertreated.

Classification

Since there are no objective biological markers of pain, multiple classification schemes have been developed in order to improve its understanding, prediction and treatment. Although a clear categorisation is not always possible, pain is conventionally classified according to its time course, underlying pathophysiology or location.

Depending on the duration of the pain process, clinical researchers have traditionally defined **acute pain** as pain of less than 30 days, differentiating it from **chronic pain** that persists for more than 6 months (Merskey and Bogduk, 1994). According to this classification, other two types of pain can be identified: **subacute pain**, which lasts continuously from the end of the first month to the beginning of the seventh month, and **recurrent acute pain**, that persists over an extended period of time but occurs mainly as isolated episodes (Thienhaus *et al.* 2001).

However new and more complex definitions have been introduced that take in consideration other features more than just time. Thus acute pain is now viewed as a complex and unpleasant emotional, sensorial and cognitive experience that occurs in response to a tissue trauma and can be easily recognised by its distinct onset, short duration and obvious cause (Ferrell 2003). Since it is usually accompanied by protective reflexes (e.g., withdrawal of a damaged limb, muscle spasm, autonomic responses) this pain serves an important biological function by warning the subject about the potential or extent of injury and by protecting tissue from being further damaged. On the other side, chronic pain has been described as a severe persisting pain of moderate or long duration that disrupts sleep and normal living and that in most cases bears little or no relationship to observable tissue damage. For this reason it is more difficult to manage and requires a multidimensional treatment including both physical and psychological strategies.

On the basis of its presumed underlying pathophysiology pain is broadly categorised as nociceptive and neuropathic. **Nociceptive pain** results from stimulation of a specialised high-threshold sensory apparatus as a consequence of tissue injury, inflammation or mechanical deformation produced for example by a trauma, burns, infections, ischemia, arthritis, surgery or sport injuries. This kind of pain helps us to detect and minimise contact with damaging or noxious stimuli and usually responds well to common analgesic treatments (opioids and nonsteroidal anti-inflammatory drugs). By contrast, **neuropathic pain** arises from lesions or dysfunctions of the peripheral or central nervous system (e.g. due to trauma, metabolic diseases, infections, tumour invasion or ischemia) that lead to a combination of negative symptoms or sensory deficits, such as partial or complete loss of sensation, and positive symptoms that include pain, paraesthesias (unpleasant not painful abnormal sensations) and dysaesthesias (uncomfortable painful abnormal sensations). Unlike nociceptive pain, it offers no biological advantage, but rather causes suffering and distress (for which reason it is also defined as “pathological” or “maladaptive” pain), and has been found to respond to non conventional analgesic drugs, such as tricyclic antidepressants and anticonvulsivants (Scholz and Woolf 2002;Nicholson 2006).

Finally, depending on the location from which it is generated, pain can be further classified in somatic or visceral. **Somatic pain** is usually well localised and may be felt as **superficial**, when arising from skin or other superficial tissues, or **deep**, when arising from ligaments, tendons, muscles, bones and blood vessels. On the other side, **visceral pain** is caused by activation of pain receptors resulting from infiltration, compression, extension, or stretching of the thoracic, abdominal, or pelvic viscera. It is usually diffuse and more difficult to localise than somatic pain and can be "**referred**" when it is perceived at a location distant from the site of the painful stimulus (e.g., pain associated with the ischemia caused by a myocardial infarction is usually perceived in the neck, shoulder and back more than in the chest, the site of injury) (Garcia and Altman 1997).

Mechanisms of pain and nociception

Before starting to describe the anatomical and physiological bases of pain generation, it is important to reiterate the difference between nociception and pain. **Nociception** refers to the process by which intense external or internal thermal, mechanical, or chemical stimuli are detected by a specific subpopulation of peripheral nerve fibres and transmitted to the central nervous system. By contrast, the perception of **pain** is only produced when the information conveyed by pathways of nociception is filtered and modulated through the affective and cognitive processes of higher brain centres. Thus, in certain conditions, nociception can occur in the absence of pain (e.g., due to spinal cord transection) (Garcia and Altman 1997;Basbaum and Jessell 2000).

The propagation of pain is initiated when noxious stimuli are converted into electrical signals in free nervous endings dispersed over the body, innervating skin, muscle, joints and internal organs. This process, known as **transduction**, is mediated by specific ion channels and receptors with high thresholds of activation to external stimuli. Once they are activated, sodium and calcium ions flow into the nociceptors peripheral terminals through the opened channels. As a result the membrane is depolarised and activates voltage-gated channels, further depolarising the membrane and initiating a train of action potentials, with a frequency and duration that will reflect the intensity and duration of the noxious stimulus. The process by which these action potentials reach the central nervous system, moving along axons from the peripheral terminal to the central terminal of nociceptors where they initiate transmitter release (mainly glutamate, but also neuropeptides and neurotrophic factors), is known as **conduction**. The synaptic transfer and modulation of input from one neuron to another is defined as **transmission** (**Figure 1**) (Woolf 2004).

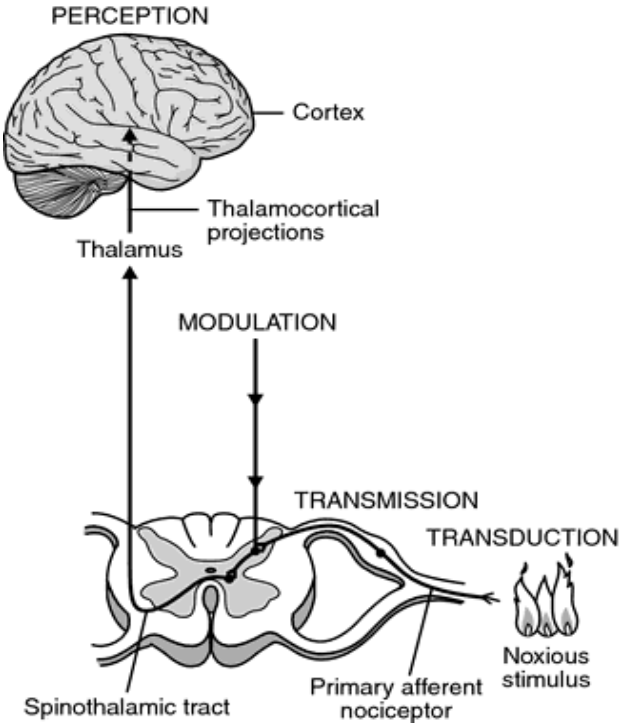

Figure 1 Phases of the pain process. Four steps occur along the pain pathway: transduction, transmission, modulation and perception (Ferrante and VadeBoncouer 1993).

The primary afferent fibres project to the dorsal horn of the spinal cord where the central terminals of nociceptors make synaptic connections with a complex array of second-order neurons that are at the origin of multiple ascending pathways, including the spinothalamic and the spinoreticulothalamic tracts. The first transmits information to the thalamus about the location and intensity of the painful stimuli, whereas the second carries pain messages to the amygdala via connections in the brainstem, contributing to the affective component of pain experience. From these loci information is finally transmitted to the somatosensory cortex. However, most inputs fail to evoke an action potential output because of local segmental circuits in the spinal cord (mainly co-releasing the inhibitory transmitters glycine and γ-aminobutyric acid, or GABA) and powerful descending mechanisms arising from the brain (mainly operating through norepinephrine and serotonin) that influence the transmission of pain messages to the cortex (Chery and de 1999;Millan 1997;Woolf 2004).

Nociceptors

The idea that nociception occurs through specialised nerve was firstly introduced by Sherrington in 1906, and confirmed later by electrophysiological studies. Today, **nociceptors** are defined as high-threshold primary sensory neurons that are normally electrically silent and transmit all-or-none potentials only when activated by stimuli capable of causing tissue damage (noxious heat, intense pressure or irritant chemicals), but not by innocuous stimuli such as warming or light touch (Sherrington 1906;Julius and Basbaum 2001).

Primary somatosensory neurons innervating the body and extremities locate their cell bodies in dorsal root ganglia (DRG), whereas those innervating neck and head project from trigeminal ganglion (TG). These neurons are pseudounipolar, meaning that from the soma a single process emanates which then bifurcates into a peripheral axon that innervates the target organ and a central branch that synapses on second-order neurons in the dorsal horn of the spinal cord (for DRG) or the trigeminal subnucleus caudalis (for TG).

Although nociceptors are all excitatory neurons that release glutamate, they can be distinguished and classified in two major classes according to their conduction velocity, which is in turn related to their axon diameter and myelination degree, and to their sensitivity to different stimulus modalities (mechanical, heat and cold) (**Figure 2**) (Belmonte and Cervero 1996).

The first type of nociceptors is constituted by medium diameter myelinated **Aδ-fibres** that support conduction velocities of approximately 5–30 m/s and convey the "first" pain (rapid, acute and sharp) (Basbaum and Jessell 2000). They are considerably different from myelinated, rapidly conducting Aβ-fibres that in normal situations do not propagate noxious potentials but rather detect innocuous stimuli (e.g. light touch) applied to skin, muscle and joints. However, these are equally important in the painful circuitry because their stimulation can reduce pain by suppressing its transmission at segmental (spinal cord) levels (Almeida *et al.* 2004). The second population of nociceptive fibres includes small diameter unmyelinated **C-fibres** that support conduction velocities of 0.4–1.4 m/s and convey the "second" pain (slow, dull and diffuse) (Julius and Basbaum 2001).

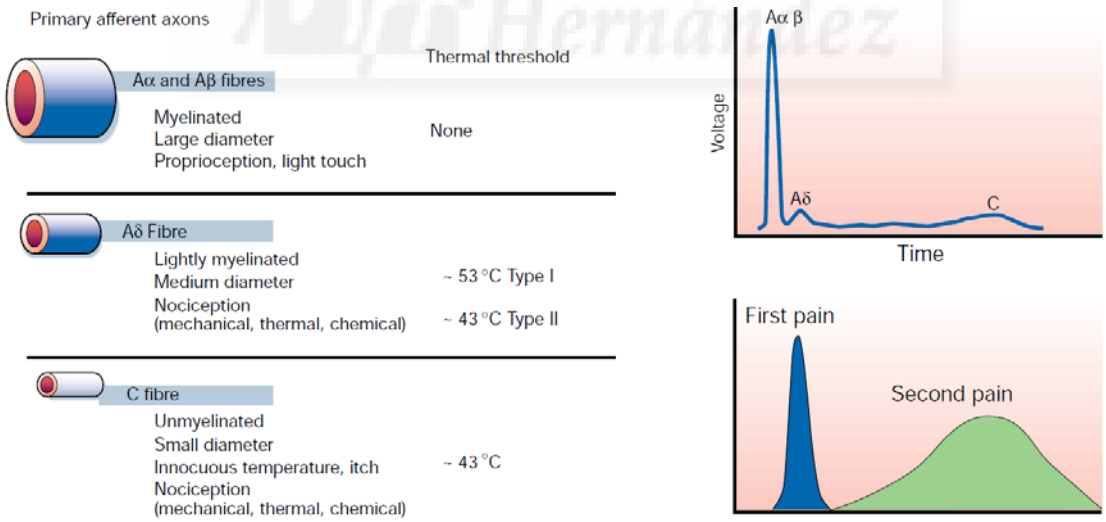

Figure 2 Different types of nociceptive fibres. Most nociceptors are Aδ and C fibres with different diameters and myelination grades which determine their conduction velocity and thus first or second pain responses (Julius and Basbaum 2001).

Aδ nociceptors have been further subdivided into two main classes, both sensitive to intense mechanical stimuli but with a different responsiveness to thermal stimuli. **Type I** fibres present a high heat threshold (~53 ºC) while **type II** fibres respond to lower temperatures (~43 ºC). However, these thresholds can be reduced by the setting of tissue injury (a process

known as sensitisation) or if the heat stimulus is maintained (Basbaum *et al.* 2009). Sensitivity to cold has also been reported (Simone and Kajander 1997;Cain *et al.* 2001).

C-fibres are quite heterogeneous. Most of them are polymodal, responding to mechanical, thermal and chemical stimuli, some are activated only by heat, others only by cold, some by mechanical and heat and others by mechanical and cold (Smith and Lewin 2009). Furthermore, there is a set of C-fibres that are not nociceptors but respond to pleasant touch, and a heat and mechanically insensitive subclass also exists (Loken *et al.* 2009). These latter fibres, also defined as "silent" or "sleeping" nociceptors, are of particular interest for their ability to become sensitive to noxious mechanical stimuli or temperature only in the setting of injury (Schmidt *et al.* 1995).

An ulterior neuroanatomical and molecular characterisation has identified two main populations of C-fibres, the so-called **peptidergic** and the **non-peptidergic**. Peptidergic fibres innervate mainly viscera and muscle, contain the pro-inflammatory neuropeptides substance P (SP) and calcitonin-gene related peptide (CGRP), require nerve growth factor (NGF) for development and express the NGF-specific tyrosine kinase receptor A (TrkA) (Lewin and Mendell 1994;Averill *et al.* 1995). By contrast, non-peptidergic fibres innervate cutaneous targets, shift its dependence from NGF to glial-derived neurotrophic factor (GDNF) during development and express the GDNF-specific c-Ret receptor (Ambalavanar *et al.* 2003;Molliver *et al.* 1997). A large percentage of this second group of fibres also binds the isolectin B4 (IB4) and expresses specific purinergic receptors (P2X3) for adenosine 5'-triphosphate (ATP). Although today CGRP, SP and IB4 are still the most common markers to subclassify nociceptors, multiple investigations have found that this classification is not always clear. For example, it has been demonstrated that CGRP is also expressed in non-nociceptive neurons, and that in rats, differently from mouse, CGRP and SP frequently colocalise in neurons that also bind IB4 (Lawson *et al.* 2002;Price and Flores 2007). Furthermore, these nociceptors classification derive largely from analysis of fibres that innervates skin, while in other tissues they present very different features (Raja *et al.* 1999).

Sensitisation

Nociceptors properties are not fixed but can be critically modified by repeated stimulation or most commonly in response to tissue damage, inflammation or injury of the nervous system (Lewin *et al.* 2004;Woolf and Ma 2007). These processes can sensitise nociceptors by reducing the threshold of activation of transducer receptors, thus increasing the excitability of the peripheral terminal membrane and inducing non-responsive neurons to become responsive (Smith and Lewin 2009). As a result, pain may arise spontaneously, so that normally innocuous stimuli are now perceived as painful (**primary allodynia**) and/or normally noxious stimuli evoke a greater and more prolonged pain (**primary hyperalgesia**). Furthermore, this sensitivity may also spread to the immediately surrounding noninjured area (**secondary allodynia** or **hyperalgesia**). These shifts in pain threshold and responsiveness are

an expression of neural plasticity, usually adaptative, promoting tissue repair and ensuring that contact with the injured tissue is minimised until repair is complete. Occasionally, the response might become maladaptive and contribute to clinical pain states (Woolf 2004). Two main mechanisms of plasticity have been described: **modulation** and **modification**. Modulation is mediated by posttranslational alterations (mainly phosphorylation) in receptors and ion channels or associated proteins through the activation of intracellular signal transduction cascades. Modification is characterised by long-lasting alterations in the expression of receptors and ion channels or in the structure, connectivity and survival of neurons that eventually produce a distortion in the normal response to stimuli (Woolf and Salter 2000). Furthermore, both these phenomenons can be localised to the peripheral terminals, a process known as **peripheral sensitisation**, or they can increase the synaptic transmission in the dorsal horn, by facilitating excitatory responses and depressing inhibition, leading to a state of hyperexcitability in the central nervous system (CNS) that is known as **central sensitisation** (Scholz and Woolf 2002;Lewin *et al.* 2004).

Peripheral sensitisation and neurogenic inflammation

Peripheral sensitisation is commonly produced when peripheral terminals are exposed to products of tissue damage and inflammation. Activated resident immune cells, mainly mast cells and macrophage at the site of injury, proliferate and degranulate, releasing inflammatory mediators which in turn mediate the recruitment of circulating immune cells (neutrophils and T cells) that release their content. Collectively all these released factors, including kinins, cytokines, chemokines, growth factors, serotonin, eicosanoids and related lipids, as well as proteases, ATP and ions such as protons (responsible for the local tissue pH decrease), are referred to as "**inflammatory soup**". In addition, activated nociceptors not only transmit afferent messages to the spinal cord but they also serve an efferent function by releasing a wide range of signalling molecules, mainly neuropeptides and neurotransmitters, from their peripheral terminals. Thus the Ca^{2+}-dependent release of the vasoactive neuropeptides SP and CGRP induces vasodilation and plasma extravasation as well as the further recruitment and activation of many non-neuronal cells, contributing to and amplifying the immune response. The resulting phenomenon is known as "**neurogenic inflammation**" and is characterised by redness and warmth, swelling and hypersensitivity (secondary to alteration in the excitability of nerve fibres) (Richardson and Vasko 2002;Julius and Basbaum 2001).

Inflammatory mediators can activate or sensitise nociceptors terminals through different mechanisms: **a)** by directly interacting with specific surface ion channels (e.g., **protons** are known to activate both Acid-Sensing Ion Channels (ASIC) and Transient Receptor Potential Vanilloid 1 (TRPV1), whereas **serotonin** binding to its ligand-gated ion channel 5-HT3 induces Na^{+} influx and nociceptor excitation); **b)** by stimulating or increasing the release of neurotransmitters and neuropeptides (mainly glutamate, SP and CGRP) and/or **c)** by modifying the function and expression of ion channels through the activation of second-messenger signalling cascades (**Figure 3**) (Woolf 2004;McCleskey and Gold 1999).

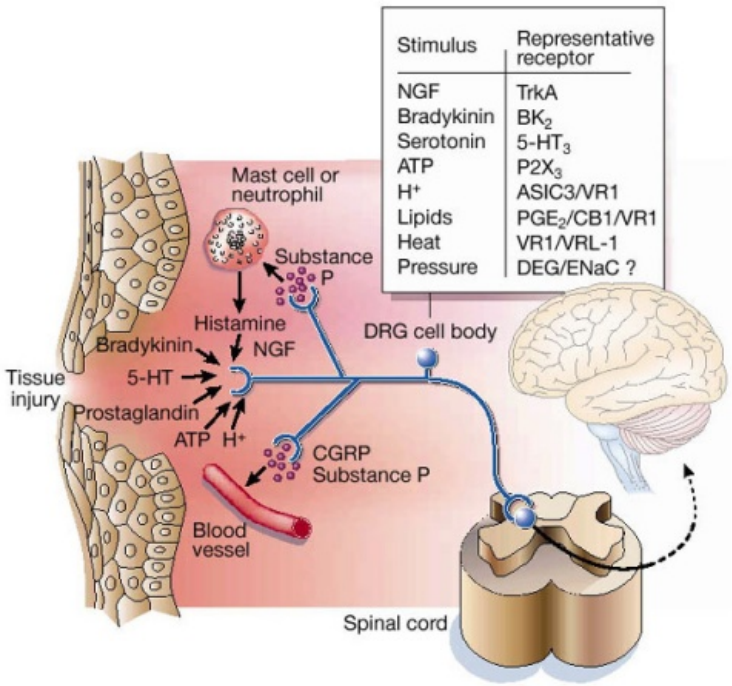

Figure 3 Neurogenic inflammation. Inflammatory mediators released at the site of tissue injury may sensitise or directly excite the terminals of the nociceptors by interacting with cell-surface receptors expressed by these neurons (Julius and Basbaum 2001).

Prostanoids are the best known lipid mediators that contribute to inflammatory pain. Among them, prostaglandin E2 (PGE2) and prostacyclin (PGI2) have the greatest impact on processing pain signals by binding different G-protein-coupled receptors (GPCR) and eventually activating specific intracellular kinases. Namely, interaction with a stimulatory G protein (**Gs**) activates **adenyl cyclase** (AC) thus increasing the levels of cyclic adenosine monophosphate (cAMP) and activating cAMP-dependent protein kinase A (PKA). The binding to other receptors subtypes (**Gq**) activates **phospholipase C** (PLC) which in turn hydrolyses phosphatidylinositol 4,5-bisphosphate (PIP2) in the plasma membrane and generates two second messengers, inositol 1,4,5-triphosphate (IP3) and 1,2-diacylglycerol (DAG): the first stimulates the release of Ca^{2+} from intracellular stores whereas the second directly activates protein kinase C (PKC). An alternative cAMP-to-PKC pathway mediated by Epac (exchange protein directly activated by cAMP) has also been described in IB4-positive neurons (Hucho *et al.* 2005). PKA and PKC kinases are able to phosphorylate serine and threonine amino acids of many ion channels and receptors (mainly Transient Receptor Potential (TRP) and voltage-gated sodium channels such as $Na_v1.8$) or associated regulatory proteins, a post-translational change that can drastically alter their activity (Cesare and McNaughton 1997;Gold *et al.* 1998;Huang *et al.* 2006).

The neurotrophic factor **NGF** has also been described as upregulated in both the inflamed peripheral tissue and upon nerve injury and to play a role in nociceptors sensitisation (Woolf *et al.* 1994). Essentially two mechanisms have been associate to NGF sensitisation: **a)** the binding to the high affinity TrkA receptor and the low affinity p75 receptor thus activating the mitogen-activated protein kinase (MAPK), the phosphatidylinositol 3-kinase (PI3K) and the

PLC downstream pathways; and **b)** the retrograde transport of NGF to the nucleus of nociceptors where it increases the synthesis of several neuropeptides such as SP and CGRP as well as of many receptors and ion channels (Chao 2003).

Bradykinin (BK), one of the most potent of these mediators, is a peptide produced by the cleavage of kininogens at sites of injury or of inflammation and whose effects are mediated by specific GPCRs, B1 and B2. Whereas B2 receptors are constitutively expressed by various neuronal and non-neuronal cell types, B1 receptors are typically inducible, present only at a low level under resting conditions, but largely upregulated upon tissue trauma, inflammation, or nerve injury. Thus, B1 receptors are considered to play a major role in chronic inflammatory pain. Both B1 and B2 receptors act mainly by stimulating PLA2 and PLC via G proteins, thus inducing the subsequent release of PGE2 and the translocation to the membrane of the ε isoform of PKC (Vellani *et al.* 2004). Apart from sensitising nociceptors, BK is also able to directly activate them by PLC- and Ca^{2+}-dependent inhibition of M-type K^{+} channels and by simultaneous opening of Ca^{2+}-activated Cl^{-} channels (CaCC) (Liu *et al.* 2010).

ATP is also known to excite nociceptors, activating ligand-gated cation channels P2X thus leading to a Ca^{2+} influx, and sensitise them by activation of G-coupled receptor P2Y, most likely the P2Y2 receptor subtype, leading to activation of PLC pathway, as well as to augment the release of neuropeptides produced by other stimuli (von, I and Wetter 2000;Bouvier *et al.* 1991;Huang *et al.* 2003).

Central sensitisation

Similar to the mechanisms found in peripheral nociceptor sensitisation, alterations in the excitability of central neurons may lead to the hyperresponsive conditions typical of postoperative pain, migraine, fibromyalgia or neuropathic pain. In these conditions central sensitisation is characterised by two phases: **a)** one immediate and acute, due to the release of neurotransmitters (glutamate) and neuropeptides (SP, CGRP) from the central terminals of nociceptors with the subsequent activation of intracellular signalling pathways and kinases, and **b)** a second slower but longer phase sustained by transcriptional changes and increased levels of protein production (Ji *et al.* 2003).

One key receptor involved in this process is the glutamate-activated N-methyl-D-aspartate (NMDA) that is usually blocked by Mg^{2+}. Once postsynaptic α-amino-3-hydroxyl-5-methyl-4-isoxazole propionic acid (AMPA) and kainate receptors are activated by glutamate released from the central terminals of nociceptors, fast and slow excitatory postsynaptic currents (EPSC) are generated. Their temporal summation results in a cumulative depolarisation that leads to removal of the Mg^{2+} blockade of NMDA receptors, allowing their activation by glutamate and the influx of Ca^{2+}, with the concurrent activation of downstream signalling pathways that contribute to increase the excitability of these neurons, an effect known as *windup* (Latremoliere and Woolf 2009).

Additional mechanisms have been described, such as a central reorganisation of low-threshold Aβ fibres, which sprout into the zone normally occupied by nociceptor terminals, or

phenotypic switches of these fibres that begin to express molecules like SP and CGRP (Neumann *et al.* 1996;Woolf *et al.* 1992).

Also a loss of GABAergic and a reduction in glycinergic inhibitory currents (disinhibition) have been observed, the former probably due to apoptosis of inhibitory interneurons resulting from NMDAR-induced excitotoxicity, the latter in part induced by PGE2 stimulation of the cAMP-PKA pathway and resultant phosphorylation of GlyRα3 glycine receptor subunits (Harvey *et al.* 2004;Scholz *et al.* 2005).

In addition, glial cells, namely microglia and astrocytes, also contribute to the central sensitisation, mainly by responding to and releasing numerous chemokynes and cytokines or specific signals (such as ATP or bone-derived neurotrophic factor, BDNF) (**Figure 4**) (Basbaum *et al.* 2009).

The global result is an increase in excitability with neurons that can be activated by subthreshold inputs (**allodynia**) or noxious stimuli that produce an amplified response (**hyperalgesia**), and innocuous stimuli from noninjured surrounding areas that elicit pain (**secondary hyperalgesia**) (Woolf 2004;Woolf and Salter 2000;Mannion and Woolf 2000).

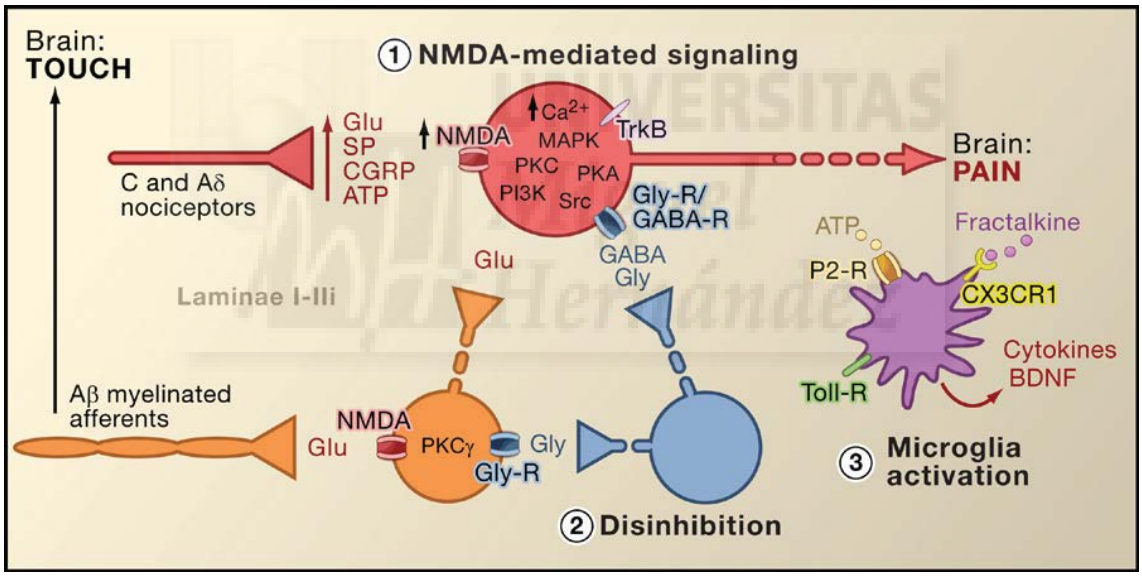

Figure 4 Central sensitisation mechanisms. 1) Activation of normally silent postsynaptic NMDA glutamate receptors by neurotransmitters released from activated C and Aδ nociceptors. **2)** Loss of interneurons inhibition and engagement of myelinated Aβ primary afferents in the pain transmission circuitry. **3)** Microglial activation resulting in the release of a host of cytokines and other factors that contribute to central sensitisation (Basbaum *et al.* 2009).

Transient Receptor Potential channels

The TRP superfamily

Most of the efforts made in the last years in order to find new pain therapies have been focused on the identification of proteins critically involved in the transduction of noxious stimuli and on the characterisation of their molecular properties and distribution in sensory neurons. Thus, different voltage-activated Na^+, Ca^{2+} and K^+ channels have been largely reported as the main channels responsible for the excitation of sensory neurons. Once activated they generate inward or outward currents which lead to cell depolarisation or hyperpolarisation, thus determining the upstroke of action potentials and the repolarisation phase after-potential. In addition, many others ion channels and metabotropic receptors have been identified, such as the previously mentioned glutamate receptors (ionotropic and metabotropic mGluRs), the purinergic receptors P2Y and P2X, ASIC channels, opioid and cannabinoid receptors, serotonin receptors and several TRP channels (Gold and Gebhart 2010).

Specifically, TRPs are a superfamily of cation channels that play a wide range of physiological functions with a huge variety of ion selectivities, modes of activation and regulation types. TRPs were first discovered in the 1960s, with a *Drosophila* mutant that displayed a transient response to continuous light instead of the sustained current observed in the photoreceptors of the wild-type flies (Cosens and Manning 1969). The defective gene, termed *trp* for transient receptor potential, was later cloned, and shown to encode a light-activated Ca^{2+} channel (Montell and Rubin 1989).

Although the crystal structure of TRPs channels has not still been solved, and the only structural data currently available comes from *in silico*, structure-function relationship and some recent cryo-electron microscopy studies (cryo-EM), they resemble voltage-gated channels with respect to their overall transmembrane topology (Yu and Catterall 2004). Thus, TRPs presumably form homo- or heterotetramers, with each subunit containing six transmembrane spanning segments (TM1-TM6), a pore-forming loop between TM5 and TM6, and intracellularly located N- and C-termini. Furthermore, many TRP channels are voltage-sensitive, albeit weakly, and the voltage sensor seems to involve the TM4 transmembrane helix similarly to voltage-gated channels, although the arginine residues sequence necessary for voltage-dependent gating is replaced by non-charged amino acids (Montell 2005;Brauchi *et al.* 2006).

To date 28 mammalian TRP channels have been identified that, according to their sequence homology, have been broadly divided into two groups and further classified into six subfamilies. Group 1 comprises subfamilies TRPC, TRPV, TRPM and TRPA. With the exception of TRPM channels, all of them contain multiple N-terminal ankyrin repeats, which are thought to interact with the cytoskeleton and other cytosolic proteins (Mosavi *et al.* 2004). There is also a TRPN subfamily included in group 1 but that has not been identified in mammals, and

a TRPY subfamily in yeast. Group 2 includes subfamilies TRPP and TRPML, which contain a large extracellular loop separating the first two transmembrane domains (Ramsey *et al.* 2006;Venkatachalam and Montell 2007). Many TRP channels also contain a homologous block of ≈25 residues (the "**TRP domain**"), located in the proximal C-terminal domain, following the sixth transmembrane segment, that is loosely conserved. This motif encompasses a highly conserved 6-amino acids sequence termed **TRP box** which function is not completely characterised yet but that seems to play an important role in channel assembly and/or function (**Figure 5**) (Garcia-Sanz *et al.* 2004;Rohacs *et al.* 2005).

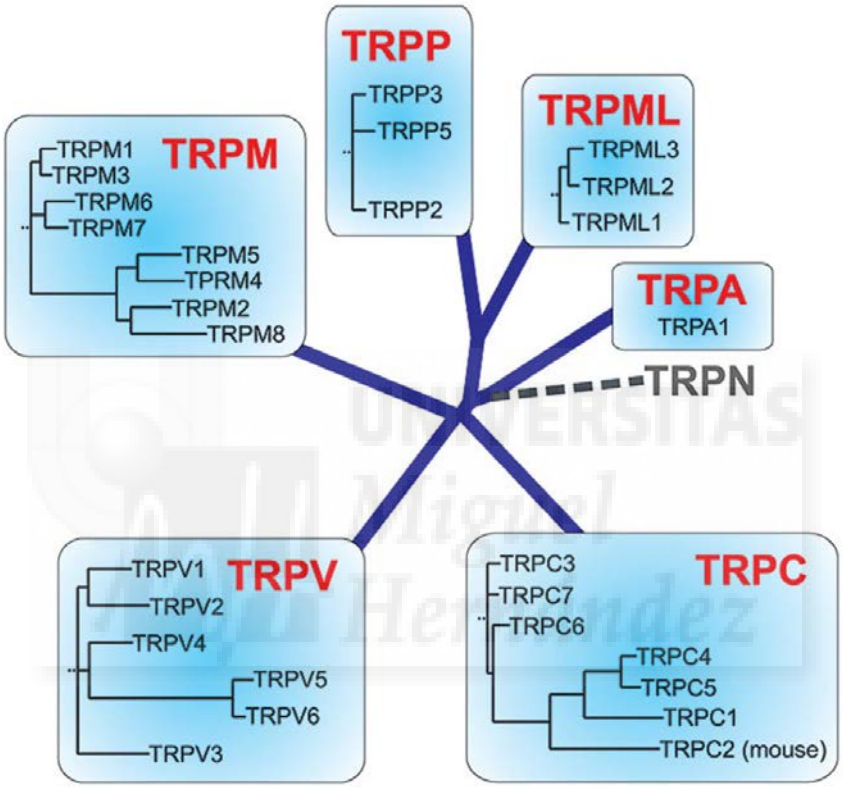

Figure 5 Phylogeny of mammalian TRP-channel superfamily. The multiple-alignment phylogenetic tree illustrates the relationship between the different TRP subfamilies. Phenograms were generated independently for each subfamily. Note that TRPC2 is a pseudogene in primates and that TRPN channels have not been identified in mammals (Voets *et al.* 2005).

ThermoTRPs

Among TRP channels, various members from the TRPV (TRPV1-4), TRPM (TRPM2-5 and TRPM8), TRPA (TRPA1) and TRPC (TRPC5) subfamilies have been shown to be activated by a wide range of temperatures that encompass from noxious heat (>42 ºC) to noxious cold (<15 ºC) as well as innocuous warmth and cold. Consequently they are usually referred to as **thermoTRPs** (**Figure 6**). Which of these channels represent the primary temperature sensors in the somatosensory system is still a matter of controversy (Vriens *et al.* 2014).

Interestingly, some of them are expressed in DRG sensory neurons and/or skin keratinocytes and, in addition to temperature, respond to a wide variety of other chemical and physical stimuli.

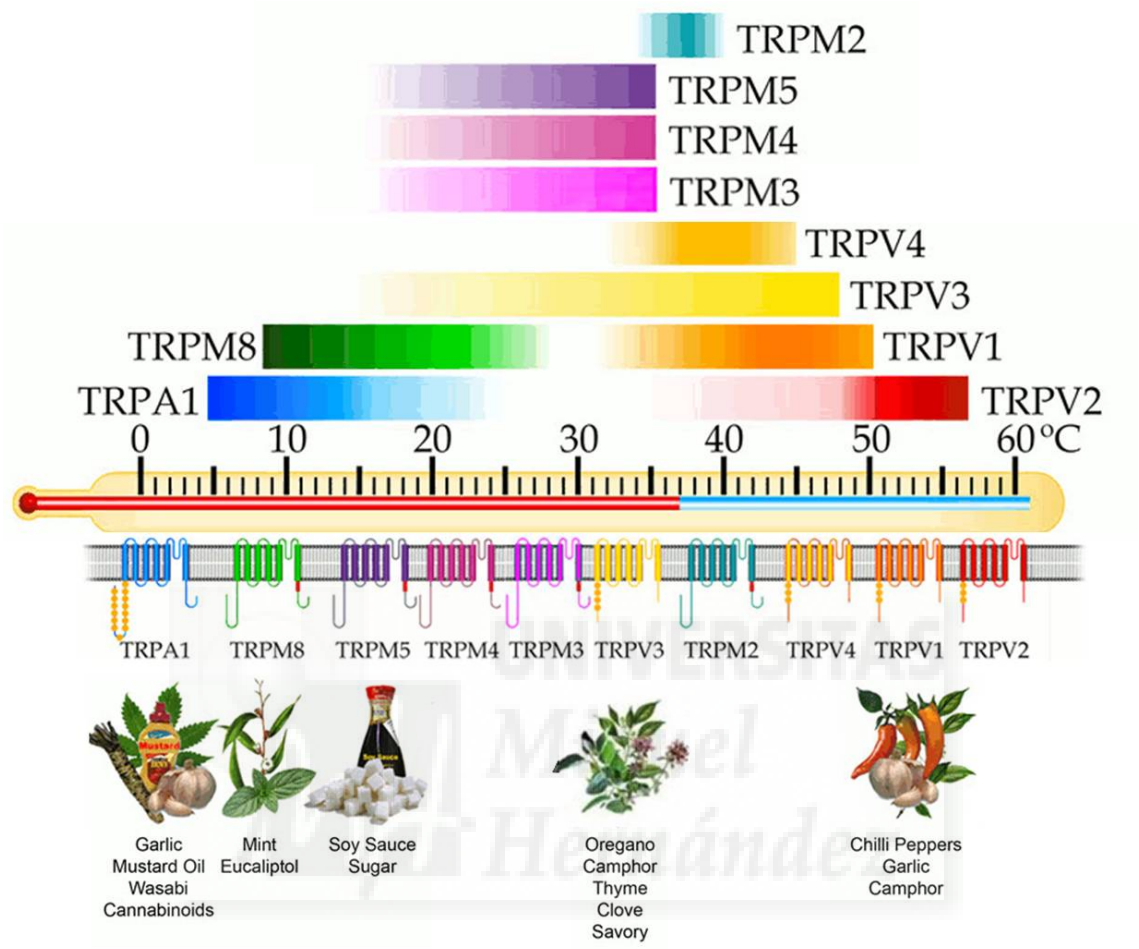

Figure 6 Schematic representation of the thermoTRPs. The figure shows the main thermally-sensitive channels in TRP family and some of the natural compounds by which they are activated (modified by (Latorre *et al.* 2009)).

The TRPM subfamily

The **TRPM** (melastatin) subfamily consists of 8 members divided into three main subgroups, on the basis of sequence similarity: TRPM1/3, TRPM4/5 and TRPM6/7. TRPM2 and TRPM8 are not placed in any particular subset, although they are most related to each other (Fleig and Penner 2004). The designation “melastatin” is based on the name of the founding member, **TRPM1**, which was originally described as a tumor suppression protein as its expression levels were inversely correlated with the metastatic potential of some melanoma cell lines (Duncan *et al.* 1998). TRPM2, TRPM6 and TRPM7 show the unique feature of containing entire functional enzymes in their C-terminal domains, therefore they are referred to as “chanzymes” (reviewed in (Nilius 2007)). Specifically, **TRPM2** is expressed in DRG, activated by warm temperatures (<35 ºC) and contributes to inflammatory and neuropathic pain (Haraguchi *et al.* 2012). Similarly, **TRPM3** is widely expressed in a variety of tissues, including pancreatic

beta cells and small-diameter DRG and TG neurons, and has been involved in insulin release, in renal osmo-homeostasis (maybe due to activation by hypotonicity) and in the development of inflammatory thermal hypersensitivity (Vriens *et al.* 2011). **TRPM4/5**, unusual among TRPs because of their selectivity to monovalent ions, have also been reported to be thermosensitive and to be involved in histamine secretion and taste perception (Guinamard *et al.* 2011). Finally, **TRPM8**, first identified as a marker of prostate cancer, was later described as a sensory channel activated by thermal (cold) stimuli as well as by a variety of natural and synthetic compounds that evoke a sensation of coolness, such as menthol, eucalyptol and icilin (Peier *et al.* 2002). It is the only TRP channel for which there is general agreement about its function in acute thermosensing: three different studies on TRPM8-null mice have demonstrated that these animals exhibit profound deficits detecting innocuous cool temperatures (15-30 ºC), although responses to noxious cold (<15 ºC) are only partially compromised, which suggests the involvement of other receptors in cold sensitivity. Moreover, TRPM8 clearly plays an important role in the enhanced sensitivity that underlies cold allodynia and hyperalgesia produced by nerve injury or inflammation, whereas, paradoxically, is also required for the analgesia provided by cooling and cooling agents (Bautista *et al.* 2007;Colburn *et al.* 2007;Dhaka *et al.* 2007;Proudfoot *et al.* 2006).

The TRPA subfamily

The subfamily **TRPA** (ankyrin) comprises only one mammalian member, **TRPA1**, mainly expressed in TG and DRG neurons, where it detects structurally diverse noxious compounds that elicit pain and neurogenic inflammation, and in hair cells (Nagata *et al.* 2005). Advances in single-particle cryo-EM have recently enabled to determine the structure of the full-length human TRPA1 to near-atomic (~4.0 Å) resolution (Paulsen *et al.* 2015). The N-terminus of TRPA1 contains between 14 and 18 ankyrin repeats that probably are important for protein–protein interactions and insertion of the channel into the plasma membrane (Gaudet 2008). This unusually long N-terminal domain may also account for the proposed role of TRPA1 in mechanosensing, potentially by acting as a gating spring capable of transducing mechanical force and facilitating channel opening. As such, the involvement of TRPA1 in noxious mechanotransduction, mostly in the maintenance of mechanical allodynia or hypersensitivity, has been reported in various models of inflammatory and neuropathic pain (da Costa *et al.* 2010;Kerstein *et al.* 2009;Kwan *et al.* 2009).

Despite the tremendous amount of research conducted since it was suggested to respond to noxious cold temperatures, TRPA1 role in cold sensation is still controversial, although it is now clear that it is not required for autonomic thermoregulation to cold in rodents (Caspani and Heppenstall 2009;de *et al.* 2014). Strikingly, it has been recently demonstrated that TRPA1 can contribute to heat nociception, in particular in the establishment of the heat threshold, although the mechanism implicated has not been determined yet (Hoffmann *et al.* 2013).

The TRPV subfamily

The **TRPV** (vanilloid) subfamily contains 6 mammalian members. TRPV1 to 4 are all activated by heat, non-selective for cations and respond to a broad array of endogenous and synthetic ligands.

TRPV1, also known as the capsaicin or vanilloid receptor 1, is the most extensively studied and best understood temperature-sensitive channel. It is activated by noxious thermal stimuli (<43 ºC) and crucial in the establishment of inflammatory thermal hyperalgesia, although mice lacking this receptor exhibit only a reduction but not elimination of acute thermal pain (Caterina *et al.* 1997;Caterina *et al.* 2000;Davis *et al.* 2000).

TRPV2, also expressed in sensory neurons, has been suggested to form heteromultimers with TRPV1, and to be activated by temperatures >52 ºC, thus representing a likely candidate for TRPV1-independent heat sensitivity (Caterina *et al.* 1999). However, there is little overlap between TRPV1- and TRPV2-expressing cells and recent studies have revealed that TRPV2 knockout mice present normal behavioural responses to noxious heat over a broad range of temperatures and mechanical stimuli, both in the basal state and under hyperalgesic conditions (Park *et al.* 2011).

TRPV3 is activated by innocuous warm temperature (30-39 ºC) and coexpress in sensory neurons with TRPV1, thus suggesting that they also can form hetero-oligomers (Smith *et al.* 2002;Xu *et al.* 2002). Moreover, TRPV3 is mainly expressed in keratinocytes where it has been shown to be critical for the heat-stimulated production of ATP, nitric oxide (NO) and PGE2, which can in turn activate or potentiate TRPV1, contributing to pain transduction in inflammatory conditions (Miyamoto *et al.* 2011;Huang *et al.* 2008). A recent study on TRPV1 and TRPV3 double knock-out mice has confirmed the predominant role of TRPV1 in perception of noxious heat temperature sensation and shown that TRPV1 and TRPV3 channels cooperate with each other to sense a well-defined window of acute moderate heat temperature (Marics *et al.* 2014).

TRPV4 is expressed in many cell types, including primary sensory neurons, skin keratinocytes and inner ear cells, and can be activated by moderate temperatures (24-38 ºC) and hypotonic stimuli in both heterologous expression systems and native tissues (Guler *et al.* 2002;Strotmann *et al.* 2000). Accordingly, multiple studies have proposed a role for TRPV4 in skin barrier homeostasis, mechanical hyperalgesia or hypotonicity-induced pain, particularly under inflammatory or nerve-injured conditions (Suzuki *et al.* 2003;Kida *et al.* 2012;Alessandri-Haber *et al.* 2003). Conversely, a more recent work on TRPV3 and TRPV4 knockout mice claimed no role of TRPV4 in mouse thermosensation, both in basal or inflammatory conditions (Huang *et al.* 2011).

TRPV1

Expression

TRPV1 was first identified from a rat DRG cDNA library through an expression cloning strategy using as a ligand the vanilloid compound capsaicin, the pungent component in chili peppers, which was already known to produce a flow of cations through nociceptor membranes (Caterina *et al.* 1997).

In agreement with an essential role in nociception, TRPV1 has been mainly detected in small-to-medium diameter neurons of primary sensory ganglia (both DRG and TG) that are known to give rise to unmyelinated (C-) and thinly myelinated (Aδ-) nociceptive fibres (Price and Flores 2007). In addition to this prominent location in sensory neurons, TRPV1 has also been encountered in many areas of the CNS system, namely in the spinal cord (both presynaptically, on the central branches of DRG ad TG neurons, and postsynaptically in the dorsal horn neurons) and in various brain nuclei known for their role in pain transmission or modulation (Spicarova and Palecek 2008;Mezey *et al.* 2000;Cavanaugh *et al.* 2011).

TRPV1 has also been reported in a multitude of non-neuronal sites, like in the inner ear, namely in the organ of Corti, in human cultured keratinocytes and melanocytes of the epidermis, in the bladder urothelium, in the arteriolar smooth muscle, in mast cells and macrophages, in the gastric epithelium, in the respiratory tract and in the pancreas, although the physiological role of TRPV1 in most of this these locations is still not clear (Bevan *et al.* 2014).

Structure

As previously mentioned the topology of TRPV1 and other TRP channels is homologous to that of voltage-gated ion channels, assembled as homo or heterotetramers around a centrally located aqueous pore, with each subunit containing six transmembrane segments and intracellularly located N- and C-termini.

The 432-amino acids **N-terminus** contains potential protein-protein interacting domains such as a relatively proline-rich region and six ankyrin repeats (ARD) which are essential for channel function and whose structure has been determined with high resolution using X-ray crystallography (Lishko *et al.* 2007). Each of these repeats consists of a pair of antiparallel α-helices followed by a “finger” loop: the concave surface formed by the inner helices and fingers has been demonstrated to be a site of protein-protein interactions in other proteins containing ankyrin repeats (Mosavi *et al.* 2004).

As for TRPC, TRPM, and TRPN channels, the 145-amino acids **C-terminal** of TRPV1 contains the TRP domain, a coiled-coil structure located just downstream of the sixth

transmembrane region that has been widely described as a transduction domain important for channel gating. Specifically, this domain includes a proline-rich region and a 6-mer conserved sequence termed TRP box that has been implicated in the allosteric coupling of stimuli sensing and pore opening (Garcia-Sanz *et al.* 2004;Valente *et al.* 2008;Gregorio-Teruel *et al.* 2014). Conversely, the proposed role for the TRP domain in subunit tetramerisation still remains controversial, as other motifs in the C-terminus have also been identified to promote TRPV1 subunit association (Zhang *et al.* 2011a;Flynn *et al.* 2014). Interestingly, the recent release of a high-resolution cryo-EM structure of an assembled TRPV1 channel has highlighted the interaction of a β sheet from one subunit, composed of both the ARD-TM1 linker and the C-terminus, with the ARD of an adjacent subunit (Liao *et al.* 2013).

Ion permeability

TRPV1 is a non-selective cation channel with moderate selectivity for the physiologically relevant divalent cations and near equal permeability to Na^+, K^+, Cs^+, Li^+ and Rb^+. Importantly, the relative permeability for Ca^{2+} when the channel is activated by capsaicin is much higher than for all other cations (PCa^{2+}/PNa^+ ~ 10 and PMg^{2+}/PNa^+ ~ 5), compared to activation by heat that confers low Ca^{2+} permeability (PCa^{2+}/PNa^+ ~ 3-4) (Caterina *et al.* 1997;Tominaga *et al.* 1998). TRPV1 is also highly permeable to protons, thus contributing to the intracellular acidification observed upon its activation, and to large polyvalent cations, maybe in association with a phenomenon called pore dilation, characterised by an increased channel selectivity for large cations upon agonist stimulation (Hellwig *et al.* 2004;Ahern *et al.* 2006;Chung *et al.* 2008;Bautista and Julius 2008). In this context, several amino acids in the pore-forming loop between the fifth and sixth transmembrane segments seem to be involved in cation selectivity and an N-glycosylation site (Asn-604) close to the pore region has been recently implicated in the uptake of large cations (Wirkner *et al.* 2005;Veldhuis *et al.* 2012).

Activation modes

TRPV1 is a polymodal channel that functions as a molecular integrator for a broad range of both physical and chemical stimuli, including noxious heat, exogenous and endogenous vanilloids, lipids, extracellular cations, changes in pH (both acidosis and alkalosis) and voltage (Tominaga *et al.* 1998;Caterina *et al.* 1997;Dhaka *et al.* 2009;Voets *et al.* 2004;Ahern *et al.* 2005). Furthermore, TRPV1 can also be activated by ethanol and venoms from jellyfish and spiders (**Figure 7**) (reviewed in (Brederson *et al.* 2013)).

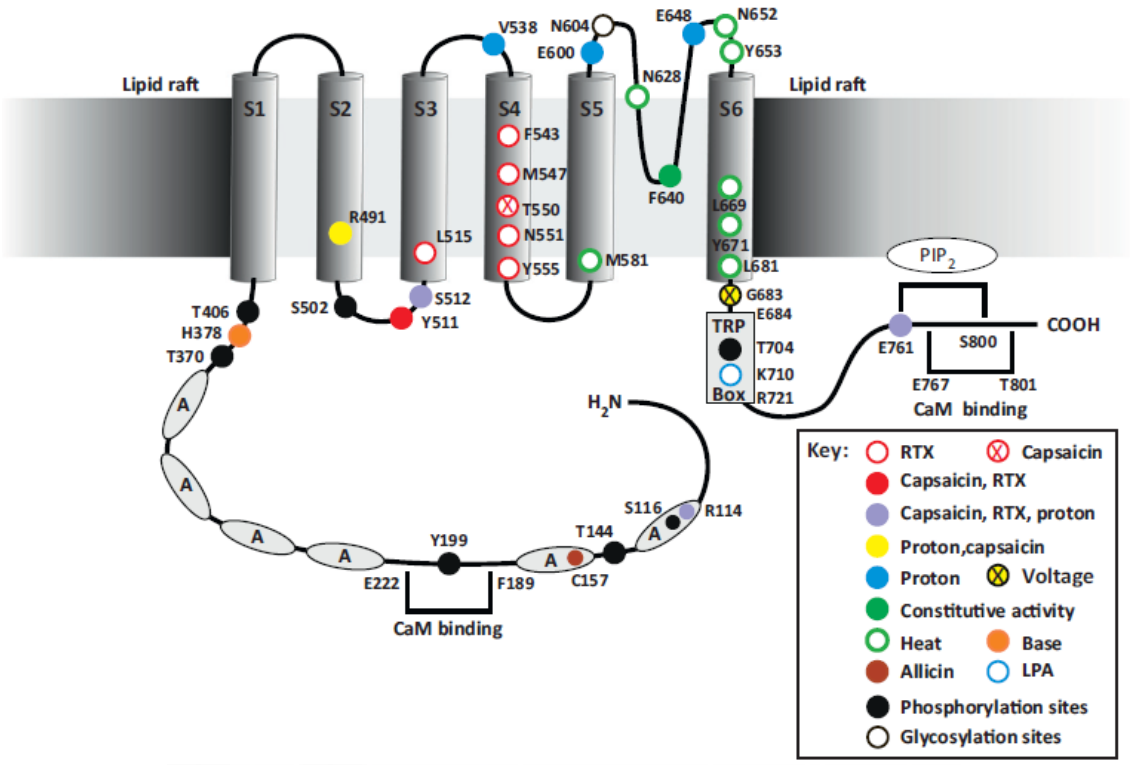

Figure 7 TRPV1 channel topology. The figure shows the key residues for channel gating by different stimuli as well as phosphorylation or glycosylation sites crucial for channel function modulation (Szolcsanyi and Sandor 2012).

Heat

TRPV1 is a noxious heat-activated channel with a thermal activation threshold of ~43 ºC and a $\mathbf{Q_{10}}$ value (defined as the relative change in current amplitude upon a 10 ºC temperature increase) of about 25, much higher than that obtained for the majority of ion channels whose Q_{10} values are typically ~2–3 (Caterina *et al.* 1997;Liu *et al.* 2003).

Despite significant efforts, the temperature-sensitive gating of thermoTRPs, including TRPV1, is still far from being fully understood and widely diverging global views have been developed. According to the hypothesis by Voets *et al.*, the channel gating, intended as a shift in the equilibrium between the open and the closed state(s) of the channel, or the active and inactive conformation of the thermosensor module, is highly temperature sensitive, and allosterically linked to chemical and voltage activation. Thus, in the particular case of a heat-activated channel like TRPV1, heating would cause a decrease in the activation energy and consequently a shift of equilibrium toward the open state of the channel (or active conformation of the thermosensor module) (Voets *et al.* 2004).

Alternatively, the existence of specific and restricted channel domains which can act as “thermosensor” modules allosterically coupled to the channel gate have been suggested. Random and directed mutagenesis studies have rendered conflicting data implicating the N- and C-termini domains and the outer pore region (reviewed in (Vriens *et al.* 2014).

Importantly, products of tissue damage and inflammation can dramatically decrease the receptor temperature threshold (either by acting allosterically or modifying the receptor

phosphorylation state) thus enabling normal body temperature to open the channel and producing a state of pain hypersensitivity and thermal hyperalgesia of which TRPV1 is thought to be a major transducer (Davis *et al.* 2000;Caterina *et al.* 2000;Basbaum *et al.* 2009).

Vanilloids

TRPV1 is the only TRP member activated by vanilloids (from what has derived its name) such as **capsaicin**, the pungent ingredient of hot chili peppers, and the ultra-potent analogue **resiniferatoxin** (RTX), a phorbol ester produced by the cactus-like plant *Euphorbia resinifera* (Caterina *et al.* 1997;Szallasi and Blumberg 1990). In addition, TRPV1 can gate in the presence of a variety of pungent plant products including piperine (the pungent ingredient in black pepper), gingerol and zingerone (from ginger), camphor and eugenol (a powerful essential oil found in cloves) (reviewed in (Brederson *et al.* 2013)).

Capsaicin and related compounds are highly lipophilic and share a vanillyl moiety in the chemical structure that seems essential for the TRPV1 activation and that has been found also in several endogenous fatty acid derivatives that act as TRPV1 agonists (so-called endovanilloids). These include anandamide (also an agonist of cannabinoid receptors), N-arachidonoyldopamine (NADA) and a number of lypoxigenase products (reviewed in (Brederson *et al.* 2013)). Studies using membrane-permeable and impermeable analogues of capsaicin, capsaicin-insensitive animal models and the competitive antagonist **capsazepine** demonstrated that these compounds bind to a putative intracellular vanilloid pocket through residues located in the cytoplasmic loop between the second and third transmembrane domains and in the forth one (Jordt and Julius 2002;Gavva *et al.* 2004). Other residues in both the N- and C-terminal domains play also a key role in ligand binding (Jung *et al.* 2002). Recent cryo-EM studies identified distinct but overlapping binding sites for capsaicin and RTX and suggested that the TM4–5 linker and the sixth transmembrane domain may also participate in the vanilloid binding mechanism (Cao *et al.* 2013).

Protons

Local tissue acidosis is a hallmark of injury and inflammation, and extracellular protons constitute a prominent component of inflammatory soup. Protons have a dual effect on the TRPV1 channel: at low concentrations (pH≤6) seem to act as partial agonists and directly gate the channel, while higher but still acidic extracellular pH values (6-7) potentiate capsaicin-, voltage- and temperature-evoked gating without directly opening the ion conduction pathway (Tominaga *et al.* 1998;Jordt *et al.* 2000). Although different residues have been correlated in the pH downstream activation pathway, two specific extracellular glutamate residues seem to be involved in pH sensitivity. The first, Glu-648, located at the loop between TM5 and the TM6, is crucial for direct activation of the channel by strong pH. The second, Glu-600, at the end of TM5, is responsible for the potentiating effect of protons at milder acidic conditions (Jordt *et al.* 2000). Interestingly, a recent study has demonstrated that protons activate and potentiate

TRPV1 by shifting the voltage dependence of the activation curves towards more physiological membrane potentials (Aneiros *et al.* 2011).

Voltage

Like most TRP channels, TRPV1 shows weak voltage sensitivity: i.e., without additional stimulation, channel opening requires strong positive potentials that are never physiologically experienced. Nevertheless, rises in temperature or addition of an agonist produce a shift in voltage-dependent activation to more negative potentials (Voets *et al.* 2004;Matta and Ahern 2007). The structural basis for voltage sensing is not fully understood yet. A recent study has identified several basic and acid residues in TM4 and the TM4-5 linker whose substitution altered the voltage gating, although also significant effects on the capsaicin and temperature sensitivities were observed (Boukalova *et al.* 2010).

Regulation

TRPV1 is not only a key integrator of a wide range of noxious stimuli but also the endpoint target of diverse intracellular signalling cascades implicated in the response to algogenic agents, inflammatory mediators and injury. All these pathways can act in concert at several levels, increasing protein biosynthesis and trafficking, inducing post-translational modifications and promoting the association with regulatory proteins and second messengers, leading to important changes in receptor expression and activity. TRPV1 activity is ultimately responsible for the consequent changes in nociceptor excitability and the related chronic effects of injury and inflammation.

Post-translational modifications

Phosphorylation

A wide variety of pro/inflammatory mediators and growth factors, released/recruited at the site of tissue injury and inflammation (such as cytokines and chemokines, ATP, bradykinin, PGE2 and NGF) activate, through their specific receptors, intracellular signalling pathways that involve different **protein kinases**, namely PKA, PKC, Ca^{2+}/Calmodulin-dependent protein kinase II (CaMKII), MAPK, PI3K, Src kinase and cyclin-dependent kinase 5 (Cdk5), and **phospatases**, like calcineurin. TRPV1 is a direct substrate of these enzymes that, through phosphorylation, dephosphorylation or re-phosphorylation of specific serine, threonine or tyrosine residues, account primarily for sensitisation, desensitisation, and re-sensitisation of the receptor (Planells-Cases *et al.* 2005;Bhave and Gereau 2004).

Accordingly, as illustrated in **Figure 7**, a number of potential phosphorylation sites have been identified in the primary sequence of TRPV1: residues Ser-116, Thr-144 and Thr-370 in the N-terminal region seem specific for PKA, while Ser-800 in the C-terminal tail is a substrate for PKC-mediated phosphorylation. Thr-704 also in the C-terminal is a substrate for both PKC

and CAMKII and Ser-502 in the intracellular loop between transmembrane domains 2 and 3 is a nonselective site for the three kinases (Numazaki *et al.* 2002;Bhave *et al.* 2002;Jung *et al.* 2004;Mohapatra and Nau 2003;Rosenbaum *et al.* 2004).

PKA- or PKC-mediated phosphorylation, for example induced by prostaglandins and BK, notably potentiates TRPV1 responses to chemical and thermal stimuli, mainly by increasing the probability of channel opening at normal membrane potentials or in response to other stimuli, whereas phosphorylation by CaMKII appears to be a prerequisite for capsaicin binding and subsequent channel activation (Bhave *et al.* 2002;Bhave *et al.* 2003;Jung *et al.* 2004). In addition, the basal activity of Cdk5, a neuron-specific, proline-directed serine/threonine kinase, which directly phosphorylates TRPV1 at Thr-407, has also been found as crucial for heat- and capsaicin-induced activation of the receptor (Pareek *et al.* 2007;Xing *et al.* 2012).

Apart from being implicated in the sensitisation of nociceptors, a role in desensitisation has also been described for these kinases. TRPV1 exhibits two types of fast desensitisation, both strongly Ca^{2+}-dependent: **acute desensitisation**, defined as a decrease of channel activity due to a continuous stimulation, and **tachyphylaxis**, which is a reduction in the response to repeated stimulus applications (Koplas *et al.* 1997). Fast desensitisation (lasting for minutes or hours) should be distinguished from the long-lasting refractory state (weeks or months) produced by prolonged agonist exposure that leads to the **defunctionalisation** of the whole nociceptive fibres (Liu *et al.* 1996). The exact mechanism responsible for desensitisation is still elusive but the general accepted hypothesis considers that at resting state some receptor residues are phosphorylated (Bhave *et al.* 2002;Mandadi *et al.* 2006). Upon activation, Ca^{2+} permeating into the cell activates the Ca^{2+}/Calmodulin dependent Ser/Thr phosphatase 2B (PP2B or calcineurin), which dephosphorylates the channel leading to its desensitisation (Docherty *et al.* 1996). Additional mechanisms have been involved in desensitisation, like interaction with calmodulin (CaM) and depletion of PIP2 from the membrane that will be described below (Numazaki *et al.* 2003;Rosenbaum *et al.* 2004;Klein *et al.* 2008).

Glycosylation

In addition to phosphorylation, N-glycosylation of TRPV1 may regulate its activity. The extracellular Asn-604, immediately adjacent to the pore-forming loop and Glu-600 important for activation by protons, was identified as the only glycosylation site in TRPV1. Notably, this residue is conserved across mammalian species but absent from the capsaicin-insensitive chicken ortholog (Jahnel *et al.* 2001;Jordt and Julius 2002). In a first study, ablation of TRPV1 glycosylation by replacement of Asn-604 with Thr increased sensitivity to capsaicin but reduced the maximal response, the pH dependency of the capsaicin response and the antagonistic effects of capsazepine, suggesting that glycosylation might regulate ligand binding or gating properties of TRPV1 (Wirkner *et al.* 2005). Interestingly, a later study did not report significant differences in the potency or efficacy of the immediate response to capsaicin neither in TRPV1 plasma membrane expression as a result of the absence of glycosylation, which seemed to be

rather required for TRPV1 acute desensitisation and capsaicin-evoked permeation of large ions (Veldhuis *et al.* 2012).

Protein expression and trafficking

Chemical modification and modulation of channel gating properties are not the only mechanisms responsible for TRPV1 potentiation or desensitisation. Under acute inflammation conditions some released mediators, like NGF, Insulin-like growth factor 1 (IGF-1) and ATP also increase TRPV1 expression in the plasma membrane (**Figure 8**). This increment has been associated with the rapid recruitment of a vesicular population of TRPV1 channels to the plasma membrane mediated by a soluble N-ethylmaleimide-sensitive factor attachment protein receptor (SNARE)-dependent, PKC- and Ca^{2+}-mediated exocytosis. A PI3K pathway has been involved in this process although the mechanism implicated is still debated. One proposal is that PI3K is able to activate Src kinase which in turn phosphorylates TRPV1 on Tyr-200 in the N-terminus, although it is unknown how this modification can induce its trafficking to the membrane (Zhang *et al.* 2005). Alternatively, a physical coupling of PI3K and TRPV1 in a signal transduction complex has been proposed to facilitate receptor trafficking to the plasma membrane (Stein *et al.* 2006). PKA also has been shown to increase the translocation of the receptor to the plasma membrane through the rapid insertion of functional multimers formed from an intracellular reservoir of inactive TRPV1 monomers (Vetter *et al.* 2008).

On the other side, the mechanism responsible for the increase in TRPV1 plasma membrane expression under chronic inflammation remains controversial although both transcription- and translation-dependent pathways have been described (Ji *et al.* 2002;Xue *et al.* 2007). Inflammation also induces activation of Cdk5, a kinase involved in vesicle transport from Golgi to neurite, which in turn increases the anterograde transport of TRPV1 to the periphery via kinesin motor proteins, thereby contributing to the development and possibly maintenance of heat hyperalgesia (Xing *et al.* 2012).

Regarding receptor retrieval, prolonged capsaicin exposure can induce a long-term receptor down-regulation by promoting receptor endocytosis, through a clathrin- and dynamin-independent mechanism, and lysosomal degradation, thus modulating the expression level of the channels. This process requires Ca^{2+} entry and can be regulated by PKA-phosphorylation of Ser-116 (Sanz-Salvador *et al.* 2012). In addition, the E3-ubiquitin ligase Myc-binding protein-2 (MYCBP2) has been involved in the regulation of activity-induced TRPV1 internalisation. Loss of MYCBP2 causes constitutive p38 MAPK activation and altered expression of several proteins involved in receptor internalisation leading to lack of capsaicin-induced desensitisation (Holland and Scholich 2011).

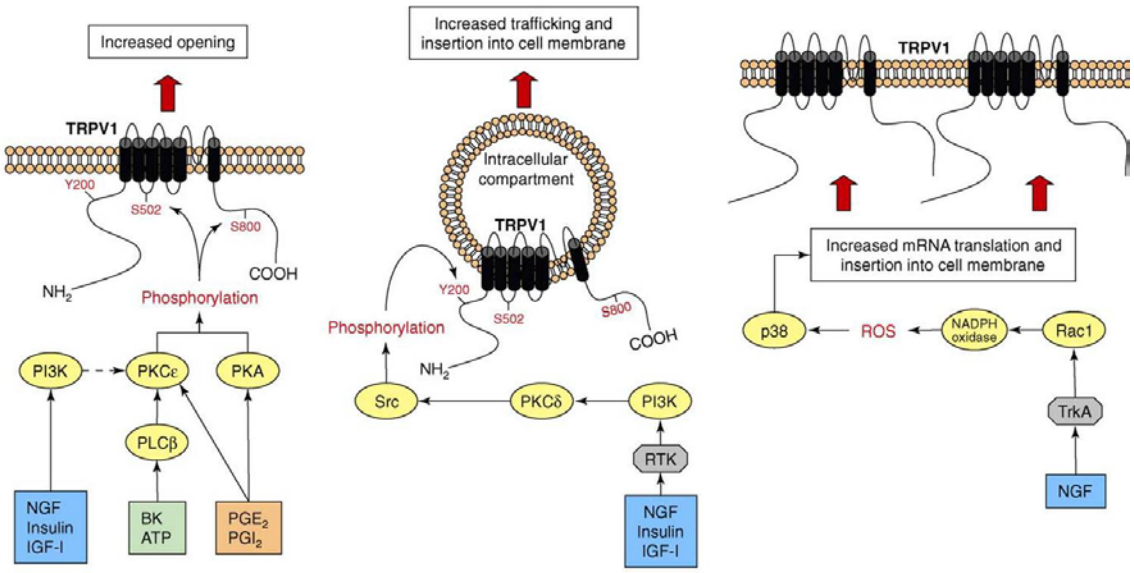

Figure 8 Regulatory mechanisms leading to TRPV1 sensitisation. *Left:* activated PKCε and PKA phosphorylate TRPV1, leading to increased open probability and thereby sensitisation. *Centre*: activated Src phosphorylates TRPV1 located in intracellular vesicles at Tyr-200, inducing exocytosis of the vesicles and insertion of functional TRPV1 into the cell membrane. *Right:* NGF also activates p38 MAPK, resulting in the increased translation of the TRPV1 mRNA and anterograde transport of TRPV1 protein to the periphery (Meents *et al.* 2010).

Modulation by lipids

Phosphoinositides

Regulation of TRPV1 activity by PIP2 is still a matter of controversy. Early whole-cell experiments indicated that PIP2 has inhibitory effects on the channel by directly interacting with positively charged amino acid residues located within the C-terminal cytoplasmic tail and that disruption of this interaction through PLC-mediated PIP2 hydrolysis contributes to channel sensitisation (Chuang *et al.* 2001;Prescott and Julius 2003). Soon, contradictory reports began to emerge. First, it was found that recovery from desensitisation requires re-synthesis of PIP2 by phosphatidylinositol 4-kinase (PI4K) and high concentrations of ATP and that the PIP2-binding region on the distal C-terminus of TRPV1 previously identified is not important for functional recovery of the channel (Liu *et al.* 2005). Moreover, it was shown that depletion of endogenous PIP2 from excised membrane patches using polylysine inhibits the capsaicin-activated currents while heterologous addition of PIP2 enhances TRPV1-mediated current (Stein *et al.* 2006;Brauchi *et al.* 2007;Lishko *et al.* 2007). Other studies support a dual role for PIP2 as a complex regulatory factor that exerts negative or positive effects on TRPV1 activity, depending on stimulus intensity (Klein *et al.* 2008;Lukacs *et al.* 2007;Ufret-Vincenty *et al.* 2011).

Cholesterol

Cholesterol is a major component of plasma membranes and modifies the function of many classes of ion channels (Levitan *et al.* 2010). Indeed, a variety of ion channels associate with cholesterol-rich membrane domains, typically called membrane or "**lipid rafts**", which are

involved in protein trafficking, regulation of cytoskeleton and formation of signalling complexes (Alonso and Millan 2001). Within lipid rafts, channels may be regulated either by direct binding of cholesterol, by an increase in membrane stiffness, or by the interactions with multiple signalling molecules segregated within the same domains.

With regard to TRPV1, although no dramatic effect on the channel response to temperature was initially found, the removal of cholesterol from the plasma membrane of both DRG/TG neurons and TRPV1-expressing HEK293 cells was later demonstrated to provoke a significant reduction in TRPV1-mediated responses to capsaicin and acidic stimuli, by a mechanism involving a decrease in TRPV1 protein levels at the cell surface (Liu *et al.* 2003;Liu *et al.* 2006;Szoke *et al.* 2010).

A more recent work performed in excised membrane patches from TRPV1-transfected HEK293 seems to confirm that modifications in cell trafficking, rather than changes in the activity of the channel in the membrane, may account for the current reduction produced by cholesterol depletion. In contrast, cholesterol enrichment significantly reduces capsaicin and temperature-induced currents, probably through a direct interaction with specific sites along the TM5 helix of the channel (described as a cholesterol recognition amino acid consensus motif) that could cause a conformational change in TRPV1 that stabilises the closed state(s) of the channel (Picazo-Juarez *et al.* 2011).

Modulation of TRPV1 by signalling complexes

Like many other ion channels, it is currently accepted that TRPV1 does not exist as an isolated protein in the membrane but rather organised in a multimeric complex with other proteins that are important in regulating the location and function of the channels (Planells-Cases *et al.* 2011). These macromolecular entities, referred to as "**signalplexes**", are composed of scaffolding, trafficking and signalling proteins, physically assembled through specific protein-protein interactions, which provide temporal and spatial specificity to signal transduction.

The first evidence for the formation of signalplexes emerged from studies of the phototransduction cascade in the *Drosophila* eye. Activation of rhodopsin upon absorption of a photon triggers the subsequent interaction with a Gq heterotrimeric protein. This leads in turn to the activation of PLC which hydrolyses PIP2 into IP3 and DAG thus causing the opening of two classes of light-sensitive channels by a still unknown mechanism: the highly Ca^{2+}-permeable TRP channel and the non-selective TRP-like (TRPL) cation channel. DAG is also responsible for activation of an eye specific PKC (ePKC), essential for response termination and light adaptation (Hardie and Raghu 2001;Katz and Minke 2009).

The several components of this cascade are coordinated into a signalling complex by the scaffolding protein Inactivation No Afterpotential D (INAD). INAD consists primarily of five protein interaction motifs referred to as PDZ domains (which will be described below), being the third one implicated in the interaction with the C-terminus of TRP (Shieh and Zhu 1996;Li and Montell 2000). Importantly, INAD can also self-multimerise via PDZ–PDZ interactions, allowing the assembly of individual complexes into a larger supramolecular network (Xu *et al.* 1998). TRP, PLC and ePKC form the core of this complex and are constitutively bound to INAD which is required for their retention in the microvillar portion of the photoreceptor cell (the rhabdomeres), the specialised subcellular compartment where visual transduction takes place. At least five additional elements, namely the TRPL transduction channel, CaM, rhodopsin, the NINAC protein (a myosin III potentially linking the complex to the cytoskeleton) and the immunophilin FKBP59 are known to be associated with the core complex but appear to bind to INAD transiently (**Figure 9**) (Tsunoda and Zuker 1999;Goel *et al.* 2001). The ability of INAD to retain all these signalling molecules in a highly organised molecular complex has been revealed as essential not only to ensure speed and efficiency of signal transduction but also the rapid regulatory feedbacks necessary for termination of the photoresponse (Adamski *et al.* 1998;Popescu *et al.* 2006).

Similar to TRP and TRPL, TRPV1 interacts with several signalling, trafficking and scaffolding proteins, as detailed below, which play significant roles in the receptor signal transduction and regulation and may represent therapeutic targets for innovative pain intervention strategies.

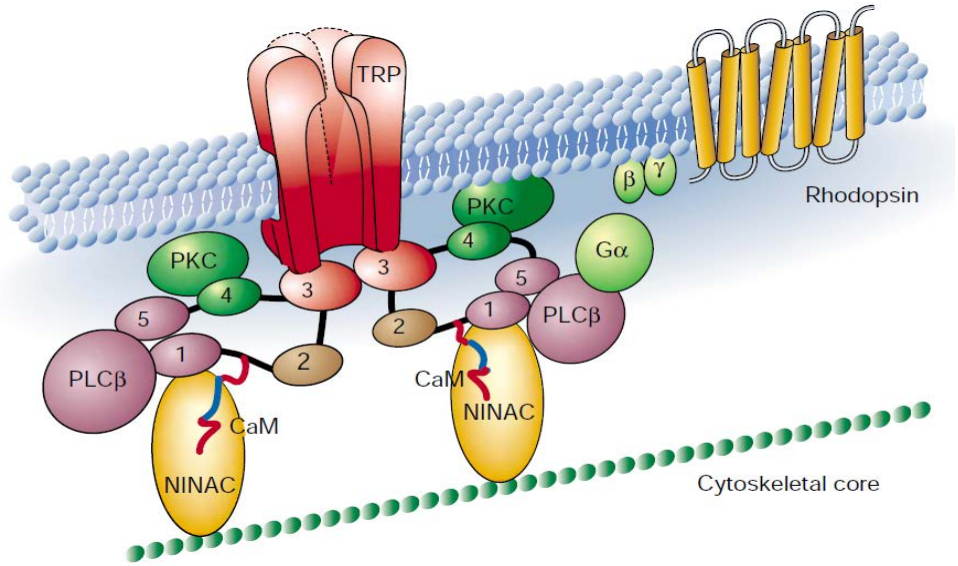

Figure 9 The INAD signalling complex. The model shows how INAD is able to scaffold different proteins through its PDZ domains thus forming a multimolecular complex crucial for visual transduction in *Drosophila* (Hardie and Raghu 2001).

Signalling proteins

As mentioned before, TRPV1 associates with a plethora of intracellular signalling enzymes like PKA, PKC, Src, PI3K, Cdk5 or CaMKII kinases and Calcineurin 2B phosphatase that are able to modulate the receptor function through phosphorylation/dephosphorylation of its cytoplasmic domains.

Physical and functional interactions with other member of the TRPV subfamily, such as TRPV2, TRPV3 and TRPV4, have also been identified, which suggest that native cells may form heteromeric channels with novel biophysical and regulatory properties (Cheng *et al.* 2007;Staruschenko *et al.* 2010). The vanilloid receptor can also form functional heteromeric channels with TRPA1, in both heterologous expression systems and sensory neurons, and a membrane adaptor protein primarily expressed in peptidergic DRG neurons (Tmem100) has been identified as a potentiating modulator of this physical association (Fischer *et al.* 2014;Weng *et al.* 2015). Similarly, the functional and physical interaction with anoctamin 1 (ANO1), a Ca^{2+}-activated Cl^- channel also activated by noxious heat over 44 ºC, has been described and proposed as a significant pain-enhancing mechanism (Takayama *et al.* 2015).

TRPV1 can also interact with other receptors and channel families like TrkA and purinergic P2X3 receptors, potassium channels KCNQ2/3, the large-conductance Ca^{2+}- and voltage-activated K^+ channel mSlo1 or the glutamate receptor NMDA (Chuang *et al.* 2001;Stanchev *et al.* 2009;Zhang *et al.* 2011b;Wu *et al.* 2013;Lee *et al.* 2012).

Binding sites for the regulatory molecules ATP, CaM and PIP2 have also been identified in the cytosolic domains of TRPV1. **ATP** has been described as a TRPV1-sensitising molecule which acts both indirectly through binding to metabotropic purinergic receptors and directly by binding to a region located in the 1-3 TRPV1 ankyrin domains (Tominaga *et al.* 2001;Lishko *et*

al. 2007). This ATP binding site partially overlaps with a **CaM**-binding site (Rosenbaum *et al.* 2004;Lishko *et al.* 2007). A second CaM-binding site has been located in the C-terminus of TRPV1. CaM seems to play an important role in desensitisation (Kwon *et al.* 2007;Numazaki *et al.* 2003). Less clear is the role of **PIP2** and contrasting studies have identified different regions within the cytosolic domains of TRPV1 as putative binding sites (Grycova *et al.* 2012). It has also been proposed that the PIP2-binding protein **Pirt** binds to TRPV1, although it is not clear if it is responsible for the actions of PIP2 on the channel (Kim *et al.* 2008;Ufret-Vincenty *et al.* 2011).

Scaffolding proteins

Scaffolding proteins play an important role in coordinating signal transduction cascades by bringing effectors and substrate in close proximity, mediating the trafficking and clustering of receptors and ion channels at defined membrane regions and connecting cytoskeletal structures with membranes.

In this context, A-kinase anchoring proteins (**AKAP**s) are well known for their ability to scaffold PKA, PKC, or calcineurin to a large number of different ion channels, promoting fast and precise phosphorylation. AKAP79/150 (orthologs in human and rodent respectively) was found to bind TRPV1 C-terminal domain and to be essential for PKA- and PKC-dependent sensitisation of TRPV1 (Zhang *et al.* 2008;Jeske *et al.* 2009;Schnizler *et al.* 2008). AKAP has also been proposed as a mediator of indirect PIP2 effects on TRPV1: while in a resting cell it is localised in PIP2-rich areas of the plasma membrane, after PLC activation and subsequent PIP2 degradation, AKAP is released from its plasma membrane anchorage and can associate with TRPV1 thereby modulating its phosphorylation and sensitisation by PKA and PKC (Jeske *et al.* 2011). Although AKAP is not required for the PP2B-mediated dephosphorylation of activated TRPV1 channels, it seems to be somehow involved also in desensitisation. Thus, upon stimulation of TRPV1 and consequent Ca^{2+} influx, CaM association with receptor prevents AKAP complex formation decreasing TRPV1 activity (Chaudhury *et al.* 2011). Additionally, adenylyl cyclase AC5 anchoring to the AKAP–TRPV1 complex facilitates cAMP/PKA-dependent sensitisation of TRPV1 to inflammatory stimuli, whereas interrupting the AKAP–AC association permits channel desensitisation (Efendiev *et al.* 2013).

A second scaffolding protein, **β-arrestin-2**, was recently implicated in the desensitisation of TRPV1 by linking the phosphodiesterase PDE4D5 to the receptor and limiting its phosphorylation status (Por *et al.* 2012). Notably, constitutive casein kinase 2-mediated phosphorylation on β-arrestin-2 limits its interaction with TRPV1 while PKA-mediated phosphorylation on TRPV1 has been shown to increase proteins association (Por *et al.* 2013).

Trafficking proteins

Several proteins have been described to participate in the regulation of TRPV1 trafficking to and from the plasma membrane, thus contributing to nociceptor sensitisation or desensitisation. Besides the aforementioned PI3K, Cdk and Src kinases, the ubiquitin ligase MYCBP2 and a kinesin motor protein, association of TRPV1 with voltage-gated K^+ channel accessory subunit beta 2 (Kvβ2) has also been described to exert a chaperone-like effect resulting in an increased cell surface expression of TRPV1 associated with an enhancement in capsaicin sensitivity (Bavassano *et al.* 2013)..

In this context, a yeast two-hybrid screening (Y2H) of a rat brain cDNA library performed by our group using the N-terminus of TRPV1 as bait, identified additional interacting partners of the receptor. TRPV1 was found to associate with the vesicular proteins **snapin** and **synaptotagmin (Syt) IX**, two components of SNARE-dependent exocytosis (Morenilla-Palao *et al.* 2004). The identification of these interactors allowed to propose the localisation of TRPV1 in a pool of synaptic vesicles near to the membrane surface and demonstrated that PKC activation was able to induce a rapid delivery of functional TRPV1 channels to the plasma membrane from these vesicular reservoir (Morenilla-Palao *et al.* 2004).

Moreover, TRPV1 was found to interact with $GABA_A$ receptor associated protein (**GABARAP**), a small cytosolic protein with an ubiquitin-like C-terminal domain, previously involved in the interaction with other receptors, and a basic N-terminal region implicated in the association with the tubulin cytoskeleton (Wang *et al.* 1999;Lainez *et al.* 2010). We found that GABARAP significantly augments the expression of TRPV1 and its targeting to the plasma membrane, but paradoxically attenuates voltage and capsaicin TRPV1 sensitivity. This apparent contradiction might be attributed to GABARAP-induced TRPV1 clustering which in turn results in a negative regulatory effect on channel gating. Notably, GABARAP also increases the previously described interaction of the C-terminal domain of TRPV1 with tubulin, and it has been recently demonstrated that the microtubule cytoskeleton helps to form the TRPV1 tetramer in the membrane. Therefore, it is possible that tubulin interaction with TRPV1 contributes to modulate TRPV1 function (Goswami *et al.* 2004;Storti *et al.* 2012).

The third putative interacting protein identified by the same Y2H screening was the calmodulin-dependent serine kinase (CASK)-interacting protein **CIP98** or **Whirlin**, which has been the object of this study.

WHIRLIN/CIP98

In 2003 a 98 kDa protein was identified as a novel interacting partner for CASK, a calmodulin-dependent serine kinase member of the membrane-associated guanylate kinase (MAGUK) family proteins, which play critical roles in the regulation of signal transduction by acting as molecular scaffolds for signalling complexes at synapses (Yap *et al.* 2003). This protein, with a wide expression in the CNS, was named CIP98 and localised at synaptic vesicle-like structures in neurons thus suggesting a role in neurotransmission. In the same year, a novel gene was identified and characterised encoding for a cytoskeletal scaffolding protein named Whirlin involved in the elongation of stereocilia in both inner (IHC) and outer (OHC) hair cells. Whirlin is the mouse ortholog of CIP98 (Mburu *et al.* 2003). The encoding gene contains 13 exons and is alternative spliced in multiple long and short C-terminal isoforms (**Figure 10**).

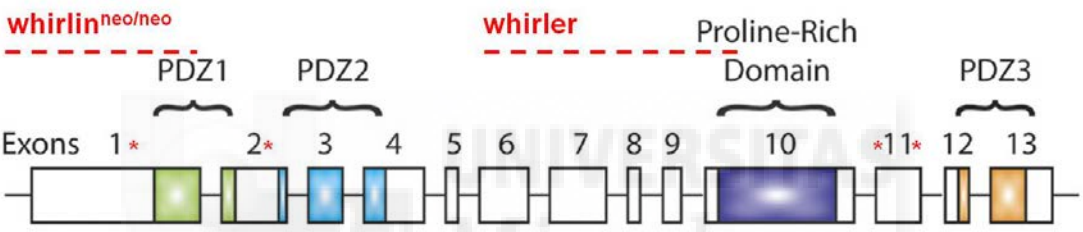

Whirlin Variants	GenBank Accession No.	Exons	Product Size (amino acids)	Calculated Molecular Weight (kDa)
1	82916.1	*1b, 2, 3, 4a, 5, 6b, 7, 9, 10, 11a, 12, 13	907	96.0
2	1008791.1	*1b, 2, 3, 4a, 5, 6b, 7, 8b, 9, 10, 11a, 12, 13	918	98.0
3	1008792.1	*1b, 2, 3, 4b, 5, 6b, 7, 9, 10, 11a, 12, 13	911	97.0
4	1008793.1	*1b, 2, 3, 4a, 5, 6b, 7, 8b, 9, 10, 11b, 12, 13	906	96.5
5	1008794.1	1b, *6b, 7, 8b, 9, 10, 11a, 12, 13	476	50.7
6	1008795.1	1a, *6b, 7, 9, 10, 11a, 12, 13	465	49.3
7	1008796.1	1a, *7, 9, 10, 11a, 12, 13	404	42.2
8	1008797.4	*6a, 7, 9, 10, 11a, 12, 13	550	58.7
9	1008798.1	6a, 7, *8a, 9, 10, 11a, 12, 13	366	38.5
WhirlinN T1	HQ148552	*1b, 2, 3	322	34.3
WhirlinN T2	HQ148553	*1b, 2, 3, 4a, 5, 6b, 7	571	61.6

Figure 10 Whirlin isoforms and mutations. *Upper panel*: Schematic representation of the Whirlin/DFNB31 gene structure: exons and encoded domains are drawn approximately to scale. The red dashed lines indicate the deletion regions of the Whirlin gene in whirlin$^{neo/neo}$ and whirler mice. The red asterisks indicate the mutations of the Whirlin gene in humans. *Lower panel*: list of known Whirlin variants, including GenBank accession numbers, details of included exons, product sizes, and calculated molecular weights. *: exon containing predicted start codon for each variant (modified from (Wright *et al.* 2012)).

The four distinct long isoforms, with an estimated molecular weight of approximately 100 kDa, contain three PDZ domains, two at the N-terminus and one at the C-terminal tail, with a few stretches of consecutive serine/alanine/glycine in the N-terminus and a proline-rich region between the second and the third PDZ. The short C-terminal isoforms, with predicted molecular weights ranging between 38.5 and 58.7 kDa, are the result of variable splicing and multiple start codons in exons 6, 7, and 8 and contain only the third PDZ domain and the proline-rich region. Recently two N-terminal transcripts have been identified, one containing exons 1 through 3 encoding only the PDZ1 domain and part of the PDZ2, and the other containing exons 1 to 7

encoding PDZ1 and PDZ2 domains but truncated before the proline-rich region (Wright *et al.* 2012). Both the PDZ domains and the proline-rich region are modular protein interaction motifs. PDZ1 usually recognise specific internal motifs or short conserved sequences at the C-terminus of target proteins, as detailed below, whereas PDZ2 binds to WW and SH3 domains (Macias *et al.* 2002).

PDZ domains

PDZ domains represent highly versatile interaction modules that act as dynamic regulators of cell signalling rather than simply static docking sites, which explains that PDZ proteins play crucial roles in a plethora of signalling pathways and biological processes, such as the establishment and maintenance of cell polarity, cell migrations and tissue growth (Harris and Lim 2001). These domains consists of 80 to 100 amino acid motifs which derive their name from the three proteins originally recognised to contain these sequences: **P**ostsynaptic density protein 95 (PSD-95), ***D****rosophila* disc large (*dlg*), and the tight-junction protein **Z**O-1 (Cho *et al.* 1992;Woods and Bryant 1993;Kim *et al.* 1995). A canonical PDZ domain contains six β strands forming a partially opened barrel, with each opening side capped by one α-helix and binds to its interaction partners in a sequence-specific fashion: a short stretch of amino acid residues (~5-7) at the C-termini of target proteins recognises a groove between the second β-sheet and the second α-helix containing the highly conserved carboxylate-binding loop **R/K-XXX-G-Φ-G-Φ** motif, where **X** is any amino acid residue and **Φ** is an hydrophobic residue (Morais Cabral *et al.* 1996;Doyle *et al.* 1996). PDZ domains are traditionally classified on the basis of their preferences for residues at 0 and -2 positions in the C-terminus of target proteins: class I PDZ domains recognise the motif **S/T-X-Φ-COOH**; class II PDZ domains recognise the motif **Φ-X-Φ-COOH**; and class III PDZ domains recognise the motif **X-X-COOH**. However, some PDZ domain interactions do not satisfy these restrictive types of recognition and so additional classes and important residues are proposed to exist for ligand specificity of PDZ domains (Songyang *et al.* 1997;Sheng and Sala 2001). For example, the PDZ3 domain of INAD was reported to bind to an internal motif of TRP although a more recent study demonstrated that the INAD interacting domain encompasses the last 14 residues at the carboxyl terminus of TRP (Shieh and Zhu 1996;Li and Montell 2000;Peng *et al.* 2008). In other cases, a stretch of ankyrin repeats can be required for the association or, if the target protein does not contain the carboxyl PDZ-binding motif (PBM) or a PDZ-like domain, unusual interactions via hydrophobic surfaces can rather be established (Feng *et al.* 2002;Maekawa *et al.* 1999).

Apart from interacting with their peptide ligands through these canonical or non-canonical binding modes, PDZ proteins, like CASK or syntenin, can also interact with lipids like PIP2, form homo- or heterodimers through PDZ-PDZ interactions or establish interdomain couplings by which one PDZ domain can function as a chaperone to stabilise the folding of a neighbouring one with its ligand (Zimmermann *et al.* 2002;Zhang *et al.* 2001;Chen *et al.* 2008). Additionally, several regulatory mechanisms like: **a)** phosphorylation of Ser/Thr/Tyr within the

PDZ ligand or on the PDZ domain itself; **b)** intramolecular disulfide bonds formation or **c)** palmitoylation of cysteine residues (the posttranslational attachment of the 16-carbon fatty acid palmitate) can modulate the tethering of PDZ-target complexes to the membrane, their sorting to particular lipid microdomains, such as lipid rafts, and their functional interactions, thus adding further functional diversity (Lee and Zheng 2010;Ivarsson 2012;Topinka and Bredt 1998;Craven *et al.* 1999). Variations in physiological buffer conditions (pH and salt concentration) can also affect the affinity between PDZ domains and their ligands (Gianni *et al.* 2005;Chi *et al.* 2006). In view of these findings it seems plausible that profound alterations previously reported to underlie inflammatory conditions (increased salt concentration and decreased extracellular pH, kinases activation and neuronal excitability enhancement) may strongly and diversely influence the establishment of PDZ-target interactions and their functional consequences.

Whirlin: a dual protein

Whirlin has been found to play an important role in vision and hearing. A spontaneous mutation in mouse was initially described which causes rapid circling locomotor activity, head shaking and deafness. These mice, named whirler, have decreased body weight and increased metabolic rate and adrenocorticosteroid activity compared with normal mice, which may account for the increased excitability and nervousness of whirler mice (Weltman *et al.* 1970). A similar mutation in the human ortholog DFNB31 underlies an autosomal recessive form of hearing loss (Mustapha *et al.* 2002). The mutation in both humans and mice lead to a truncation of the protein close to its C-terminus. Specifically, in mice the deletion encompasses the first methionine of the short C-terminal isoform and amino acids 434-631 of the long isoform, removing a portion of the proline-rich region and the entire PDZ3. In humans, a nonsense mutation in exon 10 results in a similar truncated protein of 777 amino acids lacking the third PDZ domain (Mburu *et al.* 2003). Neither patients with DFNB31 nor whirler mice manifest any retinal deficits. Conversely, mutations in the first and second exons account for both hearing and vision defects, corresponding to USH2D subtype of the **Usher syndrome** (USH), a hereditary rare disease characterised by hearing impairment, vestibular dysfunction and retinal degeneration (Yang *et al.* 2010;Yang *et al.* 2012;Ebermann *et al.* 2007). A transgenic mouse model for USH2D (whirlin$^{neo/neo}$) has been obtained by introducing a partial deletion of exon 1 thus disrupting both the complete long and short N-terminal isoforms of the protein (Yang *et al.* 2010).

Whirlin in the inner ear

The inner ear provides sensory information relating to hearing (from the cochlea) and balance (from the vestibular system). Inside the cochlea a narrow spiral of cells that constitute the sensory epithelium can be found known as the organ of Corti, mainly composed by sensory inner and outer hair cells (IHC and OHC, respectively) and accessory supporting cells. Hair cells

derive their name from the bundle located at their apex, which consists of 20-300 rigid microvilli known as stereocilia, each containing a rigid core of actin filaments closely packed with distinct sets of bundling proteins and myosins, and organised in rows of increasing height held together by extracellular filaments. Deflection toward the tallest stereocilia, caused by sound waves or changes in head position, opens the transducers ion channels and depolarises the hair cells, whereas deflection in the opposite direction closes the channels and hyperpolarise the cells (Forge and Wright 2002). The motor protein myosin XVa interacts with Whirlin and is responsible for its trafficking and localisation at stereocilia apices where it contributes to their elongation (Belyantseva *et al.* 2005;Delprat *et al.* 2005). Whirler mice, as well as a mice strain named shaker 2 (whose mutation disables the motor function of myosin-XVa), display abnormal stereocilia development, with the resulting hearing loss and balance disorders (Probst *et al.* 1998;Holme *et al.* 2002). Whirlin, and mainly the C-terminal isoform, has been found to interact at the stereocilia tips also with p55, a MAGUK protein similar to CASK, and to partially colocalise with the membrane–cytoskeleton linker 4.1R. These two proteins, p55 and 4.1R, are known to form critical complexes for actin cytoskeletal assembly in erythrocytes, and they may play a similar role in hair cells stereocilia by interacting with Whirlin (Mburu *et al.* 2006).

Whirlin in the Usher syndrome

Earliest evidences for Whirlin to be a candidate for USH2 came from different studies that reported its interaction with the transmembrane proteins Usherin (USH2A) and very large G-protein-coupled receptor-1 (VLGR1b, USH2C) at both the synaptic terminals of OHC and the ankle-link, a fine filament present in developing but no mature stereocilia that couples the bases of individual stereocilia to one another. Importantly, these interactions mainly involve the first two PDZ domains of Whirlin (Adato *et al.* 2005;van *et al.* 2006;Yang *et al.* 2010). Notably, myosin XVa, p55 and 4.1R are all present at the tips but not at the ankle-links of the stereocilia, which make them unlikely to be components of the USH2 complex. A complex with Usherin and Vlgr-1 was also identified in photoreceptor cells at both the synaptic terminals and the connecting cilium, which is the connecting link between the outer segment containing the light-sensor and the inner segment containing organelles for protein and lipid synthesis and the synaptic terminus. Here Whirlin may anchor both transmembrane proteins at specific membrane domains and simultaneously interact with the scaffolding protein containing ankyrin repeats and SAM domain (SANS, USH1G), that provides a linkage to the microtubule transport machinery (Maerker *et al.* 2008). Interestingly, Whirlin was found to interact and colocalise in the same regions with the L-type calcium channel subunit Cav1.3 (α_{1D}) thus suggesting a contribution to the organisation of Ca^{2+} channels in the photoreceptor cells, although a later study reported that Cav1.3α_1 and Whirlin were independent for their normal expression (Kersten *et al.* 2010;Zou *et al.* 2012). Furthermore, Whirlin is the nearest homologue of the USH1C protein Harmonin, a scaffolding protein with very similar structure, that has been shown to integrate all USH1 and USH2 proteins networks both in the inner ear and in the retina (Reiners *et al.* 2006;Kremer *et al.* 2006). Harmonin and Whirlin share many interaction partners, although not completely overlap,

thus it is conceivable that both play a similar role as central organisers of the Usher interactome (**Figure 11**).

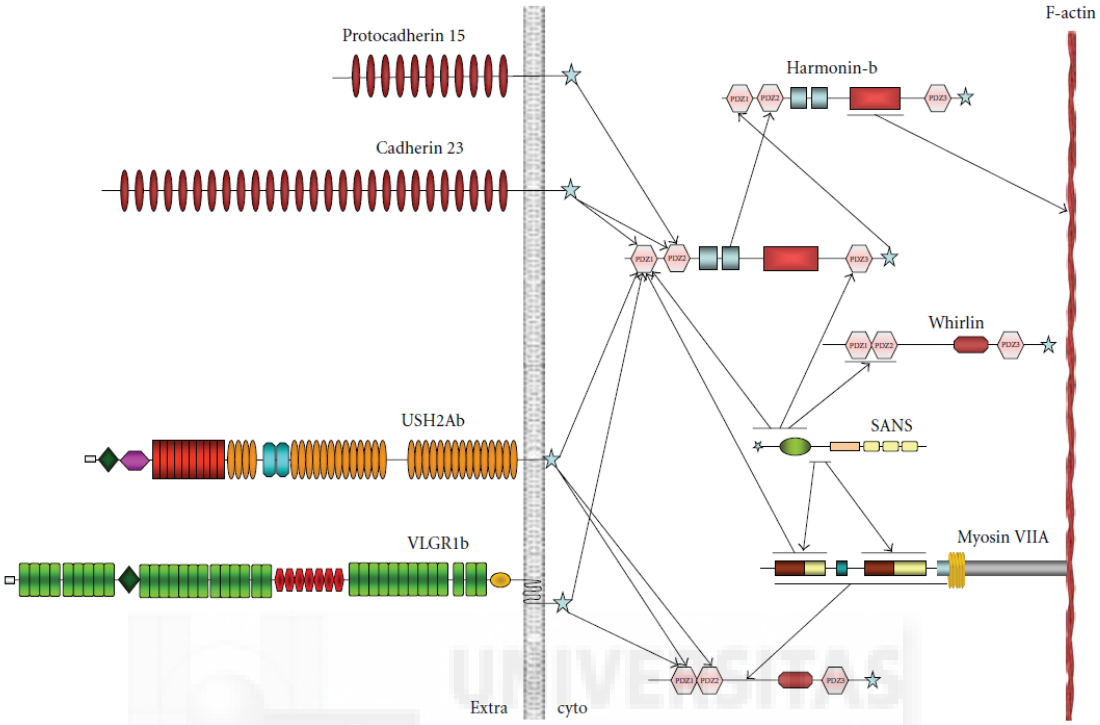

Figure 11 The Usher interactome. Schematic diagram of the Usher network in which the PDZ scaffolding proteins Whirlin and Harmonin and the microtubule-associated protein SANS form the central core (Millan *et al.* 2011).

Other functions of Whirlin

Currently, little is known about the putative function of Whirlin in other tissues or diseases. The short C-terminal isoform has been described to be upregulated in colorectal cancer tissues in clear accordance with tumour progression. Interestingly, immunocytochemistry on human colon cancer cell line detected a diffuse staining in the cytoplasm and on the plasma membrane, and immunoelectron microscopy revealed clustering along the plasma membrane where proteins were lined up (Toiyama *et al.* 2009). On the other side, Whirlin long isoform has been recently detected in mice DRG and spinal cord lysates and has been proposed to act as a cytoskeletal linker, through yet unconfirmed cytoskeletal proteins, to ensure proper paranodal compaction and stabilisation of the axonal cytoskeleton in myelinated axons (Green *et al.* 2013). Interestingly, a more recent work detected Whirlin expression in proprioceptive sensory neurons in mice DRGs, where it seems to facilitate responses to muscle stretch, substantiating a role for Whirlin in mechanoreception (de Nooij *et al.* 2015).

UNIVERSITAS
Miguel
Hernández

OBJECTIVES

UNIVERSITAS
Miguel
Hernández

Given that TRPV1 is not only a pivotal effector of cellular function in physiological conditions but plays also a crucial role in various pathological processes, and most prominently in the development of inflammatory pain, its function must be subjected to a strict and complex regulation. Many efforts have been made in order to reach a better understanding of the molecular basis of its modulation. One aspect that has attracted increasing interest in the last years is the identification and characterisation of new TRPV1 interacting partners: the comprehension of the signalplex composition and dynamics under nociceptive and inflammatory conditions may provide useful information for the development of novel therapeutic strategies to modulate TRPV1 activity. In this context, the present work is focused on the identification of Whirlin as a new putative component of TRPV1 signalplex. Specifically, the objectives of the study are the following:

- **Confirm the interaction between Whirlin and TRPV1.** Pull-down and co-immunoprecipitation assays with both full proteins. Identification of the domains implicated in the interaction. Colocalisation studies in heterologous and native expression systems (DRG).

- **Study the effect of the interaction on both receptor distribution and function.** Analysis of the effects of Whirlin overexpression or silencing on total and surface expression of the receptor in both heterologous and native expression systems, mainly through biotinylation assay and immunocytochemical staining. Functional characterisation through Ca^{2+}-imaging assays and electrophysiological recording in order to study the effect on TRPV1 responses to different stimuli.

- **Define the molecular mechanisms involved in Whirlin-mediated modulation of TRPV1.** Analysis of the effect of Whirlin overexpression or downregulation on TRPV1 total and surface stability and subcellular distribution.

- **Study eventual changes in TRPV1 activity due to Whirlin mutation or ablation.** *In vivo* nociceptive behavioural assays in whirler mutant and whirlin$^{neo/neo}$ transgenic mice in order to analyse the effect of ablation of specific Whirlin isoforms on TRPV1 activity, in both physiological and inflammatory conditions.

UNIVERSITAS
Miguel
Hernández

RESULTS

UNIVERSITAS
Miguel
Hernández

INTERACTION BETWEEN TRPV1 AND WHIRLIN

Different interaction partners for TRPV1 were identified through a Y2H assay performed by using the N-terminal domain (amino acids 1-414) of rat TRPV1 as bait. Two of them, Snapin and Sinaptotagmin IX, were shown to regulate the exocytosis and vesicular trafficking of the receptor, whereas the ubiquitin-like protein GABARAP was demonstrated to increase TRPV1 expression and clustering in the membrane and to modulate its functional activity (Morenilla-Palao *et al.* 2004;Lainez *et al.* 2010). The PDZ protein Whirlin/CIP98 was identified in the same screening. The main objective of this work has been to confirm this interaction and to analyse its capability to regulate receptor expression and functionality.

In vitro interaction between Whirlin and TRPV1

In order to confirm the interaction between TRPV1 and Whirlin, we first performed an *in vitro* pull down assay. Both the N- (amino acid 1-414) and C-terminal (amino acid 682-830) domains of TRPV1 were cloned into the pGEX-4T1 plasmid and transformed in *E.Coli* BL21. The resulting glutathione S-transferase (GST)-fusion proteins were purified, immobilised on glutathione-sepharose 4B beads and incubated with an extract of Human embryonic kidney 293 (HEK293) cells transiently expressing the human full length Whirlin protein fused to a myc-His epitope at the C-terminus to facilitate its detection by a commercial antibody (α-myc). As a negative control we immobilised GST. As illustrated in **Figure 12A**, both cytoplasmic TRPV1 domains were able to retain Whirlin at a similar level. Control with GST alone exhibited only a very weak unspecific retention of Whirlin.

We next evaluated whether Whirlin-myc interacted in cells with the full-length TRPV1 using a co-immunopurification strategy. As illustrated in **Figure 12B**, an immobilised anti-myc monoclonal antibody co-immunoprecipitated Whirlin-myc and TRPV1 from a whole HEK293 cell extract expressing both proteins (lane 2). Furthermore, TRPV1 was also able to associate with PSD95, a different protein also containing PDZ domains (**Figure 12B**, lane 3). Similarly, we could co-immunoprecipitate Whirlin-myc using a polyclonal antibody that recognised an N-terminal epitope of TRPV1. Altogether we corroborated that both proteins complex when co-expressed in mammalian cells (**Figure 12C**, lane 2).

The association of PDZ proteins with their targets usually involves a specific short amino acid motif localised either at the very C-terminus or close to it, as in the case of the fly TRP channel (Shieh and Zhu 1996). By analysing the sequence of the last stretch of amino acids of rat TRPV1 C-terminal domain we identified a putative internal Class I PBM, (**S/T)XV** (SMV at amino acids 832 to 834). In order to verify if this sequence was essential for the interaction with Whirlin, we generated a TRPV1 truncated mutant (referred to as TRPV1 V-Stop) that lacks 11 amino acids of TRPV1 containing the SMV motif at the C-end. By either using an

anti-myc (**Figure 12B,** lane 4) or anti-TRPV1 antibody (**Figure 12C**, lane 3), we confirmed that the V-Stop mutant was able to coimmunoprecipitate with Whirlin-myc, thus suggesting that other regions of TRPV1 are implicated in the interaction. This seems in accordance with the evidence that the N-terminus domain is also able to interact with Whirlin and that the putative PBM we identified in rat TRPV1 is loosely conserved among other species (**Figure 12D**).

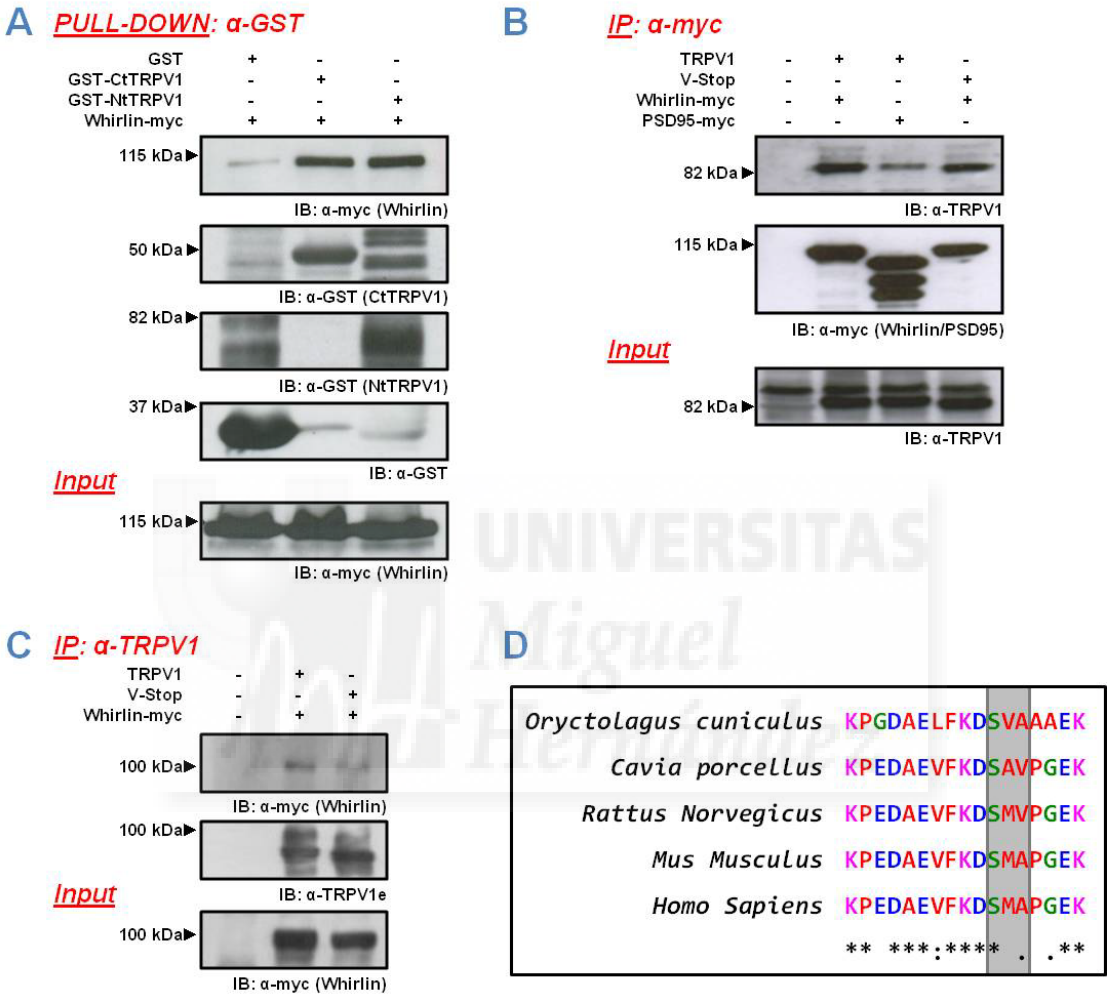

Figure 12 TRPV1 associates *in vitro* with Whirlin-myc. (A) Pull down assay in which GST, GST-NtTRPV1 and GST-CtTRPV1 were immobilised on a resin and incubated with an extract of HEK293 cells transiently expressing the full length Whirlin-myc. Both domains interact with the protein. **(B)** Coimmunoprecipitation assay from HEK293 transiently expressing TRPV1 wild-type or TRPV1-VStop and either Whirlin-myc or PSD95-myc with an immobilised anti-myc antibody. The receptor interacts with both PDZ proteins independently of the presence of the putative PBM. **(C)** Coimmunoprecipitation assay from HEK293 transiently expressing TRPV1 wild-type and V-stop and Whirlin-myc with an antibody that recognises an N-terminal epitope of the receptor. **(D)** Sequence alignment of the last 18 aa of TRPV1 C-terminal domain from different species. The gray box evidences amino acids of the putative PBM. (*) indicates positions which have a single, fully conserved residue; (:) indicates conservation between groups of strongly similar properties and (.) indicates conservation between groups of weakly similar properties.

We finally questioned which of the PDZ domains of Whirlin mediated the interaction with TRPV1. To address this question, we truncated Whirlin in two segments that were also myc-tagged, one encompassing the PDZ1 and PDZ2 domains (PDZ1+2-myc), and the other containing the proline-rich region and the PDZ3 (PDZ3-myc). Notably, this second construction resulted in a very unstable protein barely detected by western immunoblot. Blocking

proteasomal activity with the non-proteasome-specific peptide aldehyde MG132 prevented its degradation although with variable expression levels within experiments. Despite these limitations, coimmunoprecipitation assays performed with either an anti-myc (**Figure 13A**) or anti-TRPV1 (**Figure 13B**) antibody confirmed that both truncated proteins were able to strongly bind and immunopurify TRPV1, indicating that the interaction of Whirlin with the thermoTRP can be sustained by the three PDZ domains.

Taking together, these results indicate that TRPV1 and Whirlin can form a stable complex in cells mainly through an interaction of TRPV1 N-terminus and Whirlin PDZ domains.

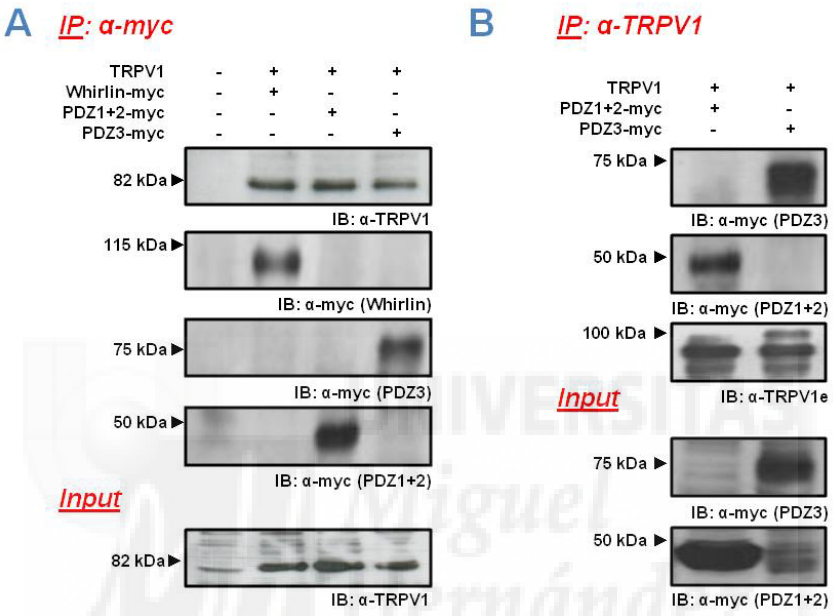

Figure 13 N- and C-terminal Whirlin truncated forms interact with TRPV1. Coimmunoprecipitation assays in which TRPV1 was coexpressed in HEK293 cells with full length Whirlin or the truncated forms PDZ1+2 and PDZ3, all fused to a myc-His epitope. Immunoprecipitation was realised with **(A)** an α-myc antibody immobilised on an agarose resin or **(B)** an antibody directed against an N-terminal epitope of the receptor. TRPV1 is able to interact with all the constructions.

Ex vivo interaction between Whirlin and TRPV1

To investigate the physiological relevance of TRPV1-Whirlin association, we determined whether both proteins co-express in sensory neurons primary cultures, the native system where the vanilloid receptor is predominantly present. First, we investigated Whirlin mRNA expression in rat DRG neuronal cultures by real-time quantitative PCR (qPCR). Furthermore, we investigated Whirlin protein expression by western immunoblot and immunocytochemical staining using a polyclonal antibody generated against an epitope located between the proline-rich region and the third PDZ domain (EVHRPDSEPDVNEV). Both techniques readily detected the presence of Whirlin in primary cultures of rat sensory neurons (**Figure 14**).

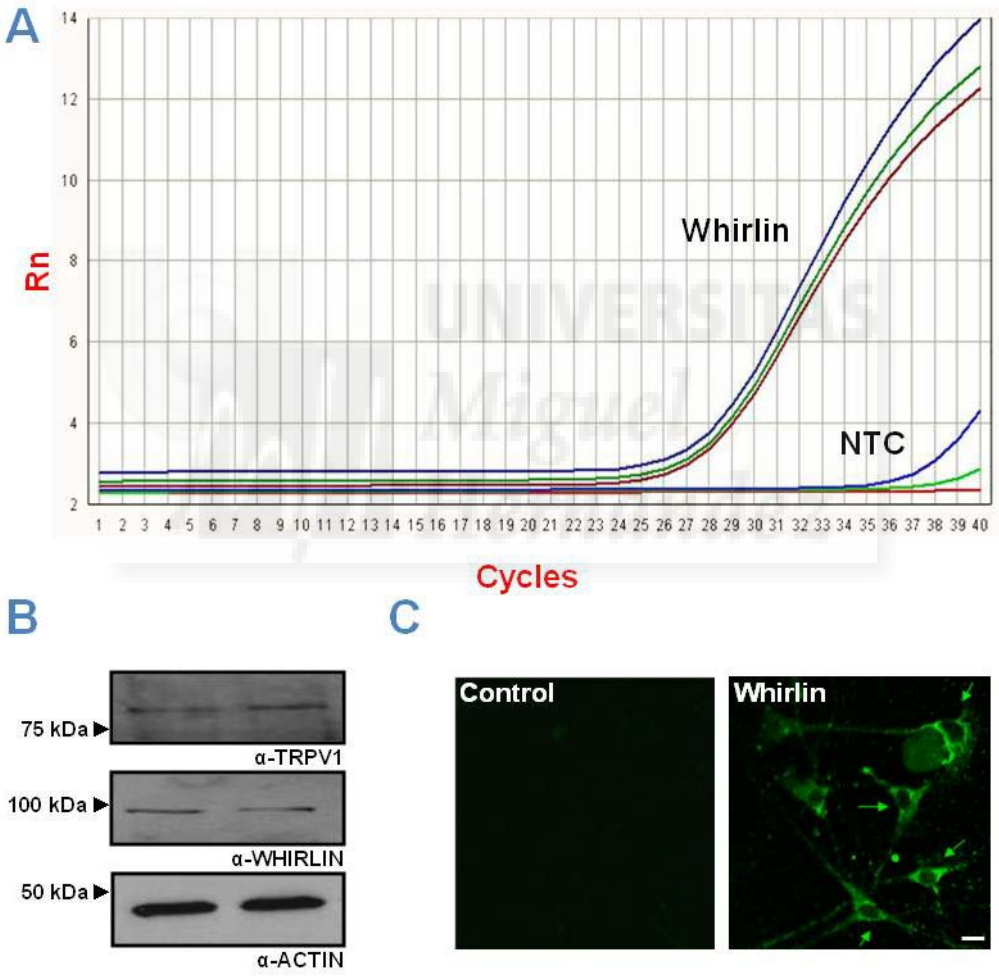

Figure 14 Rat nociceptors express Whirlin. (**A**) qPCR amplification plot in which the fluorescent signal is plotted against cycle number. Rat nociceptors extracts and specific primers for Whirlin were used. NTC: non-template control. (**B**) Immunoblots of whole nociceptor extracts probed using antibodies against TRPV1 and Whirlin. Actin was used as loading control. (**C**) Immunocytochemical detection of Whirlin expression in primary cultures of rat nociceptors. Scale bar 10 µm.

Thereafter, we used immunocytochemistry to evaluate whether Whirlin and TRPV1 co-express in the same neurons. Neonatal rats and adult mice DRG cultures were incubated with selective antibodies for TRPV1 and Whirlin, subsequently labelled with fluorophore-conjugated

secondary antibodies for their detection and analysed by confocal microscopy. Two different antibodies were independently used to detect Whirlin. For rat neuronal cultures we used the polyclonal antibody described above, generated against an epitope located between the proline-rich region and the third PDZ domain (EVHRPDSEPDVNEV). For mice DRG a commercial antibody (Abcam) was used that recognises a region between aa 600 and 700, common to all Whirlin isoforms unless the two short NT1 and NT2 (see **Figure 10**). As illustrated in **Figure 15**, a widespread cellular immunelabelling of TRPV1 and Whirlin was observed in both rats (upper panels) and mice (lower panels) sensory neurons, with a clear colocalisation at the neuronal soma.

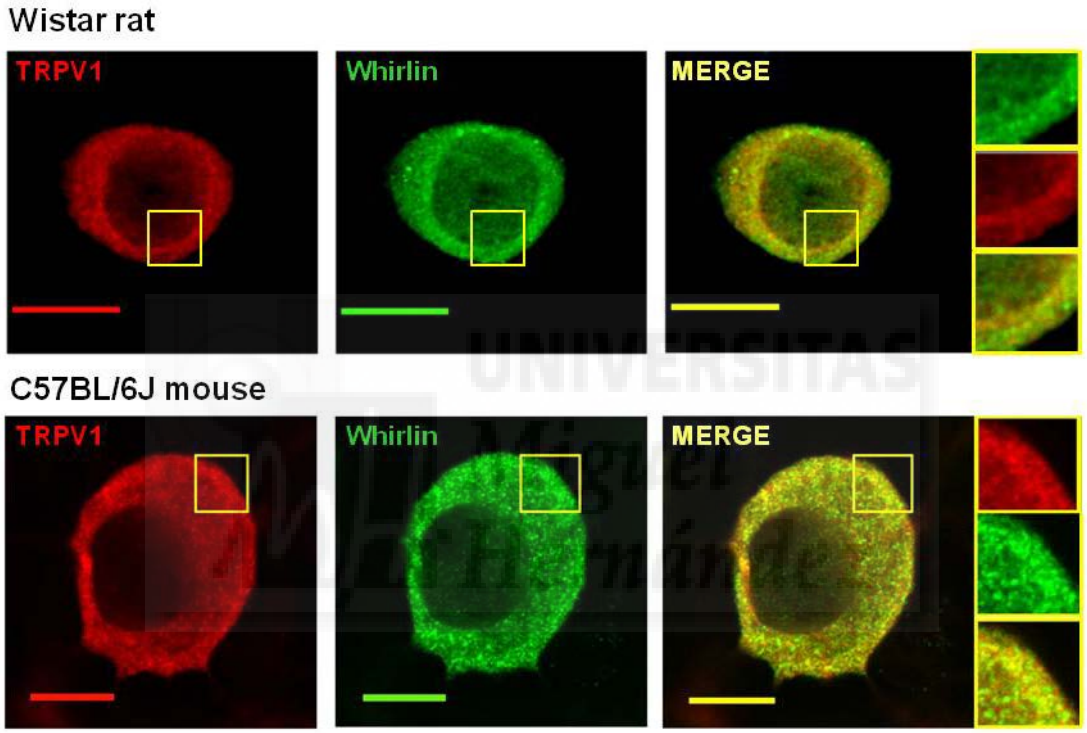

Figure 15 TRPV1 and Whirlin are widely expressed and colocalise in sensory neurons. Immunostaining of TRPV1 (red) and Whirlin (green) in neonatal rats (*upper*) and adult mice (*lower*) DRGs cultures. The inset denotes a 2X zoom of the squared area. Scale bar 10 µm.

Double immunohistochemical staining on both rats and mice DRG cryosections was also performed in order to analyse TRPV1 and Whirlin distribution in sensory fibres. In these assays a commercial antibody (Novus biological) raised against a C-terminal epitope was used to stain Whirlin in rats tissues. Two different antibodies were also used for TRPV1: a polyclonal guinea-pig (Chemicon) and a polyclonal rabbit (Alomone) for rats and mice tissues respectively. Serial pictures from each section were acquired and image analysis and quantification were performed with Zen lite™ software (Zeiss). In **Figure 16** representative immunofluorescence images are reported, depicting that in both animal models ~55% of total neurons exhibited positive staining for Whirlin, and 40% of them coexpressed TRPV1. Conversely, between 55% and 65% of TRPV1 positive neurons also coexpressed Whirlin (**Table I**). Thereafter, double immunostaining of Whirlin with the three classical molecular markers NF200 (for

mechanoreceptors and proprioceptors with large axon diameters), IB4 (for nonpeptidergic nociceptors) and CGRP (for peptidergic nociceptors) was performed and the percentage of Whirlin positive neurons that were also positive for each marker (Whirlin$^+$ x marker$^+$) calculated. As shown in **Table I**, in both species the PDZ protein displayed a wide ubiquitous expression among the three neuronal subpopulations analysed.

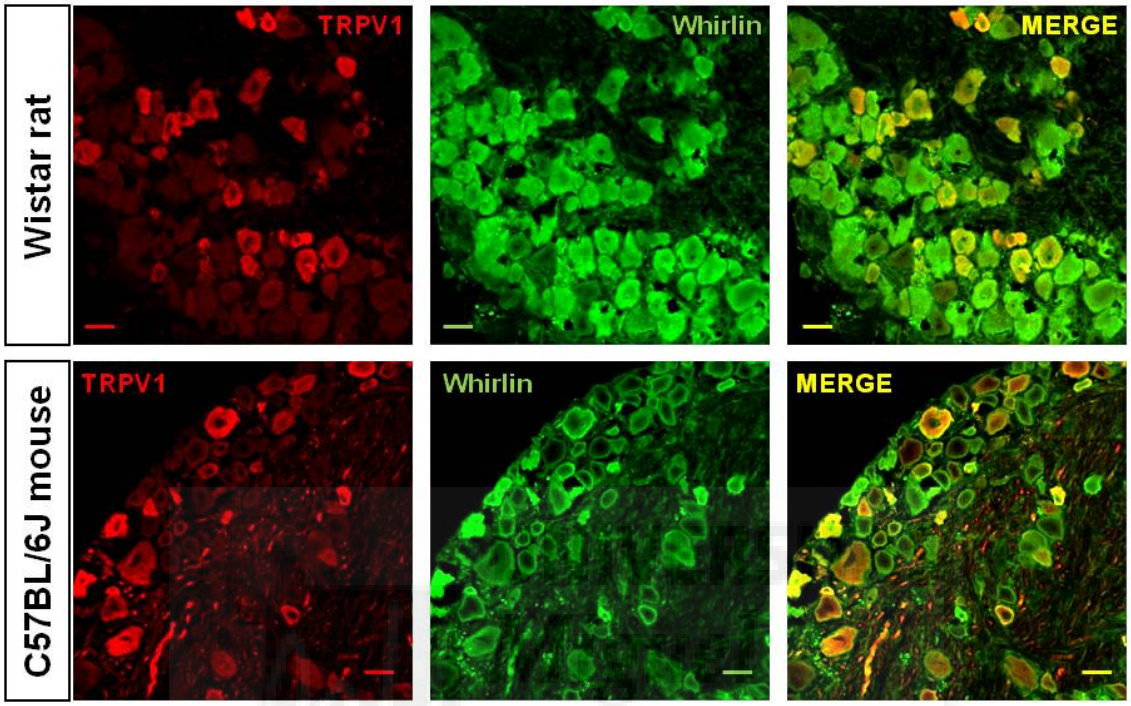

Figure 16 TRPV1 and Whirlin coexpress in a subpopulation of DRG neurons. Thin sections of DRG from Wistar rats and C57BL/6J mice were double-immunostained with antibodies for TRPV1 (red) and Whirlin (green). Representative immunofluorescent images are reported. Scale bars 20 µm.

	Wistar rat	C57BL/6J mouse
Whirlin$^+$	57 ± 2	55 ± 1
Whirlin$^+$ x IB4$^+$	42 ± 5	37 ± 3
Whirlin$^+$ x CGRP$^+$	32 ± 3	54 ± 5
Whirlin$^+$ x NF200$^+$	43 ± 5	37 ± 3
Whirlin$^+$ x TRPV1 $^+$	40 ± 4	40 ± 2
TRPV1$^+$ x Whirlin$^+$	55 ± 7	64 ± 2

Table I Immunohistochemical staining of DRG cryo-sections from Wistar rats and C57BL/6J mice was performed with polyclonal antibodies for TRPV1, Whirlin and the neuronal markers CGRP, IB4 and NF200. Three animals and a minimum of 5 sections per group were analysed. Data expressed as percentage of total neurons analysed per each section (mean ± S.E.M.).

EFFECTS ON TRPV1 EXPRESSION

Whirlin overexpression increases TRPV1 total and surface levels

Once confirmed the association between Whirlin and TRPV1, we next analysed if this interaction modulated TRPV1 expression. For this purpose, the cellular levels of both TRPV1 and Whirlin proteins were evaluated in the absence or presence of the other protein in HEK293 cells transiently transfected with TRPV1 plus Whirlin or plus Yellow Fluorescent Protein (YFP) cDNA as a control by western immunoblot. As depicted in **Figure 17A**, expression of both proteins was increased when they were coexpressed. To study this effect more precisely, a fixed amount of the receptor cDNA was cotransfected with increasing quantities of Whirlin cDNA. As observed in the immunoblots in **Figure 17B** and in the quantification of three independents experiments reported in **Figure 17C**, the protein levels of TRPV1 were enhanced in a dose-dependent manner with increasing amounts of Whirlin coexpression. The cytosolic protein β-actin was used as a loading control to normalise TRPV1 expression.

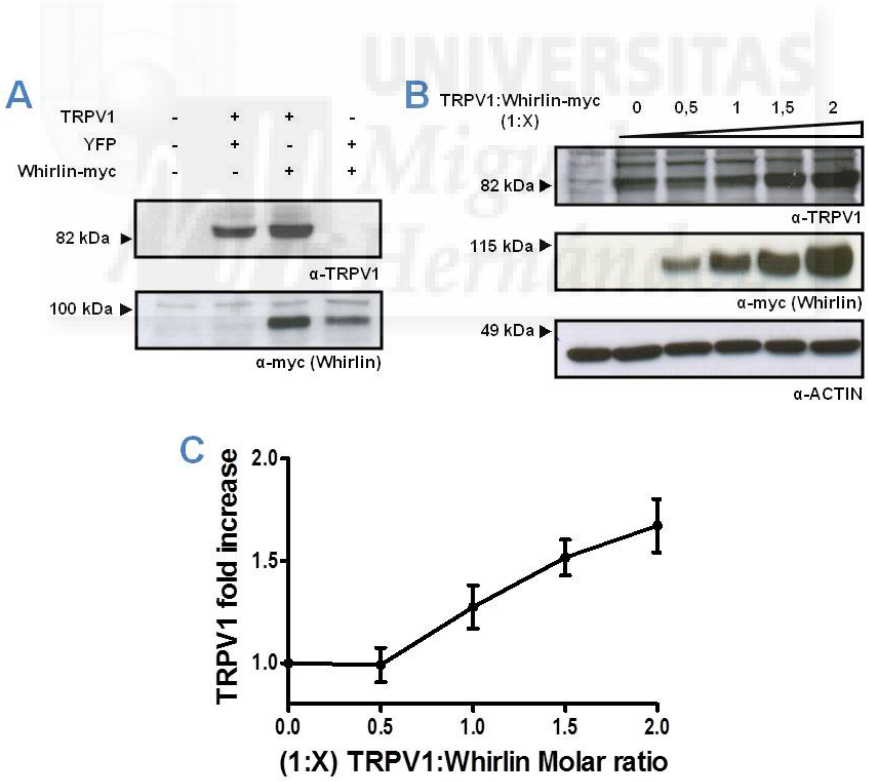

Figure 17 Whirlin increases TRPV1 expression. (A) Both Whirlin and TRPV1 total levels are increased when the two proteins are coexpressed in the same cells. **(B)** Representative immunoblots of protein extracts form HEK293 cells transfected with a fixed amount of TRPV1 and increasing doses of Whirlin. **(C)** Quantification of 3 independent experiments with data expressed as mean ± S.E.M.

As PDZ proteins are mainly known to participate in the trafficking and clustering of receptors at the cell membrane, we next determined total and surface levels of TRPV1 in presence or absence of Whirlin through biotinylation assays of cell surface membranes.

Specifically, surface proteins of HEK293 transiently transfected with TRPV1 and Whirlin plasmids, or YFP in control conditions, were covalent labelled with biotin and isolated with the high-affinity resin streptavidin. Total extracts and surface fractions were then analysed by western immunoblot (**Figure 18A**) and densitometric quantification of band intensities (**Figure 18B-C**). As Whirlin induced changes in both total and surface TRPV1 receptor expression, the fractions were individually normalised to actin levels, and the normalised percentages for surface and total proteins were plotted separately (Kantamneni *et al.* 2014). As shown in **Figure 18B**, Whirlin produced a significant increment in the expression of TRPV1 with a parallel enhancement of the plasma membrane levels. However, when surface levels were normalised to the total protein amount no significant change was detected, thus suggesting that Whirlin does not modify the receptor trafficking to the membrane (**Figure 18C**).

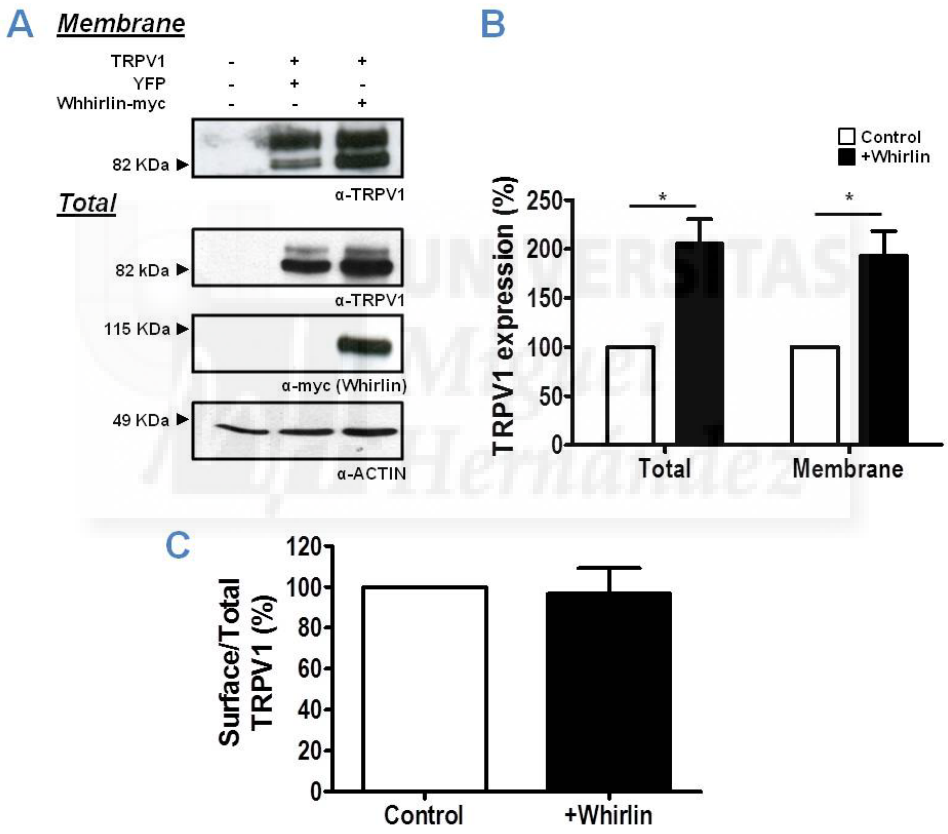

Figure 18 Whirlin increases total and surface TRPV1 levels. (A) Representative immunoblots of membrane and total fractions. HEK293 were transfected with TRPV1 plus YFP as control or plus Whirlin. Surface proteins were labelled with biotin and subsequently isolated. **(B)** Quantification of 5 independent experiments with data expressed as mean percentage increase in TRPV1 signal ± S.E.M. compared with control (100%). * p<0.05 (paired *t* test). **(C)** Normalisation of TRPV1 surface levels to the total inputs.

In order to corroborate the results obtained with the biotinylation assays we also performed immunocytochemical staining of HEK293 cells expressing TRPV1 plus Whirlin or the YFP-homologue Discosoma sp. red fluorescent protein (DsRED) as control. Non-permeabilised cells were incubated with the TRPV1e antibody to specifically recognise the receptor pool localised at the plasma membrane (Camprubi-Robles *et al.* 2009). Thereafter, the cells were

permeabilised and stained with anti-myc antibody to detect intracellular Whirlin. Confocal microscope images in **Figure 19** illustrate that, using the same acquiring conditions, Whirlin (red) positive cells displayed a significantly stronger TRPV1 immunoreactivity (green) at the cell membrane as compared to control cells.

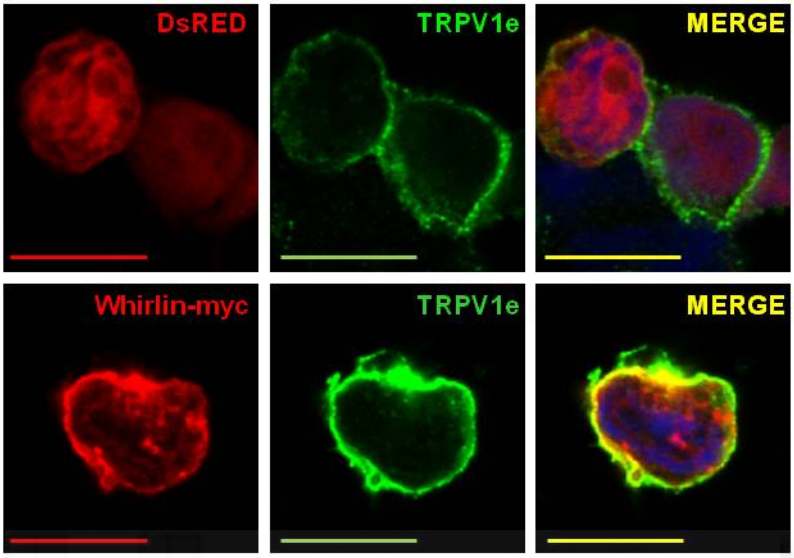

Figure 19 Whirlin increases TRPV1 surface expression. Non-permeabilised HEK293 expressing TRPV1+DsRED or TRPV1+Whirlin-myc were immunostained with TRPV1e (green), that recognises an extracellular epitope of TRPV1, and later detergent-permeabilised for Whirlin staining (red). Cell nuclei were stained with DAPI (blue). Scale bars 10 µm.

Furthermore, the higher TRPV1 levels at the plasma membrane promoted by Whirlin coexpression was evidenced in the form of large receptor aggregates, as shown by clustered membrane labelling of a YFP-fused TRPV1 construct (**Figure 20**).

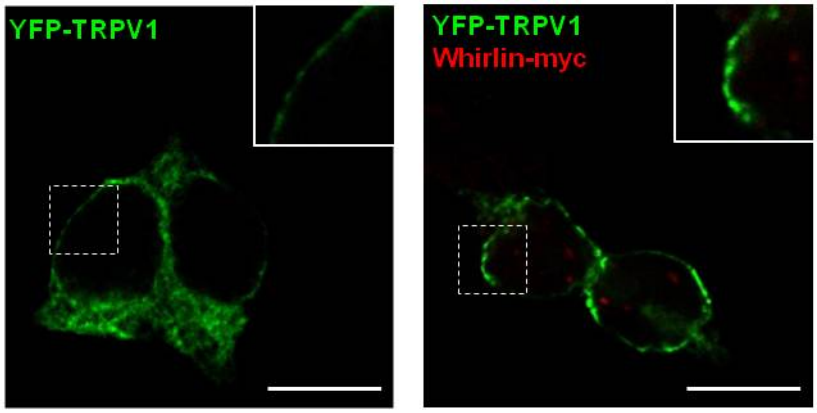

Figure 20 Whirlin increases the clustering of TRPV1. YFP-TRPV1 (green) expression in HEK293 cells in the absence or presence of Whirlin (Red). The inset denotes a 2X zoom of the squared area. Scale bars 10 µm.

The effect on native TRPV1 expression was further evaluated by transiently overexpression of Whirlin (or YFP as a control) in rat neonatal DRG cultures for 48 hours by western immunoblot and densitometrical analysis of protein extracts. As shown in **Figure 21**, overexpression of Whirlin caused a significant increase in TRPV1 total levels compared with control conditions.

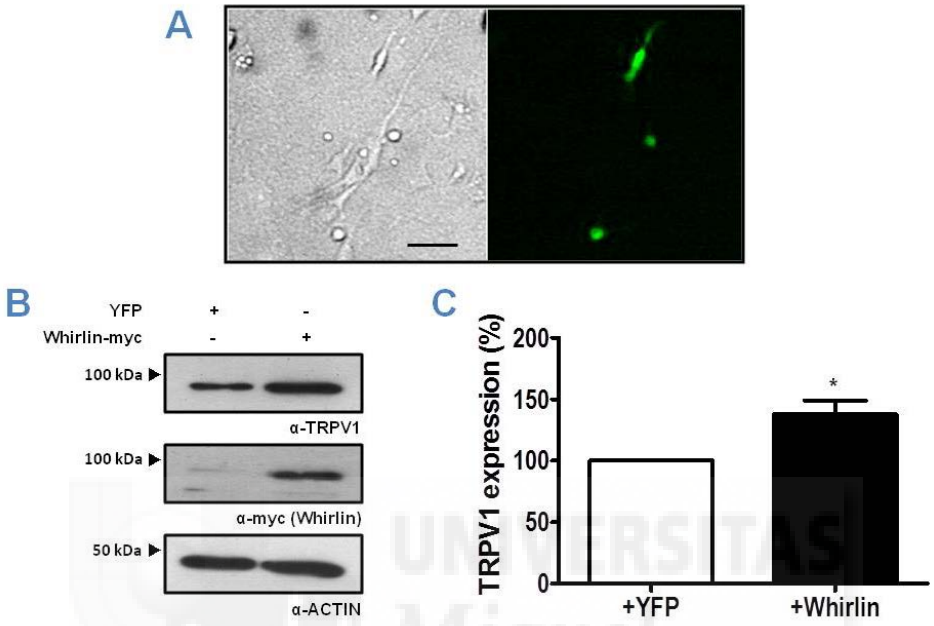

Figure 21 Whirlin increases native TRPV1 expression. (A) Phase contrast and YFP fluorescence of neonatal rats DRG 48 hours after electroporation with the expression plasmids. Scale bar 100 µm. **(B)** Representative immunoblots of total protein extracts **(C)** Quantification of 6 independents experiments with data expressed as percentage increase in TRPV1 signal ± S.E.M. compared with control (100%). * $p<0.05$ (paired *t* test).

Collectively, these results indicate that Whirlin is a PDZ-scaffold protein that increases the total and membrane expression of TRPV1 in cells, and appears to promote receptor clustering.

Whirlin silencing decreases TRPV1 expression

Once demonstrated that Whirlin overexpression produced an increase in TRPV1 levels, we evaluated the effect of Whirlin knock-down on receptor expression in F11 cells, a hybridoma of the mouse neuroblastoma cell line N18TG-2 and embryonic rat DRGs. Three different small interfering RNAs (siRNA-1 to siRNA-3) were used. siRNA-1 was directed to a sequence in exon 1, whereas siRNA-2 and siRNA-3 recognised two different sequences in exon 6. As F11 cells do not express Whirlin nor TRPV1, they were first transfected with rat TRPV1 and Whirlin cDNAs and 24 hours later re-transfected with one or a mix of the three siRNAs designed against Whirlin at two different concentrations, 30 and 50 nM. A housekeeping gene (GAPDH) and a scramble siRNA (sc-siRNA, a siRNA with a random sequence), both at 30 nM, were used as positive and negative controls, respectively. The three siRNAs were able to drastically reduce both Whirlin mRNA levels, measured by qPCR (**Figure 22A**), and Whirlin protein expression, detected by western immunoblot (**Figure 22B**). Importantly Whirlin knockdown was accompanied by a decreased TRPV1 expression and this effect was particularly evident for siRNA-1 and siRNA-2.

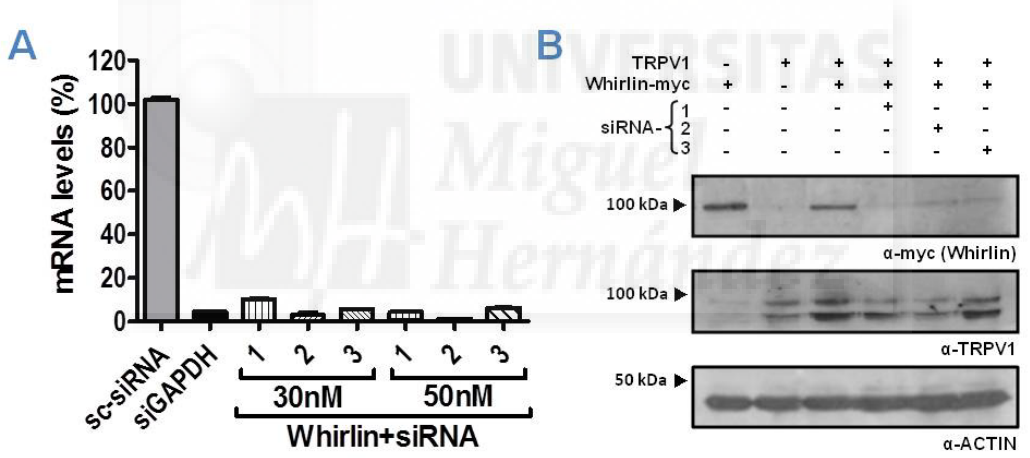

Figure 22 Silencing of Whirlin inhibits its increasing effects on TRPV1 expression. (A) Whirlin mRNA levels after transfection of three different siRNAs (-1, -2, -3) in F11 cells at two distinct concentrations, normalised to a scramble siRNA (sc-siRNA). A housekeeping gene (GAPDH) was used as a positive control. **(B)** F11 cells were transiently transfected with rat plasmids for TRPV1 and Whirlin and 50 nM siRNA-1,-2 or -3. Whirlin expression was silenced and consequently its effect on TRPV1 expression reduced.

Subsequently, the effect of these siRNAs in primary sensory neurons was tested. A Cy3-labeled sc-siRNA in a 1:10 mixture with a non-labelled sc-siRNA was used to identify transfected cells by fluorescence microscopy and evaluate lipofectamine transfection efficiency (**Figure 23A**, lower panels). Lipofectamine toxicity after 24 and 48 hours was assessed by Trypan blue exclusion test, a vital stain that allows to discriminate between viable (unstained) and non-viable (stained cells) and thus calculate cell viability, which in both conditions was ~70% (**Figure 23A**, upper panels). Finally, Whirlin mRNA levels were assessed in the same conditions at both 24 and 48 hours post-transfection with 50 nM siRNA-1, -2 or -3 (**Figure 23B**).

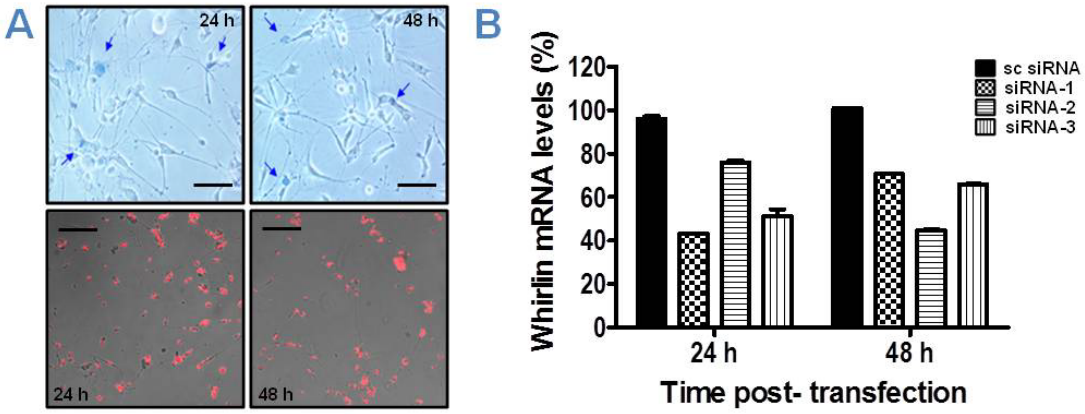

Figure 23 Whirlin mRNA levels in neonatal rat DRG cultures are reduced after siRNA transfection. (A) Trypan blue staining revealed a ~70% cell viability at both 24 and 48 hours post transfection (*upper panels*). Lipofectamine transfection efficiency was evaluated with a 1:10 Cy3-sc-siRNA:sc-siRNA mixture (*lower panels*). Scale bar 100 µm. **(B)** Whirlin mRNA levels were decreased 24 and 48 hours after 50 nM siRNA-1,-2 or -3 transfection.

In order to analyse the effect of the three siRNAs on protein expression immunocytochemical staining with specific antibodies for TRPV1 and Whirlin was performed and samples analysed by confocal microscopy. Non-transfected cells and a scramble siRNA were used as negative controls. As shown in **Figure 24** and **Figure 25**, in the same acquiring conditions, at both 24 and 48 hours post-transfection the three siRNAs induced the disappearance of Whirlin with the parallel decrease of TRPV1 staining, compared with non-transfected or sc-siRNA transfected cells. Altogether, data from both heterologous overexpression and silencing assays suggest a role for Whirlin in modulating receptor expression levels.

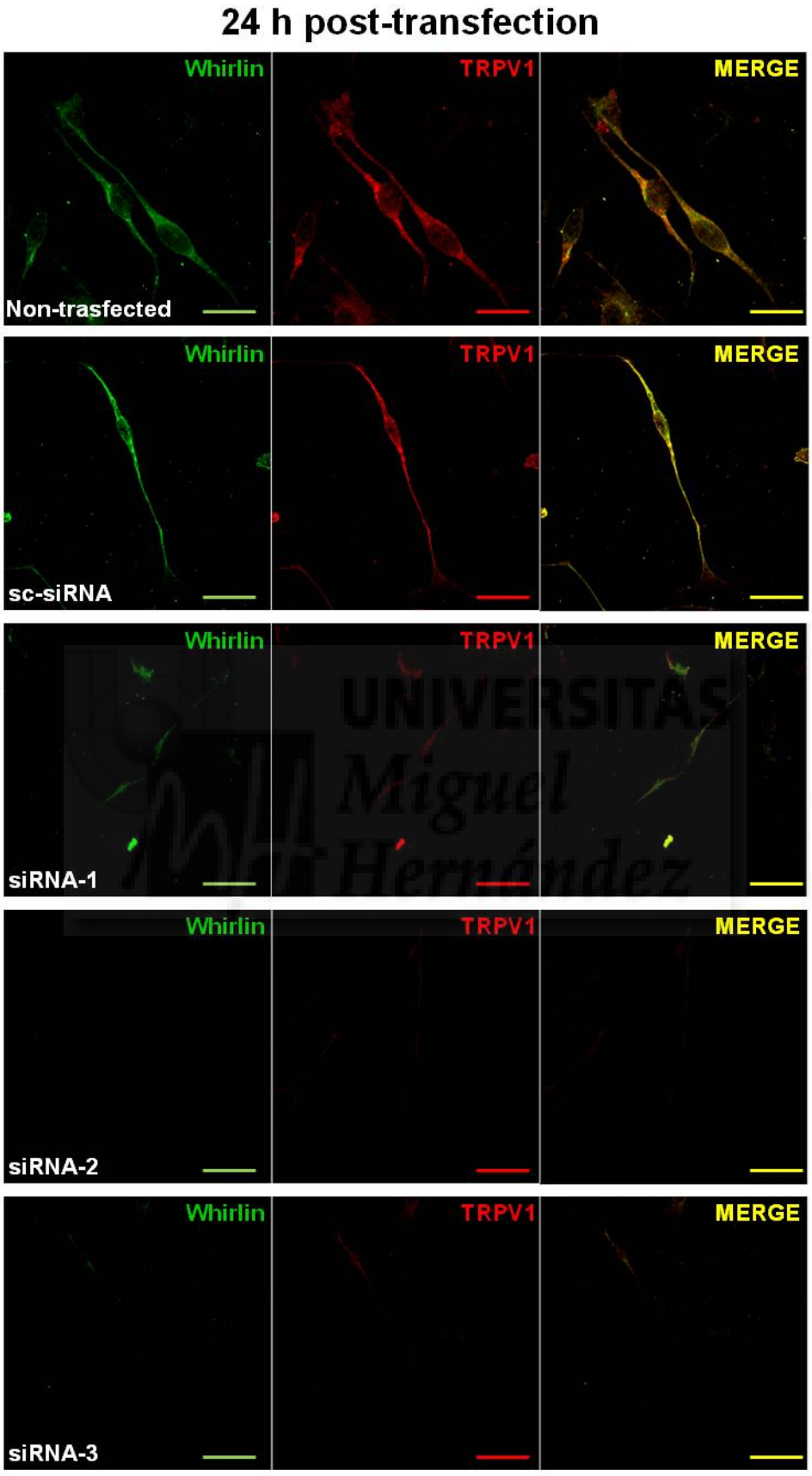

Figure 24 Whirlin silencing decreases native TRPV1 expression. Rats DRG were transfected with siRNA-1, -2, -3 or a sc-siRNA. Non-transfected DRG were used as a control. The three siRNAs silenced Whirlin (green) expression which caused a parallel decrease in TRPV1 (red) staining. Scale bars 10 µm.

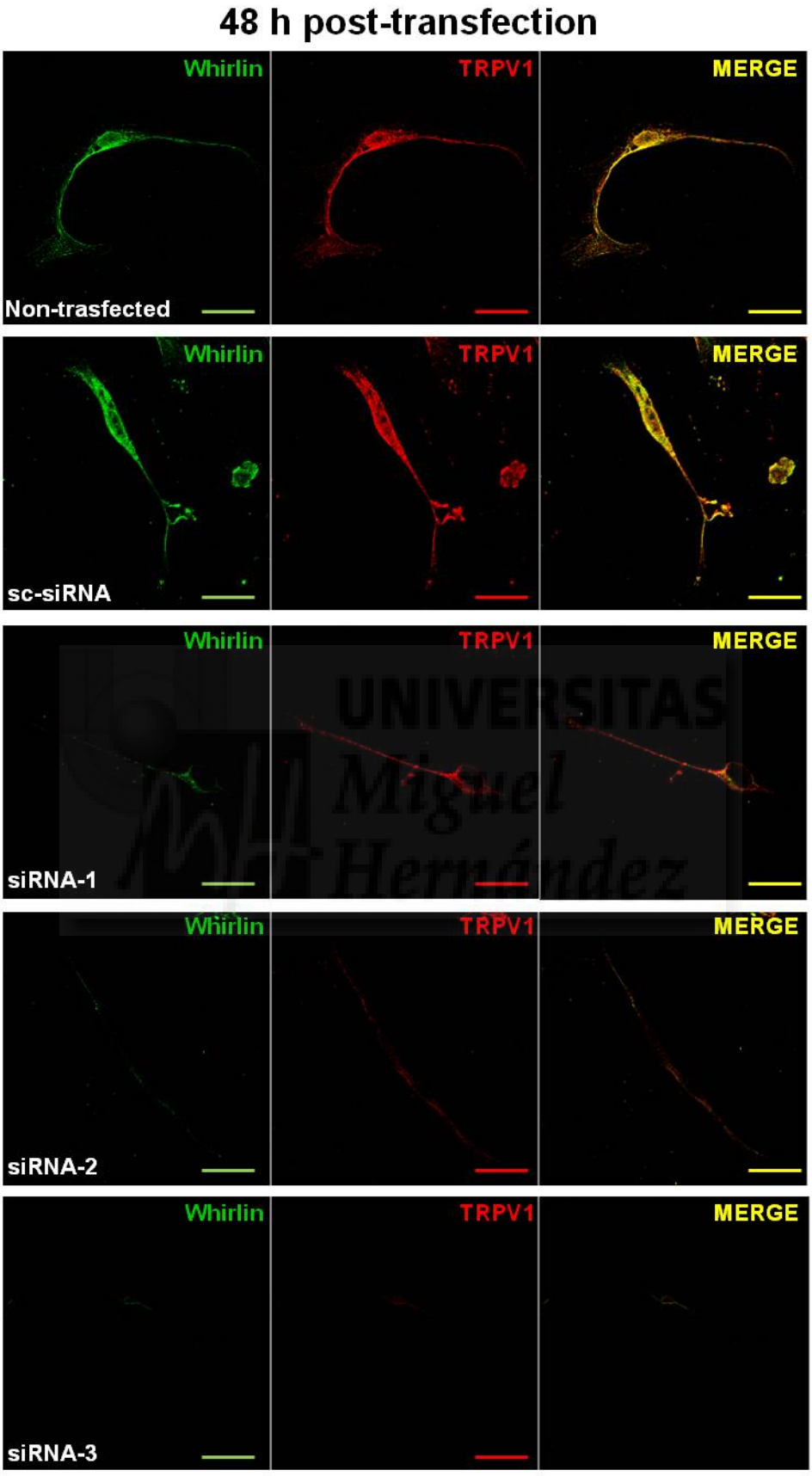

Figure 25 Whirlin silencing decreases native TRPV1 expression. Rat DRG were transfected with siRNA-1,-2, -3 or a sc-siRNA. Non-transfected DRG were used as a control. The three siRNAs silenced Whirlin (green) expression which caused a parallel decrease in TRPV1 (red) staining. Scale bars 10 µm.

EFFECT ON TRPV1 FUNCTION

Effect of Whirlin overexpression on TRPV1 mediated currents

The putative effect of Whirlin overexpression on TRPV1 function was analysed by patch clamp recordings in HEK293 cells transiently expressing TRPV1 plus YFP for controls or plus Whirlin, and using CD8 as an expression reporter protein. As TRPV1 is a polymodal channel that can be activated by different stimuli, we characterised the responses to three of them: voltage, acidic pH and the vanilloid capsaicin. The voltage-dependent activity of the channel in presence or absence of Whirlin was assayed using voltage steps protocols starting from a holding potential (V_h) of -60 mV, and applying 100 ms depolarising steps of 20 mV from -120 mV to +220 mV. Representative traces are reported in **Figure 26** characterised by low or null TRPV1 activation at negative potentials, gradually increasing with more positive potentials. Evoked currents and activation kinetics were not modified by Whirlin coexpression. Current densities (J) at +40 mV and +180 mV, calculated by dividing maximal currents (nA) by the cell capacitance (pF), an indicator of cell size, resulted in a significant decrease in the current density at high depolarising potential in cells co-expressing both the channel and Whirlin, as compared to control cells (**Figure 26B**). Conductance-voltage (G-V) curves obtained for each cell by converting the maximal current values from the voltage step protocol to conductance were fitted to the Boltzmann equation and estimated G_{max} values were used to obtain the normalised G/G_{max}-V curves (**Figure 26C**). The voltage dependence of channel gating was slightly shifted to higher voltages in the presence of Whirlin, indicating that the energetics of channel gating were marginally increased ($V_{0.5}$=96±2 mV and $V_{0.5}$=117±3 mV in the absence and presence of Whirlin, respectively). Conversely, the PDZ-scaffold protein did not alter TRPV1 voltage sensitivity, as evidenced by similar z_g values obtained from the slope of the G-V curve (0.55±0.03 and 0.58±0.02 in the absence and presence of Whirlin, respectively).

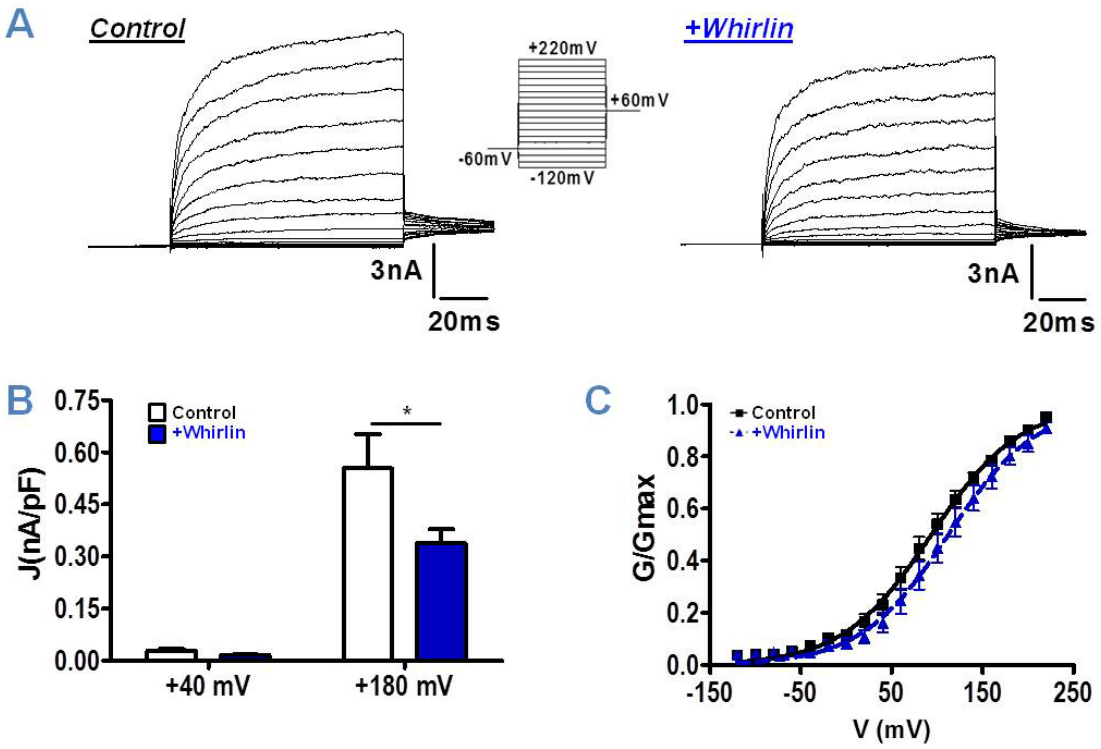

Figure 26 Effect of Whirlin on TRPV1 currents activated by voltage. (A) Representative traces of currents evoked by step potentials from -120 to +220 mV in 100 ms from V_h=-60 mV in HEK293 cells transfected with TRPV1+YFP (Control) or TRPV1+Whirlin. Evoked currents and activation kinetics were not altered by Whirlin. **(B)** Current densities (J, nA/pF) calculated from maximal currents at +40 mV and +180 mV showed a significant decrease in presence of Whirlin compared to control at the highest potential. n=23 cells for each condition. * p<0.05, Two-way ANOVA, Bonferroni post-test. **(C)** G-V relations for TRPV1 in Whirlin cotransfected or control cells. Conductance values were fitted to the Boltzamm equation $G=G_{max}/\{1 + \exp [(V-V_{0.5})/a_n]\}$, where G_{max} is the maximal conductance, $V_{0.5}$ is the voltage required to activate the half-maximal conductance, and a_n is the slope of the G-V curve.

Next, we compared TRPV1 gating by activating the channel with an acidic solution (pH=6) at a constant V_h of -60 mV. The stimulus was applied until the plateau response was reached. In **Figure 27A**, representative traces of activated inward currents are reported for control (TRPV1+YFP, *left*) and TRPV1+Whirlin (*right*) cells. Notably, the magnitude of acid-evoked currents in presence of Whirlin was significantly smaller than that recorded in its absence. Indeed, current densities were almost 2-fold smaller when Whirlin was co-expressed (-0.12±0.02 nA/pF, n=21, for control condition; -0.06±0.02 nA/pF, n=23, for TRPV1+Whirlin).

We also investigated capsaicin-evoked responses by applying a pulse of 1 µM capsaicin at a constant V_h of -60 mV until the plateau was reached. In this case, the magnitude and shape of TRPV1-mediated responses were not disturbed by Whirlin coexpression and currents densities calculated for both conditions were very similar, as shown in **Figure 27B** (control: -0.14±0.02 nA/pF, n=21; TRPV1+Whirlin: -0.12±0.01 nA/pF, n=22).

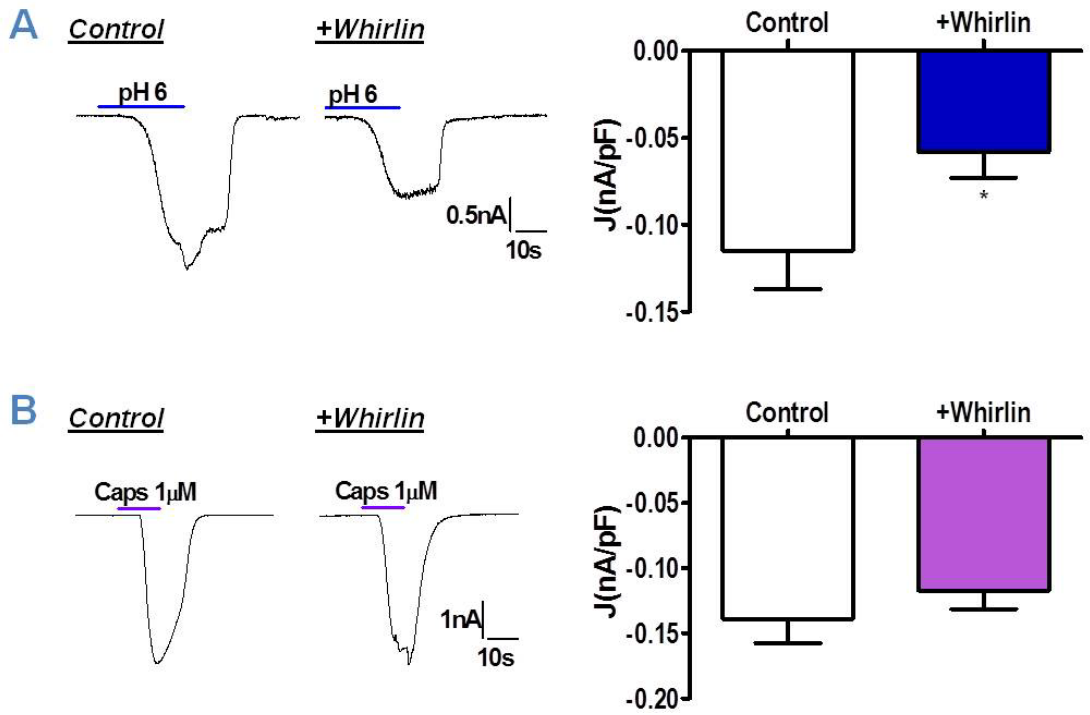

Figure 27 Effect of Whirlin on TRPV1 currents activated by acidic pH and capsaicin. (A) Representative evoked currents produced by acidic pH and current density quantification. A ~2-fold decrease in the inward current magnitude was observed in cells transfected with TRPV1+Whirlin compared with control cells. Data expressed as mean ± S.E.M. n=21 for control cells and n=23 for TRPV1+Whirlin condition * $p<0.05$ (unpaired *t* test). **(B)** Representative capsaicin evoked currents and current densities quantification. The magnitude of inward currents elicited by 1 μM capsaicin was not altered by Whirlin coexpression. n=21 for control cells and n=22 for TRPV1+Whirlin condition. Unpaired *t* test.

Taking advantage that TRPV1 is a non-selective ion channel with a high permeability to Ca^{2+}, fluorimetric assays with the green-fluorescent Ca^{2+} indicator fluo-4-acetoxymethyl ester (Fluo-4-AM) were performed to corroborate the receptor sensitivity/gating to capsaicin. As a protocol we applied a 15-s pulse of increasing capsaicin concentrations (from 0.01 to 10 μM) followed, after 5-minutes washing, by a second 15-s pulse at a saturating concentration of capsaicin (100 μM). Representative traces for control (black) and TRPV1+Whirlin cells (red) reported in **Figure 28A** show that the shape and the magnitude of the response were not altered by the presence of Whirlin. The amplitude of Ca^{2+} increase caused by stimulation with capsaicin, expressed as the ratio between the change in the fluorescence signal intensity (ΔF) and the baseline fluorescence before capsaicin application (F0), was calculated and represented (**Figure 28B**). As illustrated, coexpression of Whirlin did not significantly modify capsaicin-induced Ca^{2+} responses at any concentration of capsaicin utilised. We also calculated and represented the ratio of the second capsaicin response (Cap2) to the first one (Cap1) (**Figure 28C**). As observed, this ratio decreased as capsaicin dose increased due to receptor desensitisation, but no significant differences when Whirlin was coexpressed were detected.

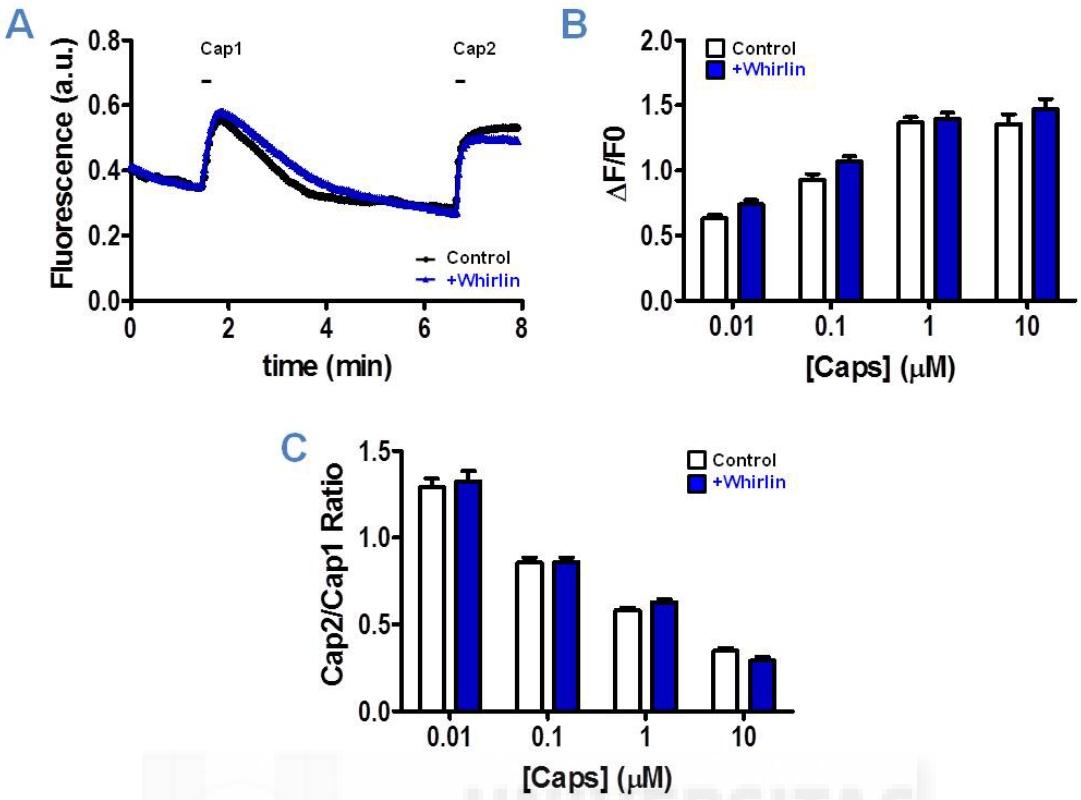

Figure 28 Whirlin does not modify capsaicin responses. (A) Representative traces of 0.01 µM (Cap1) capsaicin-evoked changes in fluorescence intensity in control (black) and TRPV1+Whirlin cells (red). Cap2=100 µm capsaicin. a.u.: arbitrary units. **(B)** ΔF/F0 (%) and **(C)** ratios between the second and the first peak responses were similar in both conditions. Data expressed as mean ± S.E.M. n>150 cells in all conditions. Two-way ANOVA, Bonferroni post- test.

Whirlin silencing reduces TRPV1 mediated currents

The functional effect of Whirlin downregulation on TRPV1 activity was also investigated. Ca^{2+} microfluorographic assays were first performed in F11 cells expressing TRPV1 in presence or absence of Whirlin and transfected or not with two different amounts (30 and 50 nM) of siRNA-1, -2 or -3 alone or a mix of them. Fluorescence emission of cells loaded with the Ca^{2+} indicator Fluo4-NW was measured during 18 cycles through the microplate reader POLARstar Omega. Ca^{2+} influx was evoked by the addition of a 100 µM capsaicin solution in the fifth cycle. **Figure 29A** illustrates calculated Area Under Curve (AUC) normalised to the response of cells coexpressing TRPV1+Whirlin. As observed, all the three siRNAs were able to abrogate TRPV1 activity.

Thereafter, Whirlin endogenous expression was silenced in rat neonatal DRG cultures with a 1:10 Cy3-siRNA-2:siRNA-2 mixture and capsaicin-induced Ca^{2+} influx in transfected nociceptors was determined by calcium imaging assays. Non-transfected (NT) or a 1:10 Cy3-sc-siRNA:sc-siRNA mixture were used as controls. 24 hours after transfection cells were loaded with the Ca^{2+} indicator Fluo-4 AM and Ca^{2+} influx was elicited by a 0.5 µM capsaicin stimulus. A pulse of 40 mM KCl solution was used to identify all viable neurons. As shown in **Figure 29B**,

the percentage of capsaicin sensitive neurons was significantly reduced by ~35% when Whirlin was silenced, compared to NT and sc-siRNA-transfected neurons.

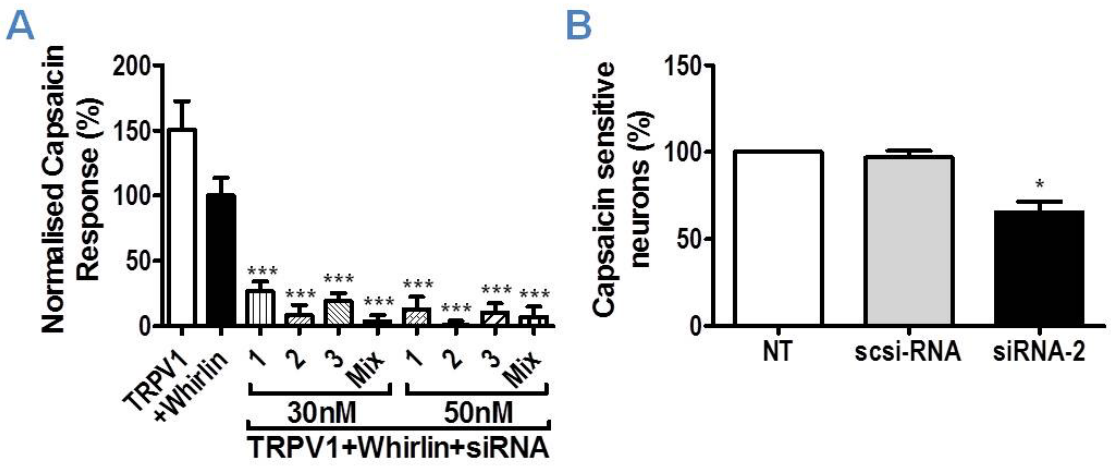

Figure 29 Whirlin silencing decreases capsaicin-induced responses. (A) Normalised capsaicin-induced calcium influx in TRPV1 or TRPV1+Whirlin F11 cells transfected with two distinct concentrations of 3 different siRNA. Silencing of Whirlin decreased TRPV1-mediated responses. Data expressed as mean ± S.E.M. *** p<0.001 (One-way ANOVA, Bonferroni post-test). **(B)** Calcium imaging assays on rat DRG neurons transfected with Cy3-siRNA-2:siRNA-2 or Cy3-sc-siRNA:sc-siRNA. NT cells were used as a control. Silencing of Whirlin was able to reduce the percentage of capsaicin sensitive neurons. * p<0.05 (One-way ANOVA, Bonferroni post-test).

MECHANISMS IMPLIED IN WHIRLIN MODULATION OF TRPV1

Whirlin modulates TRPV1 stability

To gain insight into the mechanism followed by Whirlin to modulate TRPV1 protein expression we first investigated the kinetics of TRPV1 turnover in HEK293 cells coexpressing TRPV1 with Whirlin or with YFP as a control. Cells were treated with the protein synthesis inhibitor cycloheximide (300 µg/ml) and collected at timed intervals between 0 and 24 hours. Proteins extracts were resolved by SDS-PAGE (Sodium Dodecyl Sulfate Polyacrylamide Gel Electrophoresis) and analysed by western immunoblot (**Figure 30A**). Remaining TRPV1 at each time was quantified and expressed as a percentage of initial total expression (0 hours). As we can observe in **Figure 30B**, TRPV1 was highly stable and only moderately degraded in our control condition for all the duration of the experiment (black line). Conversely, in cells coexpressing both proteins, Whirlin rapidly disappeared after 4 hours of treatment (grey hatched line) causing the parallel degradation of TRPV1 (grey line).

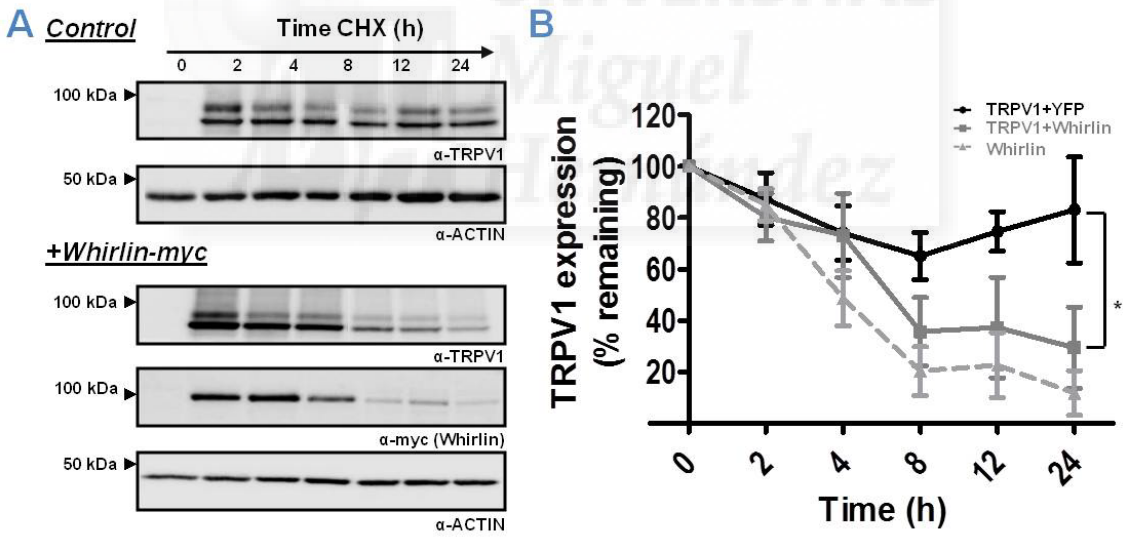

Figure 30 Whirlin degradation reduces TRPV1 stability. (A) Representative immunoblots of TRPV1 and Whirlin after treatment with the protein synthesis inhibitor cycloheximide. **(B)** Densitometric quantification of 3 independent experiments with data expressed as mean ± S.E.M. Actin was used as a loading control. The graph depicts the fraction of the remaining TRPV1 after 2-24 hours cycloheximide treatment for control TRPV1+YFP (black line) and TRPV1+Whirlin condition (gray line) compared with no treated cells (0 hours, 100%). Remaining Whirlin was also quantified and represented (Whirlin; gray hatched line). * p<0.05, paired *t* test.

One hypothesis that agrees with these results considers that both proteins form a complex, and either protein translation blockade with cycloheximide or Whirlin downregulation with specific siRNAs lead to TRPV1 destabilisation and its consequent delivery to degradation. To test this hypothesis, F11 cells co-expressing TRPV1+Whirlin and transfected with 50 nM siRNA-2 were treated with the proteasome inhibitor MG132 and then analysed by confocal

microscopy after double immunocytochemical staining of both proteins. **Figure 31** indicates that application of MG132 was able to prevent the disappearance of both expressed Whirlin and TRPV1, thus suggesting that Whirlin downregulation leads to a destabilisation and a concomitant reduction of the thermoTRP expression.

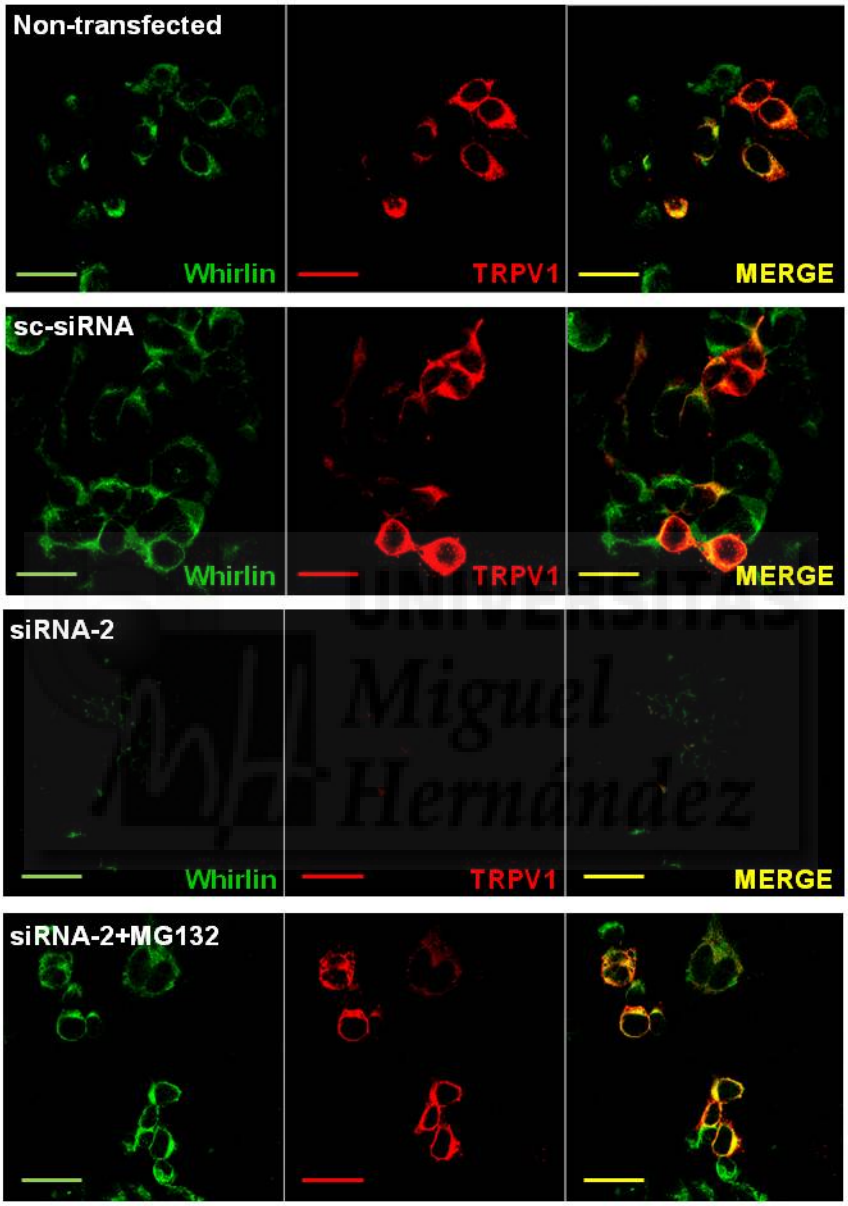

Figure 31 Proteasomal inhibition reverses the effect of Whirlin silencing on TRPV1 expression. F11 cells coexpressing TRPV1+Whirlin were transfected with 50 nM siRNA-2 or a sc-siRNA and treated or not with the proteasomal inhibitor MG132 (2 μM). Non-transfected cells were used as control condition. When proteasomal degradation was inhibited, both Whirlin and TRPV1 expression was recovered. Scale bars 10 μm.

We also evaluated the effect of Whirlin downregulation and proteasomal inhibition on TRPV1 activity by Ca^{2+} microfluorography. As previously described, siRNA-2 transfection drastically reduced capsaicin-induced responses in F11 cells co-expressing TRPV1+Whirlin (**Figure 32**). This effect required the presence of Whirlin as it was ineffective in control F11 cells that were not transfected with the PDZ-scaffolding protein and it was sequence specific since

the sc-siRNA did not abrogate TRPV1 activity. Notably, inhibition of proteasome degradation with MG132 was able to prevent siRNA-2 induced abrogation of TRPV1 activity.

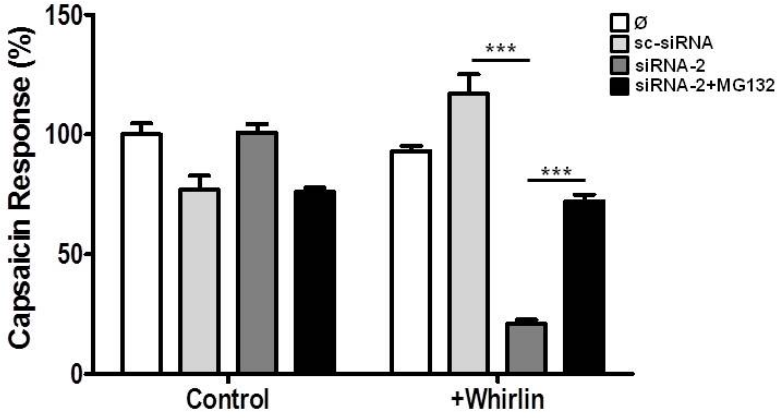

Figure 32 Proteasomal inhibition reverses the effect of Whirlin silencing on TRPV1 activity. Ca^{2+} microfluorographic assay in F11 cells expressing TRPV1 in presence or absence (Control) of Whirlin and transfected with sc-siRNA or siRNA-2. Ca^{2+} responses were evoked with 100 µM capsaicin. AUC were calculated and normalised to the response of TRPV1-expressing F11 untreated cells (Ø). siRNA-2 was transfected at 50 nM, and proteasomal inhibition was carried out with 2 µM MG132. Data expressed as mean ± S.E.M with N=5. *** p<0.001. Two-way ANOVA, followed by Bonferroni post-test.

The ubiquitin-proteasome system (UPS) and the lysosomal machinery are the two major pathways responsible for cellular proteins catabolism. Since proteasomal inhibition was able to reverse the inhibitory effect of Whirlin downregulation on both receptor expression and activity, we next sought to investigate in detail the mechanism of constitutive TRPV1 degradation in presence or absence of the PDZ protein, using specific inhibitors of both processes. HEK293 cells expressing TRPV1+YFP or TRPV1+Whirlin were treated for 12 hours with 1 µM epoxomicin (E) or with 100 µM leupeptin (L) in order to inhibit the proteasome or lysosomal proteases activity, respectively (Lee and Goldberg 1996;Meng *et al.* 1999). As shown in **Figure 33**, treatment with epoxomicin, but not with leupeptin, induced a ~35% increase in the expression levels of TRPV1 in the absence of Whirlin (L: 107±11%; E: 136±13%), which indicates that proteasomal but not lysosomal degradation is mainly implicated in basal TRPV1 catabolism. Notably, proteasome inhibition did not produce a further significant increase in TRPV1 expression when Whirlin was coexpressed (Veh E: 135±12%; E: 152±16%), which substantiates a role for the PDZ protein in stabilising the thermoTRP and preventing its degradation through the proteasome.

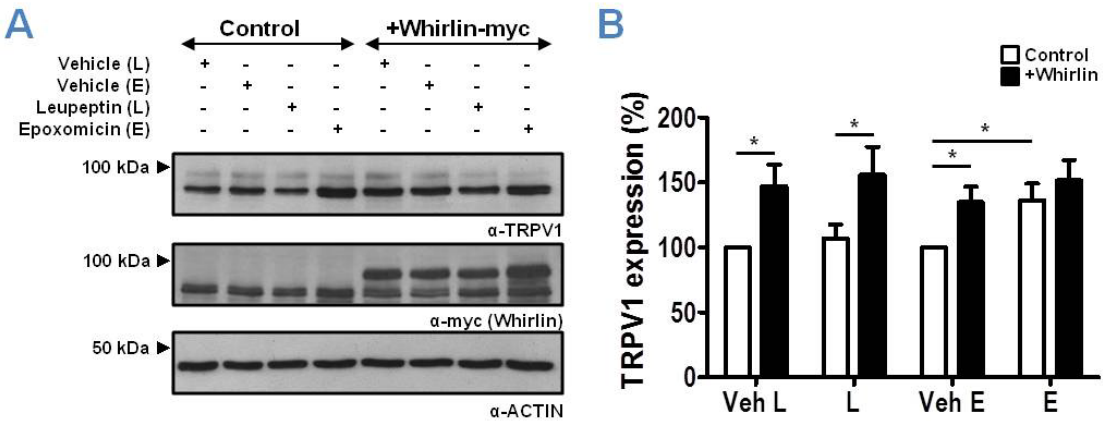

Figure 33 Whirlin reduces TRPV1 degradation through the proteasome (A) Representative immunoblots of protein extracts from TRPV1+YFP (Control) or TRPV1+Whirlin HEK293 cells treated with 100 µM leupeptin (L) or 1 µM epoxomicin (E) or their respective vehicles, water and DMSO. **(B)** Densitometry of 6 independent experiments. Data expressed as mean percentage increase in TRPV1 signal ± S.E.M. compared with control (Veh). Proteasomal but not lysosomal inhibition induced a significant increase in total TRPV1. Whirlin induced a significant increase of TRPV1 in all conditions but not in cells treated with epoxomicin. * p<0.05 (paired *t* test).

Thereafter, in order to establish whether Whirlin overexpression had any direct effect on proteasome activity, we used a reporter plasmid encoding for a protein specifically catabolised through this degradative pathway, that is a polyubiquitin chain covalently attached to the green fluorescent protein (GFP) to prevent its removal by deubiquitination machinery (Ub^{G76V}GFP) (Um *et al.* 2010). HEK293 cells were transfected with this plasmid, in presence or absence of Whirlin, and treated with the proteasomal inhibitor epoxomicin (1 µM) or its vehicle (DMSO) for 12 hours. In control cells, instead of YFP, a Dynamin construction was coexpressed with Ub^{G76V}GFP in order to avoid any cross-reactivity of the anti-GFP antibody with the yellow variant of the fluorescent tag. Protein extracts were then analysed by western immunoblot and densitometrically quantified (**Figure 34A** and **B**). As expected, treatment with the proteasome inhibitor epoxomicin increased Ub^{G76V}GFP levels compared with its vehicle (132±6% in control and 152±21% in Whirlin coexpressing cells), whereas Whirlin coexpression produced no significant effect (104±11%) in non-treated cells. Thus our results indicate that the presence of the PDZ protein does not inhibit proteasome activity.

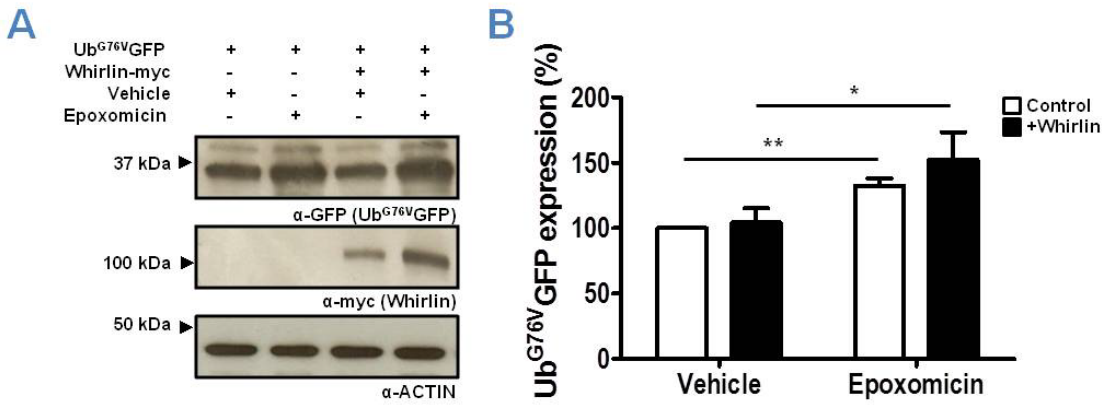

Figure 34 Whirlin does not affect proteasomal activity. (A) Representative immunoblot of protein extracts from Ub^{G76V}GFP + Dynamin (control) or Ub^{G76V}GFP+Whirlin HEK293 coexpressing cells treated with epoxomicin or its vehicle (DMSO). **(B)** Quantification of 3 independent experiments with data expressed as percentage increase in Ub^{G76V}GFP signal ± S.E.M. * $p<0.05$, ** $p<0.01$ (paired *t* test).

Subsequently, we sought to determine whether Whirlin was able to modulate TRPV1 ubiquitination, the canonical signal for proteasomal recognition (Saliba *et al.* 2008). Essentially, two types of ubiquitin modification may occur: **polyubiquitination** refers to the anchoring of a polyubiquitin chain to a lysine residue in the target substrate whereas monoubiquitination denotes the target modification by a single or multiple ubiquitins. HEK293 cells were transfected with a myc-tagged TRPV1, an untagged Whirlin and a hexahistidine (His6)-tagged Ubiquitin. An untagged TRPV1 was used as a negative control. After lysis in Radioimmunoprecipitation Assay (RIPA) buffer containing proteasome and deubiquitinases inhibitors, an immobilised anti-myc antibody was used to immunoprecipitate TRPV1. Complexes were then resolved by SDS-PAGE and analysed by western immunoblot. Two different antibodies were used to detect ubiquitin conjugates: anti-FK2, able to recognise both mono- and polyubiquitin conjugates, and anti-FK1, specific for polyubiquitinated proteins. **Figure 35A** displays a stronger ubiquitin smear with both antibodies when Whirlin was coexpressed (well 3) compared to the control (well 4), thus indicating an increased accumulation of TRPV1-ubiquitin conjugates. Importantly, the level of ubiquitination of individual TRPV1 receptors (expressed as the ratio between ubiquitin and TRPV1 signals) was not significantly altered (**Figure 35B**). However, we cannot exclude that Whirlin may be similarly ubiquitinated thus contributing to the increased smear signal detected when both proteins were co-expressed.

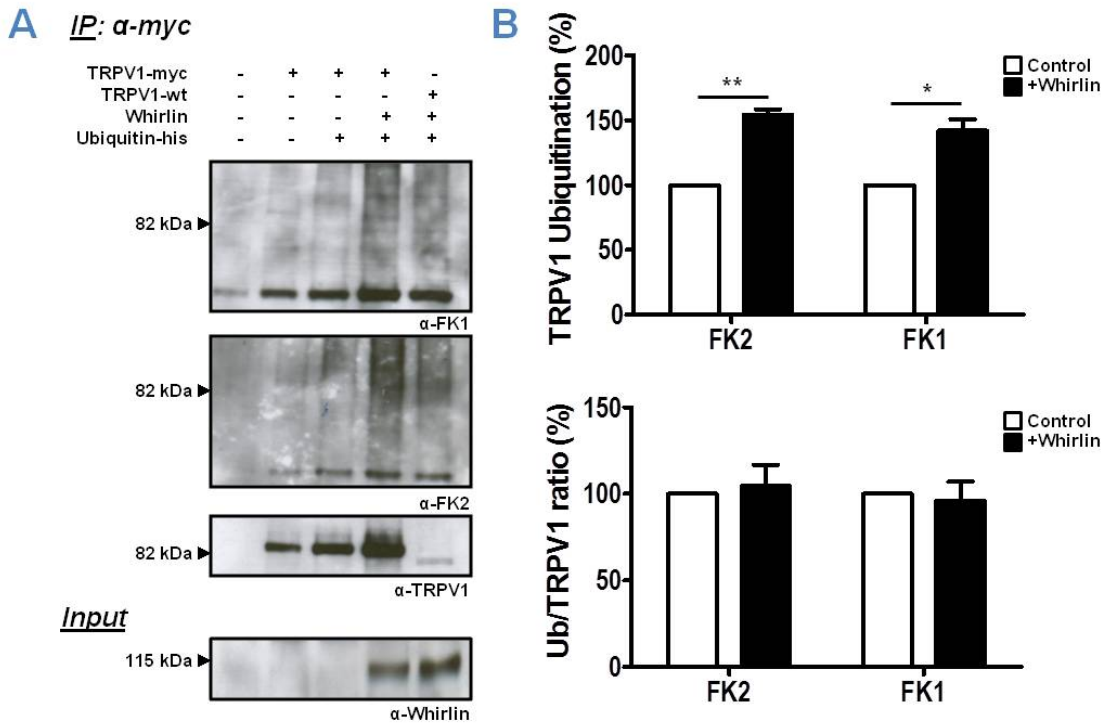

Figure 35 Whirlin increases the abundance of TRPV1-ubiquitin conjugates. (A) HEK293 cells were transfected with TRPV1-myc, Ubiquitin-his ± Whirlin and lysed in RIPA buffer plus proteasome and deubiquitinases inhibitors. Agarose anti-myc was used to immunoprecipitate TRPV1, anti-FK1 to detect polyubiquitinated proteins and anti-FK2 for both mono- and polyubiquitinated conjugates. **(B)** Densitometric quantification of 3 independent experiments with data expressed as mean percentages ± S.E.M. *Top panel*: quantification of the ubiquitin signal. *Lower panel*: ubiquitin/total TRPV1 ratio. * $p<0.05$, ** $p<0.01$ (paired t test).

The ubiquitin-dependent proteasomal elimination of TRPV1 may represent the final step of an endoplasmic reticulum (ER)-associated degradation (ERAD) process, a specialised quality control mechanism traditionally associated with the clearing of aberrant proteins and recently claimed to regulate the amount of receptors available for cell surface trafficking (Abriel and Staub 2005;Zemoura *et al.* 2013). Thus, it is tempting to hypothesise that Whirlin may act as a chaperone-like protein facilitating the folding and assembly of newly synthesised receptors in the ER, which are then subsequently exported reducing the amount of misfolded substrates available for ERAD. In this context, TRPV1 has been reported being expressed as both simple and complex glycosylated forms. Consistent with previous reports, we recognised a doublet at ~88 and ~95 kDa, corresponding to the non-glycosylated and the early N-glycosylation products occurring in the ER, and a diffuse band at ~115 kDa, corresponding to the more mature glycosylated form produced in the Golgi apparatus. The three products were detected both in total extracts and in plasma membrane fractions isolated by biotinylation (see **Figure 18**), thus confirming that N-glycosylation is not a requisite for the localisation of TRPV1 to the cell surface (Veldhuis *et al.* 2012). In order to determine the putative influence of Whirlin on immaturely and maturely glycosylated forms of TRPV1, the bands with different molecular weights were individually quantified. As the doublet could not be easily resolved, we considered it as a unique band. To overcome in part this limitation, we also performed the same biotinylation assays in cells coexpressing the glycosylation-defective mutant N604T, plus Whirlin or YFP in controls.

Western immunoblots (**Figure 36A-B**) followed by densitometric analysis revealed that Whirlin significantly enhanced the intensity of the non- and simple-glycosylated forms of TRPV1 wild-type as well as of the N604T mutant in both total and membrane fractions, reflecting as before an increase in receptor expression that could traffic normally to the plasma membrane (**Figure 36C-E**). Conversely, Whirlin had little or no effect on the post-ER mature glycosylated TRPV1 form (**Figure 36C-D**).

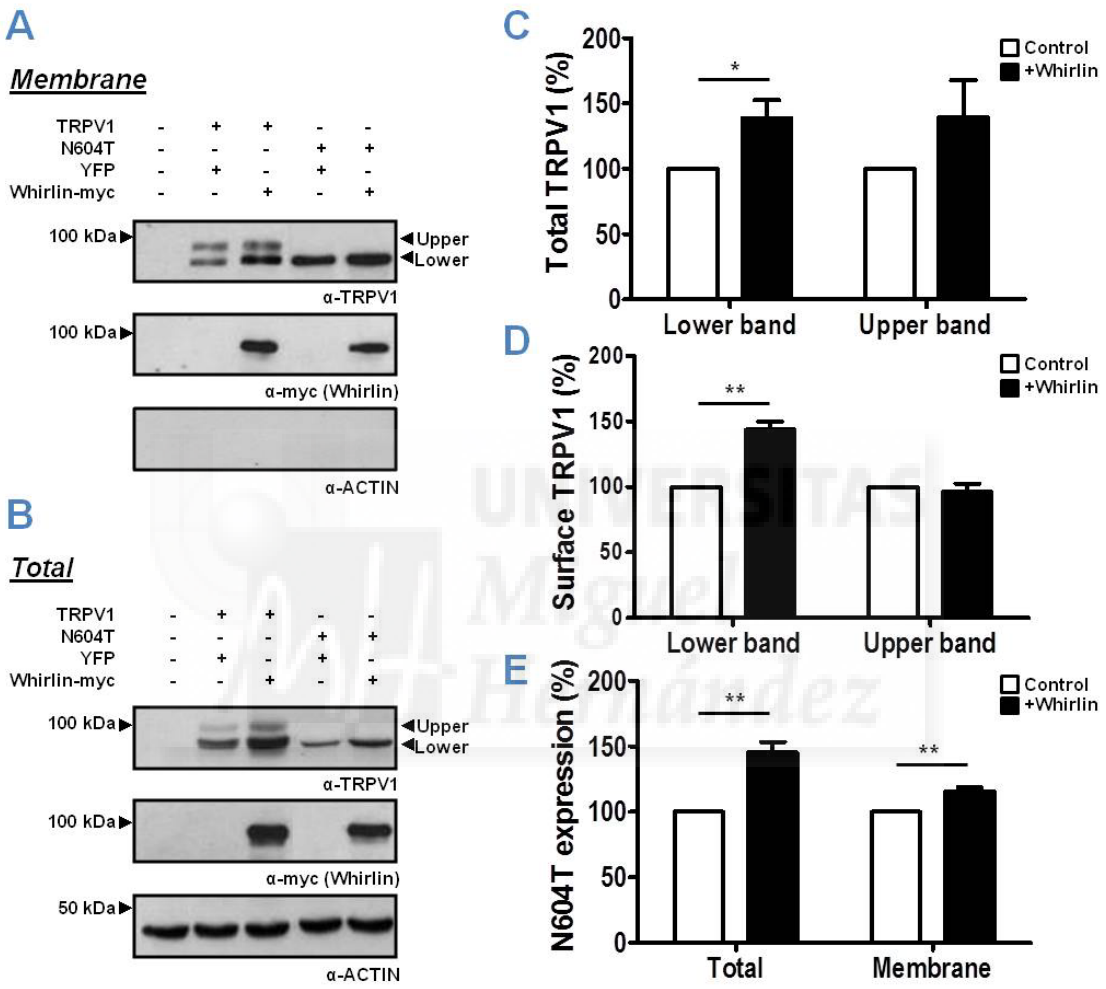

Figure 36 Whirlin mainly increases total and surface levels of non-glycosylated wild-type TRPV1 and N604T mutant. (A,B) Representative immunoblots of total and membrane fractions from biotinylated HEK293 cells expressing YFP (Control) or Whirlin with wild-type TRPV1 or the glycosylation-defective mutant N604T. **(C,D)** Densitometric quantification of simple (lower band) and complex glycosylated (upper band) forms of TRPV1 from total and surface fractions. **(E)** Densitometric quantification of total and surface fractions of N604T mutant. 5 independent experiments were realised. * $p<0.05$; ** $p<0.01$ (paired *t* test).

We next investigated if Whirlin exerted the same effect on the stability of TRPV1-AD2, a previously described TRPV1 chimeric mutant in which the TRP domain of TRPV1 was replaced by the corresponding part of TRPV2, mutation that results in a dramatic effect on protein expression and function (Gregorio-Teruel *et al.* 2014). Given the proposed role of the TRP domain in channel multimerisation, the TRPV1-AD2 phenotype has been proposed to be probably due to an impairment of protein folding causing its degradation. Western immunoblot

analysis of total protein extracts from HEK293 cells coexpressing the TRPV1-AD2 mutant with YFP as control resulted in almost undetectable levels of TRPV1-AD2, but its expression was boosted when Whirlin was coexpressed (**Figure 37A**). Strikingly, TRPV1-AD2 was not glycosylated as the wild-type receptor, and was detected as a unique band at the same molecular weight of the non-glycosylated TRPV1 wild-type form. Notably, proteasome inhibition with Epoxomicin produced a strong increase in AD2 expression. Subsequently we performed biotinylation assays in order to quantify Whirlin effect on total and surface TRPV1-AD2 expression. Representative immunoblots and densitometric quantification reported in **Figure 37B-C** confirmed that Whirlin induced a significant increase in total TRPV1-AD2 expression. The membrane levels were also slightly enhanced although without reaching statistical significance.

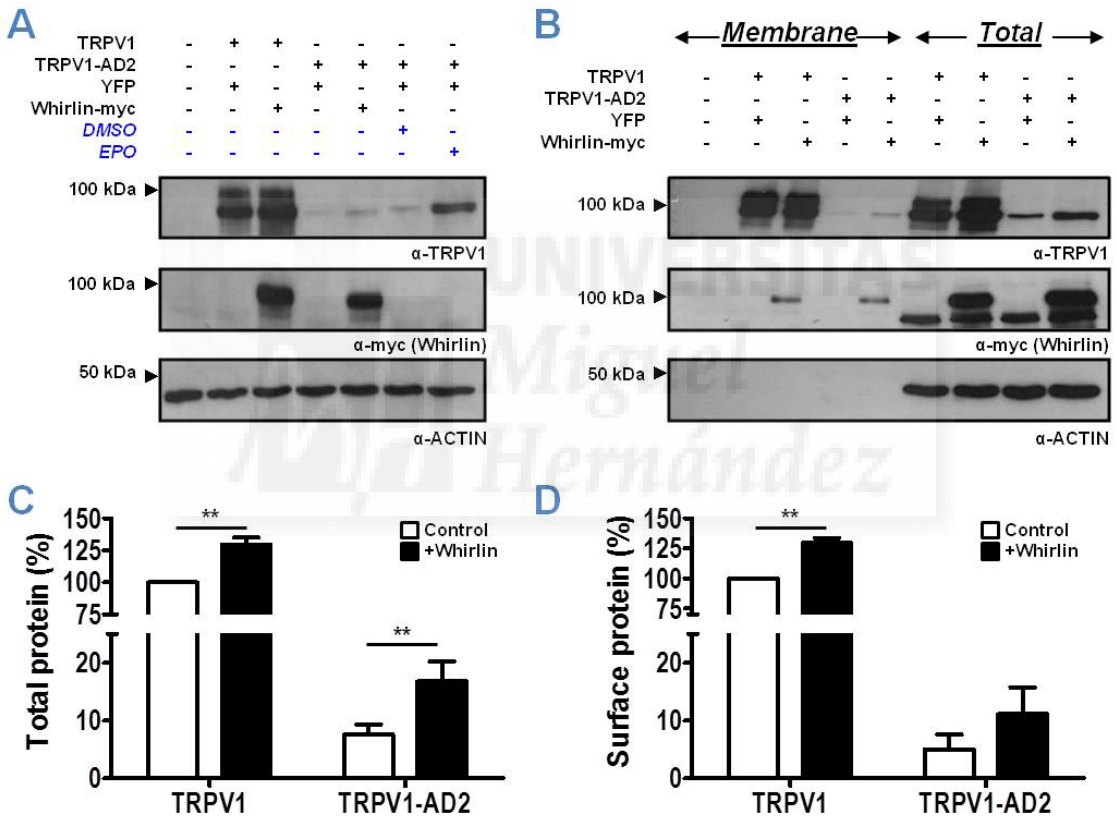

Figure 37 Whirlin increases TRPV1-AD2 total and surface expression. (A) Representative immunoblot from total extracts of HEK293 coexpressing TRPV1 wild-type or AD2 mutant and Whirlin or YFP as control. A single barely detectable band was observed for AD2. Epoxomicin (vehicle: DMSO) was used to inhibit proteasomal degradation. Total expression was increased and a higher molecular weight band was detected. **(B)** Representative immunoblots from biotinylation assays from HEK293 cells coexpressing TRPV1 wild-type or AD2 mutant and Whirlin or YFP as control. **(C)** Densitometric quantification of total (left panel) and surface (right panel) fractions from 5 independent experiments. * p<0.05; ** p<0.01. For surface AD2 p=0.0532 when control was compared to +Whirlin condition. Paired *t* test.

As for wild-type TRPV1, we also investigated if the increased expression of TRPV1-AD2 by Whirlin allowed detecting functional activity. Accordingly, we performed Ca^{2+} microfluorographic assays in HEK293 expressing either the wild-type or mutant TRPV1 constructions plus Whirlin or empty pcDNA as control. As TRPV1-AD2 is essentially inactive,

Ca^{2+} influx was evoked with two different high concentrations of capsaicin, 50 and 100 µM. Fluorescence emission was detected through the microplate reader POLARstar Omega and AUC were calculated and normalised to the response of cells expressing TRPV1 alone. As illustrated in **Figure 38**, Ca^{2+} influx through either the wild-type or mutant TRPV1 receptors was not modified by Whirlin coexpression in any of our assayed conditions. Although more extensive investigations should be performed, these preliminary results propose a chaperone-like activity for the PDZ protein Whirlin which complexes and stabilises TRPV1 by probably promoting the assembly and folding of new synthesised receptors in the ER and reducing the associated ubiquitin-mediated degradation through the proteasome.

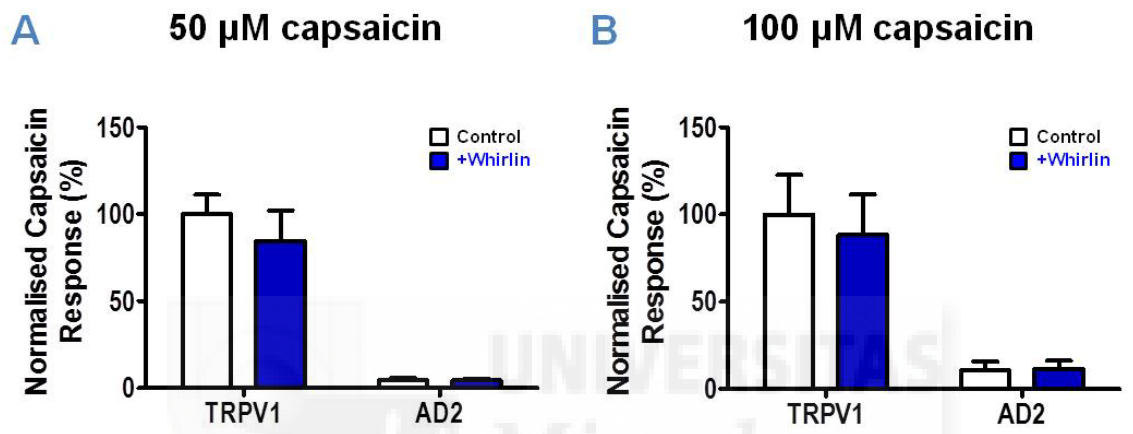

Figure 38 Whirlin does not modify Ca^{2+} influx through TRPV1 AD2 mutant. Normalised capsaicin-induced calcium influx in control or +Whirlin HEK293 cells expressing wild-type or AD2 TRPV1 constructions. **(A)** 50 µM and **(B)** 100 µM capsaicin were tested. Data expressed as mean ± S.E.M. Two-way ANOVA, followed by Bonferroni post-test. N=4.

Whirlin effect on TRPV1 stability at the cell surface

The increase in TRPV1 expression may also be a consequence of augmented stability of the receptor at the plasma membrane in the presence of Whirlin, which is a classical effect of coexpressing scaffolding proteins like those containing PDZ domains (Saliba *et al.* 2008). This possible effect was assessed by comparing TRPV1 internalisation/degradation rates in presence or absence of Whirlin. Surface membranes were biotin labelled and, after incubation for different time periods at 37 ºC to promote receptor internalisation, biotinylated proteins were then isolated with the high-affinity resin streptavidin, resolved by SDS-PAGE and analysed by western immunoblot (**Figure 39A**). The levels of remaining TRPV1 at each time point were quantified by densitometry and represented as percentage of total receptor (at 0 hours). As illustrated, similar levels of internalisation/degradation of cell surface receptor were detected in the presence of Whirlin after 24 hours compared with control (**Figure 39B**).

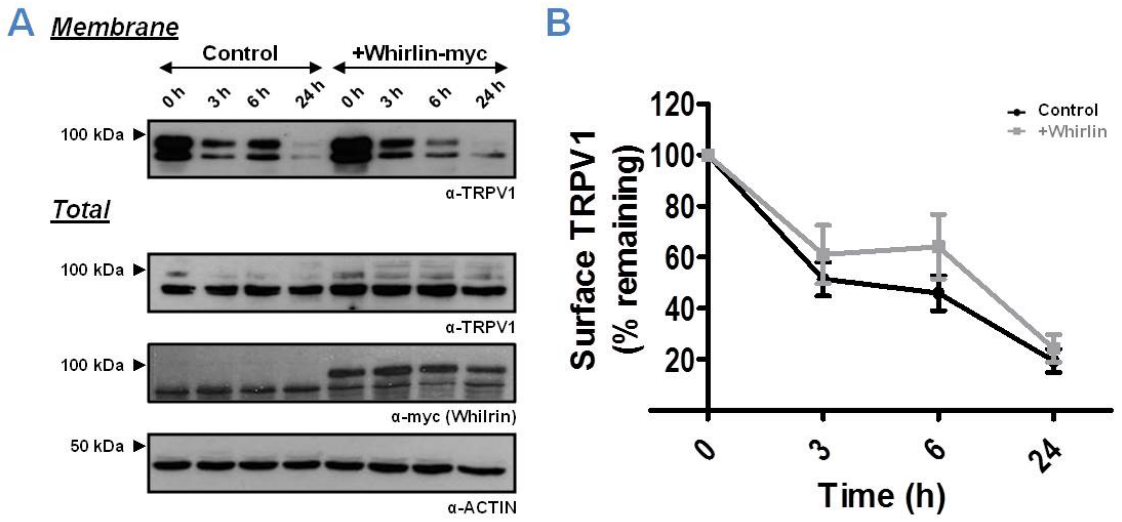

Figure 39 Whirlin does not alter constitutive surface TRPV1 internalisation/degradation. (A) Representative immunoblot of total and membrane TRPV1 fractions from HEK293 cells biotinylated and incubated at 37 ºC for different time periods. **(B)** Graph showing mean percentage of remaining surface TRPV1 ± S.E.M. at different time points compared with total receptor amount (at 0 hours) from more than 3 independent experiments. Paired *t* test.

Although global turnover of TRPV1 observed did not appear altered over a long period of time, we cannot exclude that Whirlin might stabilise TRPV1 by decreasing its endocytosis and/or increasing its recycling from an endocytic pool. To evaluate whether Whirlin coexpression renders TRPV1 more stable at the plasma membrane, we performed cell surface biotinylation experiments by applying a prolonged stimulus of 10 µM capsaicin for 20 minutes, a condition previously shown to rapidly internalise and target TRPV1 for lysosomal degradation (Sanz-Salvador *et al.* 2012). As shown in **Figure 40**, treatment with capsaicin caused a pronounced decrease in surface TRPV1 in control conditions that appeared attenuated when Whirlin was present (TRPV1+YFP: 53±11%; TRPV1+Whirlin: 72±13%), thus suggesting that TRPV1 at the plasma membrane is more stable when coexpressed with Whirlin.

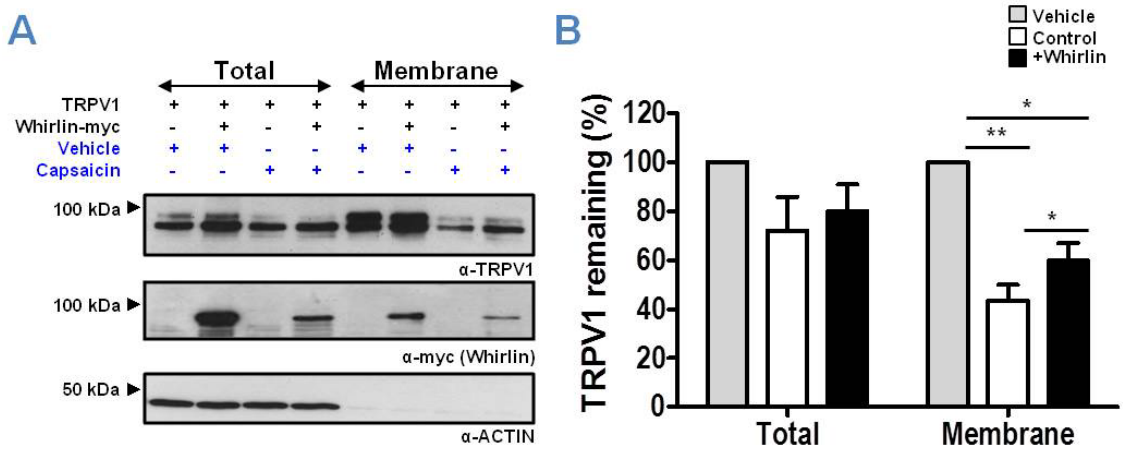

Figure 40 Whirlin reduces TRPV1 capsaicin-induced internalisation. (A) Representative immunoblots of total and membrane fractions from HEK293 cells treated with 10 µM capsaicin or vehicle (DMSO) for 20 minutes at 37 ºC and then biotinylation. **(B)** Remaining TRPV1 expressed as mean percentage ± S.E.M. of vehicle condition (100%) from 5 independent experiments. * p<0.05; ** p<0.05. Paired *t* test.

Whirlin effect on TRPV1 subcellular distribution

In order to gain further insights into the intracellular localisation of TRPV1 and Whirlin when expressed individually or both together, fractionation of HEK293 cells extracts was performed. Differential centrifugations of postnuclear supernatants yielding soluble (S100), heavy membranes (P14) and light membranes/microsomal (P100) fractions were subsequently analysed by western immunoblot and densitometry (**Figure 41A**). Markers for plasma membrane (Na^+/K^+ ATPase), early endosomes (EEA1) and lysosomes (LAMP2) were used to identify the different fractions. Consistent with previous reports, Na^+/K^+ ATPase was enriched in P14 fractions, EEA1 in the P14 and S100 fractions and LAMP2 was most abundant in the P14 fraction and present to a lesser extent in the P100 fraction (Robinson and Dixon 2005). As expected for a membrane associated receptor, TRPV1 was most abundant in P14 and P100 membrane fractions whereas Whirlin was almost equally distributed in the three fractions, but especially in the vesicle-enriched P100 fraction, suggesting that the two proteins may form a complex associated with vesicles or other light membranes.

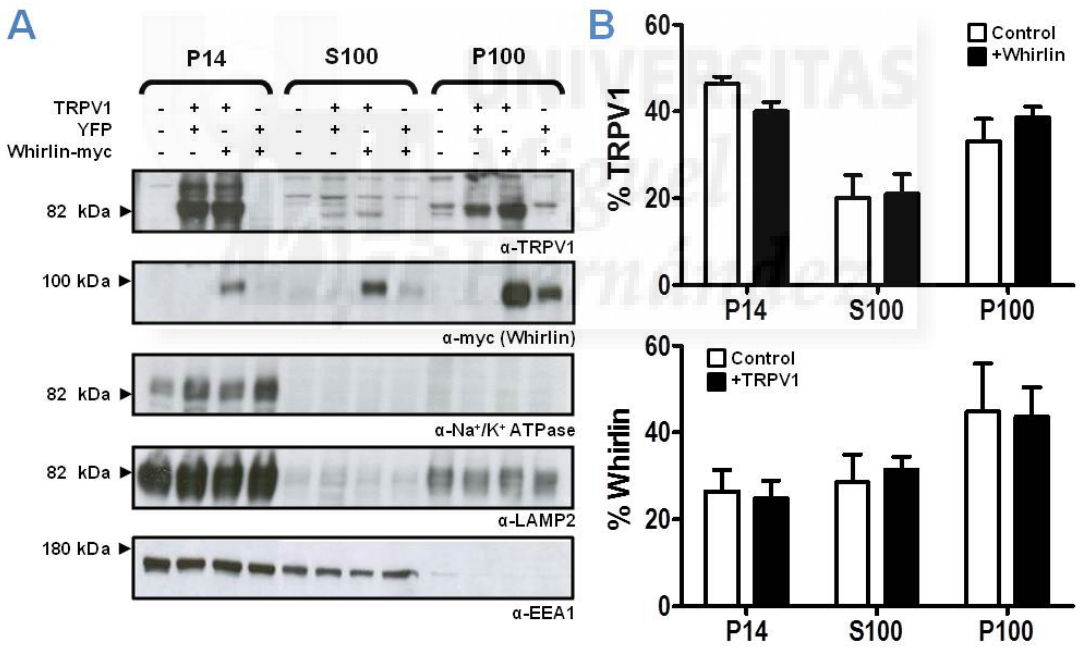

Figure 41 Subcellular localisation of TRPV1 and Whirlin in HEK293 cells. (A) HEK293 cells expressing TRPV1 or Whirlin alone or both proteins together were fractionated to yield soluble (S100), heavy membrane (P14), and microsomal (P100) fractions. The Na^+/K^+ ATPase antibody was used as a marker for the plasma membrane, EEA1 for early endosomes and LAMP2 for lysosomes. **(B)** The relative abundance of TRPV1 and Whirlin in subcellular fractions was determined by densitometric analysis of immunoblots. Data expressed as mean percentage ± S.E.M. Two-way ANOVA, followed by Bonferroni post-test. N=3.

Subsequently, to further resolve these fractions, postnuclear fractions were separated on a self-forming Percoll density gradient, widely employed for separating endocytic organelles. As shown in **Figure 42**, TRPV1 was distributed along the entire endocytic pathway with no apparent alteration produced by Whirlin coexpression. Interestingly, Whirlin was found to be enriched in the lighter fractions containing the early endosomal marker EEA1 with only little

amounts in the denser lysosomal fractions labelled by LAMP2, which could indicate a putative involvement of Whirlin in internalisation and/or recycling processes.

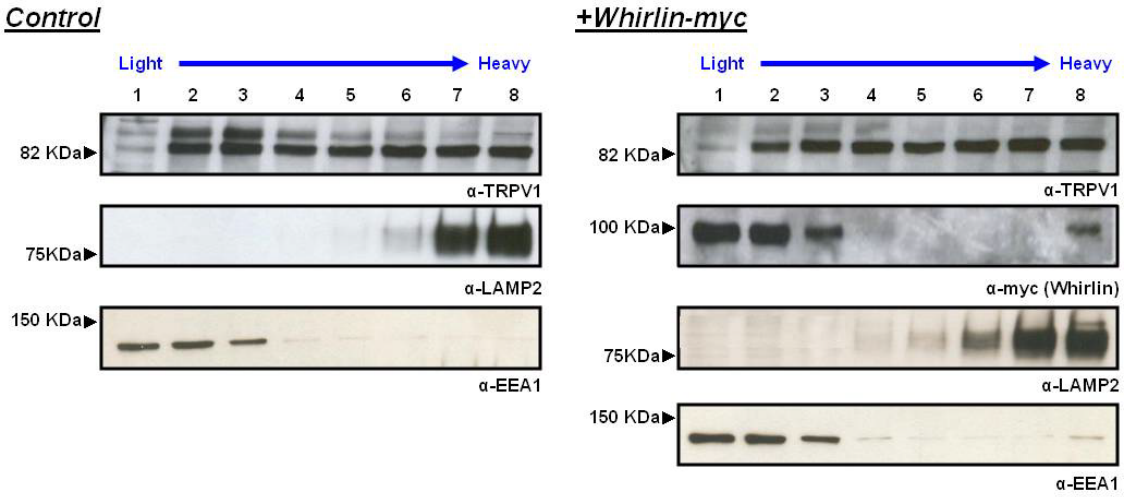

Figure 42 Subcellular distribution of TRPV1 and Whirlin along the endocytic pathway. Subcellular fractionation on Percoll density gradient centrifugation of postnuclear fractions from HEK293 cells transfected with TRPV1 plus YFP (Control) or Whirlin. Fractions were collected from the top of the gradient and analysed by SDS-PAGE and immunoblot with antibodies specific for TRPV1 and Whirlin (α-myc) and marker proteins for early endosomes (EEA1) and lysosomes (LAMP2). Representative blots from one of 3 experiments are showed.

Finally, we sought to investigate whether the receptor distribution in specific membrane domains was altered or not by the coexpression of the PDZ protein. We centred our interest on lipid rafts since TRPV1 localisation in these specialised membrane micro-environments, rich in sphingolipids and cholesterol, play a crucial role in the organisation of specific signalling pathways (like those implicated in endo- or exocytosis) by favouring protein–protein interactions (Simons and Toomre 2000). Taking advantage of the resistance of lipid rafts to extraction by Triton X-100 (or other detergents) at 4 ºC and of their low buoyant density, we isolated them from the upper floating fractions after sucrose gradient ultracentrifugation. Flotilin was used as a marker for lipid rafts, corresponding mostly to fractions 1 and 2, although a weaker signal was also visible in the last fraction (**Figure 43**). The complex glycosylated form of TRPV1 localised to lipid rafts independently of being expressed individually or with Whirlin, whereas the less mature forms concentrated primarily in the heavier fractions. Interestingly, Whirlin was especially enriched in the raft fractions, although detectable at lower levels along the entire gradient.

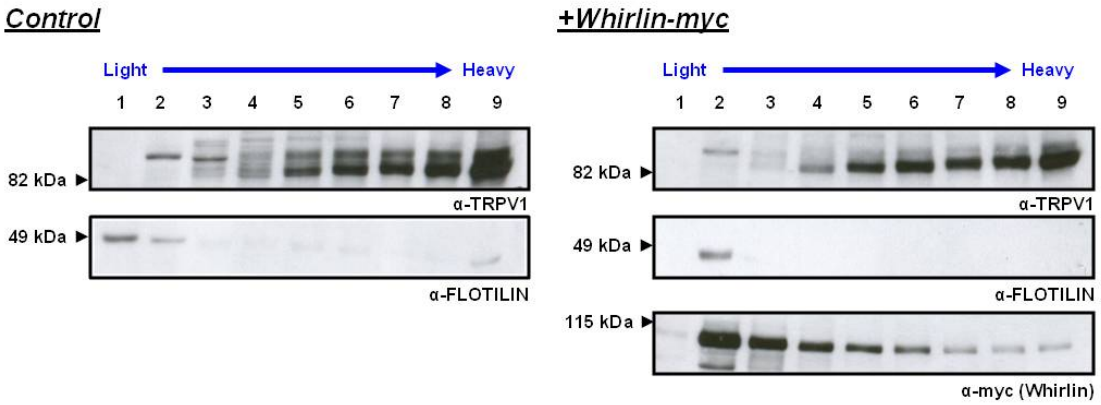

Figure 43 TRPV1 and Whirlin are present in lipid rafts. Total HEK293 free-detergents extracts were ultracentrifuged on a continuous sucrose gradient. 1 ml fractions were recollected from the top to the bottom of the gradient and the same volume from each fraction was analysed by SDS-PAGE and western immunoblot. Representative immunoblots are reported. Flotilin was used as a marker for lipid rafts.

The role of lipid rafts and Whirlin on TRPV1 function was also examined by performing Ca^{2+} fluorimetric assays on cells treated with Methyl-β-cyclodextrin (MβCD), a specific cholesterol-binding agent commonly known to disrupt lipid rafts by depleting membrane cholesterol. The applied protocol consisted of a first pulse of 1 μM capsaicin for 15 seconds (Cap1 in **Figure 44**), followed by a 5 minutes washing step and a 15 minutes treatment with 10 mM MβCD or the corresponding vehicle (Hank's balanced salt solution -HBSS- solution). A second 1 μM capsaicin pulse (Cap2) was applied for 15 seconds after another 5 minutes washing step. In **Figure 44** representative traces are displayed for the control condition TRPV1+pcDNA (**panel A**) or for cells coexpressing TRPV1+Whirlin (**panel B**). The ratio between the amplitude of the second peak versus the first one was calculated and expressed as percentage (**Figure 44C**): in both conditions MβCD induced a similar slight decrease (~20%) in the amplitude of capsaicin-induced response, thus indicating that the function of TRPV1 in cholesterol-rich membrane microdomains was not affected by the coexpression of Whirlin.

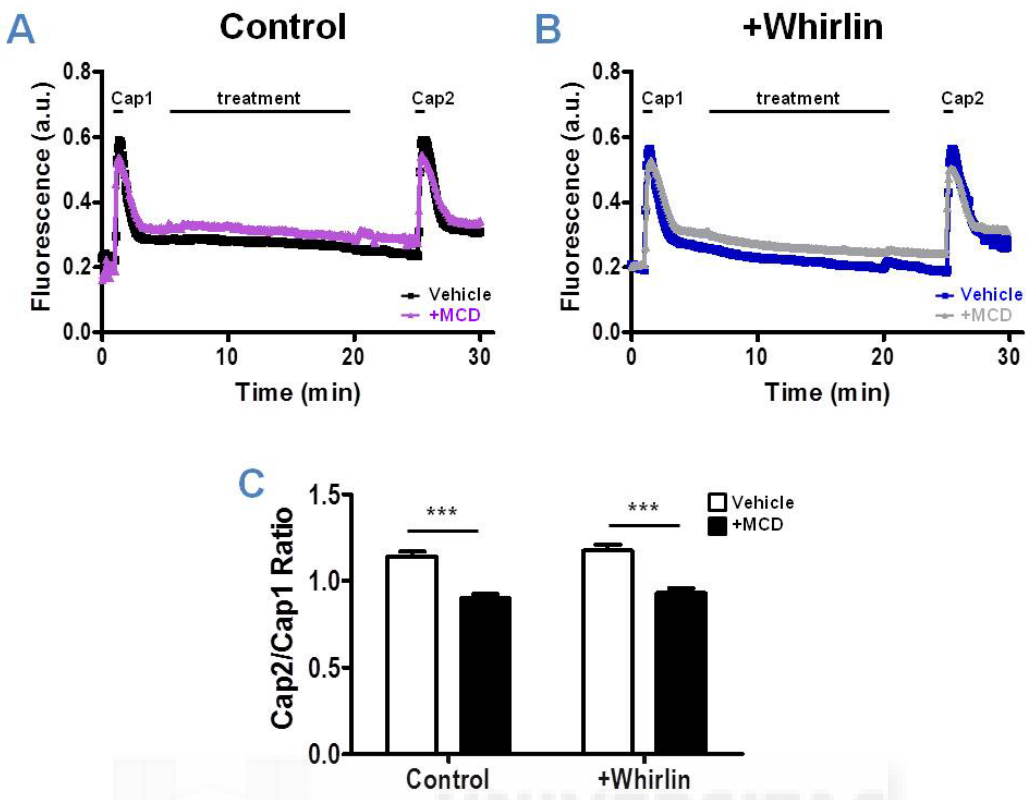

Figure 44 MβCD treatment decreases TRPV1 capsaicin-induced responses. (A) Representative traces from Ca^{2+} imaging assays in control cells (TRPV1+pcDNA). Cap1, Cap2: first and second pulse of 1 μM capsaicin. Treatment: vehicle (HBSS, black) or MβCD (purple). a.u.: arbitrary units. **(B)** Representative traces from Ca^{2+} imaging assays in cells coexpressing TRPV1+Whirlin. Cap1, Cap2: first and second pulse of 1 μM capsaicin. Treatment: vehicle (HBSS, blue) or MβCD (gray). a.u.: arbitrary units. **(C)** Ratio between the amplitude of response to the second pulse versus the first one. Data from three independent experiments and n>150 cells per condition expressed as percentage ± S.E.M., *** p<0.001. Two-way ANOVA, Bonferroni post-test.

TRPV1 EXPRESSION AND ACTIVITY IN WHIRLER MUTANT AND WHIRLIN$^{NEO/NEO}$ TRANSGENIC MICE

As previously mentioned, TRPV1 plays a crucial role in the transduction of painful thermal and chemical stimuli. Thus, once demonstrated that Whirlin was essential for TRPV1 stability *in vitro*, we investigated if different mutations of the PDZ protein in mice influenced TRPV1 receptor expression or function. For that task, we selected two different models, the whirler mutant and whirlin$^{neo/neo}$ transgenic mice. TRPV1 distribution and TRPV1-mediated responses were assessed both *ex vivo* and *in vivo*. Specifically, nociceptive behaviour was evaluated in basal conditions as well as using an inflammatory model consisting in Complete Freund's adjuvant (CFA) injection. Acute sensitivity to noxious thermal stimuli was measured by radiant plantar test (Hargreaves' Method) whereas the mechanical sensitivity was measured by a dynamic plantar Von Frey aesthesiometer.

Whirlin mRNA transcripts in whirler and whirlin$^{neo/neo}$ mice

To characterise Whirlin mRNA expression in our animal models first we performed reverse transcriptase polymerase chain reactions (RT-PCR) in DRG tissues. Specific primers to distinguish the N-terminal (Exons 1–3) from C-terminal (Exons 11-13) isoforms of Whirlin were used. Actin mRNA expression was used as a control for total RNA present. As shown in **Figure 45**, robust expression of both Whirlin (Exons 1-3) and (Exons 11-13) mRNA was observed in DRG tissue from wild-type (C57BL/6J) as well as whirler mice. As expected, no expression of Whirlin (Exons 1-3) mRNA was observed in whirlin$^{neo/neo}$ DRGs tissue, whereas Whirlin (Exons 11-13) mRNA was still detected although at a lower level.

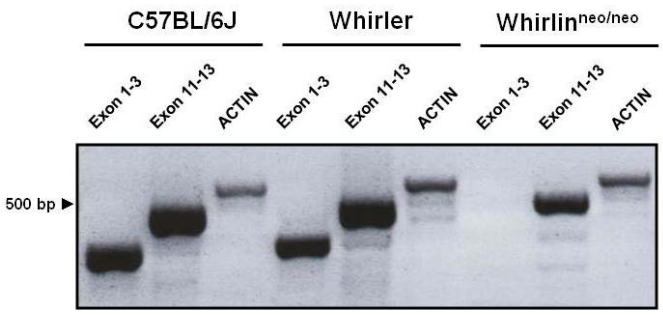

Figure 45 Both N- and C-terminal Whirlin mRNA transcripts are expressed in DRGs tissue. RT-PCR analysis from adult wild-type (C57BL/6J), whirler and whirlin$^{neo/neo}$ DRG was performed. mRNA transcripts were amplified using primers located on Whirlin exons 1-3 and 11-13 or actin exons 2 and 4. Both N- and C-terminal transcripts were detected in wild-type as well as whirler mice, whereas C- but no N-terminal transcripts were detected in the whirlin$^{neo/neo}$ transgenic mouse model.

TRPV1 and Whirlin protein expression in DRG and spinal cord tissues

Whirlin and TRPV1 protein expression in DRG extracts (two mice per group) was analysed by immunoblots with an antibody able to recognise all mouse Whirlin isoforms except the two short N-terminals. HEK293 cells expressing TRPV1 plus YFP or Whirlin were used as controls, although the antibody was supposed to recognise specifically an epitope in mouse but not human or rat sequences (that we used for heterologous expression). As observed in **Figure 46**, native TRPV1 expression was only barely detectable in mice DRG extracts after long exposure of the film. Conversely, TRPV1 was easily detected (1 mouse per group) at similar levels in spinal cord tissues from the three mice strains. Whirlin antibody did not detect any specific signal for Whirlin long isoforms either in mice tissues or in heterologous extracts, whereas different bands of lower molecular weight in spinal cord samples from the three groups were observed.

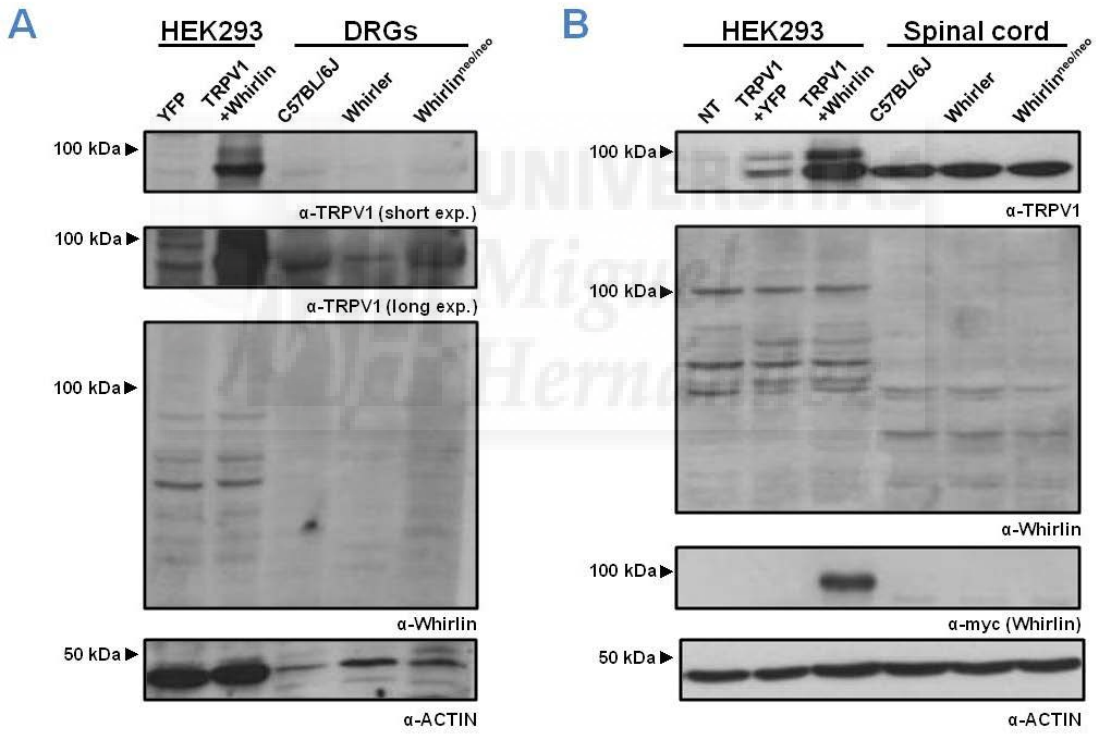

Figure 46 TRPV1 and Whirlin expression in DRG and spinal cord tissues. Immunoblots of wild-type, whirler and whirlin$^{neo/neo}$ **(A)** DRG and **(B)** spinal cord tissues extracts. HEK293 cells transfected with TRPV1 plus YFP or Whirlin were used as control for antibody specificity.

Thereafter, TRPV1 and Whirlin distribution and expression in the three mice strains was analysed by double immunohistochemical staining of DRG cryosections from wild-type, whirler and whirlin$^{neo/neo}$ mice. In **Figure 47**, representative immunofluorescence images display a neuronal subpopulation coexpressing both proteins.

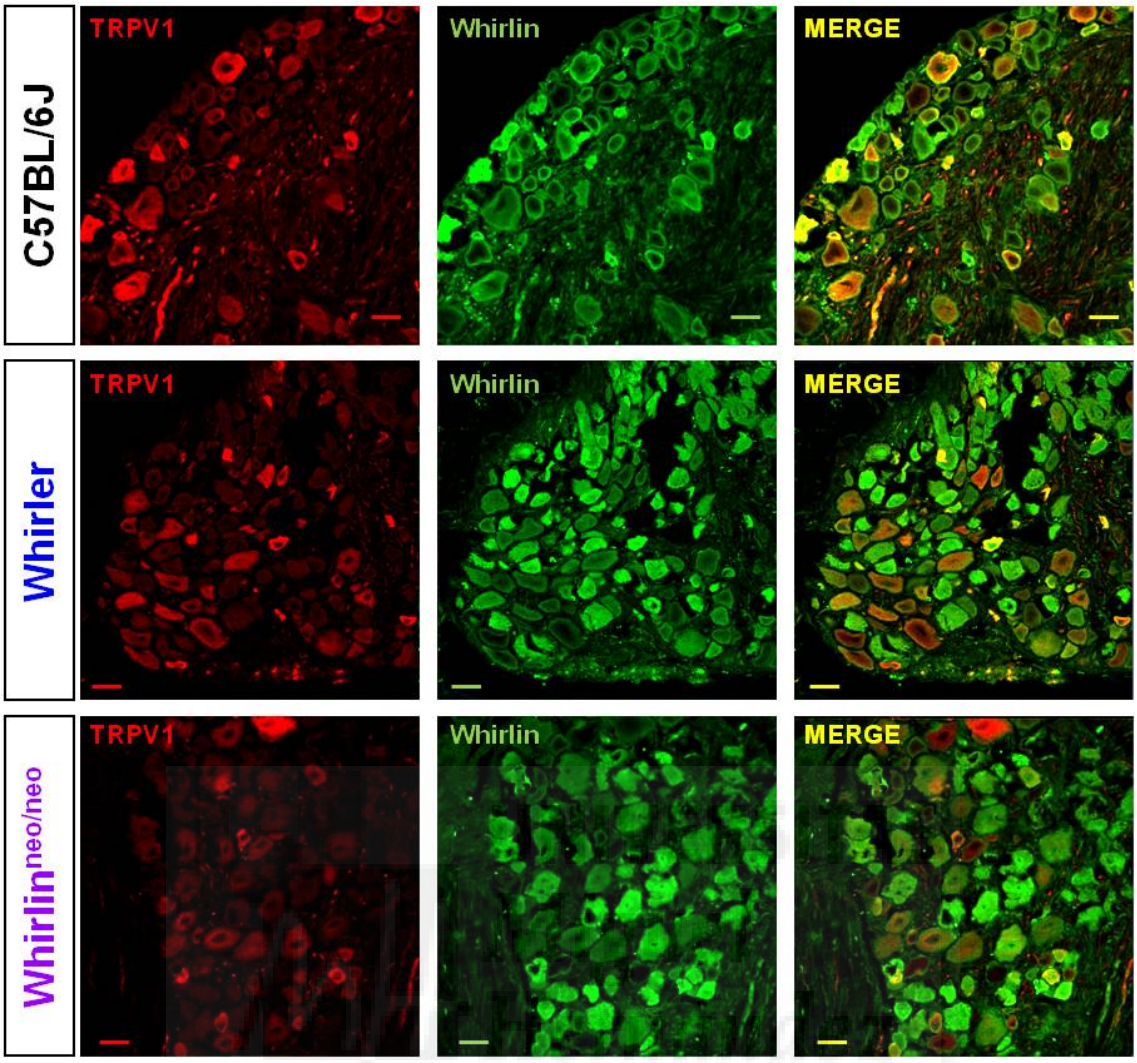

Figure 47 TRPV1 and Whirlin coexpress in a subpopulation of DRG neurons. Thin sections (14 µm) of DRG from wild-type, whirler and whirlin$^{neo/neo}$ mice were double-immunostained with antibodies for TRPV1 (red) and Whirlin (green). Representative immunofluorescent images are reported. Scale bars 20 µm.

As shown in **Table II**, about 30% of total neurons were positive for TRPV1, of which ~60% coexpressed Whirlin. On the other side, around a 50% of the global neuronal population showed staining for Whirlin, and 40% of this population also coexpressed TRPV1. Although the anti-Whirlin antibody here used is reported to detect all isoforms except NT1 and NT2, we did not detect significant differences in the number of positive neurons between wild-type compared to whirlin$^{neo/neo}$ mice, which should lack NT1 and NT2 together with the full-length PDZ protein, nor compared to whirler mice, which should lack the short C-terminal isoforms, probably due to the sensitivity of the experimental approach or the expression levels of the different isoforms.

	C57BL/6J	Whirlin$^{neo/neo}$	Whirler
TRPV1$^+$	33 ± 1	31 ± 1	34 ± 1
Whirlin$^+$	55 ± 1	51 ± 2	51 ± 2
TRPV1$^+$ x Whirlin$^+$	64 ± 2	63 ± 4	61 ± 3
Whirlin$^+$ x TRPV1$^+$	40 ± 2	40 ± 3	41 ± 4

Table II Immunohistochemical staining of serial DRG cryo-sections from wild-type, whirler and whirlin$^{neo/neo}$ mice was performed with polyclonal antibodies for TRPV1 and Whirlin. Three animals and a minimum of 5 sections per group were analysed. Data expressed as percentage of total neurons analysed per each section (mean ± S.E.M.).

Subsequent classification of the DRG population by double immunostaining of TRPV1 and Whirlin with the three molecular neuronal markers NF200, IB4 and CGRP was performed and the percentage of TRPV1 or Whirlin positive neurons that were also positive for each marker (TRPV1$^+$/Whirlin$^+$ x marker$^+$) calculated. As reported in previous studies, TRPV1 in mice was largely absent from the non-peptidergic C fibres and the myelynated fibres as defined by IB4 and NF200 respectively, whereas ~50% of TRPV1$^+$ neurons were also positive for the peptidergic marker CGRP. Conversely, Whirlin exhibited a wide distribution in the three subpopulations, at almost similar levels in the three animal models analysed (**Table III**).

	C57BL/6J	Whirlin$^{neo/neo}$	Whirler
TRPV1$^+$ x IB4$^+$	4 ± 1	6 ± 1	4 ± 1
TRPV1$^+$ x CGRP$^+$	50 ± 4	49 ± 3	40 ± 4
TRPV1$^+$ x NF200$^+$	11 ± 1	11 ± 2	11 ± 3
Whirlin$^+$ x IB4$^+$	37 ± 3	35 ± 3	45 ± 5
Whirlin$^+$ x CGRP$^+$	54 ± 5	49 ± 6	53 ± 5
Whirlin$^+$ x NF200$^+$	37 ± 3	42 ± 4	31 ± 5

Table III Immunohistochemical staining of DRG cryo-sections from wild type, whirler and whirlin$^{neo/neo}$ mice was performed with polyclonal antibodies for TRPV1, Whirlin and the neuronal markers CGRP, IB4 and NF200. Three animals and a minimum of 5 sections per group were analysed. Data expressed as percentage of total neurons analysed per each section (mean ± S.E.M.).

In vivo TRPV1 activity in whirler and whirlin$^{neo/neo}$ mice

Thermal hypersensitivity (Hargreaves' Plantar Test)

Although TRPV1 contribution to acute noxious heat sensitivity has been controversial in the last years, no doubt exists about its essential role in the development of inflammatory thermal hyperalgesia. Thus, we used Hargreaves' plantar test to assess whether Whirlin mutations had some effect in the induction of unilateral peripheral inflammation through the injection of complete Freund's adjuvant in the mice left hind paw (ipsilateral). The hyperactive phenotype of whirler mice prevented unrestrained measurement. Consequently, both control and mutant mice were gently restrained with one hand and placed on a glass plate, trying to align their hind paw with the centre of the mobile radiant heat source located below. Whirlin$^{neo/neo}$ mice, that did not exhibit any locomotor hyperactivity, were assayed without movement restrictions. A constant heat intensity pulse was applied to the glabrous surface of the hind paws and the latency to paw withdrawal measured. Mice were first challenged to measure their acute responses (baseline). A cut-off time of 30 seconds was applied in order to avoid tissue damage. As shown in **Figure 48**, no significant differences were observed in the latencies of whirler or whirlin$^{neo/neo}$ mice compared with the wild-type group, for any of the two hind paws (N=10 for each group; contralateral: right hind paw; ipsilateral: left hind paw).

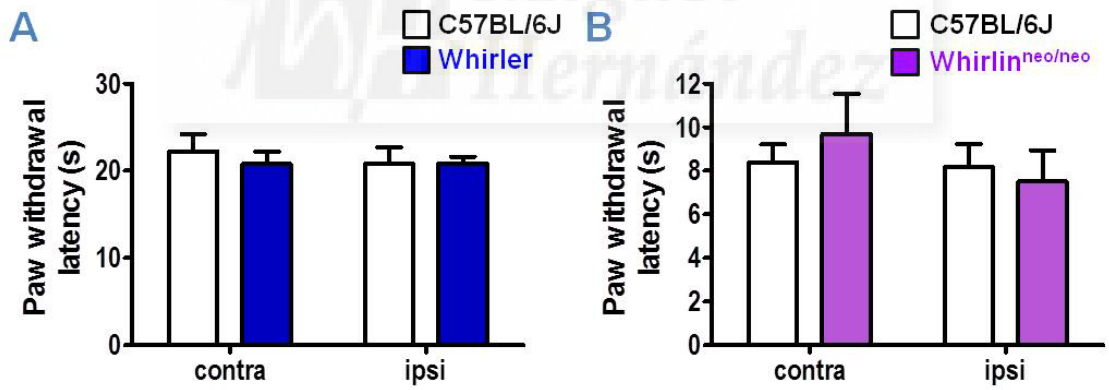

Figure 48 Whirler and whirlin$^{neo/neo}$ display normal acute noxious heat responses. A radiant heat source was used to apply an acute thermal stimulus to the mice contra- (right) and ipsilateral (left) hindpaws and paw withdrawal latencies measured. Data expressed as mean ± S.E.M. Two-way ANOVA, Bonferroni post-test. n=10 animals per each group.

Intraplantar injection of 50 µl CFA into the ipsilateral paw was then administered to produce a local inflammatory reaction and the contralateral non-injected paw was used as a control. After 24 hours significant edema formation and paw swelling were visible in the injected paws of all wild-type, whirler and whirlin$^{neo/neo}$ mice tested (**Figure 49**).

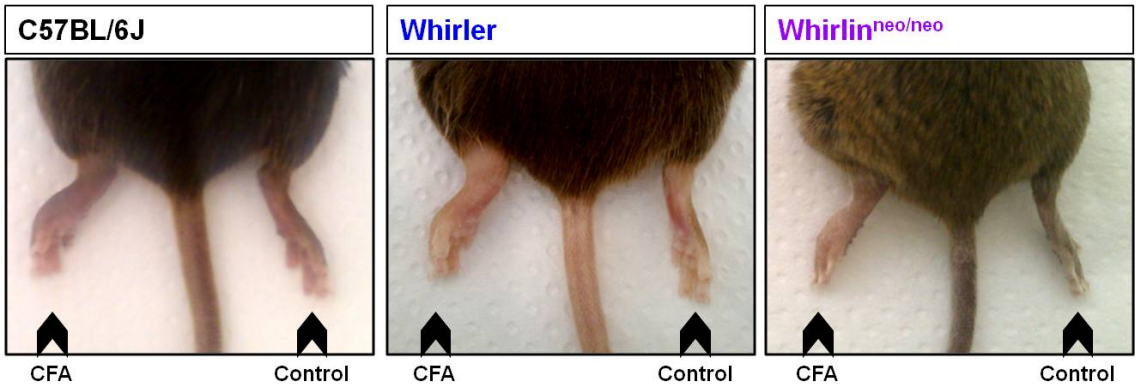

Figure 49 Edema and paw swelling produced by CFA injection. Photographs of wild-type, whirler and whirlin$^{neo/neo}$ hind paws showing the swelling produced 24 hours after CFA injection compared with the non-injected control paw.

Latencies to thermal stimuli were measured from 1 to 3-4 days post-CFA-injection and responses were normalised to that obtained the day before injection for each paw (baseline, 100%). As shown in **Figure 50**, both mice strains developed thermal hyperalgesia in the inflamed paw along the duration of the experiment, with a reduction in latencies from ~25 to ~40% of the baseline.

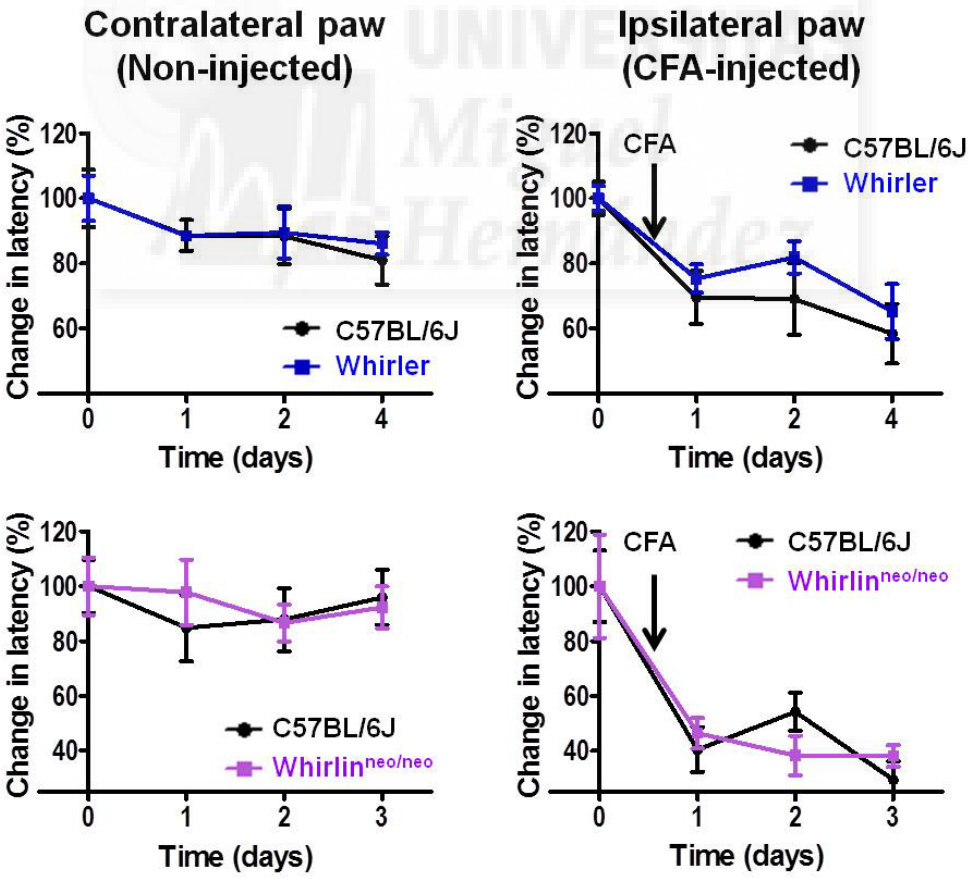

Figure 50 Whirler and whirlin$^{neo/neo}$ mice develop thermal hyperalgesia similar to wild-type. Paw withdrawal latencies were firstly measured in basal condition through Hargreaves' method (baseline at day 0:100%). After that, 50 µl of CFA were injected in the left hind paw (ipsilateral) and latencies from 1 to 3-4 days post-injection were measured and normalised to corresponding baseline. Data expressed as mean percentage ± S.E.M. n=10 animals per group. Two-way ANOVA, Bonferroni post-test.

Mechanical hypersensitivity (Dynamic Aesthesiometer Plantar Test)

Involvement of TRPV1 in mechanical sensitivity is still a matter of controversy: TRPV1 knockout seem to have normal mechanical sensitivity and mechanical hypersensitivity induced by inflammation (Caterina *et al.* 2000). However, systemic or intrathecal administration of TRPV1 antagonists in normal animals results in a reversal of both heat and mechanical hyperalgesia (Yu *et al.* 2008). Furthermore, a role for Whirlin in proprioceptor mechanotransduction has been recently proposed (de Nooij *et al.* 2015). Thus, we decided to investigate whether sensitivity to mechanical stimuli and development of mechanical allodynia were altered in our animal models. We used a Dynamic Aesthesiometer to assess "touch sensitivity". Animals were placed in Plexiglas chambers and left to acclimate at least for 30 minutes. Basal mechanical thresholds were then measured and reported as the force (in grams) at which the paw was withdrawn. As depicted in **Figure 51**, no significant differences were observed in the responses of both right (contralateral) and left (ipsilateral) hind paws from the three mice strains.

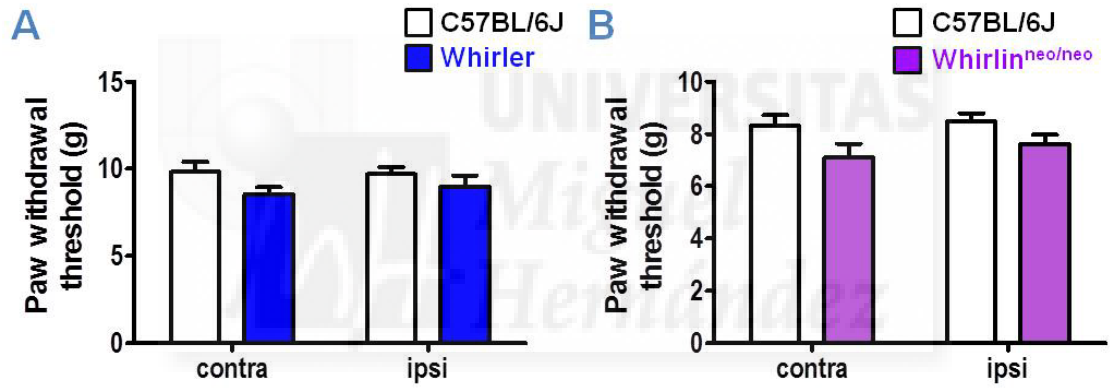

Figure 51 Whirler and whirlin$^{neo/neo}$ mice exhibit normal basal mechanical sensitivity. Wild-type, whirler and whirlin$^{neo/neo}$mice were placed in Plexiglas chambers and left to acclimate for at least 30 minutes. Mechanical sensitivity was then assessed through an automated Von Frey and the force (in grams) at which each paw was withdrawn was measured. Data expressed as mean ± S.E.M. n=10 animal per group. Two-way ANOVA, Bonferroni post-test.

Later, 50 µl of CFA were injected in the left hind paw (ipsilateral) and mechanical sensitivity was assessed from 1 to 3-4 days post-injection. Measurements were normalised to the baseline obtained for each paw (day 0, before injection). As shown in **Figure 52**, both mice strains exhibited a reduction in latencies from about a 20 to a 40% of the baseline. Thus, Whirlin mutation or deletion did not affect mechanical allodynia development.

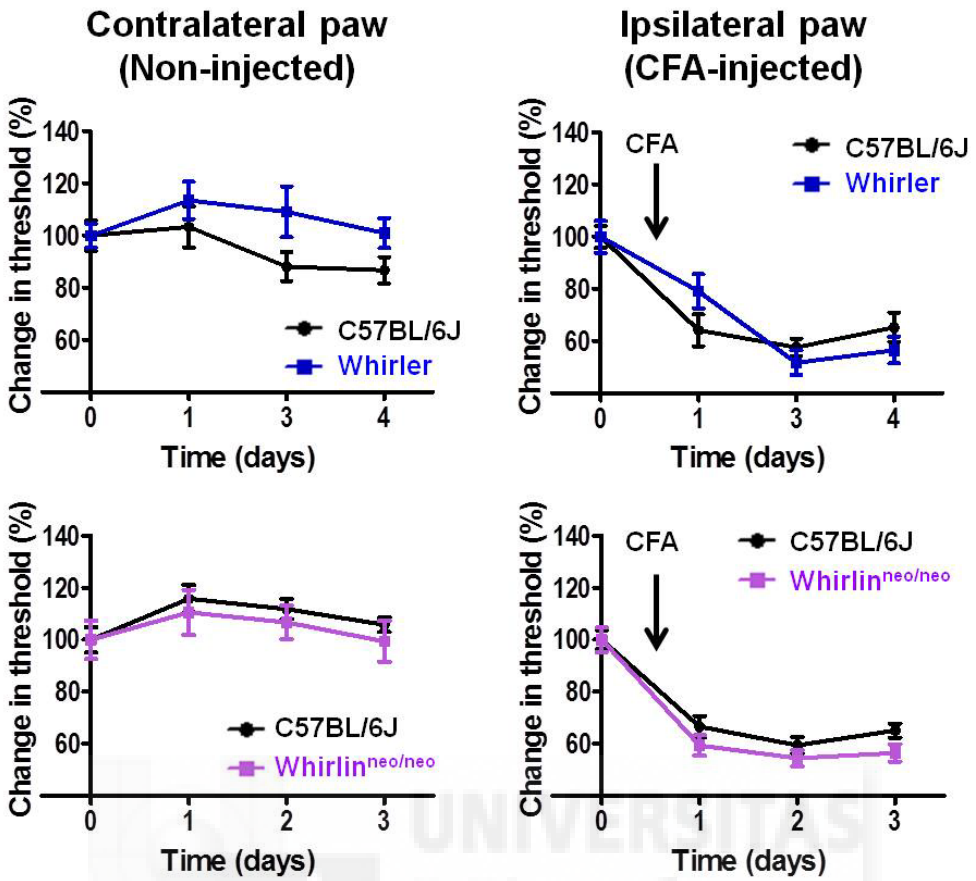

Figure 52 Whirler and whirlin$^{neo/neo}$ mice develop mechanical allodynia similar to wild-type. Basal responses to mechanical stimuli were assessed with an automated von Frey device (baseline at day 0: 100%). Subsequently, 50 µl of CFA were injected in the left hind paw (ipsilateral) and mechanical threshold were measured at days 1, 3 and 4 post-injection. Data expressed as mean percentage of baseline ± S.E.M. n=10 animals per group. Two-way ANOVA, Bonferroni post-test.

Ex vivo TRPV1 activity in whirler and whirlin$^{neo/neo}$ mice

We investigated receptor function *ex vivo* by Ca^{2+} fluorimetric assays in DRG cultures from wild-type, whirler and whirlin$^{neo/neo}$ mice. A pulse of capsaicin at two distinct concentrations (0.1 and 1 µM) was applied followed by a pulse of 40 mM KCl as a confirmation of neuronal viability. The amplitude of the capsaicin response was calculated and expressed as the ratio between the increase in the calcium fluorescence signal intensity and the baseline calcium fluorescence measured prior to capsaicin application (ΔF/F0). As shown in **Figure 53A**, a significant decrease in capsaicin-induced responses was observed in both whirler and whirlin$^{neo/neo}$ DRG neurons compared to wild-type. We also calculated the number of DRG neurons activated by capsaicin and expressed it as a percentage of total KCl-responsive neurons. As reported in **Figure 53B**, the percentage of responsive neurons was not significantly modified at any of the two doses of agonist applied in our experiments.

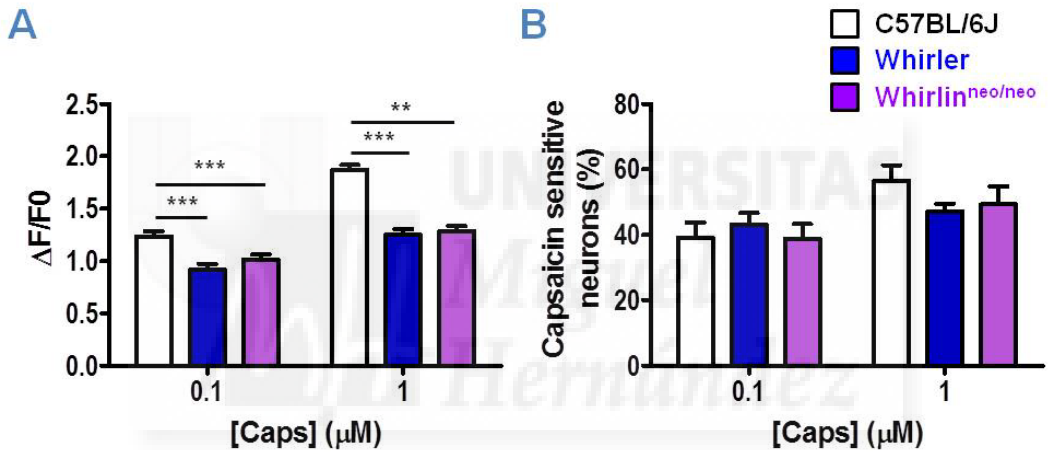

Figure 53 Capsaicin-induced responses in DRGs neurons from whirler and whirlin$^{neo/neo}$ mice were similar to wild-type. Ca^{2+} imaging assays were performed in DRGs cultures from wild-type, whirler and whirlinn$^{neo/neo}$ mice, by applying two different concentrations of capsaicin (0.1 and 1 µM). **(A)** ΔF/F0 and **(B)** capsaicin sensitive neurons (%) ± S.E.M are represented. n>200 cells per condition. ** p<0.01, *** p<0.001, Two-way ANOVA, followed by Bonferroni post-test.

DISCUSSION

UNIVERSITAS
Miguel
Hernández

Ion channels play a crucial role in many fundamental physiological processes and alterations of their function are consequently responsible for different pathological conditions such as cardiac and neurological disorders, kidney failure, blindness and pain perception. As a result, they represent an attractive potential target class for drug discovery and pharmaceutical intervention in a broad range of disease areas (Bagal *et al.* 2012). In the particular area of pain research, traditional analgesic drugs that either suppress inflammation (e.g. NSAIDs and COX-2 inhibitors) or block pain transmission (e.g. opiates) are quite efficacious, but a combination of gastro-intestinal and cardiovascular complications for the former and development of tolerance and addiction to the latter are serious problems. Other classes of drugs, such as antidepressants and anticonvulsants, are often used for multiple pain syndromes but commonly with unsatisfactory efficacy, and their mechanism of action is still not clear.

For establishing novel, selective therapeutic approaches, a targeted inhibition of pain-specific pathways or molecules would be ideal (Mathie 2010). In this context, the cloning of the capsaicin receptor TRPV1 in 1997 represented a significant step in the understanding of molecular mechanisms involved in the transduction of noxious thermal and chemical stimuli by sensory neurons. This prompted the development of a new generation of analgesic agents which, unlike traditional drugs, aim to prevent pain by specifically blocking a transducer of noxious stimuli at the site where pain is generated (Szallasi *et al.* 2007). Unfortunately, most of the first-generation small molecules **antagonists** developed against TRPV1 failed at different stages of preclinical trials, mainly due to their hyperthermia-inducing side effects and impaired noxious heat sensation, with the possible complication of accidental burn injuries (Mickle *et al.* 2015). Second generation (modality-selective) TRPV1 antagonists, that block capsaicin but not acid and/or heat activation of TRPV1, are predicted to not change core body temperature or elevate heat pain threshold (Szolcsanyi and Sandor 2012;Brederson *et al.* 2013). However, non-competitive antagonists acting as open-channel blockers are therapeutically more attractive because they preferentially recognise and block the population of pathologically-over-activated TRPV1 channels, thereby potentially reducing the unwanted side effects (Brito *et al.* 2014). On the other hand, TRPV1 **agonists** have shown great promise in the treatment of moderate to severe pain by rapidly and strongly activating TRPV1, and then promoting fast and prolonged channel desensitisation, and/or eventual degeneration/death of nociceptive fibres due to excitotoxicity. Occlusive high capsaicin concentration patches and site-specific injections are already in clinical use for treating various pain syndromes, including post-herpetic neuralgia, diabetic neuropathy, and chronic musculoskeletal pain. However, burning sensation or erythema at the site of application and poor capsaicin absorption through the epidermis limit the widespread application of this treatment option. The ultrapotent analogue RTX is an attractive alternative to capsaicin with improved desensitisation to irritancy ratio and is currently undergoing clinical trials in patients with intractable cancer pain (Kaneko and Szallasi 2014).

A deeper understanding of the molecular and structural mechanisms underlying channel function may provide novel targeting opportunities for pain intervention. Notably, as for other receptors and ion channels, several proteins have been described to interact with TRPV1 in a

supramolecular complex (signalplex) which is crucial for the establishment and maintenance of key aspects of the receptor function, including trafficking, assembly and activity. Improper regulation of these complexes seems to be intimately associated with the development of diseases and pathophysiological conditions. Therefore, understanding the complexity of this functional protein network may provide a new platform for defining the cellular mechanisms of TRPV1 pathophysiology and developing new therapeutic strategies to target TRPV1 in diseased, but not healthy, tissues.

In this context, the principal finding of this work was the scaffolding protein Whirlin as a novel interactor and modulator of TRPV1. This interaction was initially detected by performing a yeast two-hybrid screening of a rat brain cDNA library using as bait the cytosolic N-terminal domain of TRPV1 (Morenilla-Palao *et al.* 2004). Given the reported ability of Whirlin to recruit macromolecular complexes to specific subcellular locations through its three-PDZ-domains, and its important role in sensory transduction of hair cells, photoreceptors and proprioceptors, the identified protein caught our immediate attention and lead us to speculate that Whirlin may be a critical organiser of the TRPV1-transduction complex in nociceptive sensory terminals. The first objective of this study was to confirm the observed interaction through *in vitro* pull down, coimmunoprecipitation assays and immunocytochemical approaches. Interestingly, both isolated cytoplasmic domains of TRPV1 were able to bind Whirlin with a similar strength. For the binding to PDZ domains, canonical amino acid sequences have been identified in the C-termini of many TRP channels from TRPV and TRPC subfamilies (Smani *et al.* 2014). Specifically, we identified an internal **S/TXV** sequence similar to that implicated in the binding of the PDZ protein INAD to the TRP Ca^{2+} channel (Shieh and Zhu 1996). The involvement of these TRPV1 amino acids in the interaction with Whirlin was evaluated by using a truncated (TRPV1-VStop) mutant lacking this sequence motif. Importantly, the ability of this mutant TRPV1 to pull down Whirlin, similarly as the full length channel protein, implies that additional domains may be involved in this TRPV1-Whirlin interaction. The involvement of various interacting domains has been previously described for other proteins. For instance, PDZ domains from PSD95 were shown to bind both the C- and N-termini of Kv1.5 channels with comparable affinity although probably with a divergent role on either clustering or trafficking of the channel (Eldstrom *et al.* 2002). Additionally, the association of the first PDZ domain of the protein-tyrosine phosphatase PTP-BAS with the transcription factor-inhibitory protein I*κ*B*α* was found to require a stretch of the three N-terminal ankyrin repeats instead of the C-terminal region of I*κ*B*α* (Maekawa *et al.* 1999). Given the ability of Whirlin to interact with the N-terminal domain of TRPV1, the interaction may take place between the ankyrin repeats from TRPV1 and PDZ domains from Whirlin. In this context, it would be interesting to check if the PDZ-scaffold protein also associates with other ankyrin-containing TRP channels, mainly with TRPA1 and TRPV2-4 which have been described to form functional heteromultimers with the vanilloid receptor. Alternatively, the putative interaction could be assayed of Whirlin with the cold receptor TRPM8 which lacks of ankyrin domains in its N-terminus and minimally coexpress *in vivo* with the vanilloid receptor (Peier *et al.* 2002).

Given that Whirlin long and short isoforms seem to function differently in photoreceptors and hair cells, probably by establishing distinct patterns of interactions, we aimed to verify which of the N- or C-terminal regions of the PDZ protein, or both, played a central role for the interaction with TRPV1. Interestingly, the construction corresponding to the short C-terminal isoform of Whirlin, containing the proline-rich region and the third PDZ domain, resulted very unstable and not detectable in our experimental conditions. Protein instability has often been correlated to so-called PEST sequences rich in proline (P), glutamic acid (E), serine (S) and threonine (T) (Belizario *et al.* 2008). Indeed, a PEST search algorithm (**http://emboss.bioinformatics.nl/cgi-bin/emboss/help/epestfind**) revealed three putative motifs along the Whirlin sequence: 627-662, 752-778 and 728-739, all located in the C-terminal region. Accordingly, when cells were treated with the proteasome inhibitor MG132, detectable levels of PDZ3 were recovered, supporting our hypothesis that this construction is a candidate for proteolytic degradation at the PEST sequences. Using proteasomal inhibition, we were able to confirm the interaction of TRPV1 with both the first two PDZ domains and with the third PDZ domain of Whirlin, separately. Thus, our results suggest that the TRPV1 receptor may interact *in vivo* with both the long and short isoforms of Whirlin. Nevertheless, further studies are required in order to achieve a better characterisation of the specific domain(s) involved in this interaction, which may provide a starting point for the development and employment of small interfering peptides as a new therapeutic approach to modulate channel function by specifically targeting and interfering at the protein-protein interface.

Encouraging findings in the protein-protein interaction-competing peptide field have been recently reported. Thus, a peptide with sequence identical to the AKAP79 binding site has been designed which blocks sensitisation of TRPV1 *in vitro* and has a potent analgesic action in several mouse models of inflammatory pain *in vivo* (Btesh *et al.* 2013). Similarly, a cell-permeable peptide that mimics the C-terminus of a Tmem100 mutant, a membrane adaptor protein that regulates the physical association between TRPA1 and TRPV1, selectively inhibits TRPA1-mediated activity and pain in a TRPV1-dependent manner (Weng *et al.* 2015). Further supports come from investigations on PSD-95, another prominent organising PDZ protein which is crucial for the coupling of different pain-related receptors to intracellular proteins and signalling enzymes. Preclinical studies have demonstrated that intraperitoneal injection of a fusion protein comprised of the PSD-95 PDZ2-domain and the protein transduction domain (PTD) of the human immunodeficiency virus-type 1 (HIV-1) Tat protein (to confer cell-permeability), significantly inhibits CFA-induced chronic inflammatory pain behaviours in mice by disrupting protein-protein interactions between NMDA receptors and PSD-95 (Tao *et al.* 2008). Likewise, intrathecal injection of an interfering peptide comprising the nine C-terminal residues of the 5-HT2A receptor fused with the transduction domain of HIV-1 Tat protein, inhibits both thermal and mechanical hyperalgesia by disrupting *in vivo* interactions between spinal 5-HT2A receptors and their associated PDZ proteins PSD95 and SAP97 (Pichon *et al.* 2010).

One of the relevant contributions of our study was the demonstration that Whirlin significantly augmented TRPV1 expression levels in both recombinant and native neuronal expression systems. Capsaicin-induced channel activity did not parallel the increase in protein expression and a slight downregulation in responses to partial activators like voltage and acidic stimuli was observed. A similar phenomenon was previously described in SH-SY5Y cells stably expressing the TRPV1 receptor chronically exposed to insulin or IGF-I that resulted in a 3-fold overexpression of TRPV1 in the plasma membrane that was not accompanied by an augmented channel activity (Lilja *et al.* 2007). We observed a more pronounced increase of the less glycosylated form of TRPV1 that could in part account for the lack of correlation between channel expression and function. Indeed, previous studies reported that non-glycosylated channels are functional and normally trafficked to the membrane but exhibit lower responses and sensitivity to capsaicin than the wild-type (Wirkner *et al.* 2005). Furthermore, the identified glycosylation site (Asp-604) on TRPV1 is located near two glutamate residues (Glu-600 and Glu-648) involved in both acidic activation and potentiation of the channel that in our experiments were decreased by Whirlin coexpression (Wirkner *et al.* 2005;Cohen 2006;Winter *et al.* 2013). Another possibility is that overexpressed Whirlin inhibits TRPV1 activation through a direct (or indirect) interaction at the cell surface which may stabilise a closed channel conformation. Alternatively, the increase in surface expression may be responsible for the enhanced clustering of the TRPV1 channel at the plasma membrane that may have an inhibitory effect on his functionality, as previously described for GABARAP (Lainez *et al.* 2010).

Lipid rafts, plasma membrane micro-domains rich in cholesterol, sphingolipids and gangliosides, modulate the activity of several ion channels and are crucially involved in the formation of signalling complexes by regulating protein trafficking and clustering (Levitan *et al.* 2010;Simons and Toomre 2000). Disruption of these domains by cholesterol depletion decrease the amount of TRPV1 in the plasma membrane and inhibits the opening properties of the channel evoked by various agonists, in both native sensory neurons and TRPV1-transfected cell lines (Liu *et al.* 2006;Szoke *et al.* 2010). Our data suggest that a small fraction of the fully glycosylated form of TRPV1 is segregated in low density fractions, whereas the poorly glycosylated channels mostly co-localise to non-raft fractions. The glycosylation pattern as a function of the membrane subdomain was not altered by Whirlin coexpression. Moreover, disruption of lipid rafts by incubation with the cholesterol-binding oligosaccharide MβCD slightly affected TRPV1-mediated responses, as previously reported, but independently on the presence of Whirlin. Interestingly, a physical and functional interaction with lipid rafts has also been described for TRPM8, whose menthol- and cold-mediated responses, however, are potentiated when the association with lipid rafts is prevented by cholesterol depletion. Interestingly, the highly glycosylated forms of TRPM8 preferentially segregate into lipid rafts compared with the less glycosylated ones (Morenilla-Palao *et al.* 2009).

Based on these results, localisation of the TRPV1-Whirlin complex in distinct membrane microdomains seems plausible and previously described interactions for the two proteins with microtubules and actin filaments suggest cytoskeletal corrals as good candidates for further

investigations (Goswami *et al.* 2004;Wang *et al.* 2012). Consistently, a recent study has shown the existence of three dynamic channel populations: the first constituted by channels bound to caveolin-1 (a major protein component of lipid rafts) likely responsible for receptor desensitisation via caveolar endocytosis upon prolonged activation; the second, channels that freely diffuse possibly like a receptor "reservoir" not directly implicated in its functionality; and the third of channels bound to microtubules, which appears as large clusters (860 nm) of slow mobility (Storti *et al.* 2015). Thus it is tempting to speculate that Whirlin, as well as GABARAP, may favour the formation of this clustered receptor population. In support of this tenet, Whirlin attenuated capsaicin-induced TRPV1 internalisation, a process that has been partly associated to the channel subpopulation bound to caveolin-1 (Sanz-Salvador *et al.* 2012;Storti *et al.* 2015).

A more discernible effect on TRPV1 function was observed when Whirlin expression was downregulated using specific siRNAs: in both heterologous and native neuronal systems TRPV1 receptor expression was significantly decreased judged by the amplitude of capsaicin-induced responses and the percentage of neurons that were sensitive to agonist application. This effect was prevented by the proteasome inhibitor MG132, thus suggesting that Whirlin could stabilise the receptor and reduce its degradation through the proteasome. Accordingly, we demonstrated that in basal conditions TRPV1 is prone to ubiquitination and subsequent proteasomal degradation, possibly through an ERAD process, as the treatment with a proteasomal but not a lysosomal inhibitor increased *per se* the receptor expression.

A recent study supports our data and also reports that a TRPV1 Y200F mutant, which is poorly translocated to the membrane (phosphorylation at Tyr-200 is critical for plasma membrane trafficking of TRPV1), is more vulnerable to ubiquitination and subsequent proteasomal degradation, thus resulting in decreased receptor levels which are recovered after proteasomal inhibition (Stein *et al.* 2006;Shimizu *et al.* 2012). Interestingly, this residue is located in the N-terminal region, a domain also involved in the interaction of TRPV1 with Whirlin, and other trafficking proteins like Snapin and Syt IX (Morenilla-Palao *et al.* 2004).

Intriguingly, whereas degradation kinetics were virtually identical for TRPV1 and Whirlin when co-expressed, in the absence of Whirlin TRPV1 was more stable. This result suggests that the stability of TRPV1 is primarily determined by formation of the Whirlin-TRPV1 complex. Notably, a similar effect on P2X3 receptors has been recently described for the Whirlin-interacting MAGUK protein CASK, a molecular scaffold which is known to play a major role in the assembly of multiprotein complexes at specialised regions of neuronal plasma membranes and to associate with pre- and post-synaptic proteins and cytoskeleton (Cohen *et al.* 1998;Chao *et al.* 2008). As for the TRPV1-Whirlin complex, coexpression with CASK in a neuronal-free system significantly enhances P2X3 receptors levels whereas CASK downregulation in mice trigeminal neurons results in a proteasome-dependent P2X3 disassembly and reduced receptor-mediated currents, suggesting an analogous role for the MAGUK protein in modulating the stability and clustering of P2X3 receptors at the plasma membrane (Gnanasekaran *et al.* 2013). Moreover, coexpression with four CASK mutants missing different interacting domains still increased receptor expression although two of them failed in enhancing the amplitude of

P2X3-mediated currents, maybe because they were not able to recruit other intracellular adaptors required to modulate the receptor function. This provides further evidence that an increase in receptor expression is not always accompanied by a parallel increase in its function. Interestingly, CASK/P2X3 interaction was up-regulated by NGF and down-regulated by P2X3 agonist-induced desensitisation, and previous studies suggest that phosphorylation of both proteins by specific kinases may also affect the strength of this interaction, similar to what has been reported for other PDZ-mediated interactions (Huang *et al.* 2010;Fabbretti 2013). As the release of soluble mediators and the activation of protein kinases are pivotal mechanisms (among others) for the establishment of chronic pain syndromes, it is patent that investigating how they modulate protein interaction networks responsible for signal transduction from cell surface receptors is pivotal for the identification of novel targets and the development of more specific therapeutic approaches.

Once described the effect of both Whirlin overexpression and downregulation *in vitro*, we centred the last part of our study on analysing eventual alterations of TRPV1 expression and activity *in vivo* using mice models carrying mutations or deletions of different Whirlin isoforms. Specifically, we used animal models for autosomal recessive deafness DFNB31 (whirler mice) and for Usher syndrome type 2D (whirlin$^{neo/neo}$ mice). The first is associated with a mutation that leads to a truncation of the long isoform before the third PDZ domain and encompasses the first methionine of the short isoform, whereas whirlin$^{neo/neo}$ does not express the long isoform of the PDZ protein. TRPV1 expression and distribution in the two animal models were similar and, despite the decreased receptor-mediated activity registered in *ex vivo* preparations, no significant impairment in whirler or whirlin$^{neo/neo}$ mice nociceptive behaviour was observed as compared with the wild-type littermates. Apart from the intrinsic limitations of the *ex vivo* preparation compared to the complex regulatory mechanisms associated with an inflammatory response *in vivo*, multiple factors may be responsible for these discrepancies. The ability of TRPV1 to bind to any of the three PDZ domains of Whirlin *in vitro* suggests the involvement of both long and short isoforms of the PDZ-scaffold protein in the complexation and stabilisation of the receptor, which in turn may account in part for the lack of impact on both TRPV1 expression and activity in whirler and transgenic mice. Furthermore, PSD95 or CASK or other Whirlin-related PDZ proteins may produce compensatory upregulation which may counterbalance Whirlin deletion or mutation. In this sense, *ex vivo* downregulation of the PDZ domain containing protein 2 (Pdzd2) was shown to inhibit the *in vitro* activity of the voltage-gated sodium channel $Na_V1.8$ in sensory neurons although Pdzd2-decificent mice exhibited no marked change in pain behaviours. This discrepancy was attributed to the compensatory upregulation of p11, another regulatory factor for $Na_V1.8$ in dorsal root ganglia (Shao *et al.* 2009).

Notably, and in agreement with the importance of TRPV1-Whirlin interaction, an alternative Whirlin null mouse model, produced using a genome-wide generation approach and characterised using systematic phenotyping, exhibited an increased thermal nociceptive threshold in the hot plate test (White *et al.* 2013).

In conclusion, we have demonstrated that TRPV1 interacts with Whirlin, a cytoskeletal PDZ-scaffold protein, and both coexpress in a subset of nociceptors. Heterologous expression of Whirlin increases TRPV1 cellular expression and promotes receptor clustering at the plasma membrane whereas abrogation of endogenous Whirlin expression with siRNAs results in a concomitant degradation of TRPV1 that could be prevented by inhibiting the proteasome. Furthermore, the degradation kinetics of TRPV1 upon arresting protein translation mimics that of Whirlin in cells co-expressing both proteins, suggesting a parallel degradation mechanism. Noteworthy, Whirlin coexpression also significantly reduces TRPV1 internalisation induced by prolonged exposure to capsaicin. Collectively, all these results indicate that the assembly of both proteins contributes to stabilise the cellular and membrane expression of the thermoTRP. Although additional experimental support is needed, our data suggest that disruption of the Whirlin-TRPV1 complex may provide a novel pharmacological intervention for the treatment of TRPV1-mediated painful disorders.

UNIVERSITAS
Miguel
Hernández

CONCLUSIONS

UNIVERSITAS
Miguel
Hernández

- TRPV1 interacts with the scaffold protein Whirlin and both proteins coexpress in a subset of nociceptors.
- Whirlin coexpression increases TRPV1 protein levels and promotes the receptor clustering at the plasma membrane, affecting voltage- and protons- but not capsaicin-activated responses.
- Upon arresting protein translation, TRPV1 and Whirlin follow parallel degradation kinetics.
- Silencing Whirlin expression results in a concomitant degradation of TRPV1. The reduction of receptor-mediated activity induced by Whirlin knockdown can be prevented by inhibiting the proteasome.
- Coexpression of TRPV1 with Whirlin attenuates TRPV1 internalisation under prolonged exposure to the agonist capsaicin.
- TRPV1 localisation and activity in lipid rafts are not altered by Whirlin coexpression.
- Decreased TRPV1-mediated responses are observed in DRG explants cultures from Whirler and Usher syndrome mice associated to Whirlin mutation, but the receptor expression/distribution and nociceptive responses *in vivo* are not altered.

UNIVERSITAS
Miguel
Hernández

- El receptor TRPV1 interacciona con la proteína de andamiaje Whirlin y ambas son coexpresadas por un subgrupo de nociceptores.
- La coexpresión de Whirlin aumenta los niveles de expresión de TRPV1 y promueve el agrupamiento del receptor en la membrana plasmática, alterando sus respuestas a voltaje y a protones pero no a capsaicina.
- Tras inhibición de la síntesis proteica, TRPV1 y Whirlin siguen cinéticas de degradación paralelas.
- El silenciamiento de Whirlin produce una disminución concomitante en los niveles de TRPV1 y en su actividad, que puede ser bloqueada por el tratamiento con un inhibidor del proteasoma.
- La coexpresión de Whirlin disminuye la internalización del receptor tras exposición prolongada a su agonista capsaicina.
- La localización y la actividad del receptor TRPV1 en las balsas lipídicas no se ve alterada por la coexpresión de Whirlin.
- Las respuestas mediadas por el receptor TRPV1 en cultivos primarios de neuronas sensoriales se ven disminuidas en modelos animales de sordera (Whirler) y síndrome de Usher debidos a mutaciones de la proteína Whirlin, mientras la expresión/distribución del receptor y las respuestas nociceptivas *in vivo* en dichos modelos no se ven alteradas.

UNIVERSITAS
Miguel
Hernández

MATERIALS AND METHODS

UNIVERSITAS
Miguel
Hernández

CELL CULTURES

Cell lines

HEK293 cell line was mainly used for this work (Graham *et al.* 1977). These cells were cultured in Dulbecco's Modified Eagle's Medium (DMEM, Sigma) supplemented with 10% fetal bovine serum (FBS, Invitrogen) and 1% penicillin-streptomycin solution (P/S, Invitrogen), in a 5% CO_2 incubator at 37 ºC. For knockdown experiments through siRNA (described below) we used F11 cells, a hybridoma derived from mouse N18TG2 neuroblastoma and rat dorsal root ganglia (Fan *et al.* 1992). These cells (a gift from Dr. Tim Hucho) were cultured in Ham's F12 medium (Sigma) supplemented with 20% FBS, 1% L-glutamine (Gibco), 1% P/S and 1% hypoxanthine-aminopterin-thymidine medium supplement (HAT, Sigma).

For immunocytochemistry or Ca^{2+} imaging assays, cells were seeded on glass round coverslips (18 or 12 mm diameter, thickness #1.5, 0.16 – 0.19 mm, Knittel Gläser) in 12 or 24 wells plates (Costar) at a concentration of 50,000 cells/well. Coverslips were previously sterilised, treated with poly-L-lysine (Sigma) for 30 minutes at 37 ºC and extensively washed with phosphate buffered saline (PBS).

Lipofectamine™ 2000 transfection reagent (Invitrogen) or JetPel™ (Polysciences) were used to deliver plasmid DNA into the cells in order to express and study the proteins of interest. For most experiments, cells were seeded the day before the transfection in 10-cm dishes or 6 well plates (Costar) at a concentration respectively of 1.5×10^6/dish and 500,000 cells/well. Thereafter, cells were transfected following the manufacturer instructions. 4-6 hours after transfection, medium was replaced with fresh one in order to preserve cell viability. All the experiments were realised 48 hours post-transfection.

Primary cultures of DRG neurons

DRG were extracted from neonatal (P1-P3) Wistar rats after decapitation. Spinal cord was removed and DRG were dissected bilaterally and collected in 2 ml of PBS on ice. Any residual piece of nerve root or connective tissue was removed and DRG were transferred to 2 ml of DMEM supplemented with 0.25% of collagenase type IA (Sigma) and incubated at 37 ºC for 1 hour. After the enzymatic dissociation, DRG were washed two times with complete medium (DMEM supplemented with 10% FBS and 1% P/S) and resuspended in 2 ml of the same medium. Then they were dissociated into single cells by passing the cellular suspension 20-30 times through a Pasteur pipette and filtered through a cell strainer with 100 µM pores (BD Falcon). Cells were concentrated by centrifuging at 300 g for 10 minutes and then resuspended in complete medium supplemented with mouse 2.5s NGF (Promega) 50 ng/ml and cytosine arabinoside (Sigma) 1.25 µg/ml to prevent non-neuronal cell proliferation.

For adult mice (C57BL/J6, whirler or whirlin$^{neo/neo}$), animals were euthanised by cervical dislocation, spinal cord removed and DRG dissected bilaterally and collected in 2 ml of DMEM with 1% P/S solution on ice. Any residual piece of nerve root or connective tissue was removed

and DRGs were transferred to 2 ml of INC mix (155 mM NaCl, 1.5 mM K_2HPO_4, 5.6 mM 4-(2-hydroxyethyl)-1-piperazineethanesulfonic acid or HEPES, 4.8 mM Na-HEPES, 5 mM Glucose, 1% P/S) (Baker and Bostock 1997) supplemented with 0.1% of collagenase type XI (Sigma) and 0.45% dispase (Gibco) and incubated at 37 ºC for 1 hour. From this point the protocol was identical to that followed for neonatal rat DRG.

18 or 12 mm glass coverslips were sterilised, put in 12 or 24 wells plates, treated with poly-L-lysine 10 µg/ml at 37 ºC for 30 minutes, washed with PBS and subsequently treated overnight (o/n) at 37 ºC with laminin (Sigma) 5 µg/ml. After washing with PBS, the neuronal suspension was added to each well and cultured until experiments were realised (at 24 or 48 hours).

For DRGs electroporation, the Neon transfection system (Invitrogen) was used. Neurons were extracted from neonatal rats and after digestion with collagenase they were resuspended in 10 µl of resuspension buffer plus 1 µg cDNA per reaction (Whirlin or YFP as control), according to manufacter instructions. 2 pulses of 20 ms at 1200 V were applied and cells then resuspended and seeded in complete medium without antibiotics for 3-4 hours before changing to complete medium.

PLASMIDS

TRPV1

Rat wild type TRPV1 cDNA was a gift from Dr. David Julius (Physiology department, University of California, San Francisco, USA).

TRPV1-myc

TRPV1 was subcloned in the pcDNA 3.1-myc-His plasmid (Invitrogen) in order to obtain a construction with a myc epitope fused to the C-terminus that could be used for co-immunoprecipitation assays with commercial antibodies. A PCR was performed using two specific primers to introduce restrictions sites for *HindIII* at the 5' and 3' ends:

Primer name	Sequence (from 5' to 3')	
H3VR1	CTCAAGCTTCATGGAACAACGGGCTAGCTTA	95° 2' 95° 30" 45° 1' 68° 4' } x35
TRPV1-R-TMBV	GAGGAATCCCCCCCGACATGGTCGACGGTATCGATAAGC TTGATTTCTCCCCTGGGACCATGGA	

TRPV1-VStop

To verify if the C-terminus of TRPV1 contains a putative PDZ binding domain, a truncated form was generated by introducing a stop codon at position Val-828 and named TRPV1-VStop. The following primers and conditions were used:

Primer name	Sequence (from 5' to 3')	
VR1 V-Stop +	GAGGATGCTGAGTAATTCAAGGATTCC	94° 2' 94° 1' 50° 45" } x5 72° 10' 94° 1' 65° 45" } x25 72° 10' 72° 10'
VR1 V-Stop -	GGAATCCTTGAATTACTCAGCATCCTC	

GST-fused NtTRPV1 and CtTRPV1

In order to obtain a GST-fusion protein, the N-terminus of rat TRPV1 (amino acids 1-414) was cloned into the pGEX-4T1 plasmid (GE Healthcare) with *BamH*I and *EcoR*I restriction sites at the 5' and 3' ends, respectively, by performing a PCR using the following primers and conditions:

Primer name	Sequence (from 5' to 3')	
BamHITRPV1+	ATTATAGAATTCTAATGGAACAACGGGCTAGCTTAGACT	92° 2' 92° 10" 37° 30" } x5 68° 2'
EcoRINtTRPV1	CTTAAGATTACTGGACGTGGCCAGGAAGACCGAC	92° 30" 50° 30" } x25 68° 2'

Likewise, the C-terminus of rat TRPV1 (amino acids 682–830) was cloned into pGEX-4T1 with *Not*I and *Sal*I restriction sites at the 5' and 3' ends, respectively (Garcia-Sanz *et al.* 2004).

Human Whirlin-myc

Human Whirlin cDNA (encoding for the 907 amino acids of the full length protein) was obtained from Open Biosystems in the pOTB7 plasmid and subsequently subcloned in the pcDNA 3.1-myc-His plasmid for its expression in eukaryotic cells and detection by commercial antibodies. First, both the plasmid and the insert were digested with *BamH*I and *EcoR*I restriction enzymes and ligation of the two segments was performed. Then, in order to eliminate the termination codon of the protein, a PCR was run by using the following primers and conditions:

Primer name	Sequence (from 5' to 3')	
CIP861	TCTGAAGCAGAAGGCAGCGGGC	95° 3' 95° 1' 45° 1' 68° 6' } x5
CIPDEF	P-AGAGCATCACATTGAACTCAGTG	95° 1' 60° 1' 68° 6' } x35

Finally, the amplified segment and the construction obtained in the first step were digested with *Afl*II and *EcoR*I and then ligated.

Rat Whirlin-myc

Rat Whirlin was isolated by PCR from a rat brain cDNA library (Morenilla-Palao *et al.* 2004) by using the following primers and conditions and subsequently subcloned in the pcDNA 3.1-myc-His plasmid between *BamH*I and *EcoR*I restriction sites:

Primer name	Secuence (from 5' to 3')	
CIP98 rat +	GATCGAATTCATGAACGCACAGCTG	95° 2' 95° 1' 55° 1' 72° 3' } x5
CIP98 rat -	GCAGGATCCTTCAGAGCATCACGTT	95° 1' 67° 1' 72° 3' } x25 72° 10'

PDZ1+2-myc

This construction (encoding for the first 406 amino acids of the full length protein) was obtained by digesting Whirlin-myc with *Apa*I and subsequently introducing the insert in the pcDNA 3.1-myc-His plasmid digested with the same enzyme.

PDZ3-myc

This construction (corresponding to Whirlin human short isoform AK022854), was obtained by amplification from a human brain gene library using the following primers and conditions:

Primer name	Sequence (from 5' to 3')	
PDZ3L	ATGCATGGTTCTCTTGAAGCTTTG	95° 2' 95° 30'' 48° 1' 68° 3' } x10
PDZ3-3'	CTAGAGCATCACATTGAACTCAGT	95° 30'' 53° 1' 68° 3' } x30 68° 5'

As the sequence obtained presented a 210 bp deletion compared to the coding sequence for the complete short isoform, this one was finally obtained by amplification and ligation of two distinct fragments and subsequently insertion in the pcDNA 3.1-myc-His plasmid.

Primer name	Sequence (from 5' to 3')	
PDZ3L	ATGCATGGTTCTCTTGAAGCTTTG	95° 2' 95° 45'' 50° 1' } x10 68° 3' 95° 45'' 53° 1' } x30 68° 3' 68° 5'
AK762R	GGCGTGGGTGTTGAGCAGCTT	
AK762F	AAGCTGCTCAACACCCACGCC	
CIP98-3'	GGTCATCATCACCATCACCATTGA	

PSD95-myc

PSD95 cDNA was isolated by PCR from a human DRG library (Invitrogen) using the following primers and conditions that permitted to introduce an *EcoR*I restriction site at its C-terminus:

Primer name	Sequence (from 5' to 3')	
PSD95	TCTGCAGAATTCGAGTCTCTCTCGGGCTGGGACCCA	95° 3' 94° 1' 40° 1' } x35 68° 6'

Subsequently the amplified segment and the pcDNA 3.1-myc-His were digested with *Hind*III and *EcoR*I and ligated.

Ubiquitin-his

This construction was a gift from Dr. Rosa Farrás (Centro de Investigación Principe Felipe, Valencia, Spain).

$Ub^{G76V}GFP$

This construction was obtained from Addgene and consists of a ubiquitin cDNA with the Gly-76 mutated to Val and fused to the N-terminus of GFP by cloning in the EGFP-N1 plasmid.

Dynamin

Wild-type dynamin construct was a gift from M. McNiven (Mayo Clinic and Foundation).

TOTAL PROTEIN EXTRACTION

Cell extracts were obtained after 24-48 hours post-transfection using one 6-well per condition (different DNA and/or treatments). The cells were placed on ice, washed twice with cold PBS and collected. The pellet obtained by centrifuging for 5 minutes at 1000 g was resuspended in approximately 100-200 µl per well of lysis buffer (50 mM HEPES pH 7.4, 140 mM NaCl, 10% Glycerol, 1% v/v Triton X-100, 1 mM Ethylenediaminetetraacetic acid (EDTA), 2 mM Ethylene glycol tetraacetic acid (EGTA), 0.5% sodium deoxycholate) plus a proteases inhibitors cocktail (Sigma) at a 1:100 dilution. Cells were incubated for 30 minutes at 4 ºC with gentle agitation. Cellular debris were removed by centrifugation at 16,000 g for 15 minutes at 4 ºC. Total protein in the supernatants was determined with the Bicinchoninic Acid (BCA) Protein Assay Reagent (Pierce) following manufacturer instructions. Protein samples (approximately 20-40 µg of protein per condition) were denatured in Laemmli sample buffer at 100 ºC for 15 minutes on a heat block.

For spinal cord extracts, tissues were dissected, weighed and immediately frozen at -80 ºC. Upon thawing, they were homogenised in 3 ml per gram of tissue of cold RIPA buffer (50 mM Tris-Cl pH 7.4, 150 mM NaCl, 1% NP-40, 0.5% sodium deoxycholate, 0.1% SDS) containing a protease-inhibitor cocktail. The suspension was gently passed through a syringe with needles of increasing gauge number (21G, 23G and 25G) ten times per each. After centrifugation for 5 minutes at 1000 g to remove debris and insoluble material, total protein in the supernatants was determined and protein samples (approximately 50 µg of protein per condition) obtained as before.

SDS-PAGE

In our experiments, gels were made by pouring the corresponding solutions between two glass plates (1.5 mm thickness, Biorad):

Composition	Resolving gel (9%)	Resolving gel (12%)	Composition	Stacking gel (4%)
Distilled water	3.4 ml	2.6 ml	**Distilled water**	1.8 ml
Tris 1.5 M pH 8.8	2 ml	2 ml	**Tris 0.5 M pH 6.8**	0.75 ml
SDS 10%	80 µl	80 µl	**SDS 10%**	30 µl
30% Acrylamide/ 0.8% Bis-Acrylamide*	2.4 ml	3.2 ml	**30% Acrylamide/ 0.8% Bis-Acrylamide***	390 µl
Ammonium persulfate 10%	60 µl	60 µl	**Ammonium persulfate 10%**	36 µl
Tetramethylethylenediamine (TEMED)	6 µl	6 µl	**TEMED**	4 µl

*(*Protogel, National Diagnostic)*

WESTERN IMMUNOBLOT

In order to make the proteins accessible to antibody detection after their separation by SDS-PAGE, they were subsequently transferred onto a 0.45 µm nitrocellulose membrane (Biorad) using the Mini Trans-Blot Cell system connected to a power supply (Biorad). A transfer sandwich was made by overlapping a sponge, two Whatman filter papers, the gel, the nitrocellulose membrane, two filter papers and another sponge, eliminating eventual air bubbles between the gel and the membrane. The sandwich was placed into the transfer apparatus, with the membrane between the gel and a positive electrode, and covered with transfer buffer (200 mM Glycine, 25 mM Tris pH 8.3 and 20% Methanol). The proteins were transferred to the membrane for 90 minutes at 100 V at 4 ºC.

Afterwards, the membranes were blocked for 1 hour at room temperature (RT) with agitation with non-fat dry milk at 5% in Tris-buffered saline (25 mM Tris-HCl, 0.15 M NaCl, pH 7.2) with 0.05% Tween-20 (TBS-T) to prevent non-specific background binding of the primary and/or secondary antibodies to the membrane. The membranes were then incubated o/n at 4 ºC under gentle agitation with the corresponding primary antibodies dissolved in PBS with 1% bovine serum albumin (BSA) and 0.02% sodium azide. Thereafter, after three washes of 10 minutes with TBS-T, the membranes were incubated with the horseradish peroxidase (HRP)-conjugated secondary antibody. After three washes with TBS-T the membranes were incubated with a homemade ECL mix (proportion 1:1), a luminol-based chemiluminescent substrate for the detection of HRP on immunoblots. Protein bands quantification was realised using ImageJ or TotalLab QUANT softwares. Data were expressed as means ± S.E.M for number of experiments (N) in different conditions. Statistical analysis was performed with paired *t* test and significance level was preset to $p<0.05$.

Primary Antibodies

The primary antibodies and probes used in the present work and the respective working conditions are reported in the following table:

ANTIBODY	STOCK	DILUTION	INCUBATION TIME	SPECIES	MANUFACTURER
α-TRPV1 serum (C-terminus EVFKDSMVPGEK)	/	1:1000	2 hours at RT	Rabbit	DiverDrugs S.L.
α-TRPV1 (C-terminus)	0.8 mg/ml	WB: 1:3000 IC 1:500	o/n at 4 °C	Rabbit	Alomone
extracellular α-TRPV1 serum (LPMESTPHKCRGS)	1 mg/ml	1:1000	o/n at 4 °C	Rabbit	GenScript
α-TRPV1 (C-terminus)	/	1:500	o/n at 4 °C	Guinea Pig	Millipore
α-TRPV1 (N-terminus)	1 mg/ml	1:1000	o/n at 4 °C	Goat	Santa Cruz Biotechnology

ANTIBODY	STOCK	DILUTION	INCUBATION TIME	SPECIES	MANUFACTURER
α-GST	1mg/ml	1:1000	o/n at 4 °C	Mouse	Sigma Aldrich
α-myc	/	1:1000	o/n at 4 °C	Mouse	Sigma Aldrich
α-Whirlin serum (C-terminus EVHRPDSEPDVNEV)	/	1:2000	o/n at 4 °C	Rabbit	GenScript
α- Whirlin (C-terminus)	/	1:100	o/n at 4 °C	Rabbit	Novus Biologicals
α- Whirlin (aa 600-700)	/	1:100	o/n at 4 °C	Rabbit	Abcam
α-Actin	0.4-0.8 mg/ml	1:1000	o/n at 4 °C	Rabbit	Sigma Aldrich
α-FK1 (polyubiquitinated conjugates)	1 mg/ml	1:1000	o/n at 4 °C	Mouse	Enzo Life Sciences
α-FK2 (mono- and polyubiquitinated conjugates)	1 mg/ml	1:1000	o/n at 4 °C	Mouse	Enzo Life Sciences
α-LAMP2	200 µg/ml	1:1000	o/n at 4 °C	Mouse	Santa Cruz Biotechnology
α-EEA1	250 µg/ml	1:1000	o/n at 4 °C	Mouse	BD Transduction Laboratories
α-Flotilin	250 µg/ml	1:1000	o/n at 4 °C	Mouse	BD Transduction Laboratories
α-GFP	200 µg/ml	1:1000	o/n at 4 °C	Rabbit	Santa Cruz Biotechnology
α-CGRP	5 mg/ml	1:200	o/n at 4 °C	Goat	Abcam
IB4-568	1 mg/ml	1:200	1 hour at RT	/	Molecular Probes
α-NF200	/	1:500	o/n at 4 °C	Rabbit	Sigma

Secondary Antibodies

The secondary antibodies used in the present work and the respective working conditions are reported in the following table:

ANTIBODY	STOCK	DILUTION	INCUBATION TIME	SPECIES	MANUFACTURER
Goat α-rabbit HRP	/	1:5000	1 hour at RT	Rabbit	Sigma

ANTIBODY	STOCK	DILUTION	INCUBATION TIME	SPECIES	MANUFACTURER
Goat α-mouse HRP	/	1:2000	1 hour at RT	Rabbit	Sigma
α-mouse/rabbit/ guinea pig Cy3/TRITC/Alexa-488/568 conjugates	/	1:200	1 hour at RT	Multiple	Jackson Immunoresearch

PULL-DOWN ASSAY

The DNA constructions pGEX4T, GST-NtTRPV1 and GST-CtTRPV1 were expressed in BL21-Codon Plus (RIL) *Escherichia coli* (Stratagene) employing the heat shock protocol (Maniatis). For each construction a colony was inoculated in 50 ml of Luria Broth (LB)-Ampicillin medium o/n at 37 ºC with vigorous shaking. The culture was diluted in 500 ml of 2X YT medium (16 g/l tryptone, 10 g/l yeast extract, 5 g/l NaCl) to an A_{600} of 0.1 and growth to an A_{600} of 0.4-0.6. Fusion proteins expression was induced by adding Isopropyl β-D-1-thiogalactopyranoside (IPTG, Sigma) to the culture to a final concentration of 1 mM. Cultures were incubated for an additional 2 hours at 37 ºC and then pelleted for 10 minutes at 5000 g. Each pellet was resuspended in PBS (20 ml/250 ml of culture) supplemented with protease inhibitors (1 mM phenylmethylsulfonylfluoride, PMSF, and 10 mM Iodoacetamide). Cells lysis was achieved by incubating with lysozime 0.1 mg/ml, shacking for 10 minutes at RT and finally sonicating 3 times for 10 seconds. To facilitate fusion proteins solubilisation, the suspension was incubated for 30 minutes at 4 ºC with glycerol and Triton X-100 to a final concentration of 15% and 0.01% respectively. Insoluble materials were removed by centrifuging for 30 minutes at 16,000 g at 4 ºC. The supernatant was transferred to a 15 ml falcon tube with 100 µl of slurry glutathion-sepharose 4B (GE Healthcare), previously equilibrated with PBS, and incubated for 2 hours at RT with gentle agitation. After centrifuging for 3 minutes at 500 g and discharging the runthrough, the GST-fusion protein/sepharose 4B beads were washed several times (10 minutes each time) with PBS until an A_{260} of 0 was measured. Thereafter an equilibration step was included with extraction buffer (150 mM NaCl, 10 mM Tris, 5 mM EDTA, 10 mM $MgCl_2$, pH 7.5, 1% Triton X-100 and 0.5% Nonidet P-40 or NP-40) plus protease inhibitors. The immobilised protein was incubated o/n at 4 ºC with HEK293 transiently expressing Whirlin freshly solubilised in extraction buffer. After several washes with extraction buffer the proteins were eluted and denatured with SDS sample loading buffer, resolved by SDS-PAGE and analysed by Western Immunoblot.

COIMMUNOPRECIPITATION

HEK293 cells were cotransfected with wild-type TRPV1 or TRPV1-VStop mutant and myc-tagged Whirlin, PDZ1+2, PDZ3 or PSD95, using Lipofectamine™ 2000 reagent. 48 hours

after transfection cells were washed twice with cold PBS, collected and pelleted by centrifuging at 1000 g for 5 minutes. The pellets were resuspended in RIPA buffer containing a protease inhibitors cocktail and incubated for 30 minutes at 4 ºC with gentle agitation. Cellular debris were removed by centrifugation (15 minutes at 16,000 g at 4 ºC) and total protein in the supernatants was quantified. Approximately 900 µg of protein were incubated o/n at 4 ºC with 10 µl of slurry anti-c-Myc antibody immobilised to agarose beads (Pierce). Immunoprecipitated complexes were washed three times with TBS-T and eluted through the Handee™ Spin Columns with 25 µl of 2X Non-Reducing Sample Loading Buffer. After addition of 2 µl of 2-Mercaptoethanol, samples were denatured at 100 ºC for 10 minutes and analysed by Western Immunoblot.

For immunopurification with the anti-TRPV1 (N-terminus) antibody, cell lysates were precleared for 2 hours with 30 µl of slurry protein G and incubated o/n with ~4 µg of the primary antibody. After further incubation with 60 µl of slurry protein G, immunocomplexes were washed 4-5 times with RIPA-buffer, denatured at 100 ºC for 10 minutes with 2X SDS sample buffer and analysed by Western Immunoblot.

BIOTIN LABELING OF SURFACE PROTEINS

This technique allows to label and separate membrane proteins on the plasma membrane from those in the intracellular compartments. The isolation procedure uses a membrane-impermeable, cleavable biotinylation reagent to label exposed primary amines of proteins on the surface of intact adherent or suspension cells. HEK293 cells transiently coexpressing TRPV1 plus Whirlin or YFP (Clontech) in control were washed twice with cold PBS and incubated with 0.5 mg/ml sulfo-NHS-SS-Biotin (Pierce) for 30 minutes at 4 ºC (Morenilla-Palao *et al.* 2004). Plates were rinsed with 100 mM glycine in cold PBS and incubated in the same buffer for 30 minutes at 4 ºC to quench and remove excess biotin reagent. Cells were lysed for 1 hour at 4 ºC with lysis buffer (50 mM HEPES pH 7.4, 140 mM NaCl, 10% Glycerol, 1% Triton X-100, 1 mM EDTA, 2 mM EGTA, 0.5% sodium deoxycholate) containing a proteases inhibitors cocktail. Lysates were cleared of cell debris by centrifugation at 16,000 g for 15 minutes at 4 ºC. Total protein was quantified and biotin-labeled proteins were isolated incubating approximately 100 µg of cell lysates with 60 µl of slurry streptavidin agarose o/n at 4 ºC: the streptavidin is able to establish a strong non-covalent interaction with biotin thus isolating only labeled proteins localised at the cell surface. After two washes with lysis buffer, the immobilised protein were eluted and denatured with 2X SDS loading buffer, resolved by SDS-PAGE and detected by Western Immunoblot.

UBIQUITINATION ASSAY

The identification of ubiquitinated conjugates of TRPV1 was performed as described in (Choudhury *et al.* 2004) with some modifications. HEK293 cells were co-transfected with a myc-

tagged TRPV1, an untagged Whirlin (or YFP in control) and a His6-tagged Ubiquitin. At 24 hours after transfection MG132, a proteasome inhibitor, was added to the culture medium at a final concentration of 10 µM. At 48 hours after transfection cells were collected and lysed for 30 minutes at 4 ºC in RIPA buffer containing 10 µM MG132, 5 mM N-Ethylmaleimide and 5 nM Ubiquitin aldehyde (two deubiquitinases inhibitors), and proteases inhibitors. Lysates were then cleared of cell debris by centrifugation at 16,000 g for 15 minutes at 4 ºC. The supernatants (~800 µg of protein) were incubated o/n at 4 ºC with 10 µl of anti-c-myc agarose. Immunocomplexes were washed three times with a solution of TBS-T, eluted with SDS loading buffer and analysed by Western Immunoblot.

IMMUNOCYTOCHEMISTRY AND CONFOCAL MICROSCOPY

To analyse the subcellular distribution of TRPV1 and Whirlin, DRG primary cultures or transfected HEK293 cells were washed three times with cold PBS and fixed with 4% paraformaldehyde (PFA) in PBS for 15 minutes on ice. After extensive washing with PBS, cells were blocked and permeabilised for 10 minutes at RT with 0.3% Triton X-100 and blocked for 1 hour at RT in 5% serum (from the species in which the corresponding secondary antibody was raised). Thereafter cells were incubated with the appropriate primary antibodies, dissolved in blocking solution, o/n at 4 ºC with agitation. After washing twice (10 minutes each time) with High Salt PBS (0.5 M NaCl), and twice with 1X PBS, cells were incubated with the secondary antibodies dissolved in blocking solution, for 1 hour at RT. After washing two times with PBS, cell nuclei were stained with 0.2 µg/ml 4',6-diamidino-2-phenylindole (DAPI, Molecular Probes) in PBS for 3 minutes at RT. Coverslips were mounted with Mowiol (Calbiochem) onto microscope slides and stored at 4 ºC until observation. Cells were evaluated and analysed by confocal microscopy in a Zeiss LSM 5 Pascal inverted fluorescence microscope, using 40x and 63x oil-immersion objectives.

To analyse TRPV1 levels at the plasma membrane, an antibody that recognised an epitope located in the extracellular domain of the receptor was used. Specifically, this polyclonal antibody, referred to as TRPV1e, was generated against the sequence ^{607}LPMESTPHKCRGSA^{620} of rat TRPV1, located in the loop between TM5 and TM6, just after the glycosylation site (GenScript) (Camprubi-Robles *et al.* 2009). Intact HEK293 cells co-transfected with TRPV1 plus Whirlin-myc, or plus DsRed in control, were incubated for 1 hour at 4 ºC with TRPV1e (1:1000) in cold complete DMEM plus 1% BSA with agitation. After several washes, cells were fixed and permeabilised as previously described and thereafter incubated o/n at 4 ºC with mouse anti-c-myc (Sigma) to visualise Whirlin distribution. After extensive washing cells were incubated with the secondary antibodies, mounted with Mowiol and visualised with an inverted confocal microscope.

IMMUNOHISTOCHEMISTRY

Animals were over-anesthetised with pentobarbital (50 mg/kg, intraperitoneal) and then transcardially perfused through the left ventricle with cold saline followed by 4% PFA in PBS (pH 7.4). DRG were quickly removed bilaterally and post-fixed for 4 hours in the same fixative solution at 4 ºC. The tissues were placed in PBS containing increasing concentrations (10, 20, and 30%) of sucrose at 4 ºC for cryoprotection until the tissues sunk and then frozen with dry ice in mounting medium (O.C.T.™, Tissue-Tek). DRG were serially cut at 14 µm thickness on a cryostat, mounted onto polylysine-coated Menzel-Gläser Superfrost UltraPlus® slides (Thermos Scientific), and kept at -20 ºC until use.

Slides were then defrosted for 30 minutes at RT, washed, blocked with 1% BSA and 0.3% Triton-X100 in PBS for 30 minutes at RT and incubated o/n at 4 ºC with the primary antibodies diluted in the blocking solution. After washing three times with PBS (10 minutes each time), sections were incubated with the appropriate secondary antibodies for 1 hour at RT. Sections were then washed four times for 10 minutes in PBS and mounted with Mowiol.

At least 5 images per sample were captured with an inverted confocal microscope (40x oil-immersion objective) and then analysed with Zen Lite 2012 software (Zeiss) by tracing the soma perimeter in a calibrated image on a computer screen and calculating the percentage of positive neurons for each marker.

RNA silencing

Three different siRNAs (Ambion) were used to suppress Whirlin expression in F11 and DRG cultures:

siRNA	Sequence (from 5' to 3')	Location
siRNA-1	CGAUAAAUCUCUAGCCCGG	Chromosome 5-587 (Exon 1)
siRNA-2	GGAUUUACAAGGGCCCAG	Chromosome 5-1212 (Exon 6)
siRNA-3	CCAUGAUGUACUACCUAGA	Chromosome 5-1327 (Exon 6)

A siRNA to GAPDH and a scramble siRNA (a siRNA with a random sequence) were also used as positive and negative controls respectively.

F11 cells were cotransfected with rat TRPV1 and Whirlin plasmids and/or either of the siRNAs described above or a mix of them at two distinct concentrations, 30 and 50 nM.

A Cy3-labelled siRNA-2 was also used in order to verify transfection efficiency in DRG cultures and to identify transfected cells for functional assays.

RNA PREPARATION AND qPCR

Total RNA was isolated from F11 cells or rat DRG using E.Z.N.A.™ HP Total RNA Kit (Omega). RNA concentration was estimated and approximately 1 µg RNA was used for RT-PCR with Gene Amp® RNA PCR (Applied Byosistems), according to the manufacturer conditions. qPCR was performed with 20 ng cDNA using appropriate Taqman® for rat Whirlin (Reference number 00710383_m1, Applied Biosystems) and Taqman PCR Mastermix (Applied Biosystems). Three replicate for each sample were tested. Singleplex reactions were runned with an ABI PRISM 7700 thermocycler (Applied Byosystems) using the following cycling conditions: 50 ºC for 2 minutes; 95 ºC for 10 minutes; 40 cycles of (95 ºC for 15 seconds; 60 ºC for 1 minute). Whirlin expression relative to a housekeeping gene (GAPDH) was determined. A non-template sample was also used as a control.

SUBCELLULAR FRACTIONATION

HEK293 transiently coexpressing TRPV1 plus Whirlin or YFP or Whirlin plus YFP were washed and collected with PBS and resuspended in ice-cold hypotonic lysis buffer (10 mM Tris pH 7.5, 10 mM NaCl, 1 mM EDTA) containing a proteases inhibitors cocktail. The suspension was gently passed 10 times through a 27-gauge needle. Samples were centrifuged at 1000 g for 10 minutes at 4 ºC. The resulting postnuclear supernatant was centrifuged at 14,000 g for 15 minutes at 4 ºC to yield a heavy membrane pellet (P14), that contains mostly lysosomes and mitochondria, and a supernatant (S14) which was ultracentrifuged at 100,000 g for 1 hour at 4 ºC to yield a light membrane/vesicular pellet (P100) and a soluble fraction (S100) representing the cytoplasm. Each pellet was resuspended in 100 µl of ice-cold hypotonic lysis buffer plus protease inhibitors. Equal proportions of the three fractions were analysed by SDS-PAGE and Western Immunoblot (Robinson and Dixon 2005).

ENDOSOMES/LYSOSOMES ISOLATION

Percoll gradient fractionation was performed as previously described (Press *et al.* 1998). Briefly, six confluent 10-cm dishes were washed twice in PBS containing 1 mM $MgCl_2$ and 0.9 mM $CaCl_2$ (PBS^+), and the cells were scraped in PBS^- (without $MgCl_2$ and $CaCl_2$). From this point on, all buffers contained a proteases inhibitors cocktail. Cells were pelleted by centrifugation at 1,000 g for 10 minutes at 4 ºC. The cell pellet was resuspended in 10 ml homogenisation buffer (HB: 20 mM HEPES, pH 7.4, 150 mM NaCl, and 2 mM $CaCl_2$). The cells were again collected by centrifugation and resuspended in three-pellet volumes of HB. The suspension was gently passed through a 27-gauge needle eight times. Cell debris and nuclei were removed by two successive centrifugation steps at 1000 g for 5 min in a microfuge at 4 ºC. The resulting postnuclear supernatant (~1 ml) was overlaid onto 8 ml of a 20% Percoll solution prepared in TBS buffer. The samples were subjected to centrifugation at 4 ºC for 50 minutes in

a 70.1Ti fixed angle rotor (Beckman) at 20,000 g. One ml fractions were collected. NP-40 was added to each fraction to a final concentration of 1% and incubated for 1 hour on ice to solubilise all membranes. Subsequently, the Percoll was removed by centrifugation for 1 hour at 100,000 g in a TLA 100.2 rotor. Individual fractions were analysed by SDS-PAGE and Western Immunoblot.

LIPID RAFTS ISOLATION

HEK293 cells were rinsed with cold PBS, collected and resuspended in 1 ml of MES solution (25 mM 2-(N-morpholino)-ethanesulfonic acid pH 6.5, 150 mM NaCl) plus 1% Triton X-100 and protease inhibitors. After 30 minutes at 4 ºC with agitation, samples were centrifuged 30 minutes at 16,000 g to separate the Triton-extract from the insoluble pellet.

To make a continuous sucrose gradient (total volume: 8 ml per sample), two solutions at distinct sucrose percentage (45% and 5%) were prepared and loaded into a standard two chambers gradient maker connected to a peristaltic pump (Masterflex L/S Economy Drive, Cole Parmer). The gradient was prepared freshly on the day of the experiment and kept at 4 ºC until use.

One ml of the previously obtained cellular extract was applied slowly through a plastic Pasteur pipette on top of the pre-cooled gradient. The loaded gradients were placed in a SW40Ti rotor (Beckman) and ultracentrifuged at 190,000 g for 16 hours at 4 ºC. At the end, nine fractions of 1 ml were recollected starting from the top of the gradient and proteins precipitated by incubation with 20% trichloroacetic acid (TCA) (ratio 1:1) for 30 minutes on ice. After a 15 minutes centrifugation at 14,000 g at 4 ºC, any TCA residue was washed out with 200 µl of cold acetone then eliminated by centrifuging two times at 14,000 g for 5 minutes. The resulting pellets were resuspended in 2X reducing sample buffer, denatured and analysed by SDS-PAGE and Western Immunoblot.

CALCIUM IMAGING ASSAY

HEK293 cells cotransfected with TRPV1 and Whirlin, or pcDNA in control, were loaded with 5 µM Fluo-4-AM (Molecular Probes) in the presence of 0.02% pluronic F-127 acid (Invitrogen) in HBSS (140 mM NaCl, 4 mM KCl, 1 mM $MgCl_2$, 1.8 mM $CaCl_2$, 5 mM D-glucose, 10 mM HEPES pH 7.4) for 1 hour at 37 ºC in the darkness. Coverslips were then mounted in an imaging chamber continuously perfused (1 ml/min) with HBSS at ~20-22 ºC using a multibarreled gravity-driven, automatic operated perfusion system.

TRPV1 activity was evoked with a first 15-seconds pulse of capsaicin at increasing concentration (0.01-0.1-1-10 µM) and a 15-seconds pulse of a supramaximal concentration of capsaicin (100 µM) after a 5-minutes washing with HBSS. Capsaicin stock (100 mM, Fluka) was prepared in dimethylsulfoxide (DMSO, Sigma) and diluted as indicated for the experiments in HBSS the day of the experiment. The same protocol was applied for DRG cultures plus an

additional brief (15 seconds) application of 40 mM KCl to distinguish neurons from non-neuronal cells and to ensure that cells were healthy and responsive.

Fluorescence from individual cells was monitored as a function of time and measured with a Zeiss Axiovert 200 inverted microscope (Carl Zeiss) fitted with an ORCA-ER CCD camera (Hamamatsu Photonics) through a 10x or 20x air objective. Fluo-4 was excited at 500 nm using a computer-controlled Lambda-10-2 filter wheel (Sutter Instruments), and emitted fluorescence was filtered with a 535-nm long-pass filter. Images were acquired and processed with AquaCosmos package software (Hamamatsu Photonics).

The amplitude of Ca^{2+} increase caused by stimulation with capsaicin was expressed as a delta function ΔF/F0 by quantifying the ratio between the change in the fluorescence signal intensity (ΔF) and the baseline fluorescence before capsaicin application (F0). The response to capsaicin stimulus was also defined as the ratio (expressed as percentage) between the intensity of the Ca^{2+} peak of the first capsaicin application with respect to the Ca^{2+} peak of the second capsaicin application. All data were expressed as mean ± S.E.M, with n=number of cells tested and N=number of experiments realised. For statistical analysis, a Two-way ANOVA followed by Bonferroni post-test was applied and significance level was preset to $p<0.05$.

For cholesterol-depletion assays with MβCD, cells were loaded with 10 μM Fura-2/AM ester (Biotium) for 1 hour at 37 ºC. Fura-2 is a ratiometric dye which has an emission peak at 505 nM and changes its excitation peak from 340 nm to 380 nm in response to Ca^{2+} binding. Thus, by measuring the ratio of intensities on digital images captured at 340 and 380 nm the variation of Ca^{2+} concentration can be tracked. Lipid raft disruption was performed as follows. After the application of the first 1 μM capsaicin stimulus (15 seconds) and a 5 minutes washing step, a continuous perfusion of 10 mM MβCD solution was applied for 15 minutes. Then a second washing step was performed with HBSS for 5 minutes and a second agonist pulse at the same concentration was applied. The ratio of the second with respect to the first peak of capsaicin application was calculated.

CALCIUM MICROFLUOROGRAPHIC ASSAY

Cells were seeded in black 96 well-plate with clear flat bottom at 10,000-20,000 cells per well and transfected between 24-48 hours after seeding with Lipofectamine™ 2000. We used the fluorescence Ca^{2+} indicator Fluo4-NW (Molecular Probes) for detecting channel's activity. 48 hours after transfection cells were incubated with 100 μl of dye loading solution (1X HBSS, 20 mM HEPES, pH 7.4) in the presence of 2.5 mM probenecid for 45 minutes at 37 ºC and 10 minutes at RT. For fluorescence detection we used the microplate reader POLARstar Omega (BMG Labtech). The protocol used measured the Fluo-4 fluorescence signal (excitation at 494 nm and emission at 516 nm) during 18 cycles. TRPV1 activity was evoked by the addition of capsaicin in the fifth cycle using the injection system of the plate reader. We quantified the response to capsaicin by calculating the AUC between the fifth and the

eighteenth cycles, generated by the increase of fluorescence signal induced by the response to capsaicin.

PATCH CLAMP RECORDINGS

HEK293 cells were cotransfected with a mixture of TRPV1, Whirlin, and CD8 (as a reporter protein) cDNAs, in a 2:2:1 ratio, and cultured for 48 hours before being tested. In control samples, Whirlin was replaced by YFP. For selection, cells were incubated with 1 µl of anti-CD8-coated magnetic beads (Dynal).

Patch pipettes (1.5 mm external and 1 mm internal diameter) were prepared from thin-borosilicate glass (World Precision Instruments) with a P-97 horizontal puller (Sutter Instruments) and fire-polished with a microforge MF-830 (Narishige) to have a final resistance of 2-3 MΩ. Standard whole-cell voltage-clamp protocols were applied using an EPC-10 amplifier (HEKA Electronic).

Pipettes were filled with standard internal solution containing (in mM): 144 KCl, 2 $MgCl_2$, 5 EGTA and 10 HEPES. The pH was adjusted at 7.2 with KOH and the osmolarity set to 295 mosmol/kg. Standard extracellular solution contained (in mM): 140 NaCl, 4 KCl, 2 $CaCl_2$, 2 $MgCl_2$, 10 HEPES, 5 glucose and 20 mannitol. The pH was adjusted at 7.4 and the osmolarity set to 320 mosmol/kg. For acidic solution, HEPES was replaced with MES and pH adjusted to 6 and 50 µM amiloride was included to block ASIC responses. The different saline solutions were applied with a gravity-driven local microperfusion system near the recorded cell. Capsaicin stock (100 mM) was prepared in DMSO and diluted as indicated for the experiments in bath solution the day of the experiment. All recordings were performed at RT of 22-24 ºC.

Voltage-step protocols consisting of 100 ms depolarising pulses from -120 mV to +220 mV in steps of 20 mV were used. The holding potential (V_h) was -60 mV and the time interval between each pulse was 5 seconds. Conductance-voltage (G-V) curves were obtained by converting the maximal current values from the voltage step protocol to conductance using the relation $G=I/(V-V_r)$, were G is the conductance, I is the peak current, V is the command pulse potential, and V_r is the reversal potential. G-V curves for each cell were fitted to the Boltzmann equation

$$G=G_{max}/\{1 + \exp[(V_{0.5}-V)/a_n]\}$$

where G_{max} is the maximal conductance in a given cell, $V_{0.5}$ is the voltage required to activate the half-maximal conductance and a_n the slope of the G-V curve. This value can be used to calculate the valence (charge) moving across the channel during the transitions from the closed to the activated state thus obtaining an estimation of the voltage-dependence of the channel:

$$z_g=RT/a_nF$$

where z_g is the valence and F, R and T are Faraday constant, gas constant and absolute temperature respectively. Since RT/F=25.69 mV at room temperature (25 ºC), z_g = 25.69 mV/a_n. Thereafter, G_{max} values were used to obtain the normalised G/G_{max}-V curves.

Capsaicin- or acidic pH-evoked currents were elicited with V_h set at -60 mV. Pulses were applied for a time sufficient for the response to reach plateau.

Data were visualised and analised using PulseFit (HEKA Electronic), GraphPad Prism 5 statistical software (GraphPad Software) and Origin 8.0 (OriginLab Corporation). All data were expressed as means ± S.E.M, with n=number of cells tested. For statistical analysis, unpaired *t* test and Two-way ANOVA followed by Bonferroni post-test were applied and significance level was preset to $p<0.05$.

ANIMALS

Experimental procedures were approved by the Institutional Animal and Ethical Committee of the University Miguel Hernández de Elche, in accordance with the guidelines of the Economic European Community, the National Institutes of Health, and the Committee for Research and Ethical Issues of the International Association for the Study of Pain. Animals were kept in a separate, sound-attenuated animal room having controlled temperature (21-23 ºC) and air humidity and a 12 hour light–dark cycle. They were provided with food and water *ad libitum*. Wistar rats and wild type C57BL/6J mice were purchased from in house bred stock (originally from Harlan Laboratories). Whirler mutant mice were kindly provided by Dr. Philomena Mburu (Mburu *et al.* 2003). Whirlin$^{neo/neo}$ mice were kindly provided by Dr. Jun Yang (Yang *et al.* 2010). Male mice (9-10 animals/group) between 11 and 16 weeks age were used for all the behavioural tests below described.

Genotyping

Genomic DNA from mouse tails was extracted by incubating with 75 µl of Solution I (25 mM NaOH and 0.2 mM EDTA) for 1 hour at 98 ºC and then adding 75 µl of Solution II (40 mM Tris-HCl, pH 5.5). After centrifugating at 1500 g for 3 minutes 2-4 µl of the extract were used for PCR amplification. The following primers and cycling conditions were used for whirler:

Primer name	Sequence (from 5’ to 3’)	
D4Mit17	TGGCCAACCTCTGTGCTTCC	94° 3’ 94° 2’ 58° 1’ 68° 2’ } x35
D4Mit17 rev	ACAGTTGTCCTCTGACATCC	
D4Mit244	CAAAATATCTGACAAAAACAAGTGTG	
D4Mit244 rev	GGTGTCATCACCATGATGGA	

and for whirlin$^{neo/neo}$:

Primer name	Sequence (from 5' to 3')	
PDZG1	GGGTGAGTGAATGCCAGCCAG	95° 2' 95° 30" 65° 30" } x35 72° 1' 72° 5'
PDZG5R	CAGGGAAGTTGAGGCACACGG	
PNT3A	GAGATCAGCAGCCTCTGTTCCAC	

And these are the product size expected for the different strains of mice:

.

Primer name	C57BL/6J	Whirler	Whirlin$^{neo/neo}$
PDZG1/PDZG5R	894 bp		/
PNT3A/PDZG5R	/		700 bp
D4Mit17/rev	144 bp	/	
D4Mit244/rev	110 bp	130 bp	

RNA preparation and RT-PCR

DRG were removed and dissociated with dispase and collagenase, and total RNA was isolated as previously described. 1 µg RNA was used for reverse transcription, followed by PCR amplification of the obtained cDNA. The following primers and cycling conditions were used:

Primer name	Sequence (from 5' to 3')	
FW_1	CGCGTCAACGATAAATCTCTAGC	95° 1' 95° 30" 62° 30" } x35 72° 30" 72° 5'
RV_3	ACCAGTGATGTAAATGCCAAGG	
FW_10	ACACTCTCTCAGCTCTCAGACAG	
RV_12	CGTTGAACTCAGTGACCAGAAAG	
Act FW_2	GCTCCGGCATGTGCAA	
Act RV_4	AGGATCTTCATGAGGTAGT	

BEHAVIOURAL ASSAY

Tail-flick and plantar thermal or mechanical sensitivities were used to screen animals for altered nociceptive activity as they are non-invasive tests with minimised stress (Schildhaus *et*

al. 2014). For statistical analysis, Two-way ANOVA followed by Bonferroni post-test was applied and significance level was preset to $p<0.05$.

CFA inflammatory pain model

Mice received a subcutaneous injection into the left hindpaw of 50 µl CFA (Sigma) to induce local inflammation that developed over minutes, lasted for more than a week, and was associated with swelling and erythema, as well as thermal and mechanical pain hypersensitivity (Stein *et al.* 1988;Ren and Dubner 1999). The controlateral non-injected hindpaw was used as a control. 24 hours after CFA injection, thermal hyperalgesia and mechanical allodynia were assessed as described below.

Plantar Test

The method of Hargreaves was used to assess basal heat sensitivity and CFA-induced thermal hyperalgesia (Hargreaves *et al.* 1988). A standard Hargreaves' Plantar Test apparatus (Ugo Basile) was used that automatically measured the paw withdrawal latency to a thermal radiant stimulus.

Mice were placed in Plexiglas cages on a glass surface above the plantar test apparatus in a quiet testing room and allowed to acclimatise for 30 minutes before the behavioural test. For whirler mice, both mutant and wild-type animals were gently restrained to perform this test due to the former hyperactive phenotype (circling behaviour and increased locomotor activity). A movable noxious heat source was focused directly under the plantar surface of the hindpaw. When activated, the apparatus applied a continuous infrared heat stimulus to the plantar surface and a distinctive paw withdrawal reflex was elicited, which stopped an automated timer (based on infrared reflection). The elapsed time was displayed and recorded. The intensity of the beam was controlled and adjusted prior to the experiments (infrared setting 50-60). To avoid tissue injury in refractory animals, stimulation was automatically terminated after 30 seconds. The hindpaws were tested alternately, with a 5 minute interval between consecutive tests. Paw withdrawals due to locomotion or weight shifting were not counted, and the trials were repeated. Three measurements of latency were averaged for each hindpaw in each test session expressed as paw withdrawal latencies in seconds ± S.E.M.

Aesthesiometer Dynamic Test

Basal mechanical responses and mechanical allodynia were measured by using an automated von Frey Dynamic Plantar Aesthesiometer (Ugo-Basile) which does not produce tissue damage. This apparatus administers a force on the paw that increases at a constant rate. The force at which the animal pulled the paw away was used for statistical analysis.

Mice were allowed to move freely in individual plastic cage positioned on a metal mesh surface and were adapted to the testing environment for 30 minutes before any measurement

was taken. After that, the mechanical stimulus was delivered to the middle of the plantar surface of the hindpaw of the mouse from below the floor of the test chamber by an automated testing device. A blunt-end metal filament (0.5 mm in diameter) was pushed with electronical ascending force (0–50 g in 20 seconds). When the animal withdrawn its hindpaw, the mechanical stimulus was automatically halted and the force recorded. For each hind paw, the procedure was repeated 3 times at 5 minutes intervals and the average pressure to produce withdrawal was calculated and expressed as mechanical withdrawal thresholds in grams ± S.E.M.

STATISTICAL ANALYSIS

Data were visualised and analysed using GraphPad Prism 5 statistical software. All data were expressed as means±S.E.M, with n=number of cells tested and N=number of independent experiments realised. For statistical analysis, unpaired *t* test and one-way or two-way Anova followed by Bonferroni post-test were applied and significance level was preset to $p<0.05$. Significance levels are shown as: ns, no significant; * $p< 0.05$; ** $p < 0.01$; *** $p <0.001$.

Electrophysiological recordings were represented using the Origin 8.0 software.

Protein bands quantification was realised using TotalLab QUANT software. Data were expressed as mean ± S.E.M with N=number of independent experiments realised. Statistical analysis was performed with paired *t* test and significance level was preset to $p<0.05$.

BIBLIOGRAPHY

UNIVERSITAS
Miguel
Hernández

Abriel H. and Staub O. (2005) Ubiquitylation of ion channels. *Physiology (Bethesda.)* **20,** 398-407.

Adamski F. M., Zhu M. Y., Bahiraei F. and Shieh B. H. (1998) Interaction of eye protein kinase C and INAD in Drosophila. Localization of binding domains and electrophysiological characterization of a loss of association in transgenic flies. *J. Biol. Chem.* **273,** 17713-17719.

Adato A., Lefevre G., Delprat B., Michel V., Michalski N., Chardenoux S., Weil D., El-Amraoui A. and Petit C. (2005) Usherin, the defective protein in Usher syndrome type IIA, is likely to be a component of interstereocilia ankle links in the inner ear sensory cells. *Hum. Mol. Genet.* **14,** 3921-3932.

Ahern G. P., Brooks I. M., Miyares R. L. and Wang X. B. (2005) Extracellular cations sensitize and gate capsaicin receptor TRPV1 modulating pain signaling. *J. Neurosci.* **25,** 5109-5116.

Ahern G. P., Wang X. and Miyares R. L. (2006) Polyamines are potent ligands for the capsaicin receptor TRPV1. *J. Biol. Chem.* **281,** 8991-8995.

Alessandri-Haber N., Yeh J. J., Boyd A. E., Parada C. A., Chen X., Reichling D. B. and Levine J. D. (2003) Hypotonicity induces TRPV4-mediated nociception in rat. *Neuron* **39,** 497-511.

Almeida T. F., Roizenblatt S. and Tufik S. (2004) Afferent pain pathways: a neuroanatomical review. *Brain Res.* **1000,** 40-56.

Alonso M. A. and Millan J. (2001) The role of lipid rafts in signalling and membrane trafficking in T lymphocytes. *J. Cell Sci.* **114,** 3957-3965.

Ambalavanar R., Moritani M., Haines A., Hilton T. and Dessem D. (2003) Chemical phenotypes of muscle and cutaneous afferent neurons in the rat trigeminal ganglion. *J. Comp Neurol.* **460,** 167-179.

Aneiros E., Cao L., Papakosta M., Stevens E. B., Phillips S. and Grimm C. (2011) The biophysical and molecular basis of TRPV1 proton gating. *EMBO J.* **30,** 994-1002.

Averill S., McMahon S. B., Clary D. O., Reichardt L. F. and Priestley J. V. (1995) Immunocytochemical localization of trkA receptors in chemically identified subgroups of adult rat sensory neurons. *Eur. J. Neurosci.* **7,** 1484-1494.

Bagal S. K., Brown A. D., Cox P. J., Omoto K., Owen R. M., Pryde D. C., Sidders B., Skerratt S. E., Stevens E. B. and Storer R. I. (2012) Ion channels as therapeutic targets: a drug discovery perspective. *Journal of medicinal chemistry* **56,** 593-624.

Baker M. D. and Bostock H. (1997) Low-threshold, persistent sodium current in rat large dorsal root ganglion neurons in culture. *J. Neurophysiol.* **77,** 1503-1513.

Basbaum A. I., Bautista D. M., Scherrer G. and Julius D. (2009) Cellular and molecular mechanisms of pain. *Cell* **139,** 267-284.

Basbaum A. I. and Jessell T. M. (2000) The perception of pain. *Principles of neural science* **4,** 472-491.

Bautista D. and Julius D. (2008) Fire in the hole: pore dilation of the capsaicin receptor TRPV1. *Nat. Neurosci.* **11,** 528-529.

Bautista D. M., Siemens J., Glazer J. M., Tsuruda P. R., Basbaum A. I., Stucky C. L., Jordt S. E. and Julius D. (2007) The menthol receptor TRPM8 is the principal detector of environmental cold. *Nature* **448,** 204-208.

Bavassano C., Marvaldi L., Langeslag M., Sarg B., Lindner H., Klimaschewski L., Kress M., Ferrer-Montiel A. and Knaus H. G. (2013) Identification of voltage-gated K(+) channel beta 2 (Kvbeta2) subunit as a novel interaction partner of the pain transducer Transient Receptor Potential Vanilloid 1 channel (TRPV1). *Biochim. Biophys. Acta* **1833,** 3166-3175.

Belizario J. E., Alves J., Garay-Malpartida M. and Occhiucci J. M. (2008) Coupling caspase cleavage and proteasomal degradation of proteins carrying PEST motif. *Curr. Protein Pept. Sci.* **9,** 210-220.

Belmonte C. and Cervero F. (1996) *Neurobiology of nociceptors*. Oxford University Press.

Belyantseva I. A., Boger E. T., Naz S., Frolenkov G. I., Sellers J. R., Ahmed Z. M., Griffith A. J. and Friedman T. B. (2005) Myosin-XVa is required for tip localization of whirlin and differential elongation of hair-cell stereocilia. *Nat. Cell Biol.* **7,** 148-156.

Bevan S., Quallo T. and Andersson D. A. (2014) Trpv1, in *Mammalian Transient Receptor Potential (TRP) Cation Channels,* pp. 207-245. Springer.

Bhave G. and Gereau R. W. (2004) Posttranslational mechanisms of peripheral sensitization. *J. Neurobiol.* **61,** 88-106.

Bhave G., Hu H. J., Glauner K. S., Zhu W., Wang H., Brasier D. J., Oxford G. S. and Gereau R. W. (2003) Protein kinase C phosphorylation sensitizes but does not activate the capsaicin receptor transient receptor potential vanilloid 1 (TRPV1). *Proc. Natl. Acad. Sci. U. S. A* **100,** 12480-12485.

Bhave G., Zhu W., Wang H., Brasier D. J., Oxford G. S. and Gereau R. W. (2002) cAMP-dependent protein kinase regulates desensitization of the capsaicin receptor (VR1) by direct phosphorylation. *Neuron* **35,** 721-731.

Boukalova S., Marsakova L., Teisinger J. and Vlachova V. (2010) Conserved residues within the putative S4-S5 region serve distinct functions among thermosensitive vanilloid transient receptor potential (TRPV) channels. *J. Biol. Chem.* **285,** 41455-41462.

Bouvier M. M., Evans M. L. and Benham C. D. (1991) Calcium Influx Induced by Stimulation of ATP Receptors on Neurons Cultured from Rat Dorsal Root Ganglia. *Eur. J. Neurosci.* **3,** 285-291.

Brauchi S., Orta G., Mascayano C., Salazar M., Raddatz N., Urbina H., Rosenmann E., Gonzalez-Nilo F. and Latorre R. (2007) Dissection of the components for PIP2 activation and thermosensation in TRP channels. *Proc. Natl. Acad. Sci. U. S. A* **104,** 10246-10251.

Brauchi S., Orta G., Salazar M., Rosenmann E. and Latorre R. (2006) A hot-sensing cold receptor: C-terminal domain determines thermosensation in transient receptor potential channels. *J. Neurosci.* **26,** 4835-4840.

Brederson J. D., Kym P. R. and Szallasi A. (2013) Targeting TRP channels for pain relief. *Eur. J Pharmacol.* **716,** 61-76.

Brito R., Sheth S., Mukherjea D., Rybak L. P. and Ramkumar V. (2014) TRPV1: A Potential Drug Target for Treating Various Diseases. *Cells* **3,** 517-545.

Btesh J., Fischer M. J., Stott K. and McNaughton P. A. (2013) Mapping the binding site of TRPV1 on AKAP79: implications for inflammatory hyperalgesia. *J. Neurosci.* **33,** 9184-9193.

Cain D. M., Khasabov S. G. and Simone D. A. (2001) Response properties of mechanoreceptors and nociceptors in mouse glabrous skin: an in vivo study. *J. Neurophysiol.* **85,** 1561-1574.

Camprubi-Robles M., Planells-Cases R. and Ferrer-Montiel A. (2009) Differential contribution of SNARE-dependent exocytosis to inflammatory potentiation of TRPV1 in nociceptors. *FASEB J.* **23,** 3722-3733.

Cao E., Liao M., Cheng Y. and Julius D. (2013) TRPV1 structures in distinct conformations reveal activation mechanisms. *Nature* **504,** 113-118.

Caspani O. and Heppenstall P. A. (2009) TRPA1 and cold transduction: an unresolved issue? *J. Gen. Physiol* **133,** 245-249.

Caterina M. J., Leffler A., Malmberg A. B., Martin W. J., Trafton J., Petersen-Zeitz K. R., Koltzenburg M., Basbaum A. I. and Julius D. (2000) Impaired nociception and pain sensation in mice lacking the capsaicin receptor. *Science* **288,** 306-313.

Caterina M. J., Rosen T. A., Tominaga M., Brake A. J. and Julius D. (1999) A capsaicin-receptor homologue with a high threshold for noxious heat. *Nature* **398,** 436-441.

Caterina M. J., Schumacher M. A., Tominaga M., Rosen T. A., Levine J. D. and Julius D. (1997) The capsaicin receptor: a heat-activated ion channel in the pain pathway. *Nature* **389,** 816-824.

Cavanaugh D. J., Chesler A. T., Jackson A. C., Sigal Y. M., Yamanaka H., Grant R., O'Donnell D., Nicoll R. A., Shah N. M., Julius D. and Basbaum A. I. (2011) Trpv1 reporter mice reveal highly restricted brain distribution and functional expression in arteriolar smooth muscle cells. *J. Neurosci.* **31,** 5067-5077.

Cesare P. and McNaughton P. (1997) Peripheral pain mechanisms. *Curr. Opin. Neurobiol.* **7,** 493-499.

Chao H. W., Hong C. J., Huang T. N., Lin Y. L. and Hsueh Y. P. (2008) SUMOylation of the MAGUK protein CASK regulates dendritic spinogenesis. *J Cell Biol.* **182,** 141-155.

Chao M. V. (2003) Neurotrophins and their receptors: a convergence point for many signalling pathways. *Nat. Rev. Neurosci.* **4,** 299-309.

Chaudhury S., Bal M., Belugin S., Shapiro M. S. and Jeske N. A. (2011) AKAP150-mediated TRPV1 sensitization is disrupted by calcium/calmodulin. *Mol. Pain* **7,** 34.

Chen J. R., Chang B. H., Allen J. E., Stiffler M. A. and MacBeath G. (2008) Predicting PDZ domain-peptide interactions from primary sequences. *Nat. Biotechnol.* **26,** 1041-1045.

Cheng W., Yang F., Takanishi C. L. and Zheng J. (2007) Thermosensitive TRPV channel subunits coassemble into heteromeric channels with intermediate conductance and gating properties. *J. Gen. Physiol* **129,** 191-207.

Chery N. and de K. Y. (1999) Junctional versus extrajunctional glycine and GABA(A) receptor-mediated IPSCs in identified lamina I neurons of the adult rat spinal cord. *J. Neurosci.* **19,** 7342-7355.

Chi C. N., Engstrom A., Gianni S., Larsson M. and Jemth P. (2006) Two conserved residues govern the salt and pH dependencies of the binding reaction of a PDZ domain. *J. Biol. Chem.* **281,** 36811-36818.

Cho K. O., Hunt C. A. and Kennedy M. B. (1992) The rat brain postsynaptic density fraction contains a homolog of the Drosophila discs-large tumor suppressor protein. *Neuron* **9,** 929-942.

Choudhury A. D., Xu H. and Baer R. (2004) Ubiquitination and proteasomal degradation of the BRCA1 tumor suppressor is regulated during cell cycle progression. *J. Biol. Chem.* **279,** 33909-33918.

Chuang H. H., Prescott E. D., Kong H., Shields S., Jordt S. E., Basbaum A. I., Chao M. V. and Julius D. (2001) Bradykinin and nerve growth factor release the capsaicin receptor from PtdIns(4,5)P2-mediated inhibition. *Nature* **411,** 957-962.

Chung M. K., Guler A. D. and Caterina M. J. (2008) TRPV1 shows dynamic ionic selectivity during agonist stimulation. *Nat. Neurosci.* **11,** 555-564.

Cohen A. R., Woods D. F., Marfatia S. M., Walther Z., Chishti A. H. and Anderson J. M. (1998) Human CASK/LIN-2 binds syndecan-2 and protein 4.1 and localizes to the basolateral membrane of epithelial cells. *J Cell Biol.* **142,** 129-138.

Cohen D. M. (2006) Regulation of TRP channels by N-linked glycosylation, pp. 630-637. Elsevier.

Colburn R. W., Lubin M. L., Stone D. J., Jr., Wang Y., Lawrence D., D'Andrea M. R., Brandt M. R., Liu Y., Flores C. M. and Qin N. (2007) Attenuated cold sensitivity in TRPM8 null mice. *Neuron* **54,** 379-386.

Cosens D. J. and Manning A. (1969) Abnormal electroretinogram from a Drosophila mutant. *Nature* **224,** 285-287.

Craven S. E., El-Husseini A. E. and Bredt D. S. (1999) Synaptic targeting of the postsynaptic density protein PSD-95 mediated by lipid and protein motifs. *Neuron* **22,** 497-509.

da Costa D. S., Meotti F. C., Andrade E. L., Leal P. C., Motta E. M. and Calixto J. B. (2010) The involvement of the transient receptor potential A1 (TRPA1) in the maintenance of mechanical and cold hyperalgesia in persistent inflammation. *Pain* **148,** 431-437.

Davis J. B., Gray J., Gunthorpe M. J., Hatcher J. P., Davey P. T., Overend P., Harries M. H., Latcham J., Clapham C., Atkinson K., Hughes S. A., Rance K., Grau E., Harper A. J., Pugh P. L., Rogers D. C., Bingham S., Randall A. and Sheardown S. A. (2000) Vanilloid receptor-1 is essential for inflammatory thermal hyperalgesia. *Nature* **405,** 183-187.

de Nooij J. C., Simon C. M., Simon A., Doobar S., Steel K. P., Banks R. W., Mentis G. Z., Bewick G. S. and Jessell T. M. (2015) The PDZ-domain protein Whirlin facilitates mechanosensory signaling in mammalian proprioceptors. *J Neurosci.* **35,** 3073-3084.

de O. C., Garami A., Lehto S. G., Pakai E., Tekus V., Pohoczky K., Youngblood B. D., Wang W., Kort M. E., Kym P. R., Pinter E., Gavva N. R. and Romanovsky A. A. (2014) Transient receptor potential channel ankyrin-1 is not a cold sensor for autonomic thermoregulation in rodents. *J. Neurosci.* **34,** 4445-4452.

Delprat B., Michel V., Goodyear R., Yamasaki Y., Michalski N., El-Amraoui A., Perfettini I., Legrain P., Richardson G. and Hardelin J. P. (2005) Myosin XVa and whirlin, two deafness gene products required for hair bundle growth, are located at the stereocilia tips and interact directly. *Human molecular genetics* **14,** 401-410.

Dhaka A., Murray A. N., Mathur J., Earley T. J., Petrus M. J. and Patapoutian A. (2007) TRPM8 is required for cold sensation in mice. *Neuron* **54,** 371-378.

Dhaka A., Uzzell V., Dubin A. E., Mathur J., Petrus M., Bandell M. and Patapoutian A. (2009) TRPV1 is activated by both acidic and basic pH. *J. Neurosci.* **29,** 153-158.

Docherty R. J., Yeats J. C., Bevan S. and Boddeke H. W. (1996) Inhibition of calcineurin inhibits the desensitization of capsaicin-evoked currents in cultured dorsal root ganglion neurones from adult rats. *Pflugers Arch.* **431,** 828-837.

Doyle D. A., Lee A., Lewis J., Kim E., Sheng M. and MacKinnon R. (1996) Crystal structures of a complexed and peptide-free membrane protein-binding domain: molecular basis of peptide recognition by PDZ. *Cell* **85,** 1067-1076.

Duncan L. M., Deeds J., Hunter J., Shao J., Holmgren L. M., Woolf E. A., Tepper R. I. and Shyjan A. W. (1998) Down-regulation of the novel gene melastatin correlates with potential for melanoma metastasis. *Cancer Res.* **58,** 1515-1520.

Ebermann I., Scholl H. P., Issa P. C., Becirovic E., Lamprecht J. +., Jurklies B., Mill+ín J. M., Aller E., Mitter D. and Bolz H. (2007) A novel gene for Usher syndrome type 2: mutations in the long isoform of whirlin are associated with retinitis pigmentosa and sensorineural hearing loss. *Human genetics* **121,** 203-211.

Efendiev R., Bavencoffe A., Hu H., Zhu M. X. and Dessauer C. W. (2013) Scaffolding by A-kinase anchoring protein enhances functional coupling between adenylyl cyclase and TRPV1 channel. *J. Biol. Chem.* **288,** 3929-3937.

Eldstrom J., Doerksen K. W., Steele D. F. and Fedida D. (2002) N-terminal PDZ-binding domain in Kv1 potassium channels. *FEBS Lett.* **531,** 529-537.

Fabbretti E. (2013) ATP P2X3 receptors and neuronal sensitization. *Front Cell Neurosci.* **7,** 236.

Fan S. F., Shen K. F., Scheideler M. A. and Crain S. M. (1992) F11 neuroblastoma x DRG neuron hybrid cells express inhibitory mu- and delta-opioid receptors which increase voltage-dependent K+ currents upon activation. *Brain Res.* **590,** 329-333.

Feng W., Fan J. S., Jiang M., Shi Y. W. and Zhang M. (2002) PDZ7 of glutamate receptor interacting protein binds to its target via a novel hydrophobic surface area. *J. Biol. Chem.* **277,** 41140-41146.

Ferrante F. M. and VadeBoncouer T. R. (1993) *Postoperative pain management*. Churchill Livingstone.

Ferrell B. A. (2003) Acute and chronic pain, in *Geriatric Medicine,* pp. 323-342. Springer.

Fischer M. J., Balasuriya D., Jeggle P., Goetze T. A., McNaughton P. A., Reeh P. W. and Edwardson J. M. (2014) Direct evidence for functional TRPV1/TRPA1 heteromers. *Pflugers Arch.* **466,** 2229-2241.

Fleig A. and Penner R. (2004) The TRPM ion channel subfamily: molecular, biophysical and functional features. *Trends Pharmacol. Sci.* **25,** 633-639.

Flynn R., Chapman K., Iftinca M., Aboushousha R., Varela D. and Altier C. (2014) Targeting the transient receptor potential vanilloid type 1 (TRPV1) assembly domain attenuates inflammation-induced hypersensitivity. *J Biol. Chem.* **289,** 16675-16687.

Forge A. and Wright T. (2002) The molecular architecture of the inner ear. *Br. Med. Bull.* **63,** 5-24.

Garcia J. and Altman R. D. (1997) Chronic pain states: pathophysiology and medical therapy. *Semin. Arthritis Rheum.* **27,** 1-16.

Garcia-Sanz N., Fernandez-Carvajal A., Morenilla-Palao C., Planells-Cases R., Fajardo-Sanchez E., Fernandez-Ballester G. and Ferrer-Montiel A. (2004) Identification of a tetramerization domain in the C terminus of the vanilloid receptor. *J. Neurosci.* **24,** 5307-5314.

Gaudet R. (2008) A primer on ankyrin repeat function in TRP channels and beyond. *Mol. Biosyst.* **4,** 372-379.

Gavva N. R., Klionsky L., Qu Y., Shi L., Tamir R., Edenson S., Zhang T. J., Viswanadhan V. N., Toth A., Pearce L. V., Vanderah T. W., Porreca F., Blumberg P. M., Lile J., Sun Y., Wild K., Louis J. C. and Treanor J. J. (2004) Molecular determinants of vanilloid sensitivity in TRPV1. *J. Biol. Chem.* **279,** 20283-20295.

Gianni S., Engstrom A., Larsson M., Calosci N., Malatesta F., Eklund L., Ngang C. C., Travaglini-Allocatelli C. and Jemth P. (2005) The kinetics of PDZ domain-ligand interactions and implications for the binding mechanism. *J. Biol. Chem.* **280,** 34805-34812.

Gnanasekaran A., Sundukova M., Hullugundi S., Birsa N., Bianchini G., Hsueh Y. P., Nistri A. and Fabbretti E. (2013) Calcium/calmodulin-dependent serine protein kinase (CASK) is a new intracellular modulator of P2X3 receptors. *J Neurochem.* **126,** 102-112.

Goel M., Garcia R., Estacion M. and Schilling W. P. (2001) Regulation of Drosophila TRPL channels by immunophilin FKBP59. *J. Biol. Chem.* **276,** 38762-38773.

Gold M. S. and Gebhart G. F. (2010) Nociceptor sensitization in pain pathogenesis. *Nat. Med.* **16,** 1248-1257.

Gold M. S., Levine J. D. and Correa A. M. (1998) Modulation of TTX-R INa by PKC and PKA and their role in PGE2-induced sensitization of rat sensory neurons in vitro. *J. Neurosci.* **18,** 10345-10355.

Goldberg D. S. and McGee S. J. (2011) Pain as a global public health priority. *BMC. Public Health* **11,** 770.

Goswami C., Dreger M., Jahnel R., Bogen O., Gillen C. and Hucho F. (2004) Identification and characterization of a Ca2+ -sensitive interaction of the vanilloid receptor TRPV1 with tubulin. *J. Neurochem.* **91,** 1092-1103.

Graham F. L., Smiley J., Russell W. C. and Nairn R. (1977) Characteristics of a human cell line transformed by DNA from human adenovirus type 5. *J. Gen. Virol.* **36,** 59-74.

Green J. A., Yang J., Grati M., Kachar B. and Bhat M. A. (2013) Whirlin, a cytoskeletal scaffolding protein, stabilizes the paranodal region and axonal cytoskeleton in myelinated axons. *BMC. Neurosci.* **14,** 96.

Gregorio-Teruel L., Valente P., Gonzalez-Ros J. M., Fernandez-Ballester G. and Ferrer-Montiel A. (2014) Mutation of I696 and W697 in the TRP box of vanilloid receptor subtype I modulates allosteric channel activation. *J. Gen. Physiol* **143,** 361-375.

Grycova L., Holendova B., Bumba L., Bily J., Jirku M., Lansky Z. and Teisinger J. (2012) Integrative binding sites within intracellular termini of TRPV1 receptor. *PLoS. One.* **7,** e48437.

Guinamard R., Salle L. and Simard C. (2011) The non-selective monovalent cationic channels TRPM4 and TRPM5. *Adv. Exp. Med. Biol.* **704,** 147-171.

Guler A. D., Lee H., Iida T., Shimizu I., Tominaga M. and Caterina M. (2002) Heat-evoked activation of the ion channel, TRPV4. *J. Neurosci.* **22,** 6408-6414.

Haraguchi K., Kawamoto A., Isami K., Maeda S., Kusano A., Asakura K., Shirakawa H., Mori Y., Nakagawa T. and Kaneko S. (2012) TRPM2 contributes to inflammatory and neuropathic pain through the aggravation of pronociceptive inflammatory responses in mice. *The Journal of Neuroscience* **32,** 3931-3941.

Hardie R. C. and Raghu P. (2001) Visual transduction in Drosophila. *Nature* **413,** 186-193.

Hargreaves K., Dubner R., Brown F., Flores C. and Joris J. (1988) A new and sensitive method for measuring thermal nociception in cutaneous hyperalgesia. *Pain* **32,** 77-88.

Harris B. Z. and Lim W. A. (2001) Mechanism and role of PDZ domains in signaling complex assembly. *J. Cell Sci.* **114,** 3219-3231.

Harvey R. J., Depner U. B., Wassle H., Ahmadi S., Heindl C., Reinold H., Smart T. G., Harvey K., Schutz B., Abo-Salem O. M., Zimmer A., Poisbeau P., Welzl H., Wolfer D. P., Betz H., Zeilhofer H. U. and Muller U. (2004) GlyR alpha3: an essential target for spinal PGE2-mediated inflammatory pain sensitization. *Science* **304,** 884-887.

Hellwig N., Plant T. D., Janson W., Schafer M., Schultz G. and Schaefer M. (2004) TRPV1 acts as proton channel to induce acidification in nociceptive neurons. *J. Biol. Chem.* **279,** 34553-34561.

Hoffmann T., Kistner K., Miermeister F., Winkelmann R., Wittmann J., Fischer M. J., Weidner C. and Reeh P. W. (2013) TRPA1 and TRPV1 are differentially involved in heat nociception of mice. *Eur. J. Pain* **17,** 1472-1482.

Holland S. and Scholich K. (2011) Regulation of neuronal functions by the E3-ubiquitinligase protein associated with MYC (MYCBP2). *Commun. Integr. Biol.* **4,** 513-515.

Holme R. H., Kiernan B. W., Brown S. D. and Steel K. P. (2002) Elongation of hair cell stereocilia is defective in the mouse mutant whirler. *J. Comp Neurol.* **450,** 94-102.

Huang H., Wu X., Nicol G. D., Meller S. and Vasko M. R. (2003) ATP augments peptide release from rat sensory neurons in culture through activation of P2Y receptors. *J. Pharmacol. Exp. Ther.* **306,** 1137-1144.

Huang J., Zhang X. and McNaughton P. A. (2006) Inflammatory pain: the cellular basis of heat hyperalgesia. *Current neuropharmacology* **4,** 197.

Huang S. M., Lee H., Chung M. K., Park U., Yu Y. Y., Bradshaw H. B., Coulombe P. A., Walker J. M. and Caterina M. J. (2008) Overexpressed transient receptor potential vanilloid 3 ion channels in skin keratinocytes modulate pain sensitivity via prostaglandin E2. *J. Neurosci.* **28,** 13727-13737.

Huang S. M., Li X., Yu Y., Wang J. and Caterina M. J. (2011) TRPV3 and TRPV4 ion channels are not major contributors to mouse heat sensation. *Mol. Pain* **7,** 37.

Huang T. N., Chang H. P. and Hsueh Y. P. (2010) CASK phosphorylation by PKA regulates the protein-protein interactions of CASK and expression of the NMDAR2b gene. *J Neurochem.* **112,** 1562-1573.

Hucho T. B., Dina O. A. and Levine J. D. (2005) Epac mediates a cAMP-to-PKC signaling in inflammatory pain: an isolectin B4(+) neuron-specific mechanism. *J. Neurosci.* **25,** 6119-6126.

Ivarsson Y. (2012) Plasticity of PDZ domains in ligand recognition and signaling. *FEBS Lett.* **586,** 2638-2647.

Jahnel R., Dreger M., Gillen C., Bender O., Kurreck J. and Hucho F. (2001) Biochemical characterization of the vanilloid receptor 1 expressed in a dorsal root ganglia derived cell line. *Eur. J. Biochem.* **268,** 5489-5496.

Jeske N. A., Patwardhan A. M., Ruparel N. B., Akopian A. N., Shapiro M. S. and Henry M. A. (2009) A-kinase anchoring protein 150 controls protein kinase C-mediated phosphorylation and sensitization of TRPV1. *Pain* **146,** 301-307.

Jeske N. A., Por E. D., Belugin S., Chaudhury S., Berg K. A., Akopian A. N., Henry M. A. and Gomez R. (2011) A-kinase anchoring protein 150 mediates transient receptor potential family V type 1 sensitivity to phosphatidylinositol-4,5-bisphosphate. *J. Neurosci.* **31,** 8681-8688.

Ji R. R., Kohno T., Moore K. A. and Woolf C. J. (2003) Central sensitization and LTP: do pain and memory share similar mechanisms? *Trends Neurosci.* **26,** 696-705.

Ji R. R., Samad T. A., Jin S. X., Schmoll R. and Woolf C. J. (2002) p38 MAPK activation by NGF in primary sensory neurons after inflammation increases TRPV1 levels and maintains heat hyperalgesia. *Neuron* **36,** 57-68.

Jordt S. E. and Julius D. (2002) Molecular basis for species-specific sensitivity to "hot" chili peppers. *Cell* **108,** 421-430.

Jordt S. E., Tominaga M. and Julius D. (2000) Acid potentiation of the capsaicin receptor determined by a key extracellular site. *Proc. Natl. Acad. Sci. U. S. A* **97,** 8134-8139.

Julius D. and Basbaum A. I. (2001) Molecular mechanisms of nociception. *Nature* **413,** 203-210.

Jung J., Lee S. Y., Hwang S. W., Cho H., Shin J., Kang Y. S., Kim S. and Oh U. (2002) Agonist recognition sites in the cytosolic tails of vanilloid receptor 1. *J. Biol. Chem.* **277,** 44448-44454.

Jung J., Shin J. S., Lee S. Y., Hwang S. W., Koo J., Cho H. and Oh U. (2004) Phosphorylation of vanilloid receptor 1 by Ca2+/calmodulin-dependent kinase II regulates its vanilloid binding. *Journal of Biological Chemistry* **279,** 7048-7054.

Kaneko Y. and Szallasi A. (2014) Transient receptor potential (TRP) channels: a clinical perspective. *Br. J Pharmacol.* **171,** 2474-2507.

Kantamneni S., Gonzalez-Gonzalez I. M., Luo J., Cimarosti H., Jacobs S. C., Jaafari N. and Henley J. M. (2014) Differential regulation of GABAB receptor trafficking by different modes of N-methyl-D-aspartate (NMDA) receptor signaling. *J. Biol. Chem.* **289,** 6681-6694.

Katz B. and Minke B. (2009) Drosophila photoreceptors and signaling mechanisms. *Front Cell Neurosci.* **3,** 2.

Kerstein P. C., del C. D., Moran M. M. and Stucky C. L. (2009) Pharmacological blockade of TRPA1 inhibits mechanical firing in nociceptors. *Mol. Pain* **5,** 19.

Kersten F. F., van W. E., van R. J., van der Zwaag B., Marker T., Peters T. A., Katsanis N., Wolfrum U., Keunen J. E., Roepman R. and Kremer H. (2010) Association of whirlin with Cav1.3 (alpha1D) channels in photoreceptors, defining a novel member of the usher protein network. *Invest Ophthalmol. Vis. Sci.* **51,** 2338-2346.

Kida N., Sokabe T., Kashio M., Haruna K., Mizuno Y., Suga Y., Nishikawa K., Kanamaru A., Hongo M., Oba A. and Tominaga M. (2012) Importance of transient receptor potential vanilloid 4 (TRPV4) in epidermal barrier function in human skin keratinocytes. *Pflugers Arch.* **463,** 715-725.

Kim A. Y., Tang Z., Liu Q., Patel K. N., Maag D., Geng Y. and Dong X. (2008) Pirt, a phosphoinositide-binding protein, functions as a regulatory subunit of TRPV1. *Cell* **133,** 475-485.

Kim E., Niethammer M., Rothschild A., Jan Y. N. and Sheng M. (1995) Clustering of Shaker-type K+ channels by interaction with a family of membrane-associated guanylate kinases. *Nature* **378,** 85-88.

Klein R. M., Ufret-Vincenty C. A., Hua L. and Gordon S. E. (2008) Determinants of molecular specificity in phosphoinositide regulation. Phosphatidylinositol (4,5)-bisphosphate (PI(4,5)P2) is the endogenous lipid regulating TRPV1. *J. Biol. Chem.* **283,** 26208-26216.

Koplas P. A., Rosenberg R. L. and Oxford G. S. (1997) The role of calcium in the desensitization of capsaicin responses in rat dorsal root ganglion neurons. *J. Neurosci.* **17,** 3525-3537.

Kremer H., van W. E., Marker T., Wolfrum U. and Roepman R. (2006) Usher syndrome: molecular links of pathogenesis, proteins and pathways. *Hum. Mol. Genet.* **15 Spec No 2,** R262-R270.

Kwan K. Y., Glazer J. M., Corey D. P., Rice F. L. and Stucky C. L. (2009) TRPA1 modulates mechanotransduction in cutaneous sensory neurons. *J. Neurosci.* **29,** 4808-4819.

Kwon Y., Hofmann T. and Montell C. (2007) Integration of phosphoinositide- and calmodulin-mediated regulation of TRPC6. *Mol. Cell* **25,** 491-503.

Lainez S., Valente P., Ontoria-Oviedo I., Estevez-Herrera J., Camprubi-Robles M., Ferrer-Montiel A. and Planells-Cases R. (2010) GABAA receptor associated protein (GABARAP) modulates TRPV1 expression and channel function and desensitization. *FASEB J.* **24,** 1958-1970.

Latorre R., Zaelzer C. and Brauchi S. (2009) Structure-functional intimacies of transient receptor potential channels. *Q. Rev. Biophys.* **42,** 201-246.

Latremoliere A. and Woolf C. J. (2009) Central sensitization: a generator of pain hypersensitivity by central neural plasticity. *J. Pain* **10,** 895-926.

Lawson S. N., Crepps B. and Perl E. R. (2002) Calcitonin gene-related peptide immunoreactivity and afferent receptive properties of dorsal root ganglion neurones in guinea-pigs. *J. Physiol* **540,** 989-1002.

Lee D. H. and Goldberg A. L. (1996) Selective inhibitors of the proteasome-dependent and vacuolar pathways of protein degradation in Saccharomyces cerevisiae. *J. Biol. Chem.* **271,** 27280-27284.

Lee H. J. and Zheng J. J. (2010) PDZ domains and their binding partners: structure, specificity, and modification. *Cell Commun. Signal.* **8,** 8.

Lee J., Saloman J. L., Weiland G., Auh Q. S., Chung M. K. and Ro J. Y. (2012) Functional interactions between NMDA receptors and TRPV1 in trigeminal sensory neurons mediate mechanical hyperalgesia in the rat masseter muscle. *Pain* **153,** 1514-1524.

Levitan I., Fang Y., Rosenhouse-Dantsker A. and Romanenko V. (2010) Cholesterol and ion channels. *Subcell. Biochem.* **51,** 509-549.

Lewin G. R., Lu Y. and Park T. J. (2004) A plethora of painful molecules. *Curr. Opin. Neurobiol.* **14,** 443-449.

Lewin G. R. and Mendell L. M. (1994) Regulation of cutaneous C-fiber heat nociceptors by nerve growth factor in the developing rat. *J. Neurophysiol.* **71,** 941-949.

Li H. S. and Montell C. (2000) TRP and the PDZ protein, INAD, form the core complex required for retention of the signalplex in Drosophila photoreceptor cells. *J. Cell Biol.* **150,** 1411-1422.

Liao M., Cao E., Julius D. and Cheng Y. (2013) Structure of the TRPV1 ion channel determined by electron cryo-microscopy. *Nature* **504,** 107-112.

Lilja J., Laulund F. and Forsby A. (2007) Insulin and insulin-like growth factor type-I up-regulate the vanilloid receptor-1 (TRPV1) in stably TRPV1-expressing SH-SY5Y neuroblastoma cells. *J Neurosci. Res.* **85,** 1413-1419.

Lishko P. V., Procko E., Jin X., Phelps C. B. and Gaudet R. (2007) The ankyrin repeats of TRPV1 bind multiple ligands and modulate channel sensitivity. *Neuron* **54,** 905-918.

Liu B., Hui K. and Qin F. (2003) Thermodynamics of heat activation of single capsaicin ion channels VR1. *Biophys. J.* **85,** 2988-3006.

Liu B., Linley J. E., Du X., Zhang X., Ooi L., Zhang H. and Gamper N. (2010) The acute nociceptive signals induced by bradykinin in rat sensory neurons are mediated by inhibition of M-type K+ channels and activation of Ca2+-activated Cl- channels. *J. Clin. Invest* **120,** 1240-1252.

Liu B., Zhang C. and Qin F. (2005) Functional recovery from desensitization of vanilloid receptor TRPV1 requires resynthesis of phosphatidylinositol 4,5-bisphosphate. *J. Neurosci.* **25,** 4835-4843.

Liu L., Wang Y. and Simon S. A. (1996) Capsaicin activated currents in rat dorsal root ganglion cells. *Pain* **64,** 191-195.

Liu M., Huang W., Wu D. and Priestley J. V. (2006) TRPV1, but not P2X, requires cholesterol for its function and membrane expression in rat nociceptors. *Eur. J. Neurosci.* **24,** 1-6.

Loken L. S., Wessberg J., Morrison I., McGlone F. and Olausson H. (2009) Coding of pleasant touch by unmyelinated afferents in humans. *Nat. Neurosci.* **12,** 547-548.

Lukacs V., Thyagarajan B., Varnai P., Balla A., Balla T. and Rohacs T. (2007) Dual regulation of TRPV1 by phosphoinositides. *J. Neurosci.* **27,** 7070-7080.

Macias M. J., Wiesner S. and Sudol M. (2002) WW and SH3 domains, two different scaffolds to recognize proline-rich ligands. *FEBS Lett.* **513,** 30-37.

Maekawa K., Imagawa N., Naito A., Harada S., Yoshie O. and Takagi S. (1999) Association of protein-tyrosine phosphatase PTP-BAS with the transcription-factor-inhibitory protein IkappaBalpha through interaction between the PDZ1 domain and ankyrin repeats. *Biochem. J.* **337 (Pt 2),** 179-184.

Maerker T., van W. E., Overlack N., Kersten F. F., McGee J., Goldmann T., Sehn E., Roepman R., Walsh E. J., Kremer H. and Wolfrum U. (2008) A novel Usher protein network at the periciliary reloading point between molecular transport machineries in vertebrate photoreceptor cells. *Hum. Mol. Genet.* **17,** 71-86.

Mandadi S., Tominaga T., Numazaki M., Murayama N., Saito N., Armati P. J., Roufogalis B. D. and Tominaga M. (2006) Increased sensitivity of desensitized TRPV1 by PMA occurs through PKCepsilon-mediated phosphorylation at S800. *Pain* **123,** 106-116.

Mannion R. J. and Woolf C. J. (2000) Pain mechanisms and management: a central perspective. *Clin. J. Pain* **16,** S144-S156.

Marics I., Malapert P., Reynders A., Gaillard S. and Moqrich A. (2014) Acute heat-evoked temperature sensation is impaired but not abolished in mice lacking TRPV1 and TRPV3 channels. *PLoS. One.* **9,** e99828.

Mathie A. (2010) Ion channels as novel therapeutic targets in the treatment of pain. *J Pharm. Pharmacol.* **62,** 1089-1095.

Matta J. A. and Ahern G. P. (2007) Voltage is a partial activator of rat thermosensitive TRP channels. *J. Physiol* **585,** 469-482.

Mburu P., Kikkawa Y., Townsend S., Romero R., Yonekawa H. and Brown S. D. (2006) Whirlin complexes with p55 at the stereocilia tip during hair cell development. *Proc. Natl. Acad. Sci. U. S. A* **103,** 10973-10978.

Mburu P., Mustapha M., Varela A., Weil D., El-Amraoui A., Holme R. H., Rump A., Hardisty R. E., Blanchard S., Coimbra R. S., Perfettini I., Parkinson N., Mallon A. M., Glenister P., Rogers M. J., Paige A. J., Moir L., Clay J., Rosenthal A., Liu X. Z., Blanco G., Steel K. P., Petit C. and Brown S. D. (2003) Defects in whirlin, a PDZ domain molecule involved in stereocilia elongation, cause deafness in the whirler mouse and families with DFNB31. *Nat. Genet.* **34,** 421-428.

McCleskey E. W. and Gold M. S. (1999) Ion channels of nociception. *Annu. Rev. Physiol* **61,** 835-856.

Meents J. E., Neeb L. and Reuter U. (2010) TRPV1 in migraine pathophysiology. *Trends Mol. Med.* **16,** 153-159.

Meng L., Mohan R., Kwok B. H., Elofsson M., Sin N. and Crews C. M. (1999) Epoxomicin, a potent and selective proteasome inhibitor, exhibits in vivo antiinflammatory activity. *Proc. Natl. Acad. Sci. U. S. A* **96,** 10403-10408.

Merskey H., Albe-Fessard D. G. and Bonica J. J. (1979) *International Association for the Study of Pain. Pain terms: a list with definitions and notes on usage*.

Mezey E., Toth Z. E., Cortright D. N., Arzubi M. K., Krause J. E., Elde R., Guo A., Blumberg P. M. and Szallasi A. (2000) Distribution of mRNA for vanilloid receptor subtype 1 (VR1), and VR1-like immunoreactivity, in the central nervous system of the rat and human. *Proc. Natl. Acad. Sci. U. S. A* **97,** 3655-3660.

Mickle A. D., Shepherd A. J. and Mohapatra D. P. (2015) Sensory TRP channels: the key transducers of nociception and pain. *Prog. Mol. Biol. Transl. Sci.* **131,** 73-118.

Millan J. M., Aller E., Jaijo T., Blanco-Kelly F., Gimenez-Pardo A. and Ayuso C. (2011) An update on the genetics of usher syndrome. *J. Ophthalmol.* **2011,** 417217.

Millan M. J. (1997) The role of descending noradrenergic and serotoninergic pathways in the modulation of nociception: focus on receptor multiplicity, in *The pharmacology of pain,* pp. 385-446. Springer.

Miyamoto T., Petrus M. J., Dubin A. E. and Patapoutian A. (2011) TRPV3 regulates nitric oxide synthase-independent nitric oxide synthesis in the skin. *Nat. Commun.* **2,** 369.

Mohapatra D. P. and Nau C. (2003) Desensitization of capsaicin-activated currents in the vanilloid receptor TRPV1 is decreased by the cyclic AMP-dependent protein kinase pathway. *J. Biol. Chem.* **278,** 50080-50090.

Molliver D. C., Wright D. E., Leitner M. L., Parsadanian A. S., Doster K., Wen D., Yan Q. and Snider W. D. (1997) IB4-binding DRG neurons switch from NGF to GDNF dependence in early postnatal life. *Neuron* **19,** 849-861.

Montell C. (2005) The TRP superfamily of cation channels. *Sci. STKE.* **2005,** re3.

Montell C. and Rubin G. M. (1989) Molecular characterization of the Drosophila trp locus: a putative integral membrane protein required for phototransduction. *Neuron* **2,** 1313-1323.

Morais Cabral J. H., Petosa C., Sutcliffe M. J., Raza S., Byron O., Poy F., Marfatia S. M., Chishti A. H. and Liddington R. C. (1996) Crystal structure of a PDZ domain. *Nature* **382,** 649-652.

Morenilla-Palao C., Pertusa M., Meseguer V., Cabedo H. and Viana F. (2009) Lipid raft segregation modulates TRPM8 channel activity. *J Biol. Chem.* **284,** 9215-9224.

Morenilla-Palao C., Planells-Cases R., Garcia-Sanz N. and Ferrer-Montiel A. (2004) Regulated exocytosis contributes to protein kinase C potentiation of vanilloid receptor activity. *J. Biol. Chem.* **279,** 25665-25672.

Mosavi L. K., Cammett T. J., Desrosiers D. C. and Peng Z. Y. (2004) The ankyrin repeat as molecular architecture for protein recognition. *Protein Sci.* **13,** 1435-1448.

Mustapha M., Chouery E., Chardenoux S., Naboulsi M., Paronnaud J., Lemainque A., Megarbane A., Loiselet J., Weil D., Lathrop M. and Petit C. (2002) DFNB31, a recessive form of sensorineural hearing loss, maps to chromosome 9q32-34. *Eur. J. Hum. Genet.* **10,** 210-212.

Nagata K., Duggan A., Kumar G. and Garcia-Anoveros J. (2005) Nociceptor and hair cell transducer properties of TRPA1, a channel for pain and hearing. *J. Neurosci.* **25,** 4052-4061.

Neumann S., Doubell T. P., Leslie T. and Woolf C. J. (1996) Inflammatory pain hypersensitivity mediated by phenotypic switch in myelinated primary sensory neurons. *Nature* **384,** 360-364.

Nicholson B. (2006) Differential diagnosis: nociceptive and neuropathic pain. *Am. J. Manag. Care* **12,** S256-S262.

Nilius B. (2007) TRP channels in disease. *Biochim. Biophys. Acta* **1772,** 805-812.

Numazaki M., Tominaga T., Takeuchi K., Murayama N., Toyooka H. and Tominaga M. (2003) Structural determinant of TRPV1 desensitization interacts with calmodulin. *Proc. Natl. Acad. Sci. U. S. A* **100,** 8002-8006.

Numazaki M., Tominaga T., Toyooka H. and Tominaga M. (2002) Direct phosphorylation of capsaicin receptor VR1 by protein kinase Cepsilon and identification of two target serine residues. *J. Biol. Chem.* **277,** 13375-13378.

Pareek T. K., Keller J., Kesavapany S., Agarwal N., Kuner R., Pant H. C., Iadarola M. J., Brady R. O. and Kulkarni A. B. (2007) Cyclin-dependent kinase 5 modulates nociceptive signaling through direct phosphorylation of transient receptor potential vanilloid 1. *Proceedings of the National Academy of Sciences* **104,** 660-665.

Park U., Vastani N., Guan Y., Raja S. N., Koltzenburg M. and Caterina M. J. (2011) TRP vanilloid 2 knock-out mice are susceptible to perinatal lethality but display normal thermal and mechanical nociception. *J. Neurosci.* **31,** 11425-11436.

Paulsen C. E., Armache J. P., Gao Y., Cheng Y. and Julius D. (2015) Structure of the TRPA1 ion channel suggests regulatory mechanisms. *Nature*.

Peier A. M., Moqrich A., Hergarden A. C., Reeve A. J., Andersson D. A., Story G. M., Earley T. J., Dragoni I., McIntyre P., Bevan S. and Patapoutian A. (2002) A TRP channel that senses cold stimuli and menthol. *Cell* **108,** 705-715.

Peng L., Popescu D. C., Wang N. and Shieh B. (2008) Anchoring TRP to the INAD macromolecular complex requires the last 14 residues in its carboxyl terminus. *Journal of neurochemistry* **104,** 1526-1535.

Picazo-Juarez G., Romero-Suarez S., Nieto-Posadas A., Llorente I., Jara-Oseguera A., Briggs M., McIntosh T. J., Simon S. A., Ladron-de-Guevara E., Islas L. D. and Rosenbaum T. (2011) Identification of a binding motif in the S5 helix that confers cholesterol sensitivity to the TRPV1 ion channel. *J. Biol. Chem.* **286,** 24966-24976.

Pichon X., Wattiez A. S., Becamel C., Ehrlich I., Bockaert J., Eschalier A., Marin P. and Courteix C. (2010) Disrupting 5-HT(2A) receptor/PDZ protein interactions reduces hyperalgesia and enhances SSRI efficacy in neuropathic pain. *Mol. Ther.* **18,** 1462-1470.

Planells-Cases R., Garcia-Sanz N., Morenilla-Palao C. and Ferrer-Montiel A. (2005) Functional aspects and mechanisms of TRPV1 involvement in neurogenic inflammation that leads to thermal hyperalgesia. *Pflugers Arch.* **451,** 151-159.

Planells-Cases R., Valente P., Ferrer-Montiel A., Qin F. and Szallasi A. (2011) Complex regulation of TRPV1 and related thermo-TRPs: implications for therapeutic intervention. *Adv. Exp. Med. Biol.* **704,** 491-515.

Popescu D. C., Ham A. J. and Shieh B. H. (2006) Scaffolding protein INAD regulates deactivation of vision by promoting phosphorylation of transient receptor potential by eye protein kinase C in Drosophila. *J. Neurosci.* **26,** 8570-8577.

Por E. D., Bierbower S. M., Berg K. A., Gomez R., Akopian A. N., Wetsel W. C. and Jeske N. A. (2012) beta-Arrestin-2 desensitizes the transient receptor potential vanilloid 1 (TRPV1) channel. *J. Biol. Chem.* **287,** 37552-37563.

Por E. D., Gomez R., Akopian A. N. and Jeske N. A. (2013) Phosphorylation regulates TRPV1 association with beta-arrestin-2. *Biochem. J.* **451,** 101-109.

Prescott E. D. and Julius D. (2003) A modular PIP2 binding site as a determinant of capsaicin receptor sensitivity. *Science* **300,** 1284-1288.

Press B., Feng Y., Hoflack B. and Wandinger-Ness A. (1998) Mutant Rab7 causes the accumulation of cathepsin D and cation-independent mannose 6-phosphate receptor in an early endocytic compartment. *J. Cell Biol.* **140,** 1075-1089.

Price T. J. and Flores C. M. (2007) Critical evaluation of the colocalization between calcitonin gene-related peptide, substance P, transient receptor potential vanilloid subfamily type 1 immunoreactivities, and isolectin B4 binding in primary afferent neurons of the rat and mouse. *J. Pain* **8,** 263-272.

Probst F. J., Fridell R. A., Raphael Y., Saunders T. L., Wang A., Liang Y., Morell R. J., Touchman J. W., Lyons R. H., Noben-Trauth K., Friedman T. B. and Camper S. A. (1998) Correction of deafness in shaker-2 mice by an unconventional myosin in a BAC transgene. *Science* **280,** 1444-1447.

Proudfoot C. J., Garry E. M., Cottrell D. F., Rosie R., Anderson H., Robertson D. C., Fleetwood-Walker S. M. and Mitchell R. (2006) Analgesia mediated by the TRPM8 cold receptor in chronic neuropathic pain. *Curr. Biol.* **16,** 1591-1605.

Raja S. N., Meyer R. A., Ringkamp M. and Campbell J. N. (1999) Peripheral neural mechanisms of nociception. *Textbook of pain* **4,** 11-57.

Ramsey I. S., Delling M. and Clapham D. E. (2006) An introduction to TRP channels. *Annu. Rev. Physiol* **68,** 619-647.

Reiners J., Nagel-Wolfrum K., Jurgens K., Marker T. and Wolfrum U. (2006) Molecular basis of human Usher syndrome: deciphering the meshes of the Usher protein network provides insights into the pathomechanisms of the Usher disease. *Exp. Eye Res.* **83,** 97-119.

Ren K. and Dubner R. (1999) Inflammatory models of pain and hyperalgesia. *ILAR Journal* **40,** 111-118.

Richardson J. D. and Vasko M. R. (2002) Cellular mechanisms of neurogenic inflammation. *J. Pharmacol. Exp. Ther.* **302,** 839-845.

Robinson F. L. and Dixon J. E. (2005) The phosphoinositide-3-phosphatase MTMR2 associates with MTMR13, a membrane-associated pseudophosphatase also mutated in type 4B Charcot-Marie-Tooth disease. *J Biol. Chem.* **280,** 31699-31707.

Rohacs T., Lopes C. M., Michailidis I. and Logothetis D. E. (2005) PI(4,5)P2 regulates the activation and desensitization of TRPM8 channels through the TRP domain. *Nat. Neurosci.* **8,** 626-634.

Rosenbaum T., Gordon-Shaag A., Munari M. and Gordon S. E. (2004) Ca2+/calmodulin modulates TRPV1 activation by capsaicin. *The Journal of general physiology* **123,** 53-62.

Saliba R. S., Pangalos M. and Moss S. J. (2008) The ubiquitin-like protein Plic-1 enhances the membrane insertion of GABAA receptors by increasing their stability within the endoplasmic reticulum. *J. Biol. Chem.* **283,** 18538-18544.

Sanz-Salvador L., Andres-Borderia A., Ferrer-Montiel A. and Planells-Cases R. (2012) Agonist- and Ca2+-dependent desensitization of TRPV1 channel targets the receptor to lysosomes for degradation. *J. Biol. Chem.* **287,** 19462-19471.

Schildhaus N., Trink E., Polson C., Detolla L., Tyler B. M., Jallo G. I., Tok S. and Guarnieri M. (2014) Thermal latency studies in opiate-treated mice. *J. Pharm. Bioallied. Sci.* **6,** 43-47.

Schmidt R., Schmelz M., Forster C., Ringkamp M., Torebjork E. and Handwerker H. (1995) Novel classes of responsive and unresponsive C nociceptors in human skin. *J. Neurosci.* **15,** 333-341.

Schnizler K., Shutov L. P., Van Kanegan M. J., Merrill M. A., Nichols B., McKnight G. S., Strack S., Hell J. W. and Usachev Y. M. (2008) Protein kinase A anchoring via AKAP150 is essential for TRPV1 modulation by forskolin and prostaglandin E2 in mouse sensory neurons. *J. Neurosci.* **28,** 4904-4917.

Scholz J., Broom D. C., Youn D. H., Mills C. D., Kohno T., Suter M. R., Moore K. A., Decosterd I., Coggeshall R. E. and Woolf C. J. (2005) Blocking caspase activity prevents

transsynaptic neuronal apoptosis and the loss of inhibition in lamina II of the dorsal horn after peripheral nerve injury. *J. Neurosci.* **25,** 7317-7323.

Scholz J. and Woolf C. J. (2002) Can we conquer pain? *Nat. Neurosci.* **5 Suppl,** 1062-1067.

Shao D., Baker M. D., Abrahamsen B., Rugiero F., Malik-Hall M., Poon W. Y., Cheah K. S., Yao K. M., Wood J. N. and Okuse K. (2009) A multi PDZ-domain protein Pdzd2 contributes to functional expression of sensory neuron-specific sodium channel Na(V)1.8. *Mol. Cell Neurosci.* **42,** 219-225.

Sheng M. and Sala C. (2001) PDZ domains and the organization of supramolecular complexes. *Annu. Rev. Neurosci.* **24,** 1-29.

Sherrington C. S. (1906) The Integrative Action of the Nervous System Scribner. *New York*.

Shieh B. H. and Zhu M. Y. (1996) Regulation of the TRP Ca2+ channel by INAD in Drosophila photoreceptors. *Neuron* **16,** 991-998.

Shimizu T., Shibata M., Toriumi H., Iwashita T., Funakubo M., Sato H., Kuroi T., Ebine T., Koizumi K. and Suzuki N. (2012) Reduction of TRPV1 expression in the trigeminal system by botulinum neurotoxin type-A. *Neurobiol. Dis.* **48,** 367-378.

Simone D. A. and Kajander K. C. (1997) Responses of cutaneous A-fiber nociceptors to noxious cold. *J. Neurophysiol.* **77,** 2049-2060.

Simons K. and Toomre D. (2000) Lipid rafts and signal transduction. *Nature reviews Molecular cell biology* **1,** 31-39.

Smani T., Dionisio N., L+¦pez J. J., Berna-Erro A. and Rosado J. A. (2014) Cytoskeletal and scaffolding proteins as structural and functional determinants of TRP channels. *Biochimica et Biophysica Acta (BBA)-Biomembranes* **1838,** 658-664.

Smith E. S. and Lewin G. R. (2009) Nociceptors: a phylogenetic view. *J. Comp Physiol A Neuroethol. Sens. Neural Behav. Physiol* **195,** 1089-1106.

Smith G. D., Gunthorpe M. J., Kelsell R. E., Hayes P. D., Reilly P., Facer P., Wright J. E., Jerman J. C., Walhin J. P., Ooi L., Egerton J., Charles K. J., Smart D., Randall A. D., Anand P. and Davis J. B. (2002) TRPV3 is a temperature-sensitive vanilloid receptor-like protein. *Nature* **418,** 186-190.

Songyang Z., Fanning A. S., Fu C., Xu J., Marfatia S. M., Chishti A. H., Crompton A., Chan A. C., Anderson J. M. and Cantley L. C. (1997) Recognition of unique carboxyl-terminal motifs by distinct PDZ domains. *Science* **275,** 73-77.

Spicarova D. and Palecek J. (2008) The role of spinal cord vanilloid (TRPV1) receptors in pain modulation. *Physiol Res.* **57 Suppl 3,** S69-S77.

Stanchev D., Blosa M., Milius D., Gerevich Z., Rubini P., Schmalzing G., Eschrich K., Schaefer M., Wirkner K. and Illes P. (2009) Cross-inhibition between native and recombinant TRPV1 and P2X(3) receptors. *Pain* **143,** 26-36.

Staruschenko A., Jeske N. A. and Akopian A. N. (2010) Contribution of TRPV1-TRPA1 interaction to the single channel properties of the TRPA1 channel. *J. Biol. Chem.* **285,** 15167-15177.

Stein A. T., Ufret-Vincenty C. A., Hua L., Santana L. F. and Gordon S. E. (2006) Phosphoinositide 3-kinase binds to TRPV1 and mediates NGF-stimulated TRPV1 trafficking to the plasma membrane. *J. Gen. Physiol* **128,** 509-522.

Stein C., Millan M. J. and Herz A. (1988) Unilateral inflammation of the hindpaw in rats as a model of prolonged noxious stimulation: alterations in behavior and nociceptive thresholds. *Pharmacol. Biochem. Behav.* **31,** 445-451.

Storti B., Bizzarri R., Cardarelli F. and Beltram F. (2012) Intact microtubules preserve transient receptor potential vanilloid 1 (TRPV1) functionality through receptor binding. *J. Biol. Chem.* **287,** 7803-7811.

Storti B., Di R. C., Cardarelli F., Bizzarri R. and Beltram F. (2015) Unveiling TRPV1 spatio-temporal organization in live cell membranes. *PLoS. One.* **10,** e0116900.

Strotmann R., Harteneck C., Nunnenmacher K., Schultz G. and Plant T. D. (2000) OTRPC4, a nonselective cation channel that confers sensitivity to extracellular osmolarity. *Nat. Cell Biol.* **2,** 695-702.

Suzuki M., Mizuno A., Kodaira K. and Imai M. (2003) Impaired pressure sensation in mice lacking TRPV4. *J. Biol. Chem.* **278,** 22664-22668.

Szallasi A. and Blumberg P. M. (1990) Resiniferatoxin and its analogs provide novel insights into the pharmacology of the vanilloid (capsaicin) receptor. *Life Sci.* **47,** 1399-1408.

Szallasi A., Cortright D. N., Blum C. A. and Eid S. R. (2007) The vanilloid receptor TRPV1: 10 years from channel cloning to antagonist proof-of-concept. *Nat. Rev. Drug Discov.* **6,** 357-372.

Szoke É., B+Ârzsei R., T+¦th D. M., Lengl O., Helyes Z., S+índor Z. and Szolcs+ínyi J. +. (2010) Effect of lipid raft disruption on TRPV1 receptor activation of trigeminal sensory neurons and transfected cell line. *European journal of pharmacology* **628,** 67-74.

Szolcsanyi J. and Sandor Z. (2012) Multisteric TRPV1 nocisensor: a target for analgesics. *Trends Pharmacol. Sci.* **33,** 646-655.

Takayama Y., Uta D., Furue H. and Tominaga M. (2015) Pain-enhancing mechanism through interaction between TRPV1 and anoctamin 1 in sensory neurons. *Proc. Natl. Acad. Sci. U. S. A* **112,** 5213-5218.

Tao F., Su Q. and Johns R. A. (2008) Cell-permeable peptide Tat-PSD-95 PDZ2 inhibits chronic inflammatory pain behaviors in mice. *Mol. Ther.* **16,** 1776-1782.

Thienhaus O., MBA F. A. P. A. and Cole B. E. (2001) The Classification of Pain. *Pain management: A practical guide for clinicians* 27.

Toiyama Y., Mizoguchi A., Kimura K., Hiro J., Tutsumi T., Inoue Y., Miki C. and Kusunoki M. (2009) Overexpression of the signal peptide whirlin isoform 2 is related to disease progression in colorectal cancer patients. *Int. J. Oncol.* **35,** 709-715.

Tominaga M., Caterina M. J., Malmberg A. B., Rosen T. A., Gilbert H., Skinner K., Raumann B. E., Basbaum A. I. and Julius D. (1998) The cloned capsaicin receptor integrates multiple pain-producing stimuli. *Neuron* **21,** 531-543.

Tominaga M., Wada M. and Masu M. (2001) Potentiation of capsaicin receptor activity by metabotropic ATP receptors as a possible mechanism for ATP-evoked pain and hyperalgesia. *Proc. Natl. Acad. Sci. U. S. A* **98,** 6951-6956.

Topinka J. R. and Bredt D. S. (1998) N-terminal palmitoylation of PSD-95 regulates association with cell membranes and interaction with K+ channel Kv1.4. *Neuron* **20,** 125-134.

Tracey I. and Bushnell M. C. (2009) How neuroimaging studies have challenged us to rethink: is chronic pain a disease? *J. Pain* **10,** 1113-1120.

Tsunoda S. and Zuker C. S. (1999) The organization of INAD-signaling complexes by a multivalent PDZ domain protein in< i> Drosophila</i> photoreceptor cells ensures sensitivity and speed of signaling. *Cell calcium* **26,** 165-171.

Ufret-Vincenty C. A., Klein R. M., Hua L., Angueyra J. and Gordon S. E. (2011) Localization of the PIP2 sensor of TRPV1 ion channels. *J. Biol. Chem.* **286,** 9688-9698.

Um J. W., Im E., Park J., Oh Y., Min B., Lee H. J., Yoon J. B. and Chung K. C. (2010) ASK1 negatively regulates the 26 S proteasome. *J. Biol. Chem.* **285,** 36434-36446.

Valente P., Garcia-Sanz N., Gomis A., Fernandez-Carvajal A., Fernandez-Ballester G., Viana F., Belmonte C. and Ferrer-Montiel A. (2008) Identification of molecular determinants of channel gating in the transient receptor potential box of vanilloid receptor I. *FASEB J.* **22,** 3298-3309.

van H. O., Torrance N. and Smith B. H. (2013) Chronic pain epidemiology and its clinical relevance. *Br. J. Anaesth.* **111,** 13-18.

van W. E., van der Zwaag B., Peters T., Zimmermann U., Te B. H., Kersten F. F., Marker T., Aller E., Hoefsloot L. H., Cremers C. W., Cremers F. P., Wolfrum U., Knipper M., Roepman R. and Kremer H. (2006) The DFNB31 gene product whirlin connects to the Usher protein network in the cochlea and retina by direct association with USH2A and VLGR1. *Hum. Mol. Genet.* **15,** 751-765.

Veldhuis N. A., Lew M. J., Abogadie F. C., Poole D. P., Jennings E. A., Ivanusic J. J., Eilers H., Bunnett N. W. and McIntyre P. (2012) N-glycosylation determines ionic permeability and desensitization of the TRPV1 capsaicin receptor. *J. Biol. Chem.* **287,** 21765-21772.

Vellani V., Zachrisson O. and McNaughton P. A. (2004) Functional bradykinin B1 receptors are expressed in nociceptive neurones and are upregulated by the neurotrophin GDNF. *J. Physiol* **560,** 391-401.

Venkatachalam K. and Montell C. (2007) TRP channels. *Annu. Rev. Biochem.* **76,** 387-417.

Vetter I., Cheng W., Peiris M., Wyse B. D., Roberts-Thomson S. J., Zheng J., Monteith G. R. and Cabot P. J. (2008) Rapid, opioid-sensitive mechanisms involved in transient receptor potential vanilloid 1 sensitization. *J. Biol. Chem.* **283,** 19540-19550.

Voets T., Droogmans G., Wissenbach U., Janssens A., Flockerzi V. and Nilius B. (2004) The principle of temperature-dependent gating in cold- and heat-sensitive TRP channels. *Nature* **430,** 748-754.

Voets T., Talavera K., Owsianik G. and Nilius B. (2005) Sensing with TRP channels. *Nat. Chem. Biol.* **1,** 85-92.

von K., I and Wetter A. (2000) Molecular pharmacology of P2Y-receptors. *Naunyn Schmiedebergs Arch. Pharmacol.* **362,** 310-323.

Vriens J., Nilius B. and Voets T. (2014) Peripheral thermosensation in mammals. *Nat. Rev. Neurosci.* **15,** 573-589.

Vriens J., Owsianik G., Hofmann T., Philipp S. E., Stab J., Chen X., Benoit M., Xue F., Janssens A., Kerselaers S., Oberwinkler J., Vennekens R., Gudermann T., Nilius B. and Voets T. (2011) TRPM3 is a nociceptor channel involved in the detection of noxious heat. *Neuron* **70,** 482-494.

Wang H., Bedford F. K., Brandon N. J., Moss S. J. and Olsen R. W. (1999) GABA(A)-receptor-associated protein links GABA(A) receptors and the cytoskeleton. *Nature* **397,** 69-72.

Wang L., Zou J., Shen Z., Song E. and Yang J. (2012) Whirlin interacts with espin and modulates its actin-regulatory function: an insight into the mechanism of Usher syndrome type II. *Hum. Mol. Genet.* **21,** 692-710.

Weltman A. S., Sackler A. M., Lewis A. S. and Johnson L. (1970) Metabolism rate, biochemical and endocrine alterations in male whirler mice. *Physiol Behav.* **5,** 17-22.

Weng H. J., Patel K. N., Jeske N. A., Bierbower S. M., Zou W., Tiwari V., Zheng Q., Tang Z., Mo G. C., Wang Y., Geng Y., Zhang J., Guan Y., Akopian A. N. and Dong X. (2015) Tmem100 Is a Regulator of TRPA1-TRPV1 Complex and Contributes to Persistent Pain. *Neuron* **85,** 833-846.

White J. K., Gerdin A. K., Karp N. A., Ryder E., Buljan M., Bussell J. N., Salisbury J., Clare S., Ingham N. J., Podrini C., Houghton R., Estabel J., Bottomley J. R., Melvin D. G., Sunter D., Adams N. C., Tannahill D., Logan D. W., Macarthur D. G., Flint J., Mahajan V. B., Tsang S. H., Smyth I., Watt F. M., Skarnes W. C., Dougan G., Adams D. J., Ramirez-Solis R., Bradley A. and Steel K. P. (2013) Genome-wide generation and systematic phenotyping of knockout mice reveals new roles for many genes. *Cell* **154,** 452-464.

Winter Z., Buhala A., Otvos F., Josvay K., Vizler C., Dombi G., Szakonyi G. and Olah Z. (2013) Functionally important amino acid residues in the transient receptor potential vanilloid 1 (TRPV1) ion channel--an overview of the current mutational data. *Mol. Pain* **9,** 30.

Wirkner K., Hognestad H., Jahnel R., Hucho F. and Illes P. (2005) Characterization of rat transient receptor potential vanilloid 1 receptors lacking the N-glycosylation site N604. *Neuroreport* **16,** 997-1001.

Woods D. F. and Bryant P. J. (1993) ZO-1, DlgA and PSD-95/SAP90: homologous proteins in tight, septate and synaptic cell junctions. *Mech. Dev.* **44,** 85-89.

Woolf C. J. (2004) Pain: moving from symptom control toward mechanism-specific pharmacologic management. *Ann. Intern. Med.* **140,** 441-451.

Woolf C. J. and Ma Q. (2007) Nociceptors--noxious stimulus detectors. *Neuron* **55,** 353-364.

Woolf C. J., Safieh-Garabedian B., Ma Q. P., Crilly P. and Winter J. (1994) Nerve growth factor contributes to the generation of inflammatory sensory hypersensitivity. *Neuroscience* **62,** 327-331.

Woolf C. J. and Salter M. W. (2000) Neuronal plasticity: increasing the gain in pain. *Science* **288,** 1765-1769.

Woolf C. J., Shortland P. and Coggeshall R. E. (1992) Peripheral nerve injury triggers central sprouting of myelinated afferents. *Nature* **355,** 75-78.

Wright R. N., Hong D. H. and Perkins B. (2012) RpgrORF15 connects to the usher protein network through direct interactions with multiple whirlin isoforms. *Invest Ophthalmol. Vis. Sci.* **53,** 1519-1529.

Wu Y., Liu Y., Hou P., Yan Z., Kong W., Liu B., Li X., Yao J., Zhang Y., Qin F. and Ding J. (2013) TRPV1 channels are functionally coupled with BK(mSlo1) channels in rat dorsal root ganglion (DRG) neurons. *PLoS. One.* **8,** e78203.

Xing B. M., Yang Y. R., Du J. X., Chen H. J., Qi C., Huang Z. H., Zhang Y. and Wang Y. (2012) Cyclin-dependent kinase 5 controls TRPV1 membrane trafficking and the heat sensitivity of nociceptors through KIF13B. *J. Neurosci.* **32,** 14709-14721.

Xu H., Ramsey I. S., Kotecha S. A., Moran M. M., Chong J. A., Lawson D., Ge P., Lilly J., Silos-Santiago I., Xie Y., DiStefano P. S., Curtis R. and Clapham D. E. (2002) TRPV3 is a calcium-permeable temperature-sensitive cation channel. *Nature* **418,** 181-186.

Xu X. Z., Choudhury A., Li X. and Montell C. (1998) Coordination of an array of signaling proteins through homo- and heteromeric interactions between PDZ domains and target proteins. *J. Cell Biol.* **142,** 545-555.

Xue Q., Jong B., Chen T. and Schumacher M. A. (2007) Transcription of rat TRPV1 utilizes a dual promoter system that is positively regulated by nerve growth factor. *J Neurochem.* **101,** 212-222.

Yang J., Liu X., Zhao Y., Adamian M., Pawlyk B., Sun X., McMillan D. R., Liberman M. C. and Li T. (2010) Ablation of whirlin long isoform disrupts the USH2 protein complex and causes vision and hearing loss. *PLoS. Genet.* **6,** e1000955.

Yang J., Wang L., Song H. and Sokolov M. (2012) Current understanding of usher syndrome type II. *Frontiers in bioscience: a journal and virtual library* **17,** 1165.

Yap C. C., Liang F., Yamazaki Y., Muto Y., Kishida H., Hayashida T., Hashikawa T. and Yano R. (2003) CIP98, a novel PDZ domain protein, is expressed in the central nervous system and interacts with calmodulin-dependent serine kinase. *J. Neurochem.* **85,** 123-134.

Yu F. H. and Catterall W. A. (2004) The VGL-chanome: a protein superfamily specialized for electrical signaling and ionic homeostasis. *Sci. STKE.* **2004,** re15.

Yu L., Yang F., Luo H., Liu F. Y., Han J. S., Xing G. G. and Wan Y. (2008) The role of TRPV1 in different subtypes of dorsal root ganglion neurons in rat chronic inflammatory nociception induced by complete Freund's adjuvant. *Mol. Pain* **4,** 61.

Zemoura K., Schenkel M., Acuna M. A., Yevenes G. E., Zeilhofer H. U. and Benke D. (2013) Endoplasmic reticulum-associated degradation controls cell surface expression of gamma-aminobutyric acid, type B receptors. *J Biol. Chem.* **288,** 34897-34905.

Zhang F., Liu S., Yang F., Zheng J. and Wang K. (2011a) Identification of a tetrameric assembly domain in the C terminus of heat-activated TRPV1 channels. *J. Biol. Chem.* **286,** 15308-15316.

Zhang Q., Fan J. S. and Zhang M. (2001) Interdomain chaperoning between PSD-95, Dlg, and Zo-1 (PDZ) domains of glutamate receptor-interacting proteins. *J. Biol. Chem.* **276,** 43216-43220.

Zhang X., Huang J. and McNaughton P. A. (2005) NGF rapidly increases membrane expression of TRPV1 heat-gated ion channels. *EMBO J.* **24,** 4211-4223.

Zhang X., Li L. and McNaughton P. A. (2008) Proinflammatory mediators modulate the heat-activated ion channel TRPV1 via the scaffolding protein AKAP79/150. *Neuron* **59,** 450-461.

Zhang X. F., Han P., Neelands T. R., McGaraughty S., Honore P., Surowy C. S. and Zhang D. (2011b) Coexpression and activation of TRPV1 suppress the activity of the KCNQ2/3 channel. *J. Gen. Physiol* **138,** 341-352.

Zimmermann P., Meerschaert K., Reekmans G., Leenaerts I., Small J. V., Vandekerckhove J., David G. and Gettemans J. (2002) PIP(2)-PDZ domain binding controls the association of syntenin with the plasma membrane. *Mol. Cell* **9,** 1215-1225.

Zou J., Lee A. and Yang J. (2012) The expression of whirlin and Cav1.3alpha(1) is mutually independent in photoreceptors. *Vision Res.* **75,** 53-59.

UNIVERSITAS
Miguel
Hernández

ANNEX

UNIVERSITAS
Miguel
Hernández

WHIRLIN INCREASES TRPV1 CHANNEL EXPRESSION AND CELLULAR STABILITY

Maria Grazia Ciardo[1,2], Amparo Andrés-Bordería[2], Natalia Cuesta[1], Pierluigi Valente[1], María Camprubí-Robles[1], Jun Yang[3], Rosa Planells-Cases[2,*] and Antonio Ferrer-Montiel[1,*]

[1]Instituto de Biología Molecular y Celular. Universitas Miguel Hernández, Alicante, Spain.
[2]Centro de Investigaciones Príncipe Felipe. Valencia. Spain
[3]John A Moran Eye Center. The University of Utah. Salt Lake City, Utah 84132. USA.

*To whom correspondence should be addressed: Antonio Ferrer-Montiel, E-mail aferrer@umh.es or Rosa Planells-Cases, E-mail: Rosa.Planells-Cases@mdc-berlin.de.

Abstract

The expression and function of TRPV1 is influenced by its interaction with cellular proteins. Here, we identify Whirlin, a cytoskeletal PDZ-scaffold protein implicated in hearing, vision and mechanosensory transduction, as an interacting partner of TRPV1. Whirlin associates with TRPV1 in cell lines and in primary cultures of rat nociceptors. Whirlin is expressed in 55% of mouse sensory C-fibers, including peptidergic and non-peptidergic nociceptors, and co-localizes with TRPV1 in 70% of them. Heterologous expression of Whirlin increased TRPV1 protein expression and trafficking to the plasma membrane, and promoted receptor clustering. Silencing Whirlin expression with siRNA or blocking protein translation resulted in a concomitant degradation of TRPV1 that could be prevented by inhibiting the proteasome. The degradation kinetics of TRPV1 upon arresting protein translation mirrored that of Whirlin in cells co-expressing both proteins, suggesting a parallel degradation mechanism. Noteworthy, Whirlin expression significantly reduced TRPV1 degradation induced by prolonged exposure to capsaicin. Thus, our findings indicate that Whirlin and TRPV1 are associated in a subset of nociceptors and that TRPV1 protein stability is increased through the interaction with the cytoskeletal scaffold protein. Our results suggest that the Whirlin-TRPV1 complex may represent a novel molecular target and its pharmacological disruption might be a therapeutic strategy for the treatment of peripheral TRPV1-mediated disorders.

Keywords: nociception; thermosensory; PDZ; synapses; cytoskeleton; pain

Published in Biochimica et Byophisica Acta-Molecular and Cell Research, October 2015

UNIVERSITAS
Miguel
Hernández

Sobre todo,

no temas a los momentos difíciles.

Lo mejor viene de ellos.

Rita Levi Montalcini

UNIVERSITAS
Miguel
Hernández

ACKNOWLEDGEMENTS

UNIVERSITAS
Miguel
Hernández

~ Agradecimientos ~

Y ha llegado el gran final, se apagan las luces, se cierra el telón, es tiempo de reverencias, aplausos y agradecimientos.

A mis mentores, ante todo. A Rosa, por haberme acompañado en mis primeros pasos en la ciencia con sus enseñanzas y su experiencia, por la confianza depositada y la oportunidad de emprender este increíble camino. A Antonio, por haberme permitido llevarlo a cabo "adoptándome" en su laboratorio, por escucharme y animarme en los últimos críticos momentos.

A Natalia Cuesta, Amparo Andrés, María Camprubí Y Pierluigi Valente por su valiosa contribución científica a esta tesis y al correspondiente articulo.

A mi gran familia española debería dedicar otra tesis entera, o más bien un musical estilo

Sonrisas y Lágrimas

ACTO I: del convento al otro lado de los Alpes a la Villa von Felipe

Corría el año 2008 cuando una joven y alegre italiana del sur aterrizaba en un boeing Ryanair en la tierra de la pólvora y las naranjas con su maletita llena de abrazos rotos, sueños y esperanzas. No era su primera visita en suelo hispánico, pero esta vez la estancia iba a ser más larga y aún más trepidante.

Una efervescente rubia de pura estirpe aragonesa con mucho arte flamenco la acompañaría entre probetas y western blots con sus protocolos, sus clases de castellano autentico, sus sabios consejos, sus regañinas de madre, su fuerza ejemplar, la complicidad de una hermana y la lealtad de una amiga insustituible. Y hasta este día y (espero) muchos más desde entonces. A mi Luci, por ser como eres y estar siempre allí.

No estaría sola en esta ardua tarea. Un gracias infinito va también a mis chicas: a Amparo, que entre sello y sello salía de la oscuridad del patch para buscarnos con sus abrazos; a Imelda, por ayudarme en mi comienzos, con esas primeras PCR, y por el apoyo mutuo hasta el final; a Laura, por su pegadiza gracia gallega; a Judith, por esa sonrisa tan risueña y contagiosa; a María por su "apañadez" y su inteligente ironía; a Majda, siempre dispuesta a echar una mano; a Lauri, por esas risas mañaneras y por haberme abierto tantas veces las puertas de su(s) casa(s); a Arantxita, siempre tan dulce y amable. A todas gracias por hacer todo más fácil, y por esos incontables e increíbles momentos dentro y fuera del lab.

Pero muchos otros actores llenan el escenario y los títulos de cola: los que compartieron laboratorio y plantas con el I-17, los que se cruzaban por los pasillos o los ascensores, los que lucharon hasta el final y volvieron a empezar con el mismo amor por este trabajo no obstante todo. Aunque no os nombre, a todos y cada uno gracias por haberme aportado tanto científica y personalmente y por haberme hecho sentir como en casa en todo momento.

Y como olvidar mis primeras compañeras de piso, Susana y Lorena, y la única conterránea a mi alrededor por mucho tiempo, Fabiana, las carreras en bici hacía el CIPF, las cenas en el piso, los golpes del vecino de abajo, las fiestas de pueblo y los viajes por España, todo salazonado con esas charlas y esa risas que tan bien sientan al corazón.

A mi Chusa, por esos viernes de cena y peli, por esas disertaciones filosóficas sobre la vida y las personas, por decir siempre lo que piensas, por ser tan única, por estar allí ahora y siempre.

A mi literato Jose, mi primer apoyo en el “exilio”, por aguantarme cuando me meto con él o en mis momentos negros, por su humor, su inteligencia y su arte. Siempre nos quedará ese porche en la Toscana amigo.

A Manu y Soraya, por esas risas y esos momentos místico-culturales que seguimos compartiendo.

ACTO II: la fuga

Y cando todo parecía ir viento en popa, con alguna borrasca pasajera, una abrupta tormenta de recortes y mala gestión obligó nuestra heroína a dejar todo lo construido para ir en busca de una nueva patria donde poder acabar sus estudios. Y los que iban a ser solos unos meses se convirtieron en años. Y en tanto tiempo, como no, al final acabó reconstruyendo su vida y conociendo a muchas otras maravillosas personas.

Loramiguicos, que decir… ¡sencillamente me habéis robado el corazón! A los Robertos, Cloti, Ángeles, Luci, Sakthi, Ainara, Isa, Maite, Gema, Vero, Pier, Nuria, Paco, Jan, Chris, Efrén, Monica y Antonio Z. A los que han estado desde el principio, a los que han llegado después, a los que se han ido y han vuelto, a los que han ido yendo y viniendo, a los que se han ido pero siguen allí, gracias por cada momento, por cada risa, por cada consejo, por abrirme un mundo de posibilidades, multiversos y buenorror.

A Rober c/pelitos, por esas pacientes sesiones de coaching personal y profesional, por esa extrema sensibilidad, por los abrazos “achuchables”, por apreciar tanto mis pizzas-galletas y mis pasteles quemados, por tener siempre un detalle especial con todos, por todo y mucho más, no cabría ni en mil fichas. A Cloti, mi hermana “emocional” separada al nacer, por tu arte científico, por las confesiones y las risas tontas, por esa conexión que no necesita palabras. A Rober s/p, por esa sonrisa inmensa que te alegra el corazón, por esa lógica contundente que acaba con toda tontería innecesaria, por esa mirada que lo dice tó, “no puedo estar sin ti”. A Wen, por dar siempre ese toque tan tuyo y tan único, por las inquietudes y los intereses compartidos, por los sueños conquistados, por esos viajes de “piradas”, siempre smile y llegarás lejos amiga porque te lo mereSes. A Sakthi, por esos difíciles meses en los que te ha tocado compartir despacho conmigo, por esas discusiones científico-filosóficas, por ser tan chungo y tan gracioso a la vez, I will miss you a lot. Y como podía faltar otra Luci en mi vida, igual de graciosa, igual de flamenca, igual de especial. Y qué maravilla nuestro encuentro transoceánico. A Ainarufa, porque no hemos compartido pisazo pero hemos compartido mucho más en esos pocos pero intensos meses, y por lo que nos queda pingüinufa. A Isa, por su sabiduría en la ciencia y en la vida y por salvarme más de una vez de la maldición del cercanías acogiéndome en su casa. A Maitechu, valiosa aliada con la que refunfuñar en el labo, por los momentos vividos fuera y por sus maravillas culinarias. A Gemita, por esa resolución, esas regañinas y esa alegría tan esenciales en el grupo. A Vero, por su contagiosa vitalidad (seguiremos hablando de ese plan B). A Nuri, por escucharme y animarme como una madre y por alegrarme las mañanas con su chispa. A Paco, por tener siempre una respuesta a mis dudas. A Monikufa, Efrén y Antonio, por su ayuda imprescindible.

Y como no a la secretaria del IBMC, May, Javier, Carmen y Raquel por ser tan amables y eficientes, a Asia por esas peleas con el confocal y a Grego por su continuo interés.

A Lodiana, por ser la mejor compi de piso que pude tener en esos primeros y complicados meses en Alicante.

A mis amigos alicantinos, y sobre todo a mis ladies Raquel y Laura, por las charlas y las risas, los bailes, las tardes de playa, la remolacha y todos los buenos momentos pasados juntos!

A todas las familias que me han acogido en sus casas como otra hija más.

Agli amici di sempre, che sono rimasti al mio fianco oltre la distanza.

Ma il ringraziamento piú grande va alla mia Famiglia, a mamma Rosalia e papá Franco e al mio fratellone Roberto, che hanno sopportato duramente la lontananza e gli alti e bassi telefonici di questi anni, per avermi appoggiato in tutte le mie scelte, per i momenti persi e per tutti quelli ancora da vivere insieme, per essere il mio pilastro, il mio centro di gravitá permanente. Vi voglio bene.

ACTO FINAL: el futuro

Sube montañas sin desistir,
sigue el arco iris
y hallarás por fin un sueño
que habrás de cuidar y querer.

Y llegados a este punto

Agradecida y emocionada, solamente puedo decir, gracias por venir.

~The end~

UNIVERSITAS
Miguel
Hernández